UNIVERSITAT DE BARCELONA

Analysis and characterization of fullerene nanoparticles

Alina Astefanei

ADVERTIMENT. La consulta d'aquesta tesi queda condicionada a l'acceptació de les següents condicions d'ús: La difusió d'aquesta tesi per mitjà del servei TDX (**www.tdx.cat**) i a través del Dipòsit Digital de la UB (**diposit.ub.edu**) ha estat autoritzada pels titulars dels drets de propietat intel·lectual únicament per a usos privats emmarcats en activitats d'investigació i docència. No s'autoritza la seva reproducció amb finalitats de lucre ni la seva difusió i posada a disposició des d'un lloc aliè al servei TDX ni al Dipòsit Digital de la UB. No s'autoritza la presentació del seu contingut en una finestra o marc aliè a TDX o al Dipòsit Digital de la UB (framing). Aquesta reserva de drets afecta tant al resum de presentació de la tesi com als seus continguts. En la utilització o cita de parts de la tesi és obligat indicar el nom de la persona autora.

ADVERTENCIA. La consulta de esta tesis queda condicionada a la aceptación de las siguientes condiciones de uso: La difusión de esta tesis por medio del servicio TDR (**www.tdx.cat**) y a través del Repositorio Digital de la UB (**diposit.ub.edu**) ha sido autorizada por los titulares de los derechos de propiedad intelectual únicamente para usos privados enmarcados en actividades de investigación y docencia. No se autoriza su reproducción con finalidades de lucro ni su difusión y puesta a disposición desde un sitio ajeno al servicio TDR o al Repositorio Digital de la UB. No se autoriza la presentación de su contenido en una ventana o marco ajeno a TDR o al Repositorio Digital de la UB (framing). Esta reserva de derechos afecta tanto al resumen de presentación de la tesis como a sus contenidos. En la utilización o cita de partes de la tesis es obligado indicar el nombre de la persona autora.

WARNING. On having consulted this thesis you're accepting the following use conditions: Spreading this thesis by the TDX (**www.tdx.cat**) service and by the UB Digital Repository (**diposit.ub.edu**) has been authorized by the titular of the intellectual property rights only for private uses placed in investigation and teaching activities. Reproduction with lucrative aims is not authorized nor its spreading and availability from a site foreign to the TDX service or to the UB Digital Repository. Introducing its content in a window or frame foreign to the TDX service or to the UB Digital Repository is not authorized (framing). Those rights affect to the presentation summary of the thesis as well as to its contents. In the using or citation of parts of the thesis it's obliged to indicate the name of the author.

Universitat de Barcelona

Programa de Doctorado "Química Analítica del Medio Ambiente y la Polución"

ANALYSIS AND CHARACTERISATION OF FULLERENE NANOPARTICLES

Tesis doctoral presentada para optar al título de
Doctor por la Universidad de Barcelona por

Alina Astefanei

Directores de la tesis

Dra. Maria Teresa Galceran i Huguet
Departamento de Química Analítica
Universidad de Barcelona

Dr. Oscar Núñez Burcio
Departamento de Química Analítica
Universidad de Barcelona

Barcelona, Julio de 2015

To my mother

TABLE OF CONTENTS

ABSTRACT.....III

AIMS AND STRUCTURE OF THE THESIS.....VII

ABBREVIATIONS.....IX

CHAPTER 1. INTRODUCTION.....1

1.1. Nanotechnology.....3

1.2. Nanoparticles.....4

1.2.1. Classification and uses.....4

1.2.2. Exposure and potential hazards.....7

1.3. Fullerene nanoparticles.....9

1.3.1. *Scientific article I: Characterisation and determination of fullerenes: A critical review*.....13

CHAPTER 2. ANALYSIS OF FULLERENES.....37

2.1. Introduction.....39

2.2. *Scientific article II: Analysis of C60-fullerene derivatives and pristine fullerenes in environmental samples by ultrahigh performance liquid chromatography-atmospheric pressure photoionization-mass spectrometry*.....47

2.3. *Scientific article III: Non-aqueous capillary electrophoresis separation of fullerenes and C60 fullerene derivatives*.....61

2.4. Discussion of results.....71

2.5. Conclusions.....85

CHAPTER 3. CHARACTERISATION OF FULLERENES.....91

2.6. Introduction.....93

2.7. *Scientific article IV: Aggregation behavior of fullerenes in aqueous solutions: a capillary electrophoresis and asymmetric flow-field flow fractionation study*.....103

2.8. *Scientific article V: Characterization of aggregates of surface modified fullerenes by asymmetrical flow field-flow fractionation with multi angle light scattering detection*.....127

2.9. Discussion of results.....151

2.10. Conclusions.....167

CHAPTER 4. CONCLUDING REMARKS.....171

RESUMEN.....177

REFERENCES.....207

ACKNOWLEDGMENTS

ABSTRACT

Fullerenes or *Buckyballs* are a group of carbon nanoparticles formed as nanocages, classified as engineered nanoparticles which are made up of multiple pentagons and hexagons. In the last years there has been rapid growth of investment in fullerene production and widespread use by public and private sectors worldwide and they are expected to become an important contributor to achieve economic and social benefits. The advent of fullerene nanoparticles in commercial, industrial and biomedical applications raises concern about their potential ecological and human health risks and there is a continuing uncertainty and controversy on this topic due to the lack of scientific evidences. Fullerenes have not been regulated, although the European Commission (European Commission, 2002), the European Parliament (European Parliament, 2008) and the US Environmental Protection Agency (EPA, 2015) have prioritised legislation on nanomaterials handling and disposal. Given the current lack of studies regarding their presence, fate and behaviour in consumer products and environmental matrices and their associated human and environmental risks it is becoming increasingly important to be able to characterise and quantitate fullerene nanoparticles, especially derivatives, in a wide range of matrix types.

The toxicity of fullerenes is size and shape dependent and knowledge of their aggregate size is crucial since their mobility and deposition in the aquatic environment strongly depends on this characteristic. The ability to obtain such data more efficiently is expected to aid researchers in focusing their efforts to evaluate the potential exposures and risks posed by fullerene nanoparticles. Moreover, in industrial processes the particle size distribution has a critical effect on the quality and performance of the final manufactured product and consequently, through their more accurate measurement, the success of manufacturing businesses can also be improved. There are very few reports on the physico-chemical characterisation of fullerenes, and most of them are focused on C_{60} and C_{70} fullerenes. Several techniques can be used under laboratory conditions, including transmission and scanning electron microscopy (TEM and SEM), atomic force microscopy (AFM), light scattering, asymmetrical flow-field flow fractionation (AF4) and capillary electrophoresis (CE). Such methods enable the investigation of properties at the level of individual particles as well as aggregates. However, up to now no ideal technique has been found for fullerenes characterisation. Therefore, several methodologies should be combined for a complete picture on their aggregation behaviour. With regard to their detection and quantitation in complex samples, liquid chromatography coupled to UV-Vis detection or mass spectrometry and CE-UV are the most commonly used techniques. So far the reported studies are focused mainly on the analysis of pristine compounds, very few

have included several fullerene derivatives, and only a limited number of environmental matrices have been addressed.

To fill these knowledge gaps, one of the objectives of this thesis was the development of analytical methodologies for the determination of pristine and surface modified fullerenes by ultra-high performance liquid chromatography coupled to MS (UHPLC-MS) and by nonaqueous capillary electrophoresis (NACE) and micellar electrokinetic capillary chromatography (MECC) with UV-Vis detection in different environmental matrices (water and sediment samples) and cosmetic products, respectively. In addition, in this thesis the size and shape characterisation of surface modified fullerenes in aqueous solutions of different pH and ionic strength values was studied by combining several techniques (CE, AF4-MALS and TEM).

The chromatographic separation of five pristine (C_{60}-C_{84}) and three surface modified fullerenes (PCBM, PCBB and C_{60}-pyrr) was achieved in less than 4.5 min by employing a sub-2 μm C18 column and toluene:methanol as a mobile phase. The use of atmospheric pressure photochemical ionisation (APPI) as an ionisation source, and of highly selective-selected ion monitoring (H-SIM) mode for pristine fullerenes (working at enhanced resolution in Q3 (0.06 m/z full width at half maximum (FWHM), mass resolving power >12,500)), and selective reaction monitoring (SRM) mode (Q1 and Q3 at 0.7 m/z FWHM) for fullerene derivatives improved the selectivity and sensitivity of the method achieving MLODs between 0.9 pg L^{-1} and 1.6 ng L^{-1} for the water samples and between 45 pg Kg^{-1} and 158 ng Kg^{-1} for the sediments. For the extraction of the water samples, liquid-liquid extraction (LLE) with toluene and the addition of salt, to disrupt the stability of fullerene aggregates and facilitate their partition in the toluene phase, was used. Using this extraction method, slightly higher recoveries were obtained for fullerene derivatives (93-96 %) than for pristine fullerenes (83-89 %), values that are similar to the ones previously reported by LLE for some of these compounds. The advantage of the extraction method used in this thesis is that both suspended particulate and dissolved fullerene aggregates are extracted in one step, whereas by ultrasound assisted extraction (UAE) and solid phase extraction (SPE) a previous filtration step is required, and the analysis of both the suspended matter and the remaining aqueous phase is needed for an accurate determination. For sediments we propose the use of pressurised liquid extraction (PLE) performed at a high extraction temperature (150 °C) using one extraction cycle of 10 min. This method allowed us to achieve good recoveries for the selected fullerenes (70-92 %). Higher recoveries were obtained for fullerene derivatives (87-92 %) being also superior to the ones reported by UAE for the same compounds. In addition, our method is faster (10 min) and involves lower solvent consumption

than UAE and Soxhlet methods which require up to 4 h and higher toluene amounts. The developed UHPLC-(-)APPI/MS(MS) methodology allowed us to report for the first time the presence of C_{60}-pyrr, PCBM and PCBB in sediments (2.0 - 8.5 ng Kg^{-1} levels) and in pond water samples (0.1 - 5.1 pg L^{-1} levels). C_{60} and C_{70} fullerenes were detected in most of the analysed samples and quantified at levels up to 25 ng L^{-1} and 330 ng L^{-1} (water samples) and up to 1 ng kg^{-1} and 7 ng kg^{-1} (sediments), respectively.

The separation of two pristine compounds (C_{60} and C_{70}) and two C_{60}-derivatives (C_{60}-pyrr and C_{60}CHCOOH) by NACE was achieved by employing a long alkyl chain tetraalkylammonium salt (TDAB, 200 mM) able to interact with the target analytes providing them charge, and consequently electrophoretic mobility, and a short alkyl chain tetraalkylammonium salt (TEAB, 40 mM) which was needed to decrease the electroosmotic flow (EOF) in a solvent mixture containing 6 % methanol, 10 % acetic acid in acetonitrile/chlorobenzene (1:1, v/v) as the background electrolyte (BGE). The calculated detection limits, based on a signal-to-noise ratio of 3:1, were between 1 and 3.7 mg L^{-1}. The established methodology has been applied for the first time for the quantitation of C_{60} in a cosmetic product and the result (2.10 ± 0.20 mg L^{-1}) was in agreement with that obtained by analysing the same product by LC-MS (1.93 ± 0.15 mg L^{-1}). These results allowed proposing the developed NACE method as an alternative to conventional LC for the determination of C_{60} in cosmetic samples where this compound is present at a relatively high concentration and presenting the advantages of being less expensive and involving less solvent consumption.

In addition, MECC using SDS micelles (100 mM) and 10 mM sodium tetraborate-10 mM sodium phosphate as BGE is proposed for the analysis of individual hydrophobic fullerenes (C_{60}, C_{70} and C_{60}-pyrr) showing good repeatability and reproducibility, and achieving LODs between 0.6 and 2.2 mg L^{-1} being lower than the ones found by NACE (see above). The applicability of the method was evaluated by quantifying C_{60} in two cosmetic products which was found at 1.86 ± 0.07 mg L^{-1} (anti-aging serum) and 2.77 ± 0.16 mg kg^{-1} (face mask) concentration levels. The same anti-aging serum was also analysed by the previously proposed NACE method and by LC-MS and similar results were found (see above). Therefore, MECC could be used as an alternative to NACE and LC-MS for the analysis of C_{60} in cosmetic products presenting the advantage of being less contaminant than the other two since no organic solvents are used.

Regarding the characterisation of fullerene aggregates, the AF4-MALS results have shown that polyhydroxy fullerenes ($C_{60}(OH)_{24}$, $C_{120}(OH)_{30}$) present significantly smaller sizes (e.g. hydrodynamic radii (r_H): 4 nm and radii of gyration (r_G) up to 60 nm for $C_{60}(OH)_{24}$) than

carboxy-fullerenes (C_{60}CHCOOH and C_{60}-pyrr tris acid) (e.g. r_H : 10-95 nm and r_G: 10-310 nm for C_{60}-pyrr tris acid) in Milli-Q water. The fractograms of $C_{60}(OH)_{24}$, $C_{120}(OH)_{30}$ revealed tailed peaks whereas for C_{60}CHCOOH and C_{60}-pyrr tris acid multiple peaks corresponding to particles of different aggregation degree were obtained. The shapes of the aggregates formed were studied by correlating the r_G peak-top values from the MALS results with the r_H calculated from the retention times in AF4 at the maximum of the peak height, and also by TEM. The AF4-MALS results indicated a significant deviation from the spherical shape for polyhydroxy-fullerenes, and the presence of both spherical and irregular shaped particles for the carboxy-fullerenes. These results were in agreement with the results obtained by TEM which showed highly branched structures for polyhydroxy-fullerenes and the presence of both spherical and irregular clusters for the carboxy-fullerene derivatives.

The increase in the ionic strength promoted the aggregation of the particles revealing broad, multiple and distorted peaks in MECC and their peak shapes improved by working in capillary zone electrophoresis (CZE) conditions. The sizes of the polyhydroxy-fullerenes as determined by AF4 showed up to a 10-fold increase in their average r_H at 0.2 ionic strength whereas for the carboxy-fullerenes such high ionic strength values led to their adsorption to the AF4 membrane due to a significant increase in their sizes. In agreement, an increase in the r_G determined by AF4-MALS was observed for polyhydroxy-fullerenes and a slight decrease for the carboxy-fullerenes due to the adsorption of the bigger aggregates on the AF4 membrane after the fractionation. TEM micrographs also showed an increase in the aggregation degree of the particles and revealed the formation of highly branched aggregates structures. The increase in the SDS concentration allowed distinguishing between particles of different aggregation degree present in the samples, revealing multiple peaks in the electropherograms obtained by MECC and a higher number of discernable peaks in the AF4 fractograms.

AIMS AND STRUCTURE OF THE THESIS

Fullerenes are increasingly being used in medical (e.g. drug-delivery), environmental (e.g. remediation) and energy and electronic (e.g. solar cells) applications due to their unique structural and electronic properties. In this context, it is important to increase the current knowledge regarding the characteristics, behaviour, fate and toxicity of fullerenes, a new class of organic emerging contaminants that scientists have very little understanding of. Therefore, it is becoming increasingly important to be able to characterise and quantitate fullerene nanoparticles in a wide range of matrix types and for this purpose the development of analytical methods for their quantitative and qualitative analysis is needed. Furthermore, besides the determination of fullerene concentrations in complex matrices, their characterisation in terms of degree of aggregation, size distribution and surface morphology in aqueous solutions of different characteristics (e.g., ionic strength and pH) is required in order to provide tools for their risk assessment legislation.

The **general objective** of this thesis is the development of analytical methodologies for the analysis (identification and quantitation) and characterisation (aggregate sizes and shapes) of fullerenes and the evaluation of their presence in environmental and cosmetic samples.

This general objective is structured around several **specific objectives** as follows:

- To establish methodology for the analysis of hydrophobic fullerenes in environmental samples (water and sediments) by liquid chromatography coupled to mass spectrometry.
- To develop methodology for the analysis of hydrophobic and water soluble fullerenes by capillary electrophoresis and apply the methodology for the analysis of pharmaceutical and/or cosmetic samples. In this context, non-aqueous capillary electrophoresis (NACE) and micellar electrokinetic capillary chromatography (MECC) are going to be evaluated.
- To study the aggregation behaviour of fullerenes in aqueous media. For this purpose, several techniques such as capillary electrophoresis, asymmetrical flow-field flow fractionation (AF4) and transmission electron microscopy (TEM) are going to be used.
- To study the effect of conditions such as pH and ionic strength on the aggregation degree, size distribution and shape of fullerene aggregates in aqueous solutions. The technique to be used for this purpose is asymmetrical flow-field flow fractionation coupled to multi-angle light scattering (AF4-MALS).

This thesis is structured in 4 chapters:

- **Chapter 1** includes an introduction to nanotechnology, a classification of nanoparticles, their uses and applications, routes of exposure and potential risks posed for the environment and human health. This chapter ends with a section dedicated to fullerene nanoparticles which includes a brief description of fullerenes and a review recently published about these compounds, entitled: *"Characterisation and determination of fullerenes: A critical review",* published in Analytica Chimica Acta, **882**: 1-21 (2015).

- **Chapter 2** is devoted to the development of methodologies for the analysis of fullerenes in complex samples, environmental (water and sediments) and cosmetics. Two separation techniques are proposed: LC-MS for environmental samples and NACE for the cosmetic ones. The development of these methods and the obtained results can be found in two scientific papers entitled "*Analysis of C60-fullerene derivatives and pristine fullerenes in environmental samples by ultrahigh performance liquid chromatography-atmospheric pressure photoionization-mass spectrometry*" published in the Journal of Chromatography A, **1365**: 61-71 (2014) and "*Non-aqueous capillary electrophoresis separation of fullerenes and C60 fullerene derivatives*" published in Analytical and Bioanalytical Chemistry, **404**: 307-313 (2012).

- **Chapter 3** refers to the study of the aggregation behaviour of fullerenes and the development of methods for their characterisation by CE techniques, AF4-MALS and TEM. The methods and results obtained are included in two scientific papers entitled "*Aggregation behavior of fullerenes in aqueous solutions: a capillary electrophoresis and asymmetric flow-field flow fractionation study*" sent for publication in Analytical and Bioanalytical Chemistry and "*Characterization of aggregates of surface modified fullerenes by asymmetrical flow field-flow fractionation with multi angle light scattering detection*" accepted for publication in Journal of Chromatography A (2015).

- **Chapter 4.** In this last chapter the concluding remarks of this thesis are included.

ABBREVIATIONS

AF4	Asymmetric flow field-flow fractionation
AFM	Atomic force microscopy
APCI	Atmospheric pressure chemical ionisation
APPI	Atmospheric pressure photoionisation
BGE	Background electrolyte
CE	Capillary electrophoresis
CNPs	Carbon nanoparticles
CZE	Capillary zone electrophoresis
DLS	Dynamic light scattering
ENPs	Engineered nanoparticles
ESI	Electrospray ionisation
H-SIM	Highly selective-selected ion monitoring
FWHM	Full width at half maximum
LC-MS	Liquid chromatography coupled to mass spectrometry
LLE	Liquid-liquid extraction
LODs	Limits of detection
LOQs	Limits of quantification
MALS	Multi-angle light scattering
MECC	Micellar electrokinetic capillary chromatography
NACE	Non-aqueous capillary electrophoresis
PAHs	Polyaromatic hydrocarbons
PES	Polyethersulfone
PLE	Pressurised liquid extraction
REACH	Regulation on Registration, Evaluation, Authorisation and Restriction of Chemicals
RC	Regenerated cellulose

r_H	Hydrodynamic radius
r_G	Radius of gyration
SDS	Sodium dodecyl sulfate
SEM	Scanning electron microscopy
SPE	Solid phase extraction
SRM	Selective reaction monitoring
TDAB	Tetradecylammonium bromide
TDE	Time delayed exponential
TEAB	Tetraethylammonium bromide
TEM	Transmission electron microscopy
UHPLC-MS/MS	Ultrahigh-pressure liquid chromatography coupled to mass spectrometry in tandem
UAE	Ultrasound assisted extraction

CHAPTER 1

INTRODUCTION

1.1. Nanotechnology

"I want to build a billion tiny factories, models of each other, which are manufacturing simultaneously. The principles of physics, as far as I can see, do not speak against the possibility of manoeuvring things atom by atom. It is not an attempt to violate any laws; it is something, in principle, that can be done; but in practice, it has not been done because we are too big"

Richard Feynman, "There's Plenty of Room at the Bottom" 1959

As the renowned physicist Richard Feynman proposed in 1959, the concept of "nanotechnology" in its original sense refers to the projected ability to construct items from the bottom up, with atomic precision. Though he never explicitly mentioned "nanotechnology", Feynman suggested that it will eventually be possible to precisely manipulate atoms and molecules. Hence, long before scanning tunneling microscopes and atomic force microscopes were invented, Feynman proposed these revolutionary ideas to his peers.

In 1979 Eric Drexler encountered Feynman's talk which inspired him to put this concept into motion and so, the term "nanotechnology" was coined and researchers, starting with Eric Drexler, built up this field from the foundation that Feynman previously constructed. Nowadays, nanotechnology research is developed as a cutting-edge interdisciplinary technology involving chemistry, physics, material science, biology and medicine and represents a new trend within scientific development, using the properties of the molecules in a unique fashion to produce and design new and fascinating materials and products.

Today, nanotechnology has become a top research priority in most of the industrialised world, including the USA, the EU and Japan. Its rudimentary capabilities for systematic control and manufacture at the nanoscale are envisioned to evolve in several generations of new nanotechnology products within different research areas ranging from a first generation of simple and passive nanostructures through a fourth generation of highly functionalised molecular systems (Roco, 2004). As depicted in Figure 1, the first generation is illustrated by nanostructured coatings, dispersion of nanoparticles and nanostructured materials (metals, polymers, and ceramics). The second generation represented by active nanostructures refers to adaptive nanostructures, transistors, amplifiers, targeted drugs and chemicals, and actuators. The third generation, 3-D nanosystems and systems of nanosystems, includes various syntheses and assembling techniques, such as bioassembling; networking at the nanoscale and multiscale architectures. Regarding the fourth generation, the research focus will be on atomic manipulation for design of molecules and supramolecular systems, molecular machines and design of large heterogeneous molecular systems, creating multifunctional molecules, catalysts for synthesis,

electromechanical nanosystems, subcellular interventions, and biomimetics for complex system dynamics and control (Roco, 2004).

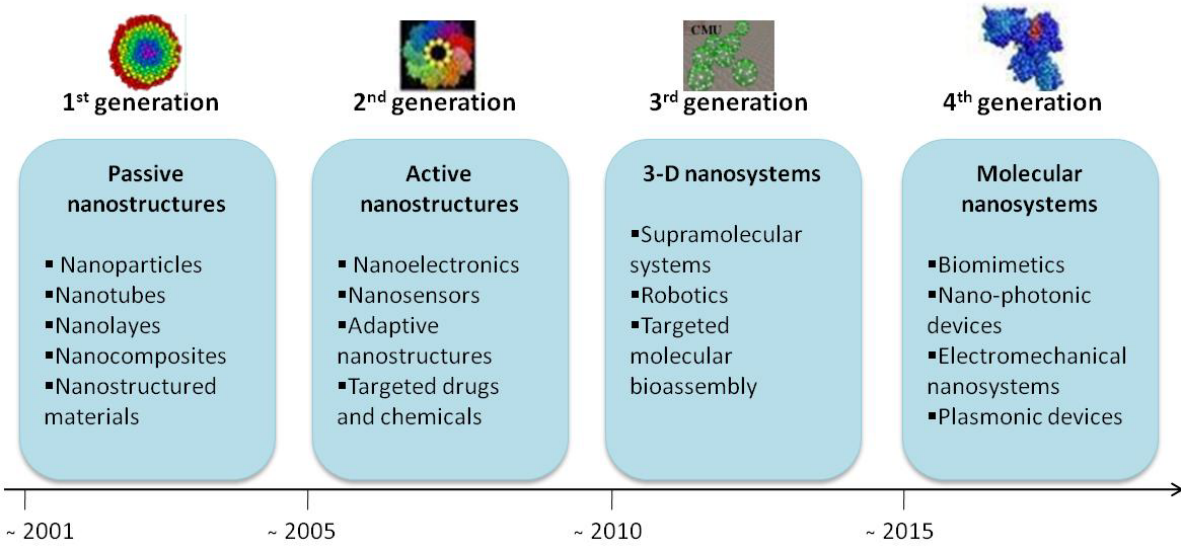

Figure 1. Evolution and applications of nanotechnology (based on: Roco, 2004).

1.2. Nanoparticles

Nanoparticles are considered substances that are less than 100 nm in size in more than one dimension, although these limits are not generally accepted and there are several nanomaterials that fall outside this range which are usually taken as being products of nanotechnology. They may be spherical, tubular, or irregularly shaped, can exist in fused, aggregated or agglomerated forms and can differ from other materials because of their relatively large specific surface area. Nanomaterials and nanoparticles exhibit high strength, high thermal stability, low permeability and high conductivity properties, among other unique properties which stimulate the scientific community to focus their research on developing new applications and products related to nanotechnology. In addition, physical or chemical modifications of "native" nanomaterials, such as surface functionalisation, are commonly performed to modify or enhance their physicochemical properties. These kinds of nanoparticles receive the prefix 'engineered', which is also used for the nanomaterials of anthropogenic origin.

1.2.1. Classification and uses

Nanoparticles can be classified as inorganic or organic (carbon-based) compounds and these two main groups are further sub-classified taking into account their physicochemical properties, as shown in Figure 2. Inorganic nanoparticles include metals, metal oxides and

quantum dots (silver, titanium dioxide and cadmium selenide nanoparticles). Organic nanomaterials occupy a prominent place among engineered nanoparticles (ENPs) enclosing carbon nanotubes, fullerenes, graphene sheets and many others (Figure 3) for the improvement of technological, industrial and medical products. Nonetheless, the list of both inorganic and organic nanomaterials is much more extensive and new ENPs are nowadays being produced in increasing quantities and finding application in a wide range of sectors.

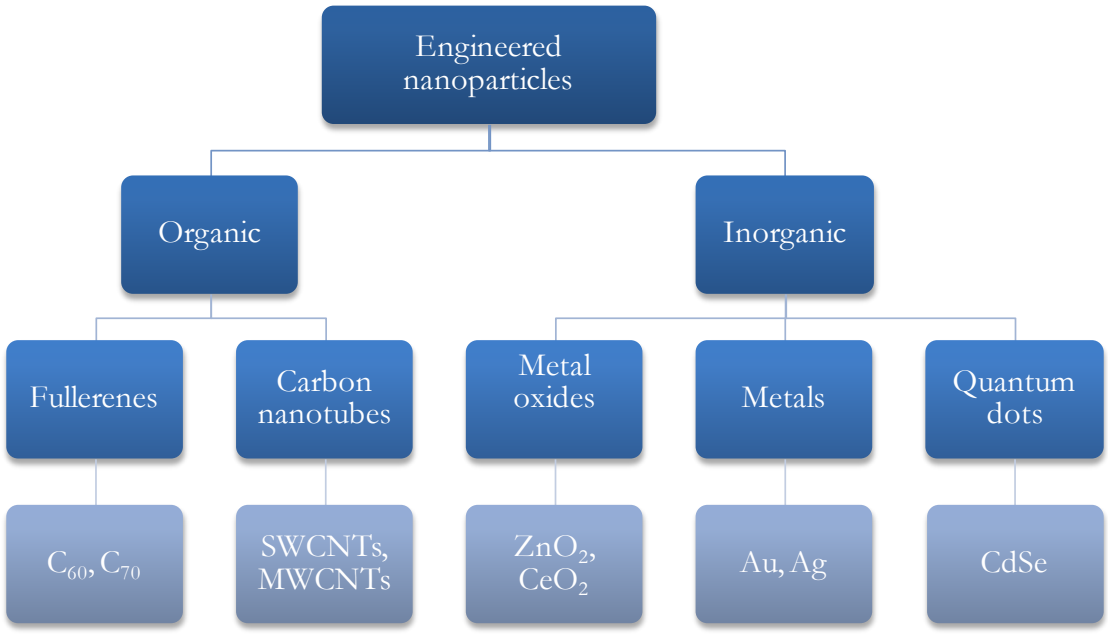

Figure 2. Nanomaterial classification according to their physicochemical properties.

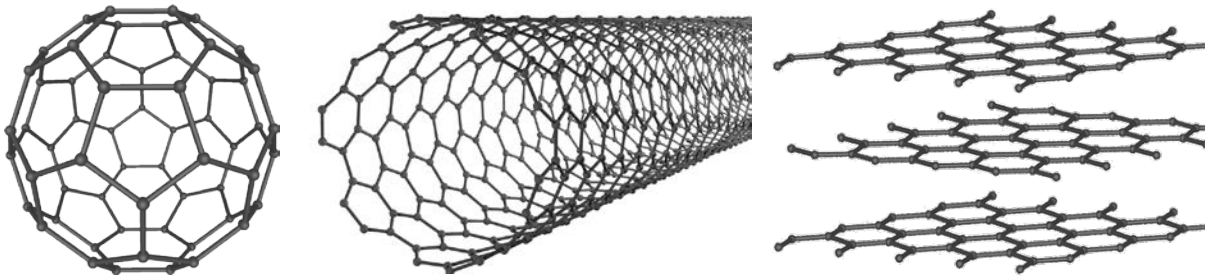

Figure 3. Example of carbon nanoparticles (from the left to the right: fullerenes, carbon nanotubes and graphene sheets).

ENPs are used, or being evaluated for use, in many fields, from biological and medical applications to environmental sciences revealing enormous prospects for progress in both life

sciences and information technology. They can contribute to stronger, lighter, cleaner and "smarter" surfaces and systems since at the nanoscale, the properties of particles may change in unpredictable ways.

Current estimates suggest that more than 1,600 consumable products, including cell phone batteries, sporting equipment, and cosmetics, already contain ENPs (Fears et al., 2011). In addition to these everyday items, work is being conducted to investigate the potential of ENPs in environmental remediation strategies, to detect and eliminate toxic substances, energy generation and storage (Tratnyek and Johnson, 2006; Theron et al., 2008; Otto and Floyd, 2008; Karnt et al., 2009) and advanced medical procedures (Freitas, 2005; Lacerda et al., 2006). It is expected that many of the applications will help to improve human health and quality of life. For instance, the medical application of nanotechnology is probably one of the fastest growing fields, with developments in therapeutic, diagnostic and imaging uses (e.g. cancer). Figure 4 presents the nanotechnology consumer products inventory published in 2013 (Inventory of nanotechnology, 2013) according to relevant main product categories (Figure 4a) and to the most common nanomaterials used (Figure 4b). As shown in Figure 4a the largest main category (50%) is health and fitness which includes mainly products like cosmetics, sunscreens and clothing followed by home and garden products and food and beverages (13-14 %). The most common material mentioned in the product descriptions is silver (51% of the products) followed by titanium (24 %) which has surpassed carbon nanomaterials (which include fullerenes) (11%), followed by silica (7%), zinc (including zing oxide) (5%), and gold (2%).

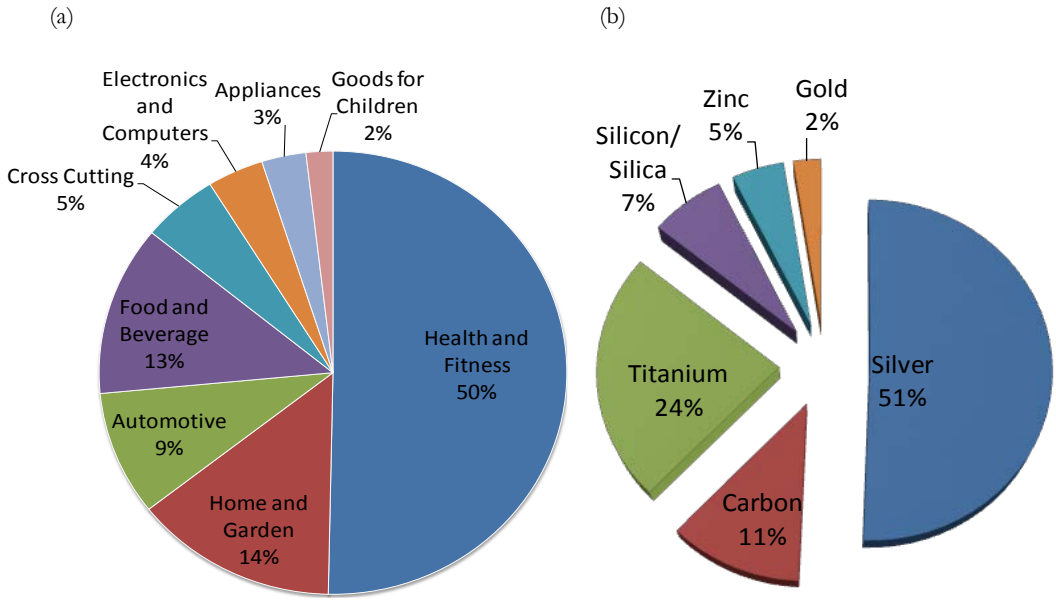

Figure 4. Inventory of nanotechnology-based consumer products according to (a) relevant main product categories and (b) the most common nanomaterials used. Based on: Inventory of nanotechnology, 2013.

1.2.2. Exposure and potential hazard

The unique features of nanotechnology may yield many far-reaching societal benefits, but they can also pose hazards and risks. As more nanotechnology applications are commercialised, it is likely that increasing exposure to ENPs will occur causing concerns about the safety of these materials to human health and the environment.

Figure 5 shows a scheme of the production, use and disposal of nanomaterials in air, water, soil and organisms. Their release into the environment may come from point sources, such as consumer products, disposal, factories or landfills, and from nonpoint sources, such as wet deposition from the atmosphere, storm-water runoff and through effluent and spillage (Yah et al., 2012). Biochemical cycling of nanomaterials may involve photochemical reactions in the atmosphere, aggregation, uptake, accumulation, transformation, and degradation in organisms. For their removal from groundwater and surface water (used for drinking water) conventional treatment methods are used, such as flocculation, sedimentation, and sand or membrane filtration. Air filters and respirators can be used to remove nanomaterials from air. Human exposure to nanomaterials is most likely to occur during nanomaterial manufacturing, but inhalation of nanomaterials released to the atmosphere, ingestion of drinking water or food (e.g., fish) that have accumulated nanoparticles and dermal exposure from sunscreens and cosmetics are also likely (Hoet et al., 2004; Yah et al., 2012). The intake is usually tolerated by the organism system but when a certain range is exceeded, it would cause toxic effects and even deaths. Since nanoparticles have environmental and human health risks, it is, therefore, crucial to carry out research to understand and anticipate them through risk assessment and risk management However, in view of scarce health information arising from nanoparticles it is of paramount importance to take some remedial actions so as to reduce the hazards to workers and the environment. Until a clearer picture emerges, the limited data available suggest that caution must be taken when potential exposures to nanoparticles arise.

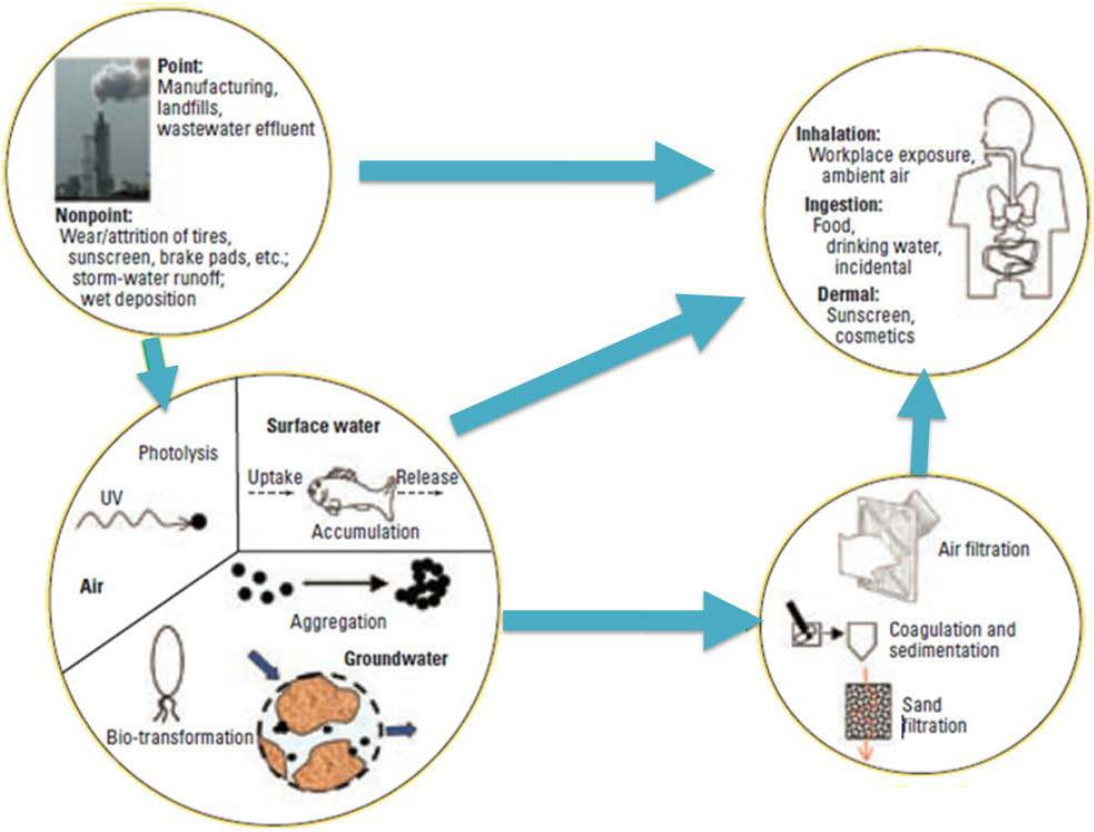

Figure 5. Scheme of the production, use and disposal of nanomaterials in air, water, soil and organisms. Reprinted with permission from (Wiesner et al., 2006). Copyright (2006) American Chemical Society.

The safety issues derived from ENPs routes of entry and their potential bio-distribution are governed by surface area, shape, agglomeration, aggregation, solubility and size interactions within the host (Yah et al., 2012). A detailed examination of these properties is required to assess the risks posed by them. Moreover, characterising starting materials is essential, since the purity of these nanoparticles, based only on the manufacturer's information is frequently unreliable and they may contain substances (including chemicals known to be toxic) in addition to the nanoparticles themselves (Liu et al., 2007; Jakubek et al., 2009; Hull et al., 2009). Large differences in reported toxicity of nanoparticles in the literature are likely a consequence of investigators actually testing different materials containing varying amounts of contamination, and variable aggregation of the particles occurring in the test solution.

These items are not currently regulated, although the European Commission (European Commission, 2002) and the European Parliament (European Parliament, 2008) has prioritised legislation on nanomaterials handling and disposal. Additionally, US Environmental Protection Agency is pursuing a comprehensive regulatory approach under the Toxic Substances Control Act (EPA, 2015) to ensure that nanoscale materials are manufactured and used in a manner that protects against unreasonable risks to human health and the environment. Assessment

of exposure concentrations of dispersed nanomaterials requires detailed insight into the processes that act on these materials in the environment and currently the available knowledge of these processes is insufficient to allow quantitative predictions of the environmental fate of nanomaterials Moreover, regulation is challenging today because of uncertainties in definition, behaviour and application of nanomaterials in many industrial sectors and the lack of appropriate standards and validated testing procedures. Hence, reference materials and methods for measuring ENPs versus natural occurring nanoparticles as well as methods for their determination after release are crucial. Additionally, in vivo assays involving long-term exposure studies are also needed to increase the knowledge of possible risks to humans and the environment.

1.3. Fullerene nanoparticles

Fullerenes or Buckyballs are a group of carbon nanoparticles (CNPs) formed as nanocages of different shapes ranging from C_{20} to C_{720} (and larger), which are made up of multiple pentagons and hexagons (Figure 6). Their potential impact on the environment is perhaps the highest profile of contemporary concerns.

An important property of fullerenes is the capacity to cross membranes (Jensen et al., 1996) enabling their use in medicine for drug and gene delivery (*i.e.,* in the context of diabetes) and for DNA photo-cleavage (da Ros et al., 1999; da Ros, 2008). Their cage like structure allows them to encapsulate other molecules such as single metal atoms to serve as absorbers in biomarkers (Zhang et al., 2010) and in combination with biomolecules, to promote specific functions, such as catalysis (Willner and Willner, 2010). Their direct application in medicine has demonstrated the ability of fullerenes to down-regulate the oxidative stress in the lung tissue of tumor bearing mice (Jiao et al., 2010). In addition, fullerenes are used in environmental remediation, for pathogen decontamination (Mauter and Elimelech, 2008) and in energy systems such as in organic solar cells (Shrotriya et al., 2006; Yuan et al., 2011) where fullerene derivatives are added as acceptor molecules to a conducting polymer to create a donor/acceptor material (Anctil et al., 2011). However, some the health-adverse aspects of fullerenes carried on rats (i.e., oxidative damage to liver and lungs and oxidative stress to the brain) have been reported, debated and opposed since the early 1990s (Aschberger et al., 2010).

The buckyballs are insoluble in water but they form colloidal suspensions or aggregates that are stable in aqueous environments (Andrievsky et al., 1995; Chen and Elimelech, 2006). For instance, when placing C_{60} into an aqueous media, the fullerene molecule arranges in an icosahedral water cluster because the size of fullerene molecule and the inner diameter of the

water cluster are similar (Figure 7). These water-fullerene clusters have acidic properties due to an acid-base reaction by electron-donor-acceptor complexation between the water and fullerene sp^2 carbons, resulting in a negatively charged surface which increases the solubility of C_{60} in more than eight orders of magnitude (Isaacson et al., 2009). Furthermore, these spherical water-fullerene clusters aggregate into larger irregular shaped structures, with sizes up to 5 μm (Brant et al., 2005; Lyon et al., 2006).

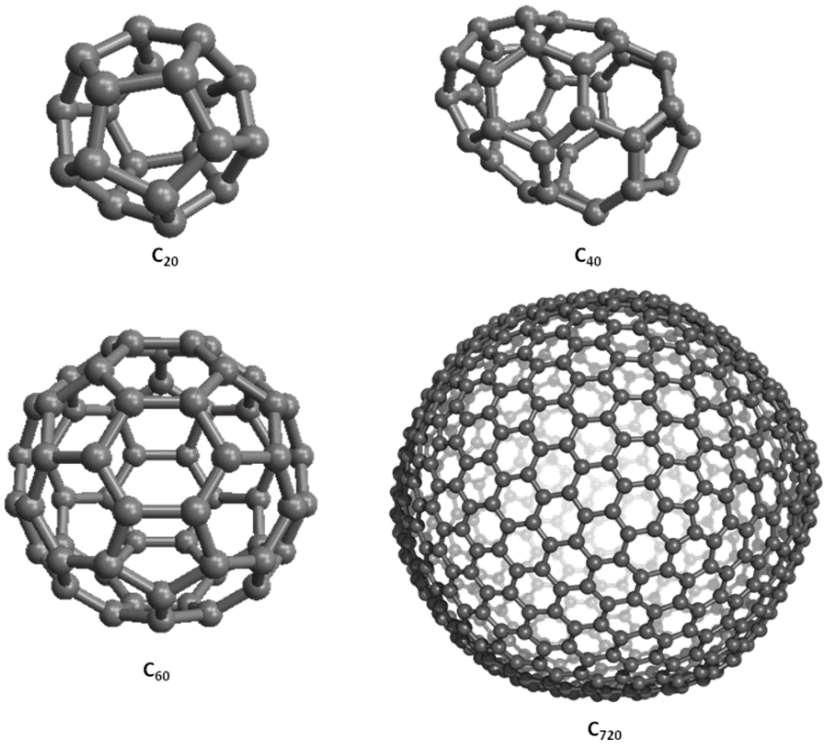

Figure 6. Structures of C_{20}, C_{40}, C_{60} and C_{720} fullerene (Tomanek, D. and Frederick, N., 2015).

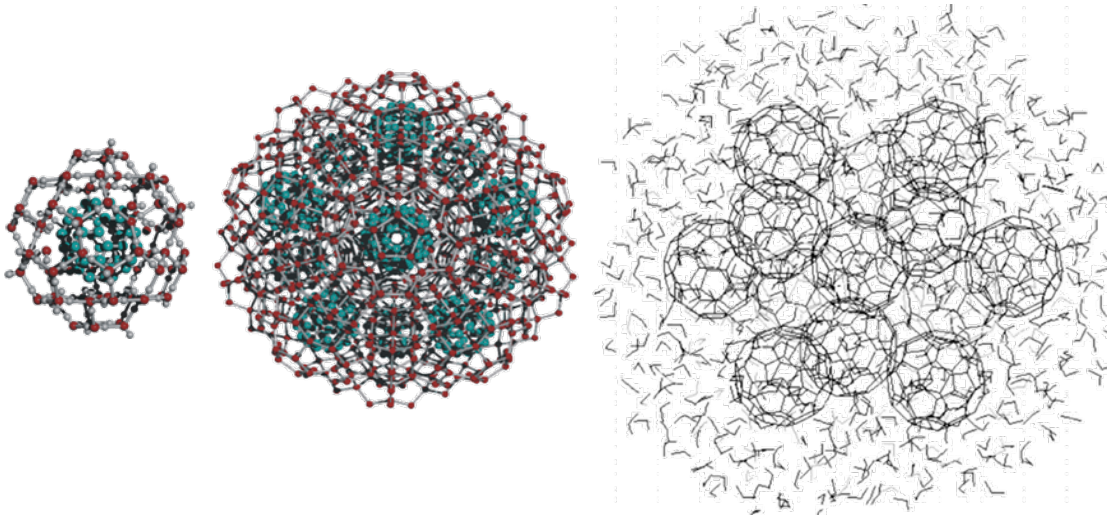

Figure 7. Single water-fullerene cluster, aqueous fullerene cluster (modified after Chaplin M., 2015) and fullerene aggregates (right). Reprinted with permission from (Andrievsky et al., 2002). Copyright (2002) Elsevier.

The colloidal stability of fullerenes depends on their physicochemical properties within the given aqueous medium and is ultimately reflected in the particles aggregation and deposition behaviour. Assessing the risks posed by them requires a better understanding of their mobility, bioavailability, and toxicity. Additionally, fullerene compounds can have very different properties depending on the functionalisation or the synthesis and cleaning method which will also have important implications for assessing their environmental behaviour.

In order to understand the behaviour of fullerenes in both, consumer products and environmental matrices, and also their fate and toxicity to humans, reliable methods for their quantitative and qualitative analysis are required. To accomplish this, access to robust analytical methodologies is essential for detecting and characterising fullerene nanoparticles in a wide range of matrix types.

The most commonly used methods for the size measurements of fullerenes (particle size, size distribution, shape, degree of aggregation, etc.), the effect of sampling and sample treatment on these characteristics and the analytical methods proposed for their determination in complex matrices are discussed in the review included below entitled: *"Characterisation and determination of fullerenes: A critical review"*.

CHAPTER 1

INTRODUCTION

1.3.1. Scientific article I: Characterisation and determination of fullerenes: A critical review

A. Astefanei, O. Núñez and M.T. Galceran

Analytica Chimica Acta **882**: 1–21 (2015).

Analytica Chimica Acta 882 (2015) 1–21

Contents lists available at ScienceDirect

Analytica Chimica Acta

journal homepage: www.elsevier.com/locate/aca

Review

Characterisation and determination of fullerenes: A critical review

Alina Astefanei [a], Oscar Núñez [a,b], Maria Teresa Galceran [a,*]

[a] Department of Analytical Chemistry, University of Barcelona, Martí i Franquès 1-11, E08028 Barcelona, Spain
[b] Serra Hunter Fellow, Generalitat de Catalunya, Spain

HIGHLIGHTS

- Methodologies for fullerene aggregate characterization are discussed.
- Chromatographic and electrophoretic techniques for fullerene analysis are presented.
- Accurate identification and detection of fullerenes by LC–MS are critically reviewed.

GRAPHICAL ABSTRACT

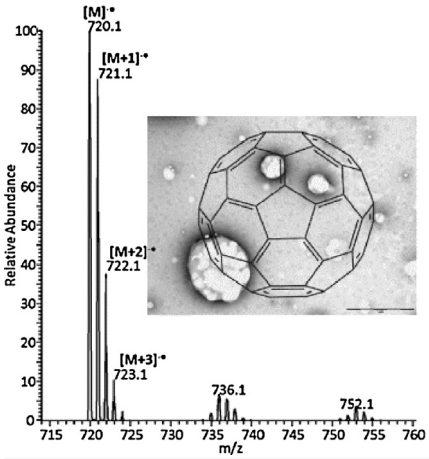

ARTICLE INFO

Article history:
Received 22 December 2014
Received in revised form 13 March 2015
Accepted 16 March 2015
Available online 25 March 2015

Keywords:
Fullerenes
Aggregates
Particle size and shape analysis
Identification
Detection and quantitation
Complex matrices

ABSTRACT

A prominent sector of nanotechnology is occupied by a class of carbon-based nanoparticles known as fullerenes. Fullerene particle size and shape impact in how easily these particles are transported into and throughout the environment and living tissues. Currently, there is a lack of adequate methodology for their size and shape characterisation, identification and quantitative detection in environmental and biological samples. The most commonly used methods for their size measurements (aggregation, size distribution, shape, etc.), the effect of sampling and sample treatment on these characteristics and the analytical methods proposed for their determination in complex matrices are discussed in this review. For the characterisation and analysis of fullerenes in real samples, different analytical techniques including microscopy, spectroscopy, flow field-flow fractionation, electrophoresis, light scattering, liquid chromatography and mass spectrometry have been reported. The existing limitations and knowledge gaps in the use of these techniques are discussed and the necessity to hyphenate complementary ones for the accurate characterisation, identification and quantitation of these nanoparticles is highlighted.

© 2015 Elsevier B.V. All rights reserved.

Abbreviations: C_{60}-pyrr, C_{60} pyrrolidine; PCBM, [6,6]-phenyl-C_{61}-butyric acid methyl ester; bis-PCBM, [6,6]-bis-phenyl-C_{61}-butyric acid methyl ester; C_{70}-PCBM, ([6,6]-phenyl-C_{71}-butyric acid methyl ester; PCBB, [6,6]-phenyl-C_{61}-butyric acid butyl ester; ThCBM, [6,6]-thienyl-C_{61}-butyric acid methyl ester; PCMO, [6,6]-phenyl-C_{61}-butyric acid octyl ester; MSAD-C_{60}, bis(monosuccimide) derivative of *p,p′*-bis(2-aminoethyl)diphenyl-C_{60}.

* Corresponding author. Tel.: +34 93 402 1275; fax: +34 93 402 1233.
E-mail address: mtgalceran@ub.edu (M.T. Galceran).

http://dx.doi.org/10.1016/j.aca.2015.03.025
0003-2670/© 2015 Elsevier B.V. All rights reserved.

Contents

1. Introduction . . . 2
2. Characterisation of fullerenes . . . 4
2.1. Effect of the preparation method on the morphology and size distribution of fullerene aqueous suspensions . . . 5
2.2. Effect of the composition and characteristics of the aqueous media on fullerenes aggregation behaviour . . . 7
3. Determination of fullerenes . . . 11
3.1. Separation . . . 11
3.1.1. Liquid chromatography . . . 11
3.1.2. Capillary electrophoresis . . . 13
3.2. Detection . . . 14
4. Analysis of complex matrices . . . 15
4.1. Sampling and sample treatment . . . 15
4.2. Identification, quantitation and detected levels . . . 16
5. Conclusions and future trends . . . 17
Acknowledgements . . . 18
References . . . 18

Alina Astefanei is a Ph.D. student at the Department of Analytical Chemistry of the University of Barcelona. Her research concerns the emerging and exciting field of fullerene nanoparticles. She has been working with liquid chromatography, capillary electrophoresis, flow field flow fractionation and mass spectrometry for the analysis and characterisation of these compounds. The unique features and versatility of the research topic demanded her to investigate a wide range of different techniques exploring and combining them to enhance the understanding of the benefits and risks of these compounds. She has reported her results in leading international journals and international conferences.

M. Teresa Galceran is professor of Analytical Chemistry at the University of Barcelona since 1990. She was vice-chancellor of this university from 1978 to 1986. She mainly works in Separation Techniques and in Mass Spectrometry, especially in the coupling of both techniques. She has been involved in the introduction of these techniques in the curriculum of Analytical Chemistry in Spain. In the last 10 years she has published more than 130 scientific papers in international journals. She is the head of a research group named "Chromatography, capillary electrophoresis and mass spectrometry" of the University of Barcelona.

Oscar Núñez is an associate professor (Serra Húnter Fellow, Generalitat de Catalunya, Spain) working in the chromatography, capillary electrophoresis and mass spectrometry group at the Department of Analytical Chemistry (University of Barcelona). With more than 50 scientific papers and book chapters, and one co-edited book to his name, he has been working for several years on the development of capillary electrophoresis, liquid chromatography, mass spectrometry, and high resolution mass spectrometry methods for the analysis of environmental and food samples.

1. Introduction

The carbon nanotechnology era was born with the discovery of C_{60}: Buckminsterfullerene by Kroto et al. [1] named after the architect Buckminster Fuller who designed geodesic domes in the 1960s. C_{60} and other clusters with a variable number of carbon atoms were produced by carbon vaporization from graphite into a high-density helium flow using a pulsing vaporization laser. The discovery of fullerenes, the third carbon allotrope, resulted in the award of the Chemistry Nobel Prize to Curl, Kroto and Smalley in 1996. Their structure is composed of closed carbon cages formed by 12 pentagons and a number of hexagons that increases with the size of the fullerene ($[(2n/2) - 10]$, n = number of C atoms). Fig. 1 shows the structure of C_{60}, C_{70}, and of two surface modified fullerenes.

The sources of nanomaterials in the environment can be natural (*e.g.*, forest fires and volcanoes and anthropogenic (*e.g.*, fossil fuel combustion and engineered nanomaterials). However, it is very difficult to distinguish between carbon nanoparticles of engineered origin and those from other, natural or anthropogenic, sources [2]. The labelling of engineered nanomaterials using fluorescent, radioactive-labelling and entrapment of rare elements could be useful for this purpose [3,4].

Despite the fact that fullerenes are very hydrophobic with very low solubility in water, around 8 ng L^{-1} for C_{60} [5], several methods have been developed to disperse these compounds in aqueous media [6–13] leading to the formation of stable colloidal aggregates (nC_{60}), a highly hydrophilic supramolecular complex consisting of C_{60} enclosed into a hydrated shell containing 24 water molecules: $C_{60}@(H_2O)_{24}$. The aqueous suspensions of nC_{60} are amber colored and are stable for months to years at very low ionic strength [14,15]. To increase the solubility in water, fullerenes surface chemical derivatisation with polar functional groups has been performed [16–18]. A large number of derivatives that combine the desirable properties of C_{60} with the solubilising power of the side chains have been produced. One common example is the fullerol molecule ($C_{60}(OH)_{24}$), a water soluble compound obtained by the addition of hydroxyl groups to the C_{60}

A. Astefanei et al./Analytica Chimica Acta 882 (2015) 1–21

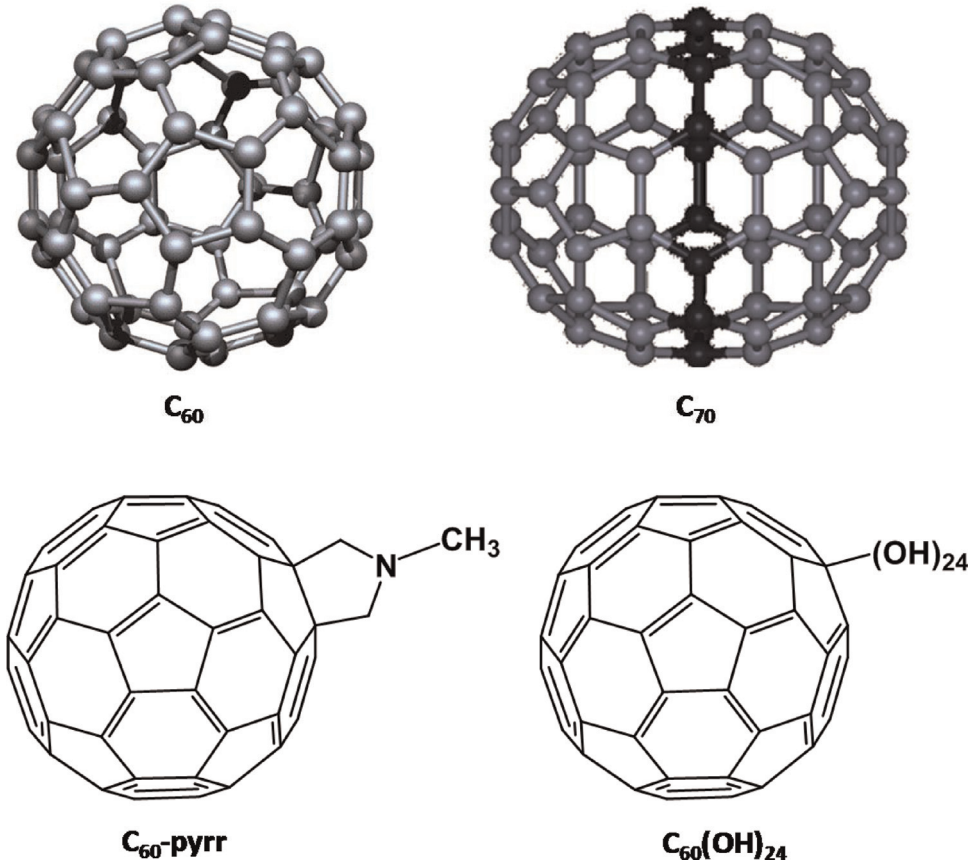

Fig. 1. C_{60}, C_{70}, C_{60}-pyrr and $C_{60}(OH)_{24}$ structures.

cage. However, even with very polar functional chains, fullerenes undergo aggregation since the spheres agglomerate forming micelle-like aggregates [19].

Today, fullerenes and surface functionalised fullerenes are used in optical, electronic, cosmetic, and biomedical applications [20–26] and in the last past years surface-functionalised fullerenes have been produced in larger quantities than pristine fullerenes [27–29] in an attempt to create more biologically compatible forms [28–30]. After the discovery of C_{60}, the formation of the endohendral fullerene La@C_{60}, proved for the first time that the interior space of fullerenes can host atoms or molecules [31]. These materials display remarkable electronic and structural properties associated with the charge transfer from the encaged metal or cluster to the carbon cage. During the past decade, intense research lead by several worldwide groups has allowed the inclusion of a variety of atoms and small molecules inside carbon cages, such as metallic nitrides [32], carbides [33], sulphides [34,35] and up to three individual metal atoms [36,37]. The new properties of metallofullerenes expand their applications in biomedicine and material sciences fields [38,39].

The need for an understanding of health and ecological risks of nanotechnology was recently stressed by the EU commission and by the US Environmental Protection Agency. Within the context of the European Registration, Evaluation, Authorisation and Restriction of Chemicals (REACH) regulation (EC) 1907/2006 a specific approach for manufactured nanoparticles (MNPs) is under discussion [40] and the European Parliament resolution on (2008/2208(INI)) also calls for legislation to adequately address nanomaterials [41]. Hence, the analysis of these particles is not only a social concern but also a legal necessity. The anticipated market growth of fullerenes in combination with the potential for direct human exposure *via* several applications [23] has led to widespread concerns about the possibility to cause adverse effects on human health. However, their effects on humans and the environment are poorly understood and there are conflicting reports on their hazard. Risk assessment is necessary in order to produce and use these materials in a responsible and sustainable way.

Early toxicity studies of fullerenes have been focused on the colloidal form of C_{60} (nC_{60}) [42,43]. Some reports indicate that pristine fullerenes are non-toxic, and that fullerene water systems have a wide spectrum of positive and unique biological activities [44]. For instance, there are studies showing that water-soluble fullerenes scavenge reactive oxygen species (ROS) in human skin cells [45] and that they are powerful antioxidants with no acute or sub-acute toxicity [46]. Fullerenes ecotoxicological studies present a major difficulty because of their poor aqueous solubility [47]. The properties and reactivity of fullerenes are affected by the solubilisation method and organic solvent used [6,7]. The choice of a dispersant is problematic, since some of the best dispersants from a chemical point of view are also likely to be toxic to organisms. For example, tetrahydrofuran (THF) is a good dispersant for C_{60} fullerenes in water but there are concerns about its toxic effects [15,48]. Henry et al. [49] showed that C_{60} toxic results in zebra fish were attributable to THF metabolites inadvertently formed during the dispersion in THF and this was further confirmed in subsequent research [50]. Regarding the potential toxicity of other fullerenes, Seda et al. [51] reported that aqueous colloidal suspensions of gallic acid-stabilized C_{70} reduce significantly the fecundity in *Daphnia magna*.

In general the water soluble C_{60} derivatives are less toxic than nC_{60} and the toxicity decreases with the number of polar functional

groups attached to the C_{60} molecule [52]. Moreover, several positive effects of fullerene derivatives have been described. For example, surface modified fullerenes with pyrrolidine groups showed antibacterial effect and inhibit cancer cell proliferation [53] and polyhydroxyfullerenes are good candidates for the treatment of neuro-degenerative disorders (*e.g.*, Parkinson's and Alzheimer's disease) [54]. However, some studies indicated that polyhydroxy fullerenes show oxidative eukaryotic cell damage [55] and Roberts et al. [56] found that fullerol is both cytotoxic and phototoxic to human lens epithelial cells. Although its acute toxicity was proved to be low, fullerol is retained in the body for long periods [57], raising concerns over its chronic toxic effect.

Several reviews have been published on methods for the characterisation of nanomaterials (*e.g.*, size, surface charge, surface area) [3,58], their occurrence and behaviour in the environment [59,60], the potential risk that fullerene nanoparticles pose to the environment and human health [61,62] and the chromatographic separation and quantitative analysis of fullerenes in environmental samples [63–65]. The accurate analysis of particles involves their detection, identification, quantitation and detailed characterisation and each step is an individual challenge in complex and heterogeneous samples. There is a lack of specific analytical methods for fullerenes and especially for functionalised fullerenes which are produced nowadays in larger amounts. The general aim of this review is to provide an overview of the techniques available for the physicochemical characterisation, and for the detection and quantitation of fullerenes. As limited studies have been carried out on real samples, the principal challenges in method development for their characterisation and analysis in complex matrices will be discussed. Given the broad range of particle properties that have to be taken into account, the need for combining complementary techniques for a better understanding of the behaviour and fate of these particles in the environment is highlighted.

2. Characterisation of fullerenes

Fullerene nanoparticles challenge the limits of colloidal science due to their small size, variable shape, structure, composition and potential interaction with organic molecules. One of the most prominent physicochemical properties of these compounds is their tendency to undergo aggregation, leading to the formation of clusters with various shapes and sizes. Knowledge of the aggregation degree, size distribution and shape of fullerenes is crucial for toxicity assessment and to track their transport and fate in the environment [66,67]. In industrial processes the particle size distribution has a critical effect on the quality and performance of the final manufactured product. Up to now, no ideal technique has been found for characterising fullerenes and there are very few reports on their size distribution behaviour in complex matrices [13,68–70].

In Table 1, the techniques most commonly used for the characterisation of nanoparticles and the measured properties (*i.e.*, size, shape, aggregation, and specific surface area) are summarized. The most popular tools to study the size and morphology of particles are microscopic techniques: transmission electron microscopy (TEM), scanning electron microscopy (SEM) and atomic force microscopy (AFM). Of the three techniques, TEM provides the highest magnification power covering the widest size range (0.1–1000 nm) and can supply detailed information on particles structure.

High-resolution TEM (HRTEM) has been used to investigate the individual C_{60} fullerene morphology, crystallography, and microstructure. For instance, Goel et al. [71] reported a crystalline structure for C_{60} in toluene with a diameter of about 0.7 nm, and a two-fold symmetry. Smith et al. [72] and Sloan et al. [73] reported HRTEM images of round closed shells of fullerenes with diameters smaller and larger than C_{60} (0.4–1.6 nm) encapsulated within the hollow central region of individual single walled carbon nanotubes (SWCNTs) [72,73] and Burden and Hutchison [74] provided real-time evidence of C_{60} and C_{70} formation on the surface of carbon black particles irradiated with an electron beam. However, TEM produces a high level of sample perturbation because the grids must be dried prior to imaging and the particles are likely to aggregate to some degree. Thus, it does not guarantee the original integrity of the particles and aggregates.

For the determination of the size distribution of particles in a fluid, dynamic and static light scattering (DLS and SLS, respectively), covering a size range between 10 and 1000 nm, are the most commonly used techniques. These methodologies enable the study of the stability, degree of aggregation, complex formation and conformation of molecules, and moreover, the sample can be recovered at the end of the measurement. DLS was used to study fullerene particle sizes in several organic solvents and binary solvent mixtures showing that they form aggregates of different sizes depending on the solvents used [75,76]. Light scattering techniques are usually combined with microscopic ones and more recently coupled to flow field-flow fractionation (flow FFF) for both characterisation and separation of particles in aqueous solutions. Flow-FFF is a powerful tool for both the characterisation and separation of aggregates over a wide size range (1–1000 nm). Since the separation occurs in a channel which does not contain a stationary phase as in liquid chromatography, there is no mechanical or shear stress applied to the sample components. Asymmetric flow-FFF (AF4) coupled to light scattering techniques has been reported for the determination of the size distribution of fullerene aggregates [77–79]. For instance, AF4 coupled to DLS was used for the characterization of aqu/C_{60} aggregates reporting sizes between 80 and 260 nm [78] and to multi angle light scattering (MALS) for the determination of the size distribution of aqu/nC_{60} and that of two C_{60}-derivatives [79] presenting radii of gyration (R_g) values from 20 to 80 nm. It must be noticed that the R_g radius obtained by MALS is different from the DLS hydrodynamic radii, thus these values cannot be compared.

Additionally, asymmetric flow-FFF combined with AFM was proposed to study the morphology and aggregate sizes of fullerol nanoparticles obtaining sizes of approx. 2 nm [80]. AFM allows the observation of particles in their natural environment with atomic resolution over a wide size range (0.5–1000 nm) and

Table 1
Nanoparticle characterisation techniques.

Method	Measured property	Approximate size range (nm)	Level of perturbation
TEM, SEM	Size (r_H), degree of aggregation, morphology	0.1–1000	High
AFM	Size and morphology	0.5–1000	Minimum
DLS, SLS	Size distribution (r_H,R_g) and degree of aggregation	10–1000	Minimum
Flow FFF	Size separation (r_H)	1–1000	Low
NTA	Size distribution, degree of aggregation, zeta potential and concentration	10–2000	Minimum
BET	Surface area and porosity	1–1000	High

r_H: hydrodynamic radius; R_g: radius of gyration.

Table 2
Preparation methods of fullerene aqueous suspensions.

Preparation method		Ref.
Abbreviation	Procedure	
Krätschmer method	A solution of C_{60} and C_{70} (ratio 10:7) in toluene is added to water and subjected to sonication until the complete evaporation of toluene, then filtered (0.22 μm).	[8]
Hand ground C_{60}	Hand ground C_{60} is added to pure water and sonicated or stirred for 1 day and then filtered (5 μm).	[12]
Hand ground C_{60} with SDS	Hand ground C_{60} is mixed with SDS in water followed by ultrasonic treatment (30 min), and subsequent filtration (5 μm).	
Toluene and ethanol	A solution of C_{60} in toluene is added to water and ethanol mixture. The solution is sonicated for 3 h to evaporate the toluene and ethanol, filtered through 0.45 μm/0.22 μm.	[11]
THF/nC$_{60}$	C_{60} is added to THF, stirred (overnight) and the excess filtered through 0.45 μm filter. Water is added to this solution and then purged with nitrogen to remove the THF. The solutions are filtered (0.45 μm/0.22 μm).	[6,7,10,13,15]
TTA/nC$_{60}$	C_{60} in toluene is added to THF and acetone. Then water is added slowly and then the solvents are evaporated and the solutions filtered (0.45 μm/0.22 μm).	[6,7,14,82]
SON/nC$_{60}$	C_{60} in toluene solution is mixed with water (sonication for several hours). After the evaporation of toluene the solutions are filtered (0.45 μm/0.22 μm).	[6,13]
PVP/nC$_{60}$	PVP in chloroform is added to C_{60} in toluene and stirred/sonicated at 45 °C/25 °C for several hours until the solvents evaporated and then is suspended in water and filtered (0.45 μm/0.22 μm or 0.1 μm).	[13,87,88]
Aqu/nC$_{60}$	C_{60} powder is added to water, stirred for several weeks and then filtered (0.45 μm/0.22 μm).	[6,7,13]

preserves their original morphology. Moreover, this technique gives true 3-dimensional information even in water and in contrast to electron microscopy, specimen preparation is less constringent.

Nanoparticle tracking analysis (NTA) is a laser technique able to simultaneously visualise and determine the particle size distribution and concentration of particles in liquids from 10 to 1000 nm (depending on the material). Recently, Sanchis et al. [70] used NTA for the analysis of fullerenes in river water samples, reporting the presence of C_{60} and C_{70} as both colloidal fractions (<450 nm) and large agglomerates (<450 nm). The Brauner, Emmett and Teller (BET) method is also used as an additional tool for the specific surface area and porosity determination of the particles. Recently, thermal-lens spectrometry, a method suitable for optical and thermophysical studies, was used for the characterisation of fullerene aqueous suspensions confirming the formation of large clusters (>130 nm) [81].

2.1. Effect of the preparation method on the morphology and size distribution of fullerene aqueous suspensions

Despite its hydrophobic structure, C_{60} can be solubilised in water forming stable suspensions whose properties differ from those of bulk solid C_{60} [8]. Several procedures were reported (Table 2), mostly involving the solubilisation in water by solvent exchange using different organic solvents (ethanol, toluene, THF and acetone) *via* sonication or mechanical stirring [6,8,10–15,82]. Additionally, the direct solubilisation of C_{60} in water was also reported *via* sonication [12] or extended stirring [13–15]. The preparation conditions vary from one study to another in terms of stirring rate, sonication power, time used for sonication and/or stirring, amount of organic solvent and the filtration step.

Several studies have investigated the characteristics of nC$_{60}$ formed *via* direct addition of C_{60} to water (aqu/nC$_{60}$) and by solvent exchange [6,7,10,13,68]. In most of the works several

Table 3
Effect of the preparation method on the formed aggregates.

Preparation method	Methodology used for characterisation and results				Ref.
	TEM	SLS	DLS	Zeta potential (mV)	
TTA/nC$_{60}$ (unfiltered)	Hexagonal shapes with faceted edges (100–200 nm)	170 ± 20 nm R_g: 57.22 nm	Average size: 237 nm (unfiltered)	0.01–100 mM NaCl: −31 to −4	[6]
SON/nC$_{60}$ (sonication for 3 h) Unfiltered and filtrated solutions (0.45 μm)	Spherical particles (5–86 nm)	160 ± 20 nm R_g: 57.87 nm	Average size: 277 nm (unfiltered and filtered)	0.01–100 mM NaCl: −34 to −16	
THF/nC$_{60}$ (12 h stirring) Unfiltered and filtrated solutions (0.45 μm)	Spherical particles (≤50 nm) and elongated aggregates (≈200 nm)	160 ± 20 nm R_g: 70.47 nm	Average size: 271 nm (filtered); 300 nm and 5 μm (unfiltered)	0.01–100 mM NaCl: −52 to −26	
Aqu/nC$_{60}$ (stirring for 2 weeks at 500 rpm) Unfiltered and filtered solutions (0.45 μm)	Spherical particles and random shaped aggregates (20–500 nm)	180 ± 20 nm R_g: 80.10 nm	Average size: 357 nm (filtered); 300 nm and 5 μm (unfiltered)	0.01–100 mM NaCl: −32 to −17	
SON/nC$_{60}$ (sonication at 80–100 W for 15 min)	Spherical particles (10–25 nm)		Average size ≈2 nm[a] (small and large)		[13]
THF/nC$_{60}$ (12 h stirring and heated at 60 °C)	Random shapes (hexagonal, tubular, square) (50–150 nm)		Average size: 74.6 nm Small: 39.1 nm Large: 97.4 nm		
Aqu/nC$_{60}$ (Stirring for 2–4 weeks at 1000 rpm and filtered (0.45 μm and 0.22 μm)	Spherical and elongated shapes (30–100 nm)		Average size: 74.9 nm Small: 2 nm[a] Large: 142.3 nm		
PVP/C$_{60}$	Spherical and uniform particles (10–25 nm)		Average size ≈2 nm[a] (small and large)		

R_g: radius of gyration.
[a] Bellow DLS detection limit.

characterisation techniques were used in order to increase the amount of information available. Microscopy provides a basis for comparison and is suitable for elucidating particle shape and to some degree aggregate structures but cannot provide information about the size distribution of the aggregates. Hence, for the accurate knowledge of the morphology, aggregation state and size distribution of fullerenes in aqueous solutions, other techniques and mostly light scattering (LS) must be also used [6,7,10,11,15,63,83–86]. For instance, Brant et al. [6] investigated the characteristics of nC_{60} obtained using four different preparation procedures by TEM, DLS and SLS (Table 3). The authors studied and compared the sizes and shapes of the nC_{60} obtained using three solvent exchange methods (SON/nC_{60}, THF/nC_{60}, TTA/nC_{60}) (Table 3) and by extended mixing of C_{60} with pure water (aqu/nC_{60}). DLS measurements (Fig. 2a) showed that the different preparation procedures produced suspensions of nC_{60} with similar size distributions, (50–2000 nm) but with important differences in the size distribution (Fig. 2b). Also, TEM micrographs showed differences in the size, shape and structure of the nC_{60} formed (Fig. 3). For instance, homogeneous hexagonally shaped structures were found for TTA/nC_{60} and heterogeneous spherical and large elongated aggregates were obtained by mechanical mixing (THF/nC_{60}) and sonication (SON/nC_{60}), respectively. The aqu/nC_{60} suspensions were highly polidisperse in size (20–500 nm) appearing as small spherical aggregates and large blunt-angular random structures. Lyon et al. [13] also studied the size and morphology (Table 3) of nC_{60} aggregates obtained by four different preparation techniques (THF/nC_{60}, SON/nC_{60}, aqu/nC_{60} and PVP/C_{60}) using TEM and DLS. TEM micrographs showed more rounded edges and less crystallinity for aqu/nC_{60} compared to the other suspensions in agreement with Brant et al. [6]. The DLS average sizes of the THF/nC_{60}, SON/nC_{60} and aqu/nC_{60} suspensions obtained in this study are significantly lower (2–142 nm) than those given by Brant et al. [6] (237–354 nm) although the same preparation methods were used (Table 3). The different results obtained with the same technique can be due to the use of different filter sizes for the filtration of the suspensions prior to the analysis, 0.22 μm [13] and 0.45 μm [6], respectively. Besides, the differences in the operation conditions such as stirring/sonication time and power used in each study could also explain the differences in the characteristics of the aggregates formed. Lyon et al. [13] also evaluated the effect of the size and morphology on the antibacterial activity of nC_{60} toward the Gram-positive bacterium *Bacillus subtilis* and observed that the smaller aggregates with higher surface areas showed the highest level of antibacterial activity. However, it is unclear whether this behaviour can be attributed to the smaller size or to the presence of an amorphous structure. Even though, the observed bactericidal effects of nC_{60} suggest the need for caution against accidental releases and disposal of fullerenes.

The radical scavenging properties of fullerene C_{60} aggregates stabilised by poly(vinylpyrrolidone) (PVP/nC_{60}) reported by various research groups [13,87,88] have led cosmetic manufacturers to use this nanomaterial as skin 'anti-aging' and whitening [89–91]. Dadalt Souto et al. [88] studied the characteristics of PVP/nC_{60} suspensions that can affect the distribution and interaction with the skin and its dermal absorption profile by NTA, TEM and DLS since the size distribution of the particles is considered a key parameter in determining its interactions with living systems [92]. The size distributions determined by DLS and NTA were in agreement (116 ± 18 and 129 ± 54, respectively) and TEM micrographs showed polydisperse samples with irregular shapes and sizes between 100 and 200 nm. Moreover, NTA measurements indicated that only 2.7% of fullerene aggregates were smaller than 40 nm, value that can be correlated with the skin pores (0.4–36 nm) meaning that most of the PVP/C_{60} aggregates will not penetrate the skin. Nevertheless, some concerns about the utilisation of cosmetic formulations containing PVP/nC_{60} still remain because the short- and long-term exposure effects of fullerenes on the skin are not well known yet.

It is clear that many characteristics of the aggregates are dependent upon the preparation method and this makes difficult to reach conclusions about the risks associated with the release of fullerenes into the environment. The lack of standardised procedures for fullerene characterisation makes difficult the comparison of the results reported in the literature on various samples and obtained by different techniques limiting the advance of research in this field. The aggregates formed in the environment will probably be more similar to aqu/nC_{60} than to aggregates produced *via* solvent exchange methods, but little research has been conducted on this form. Studies on the formation and behaviour of aqu/nC_{60} in aqueous solutions with different properties are essential to help the understanding of the fate of fullerenes upon release in the environment and represent crucial advances in this field.

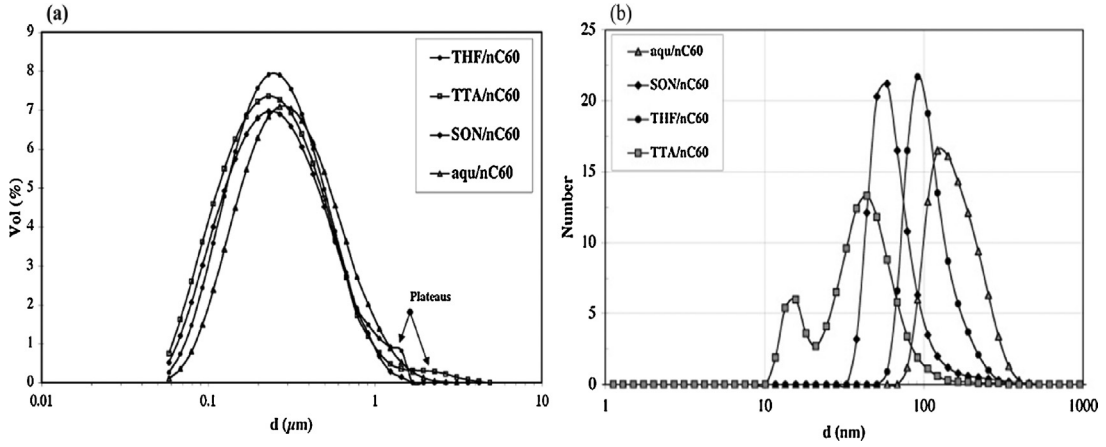

Fig. 2. (a) Intensity-weighted size distributions for the nC_{60} suspensions produced using the four different techniques by DLS (pH) 5.6, (*T*) 20 °C. The *x*-axis is plotted on a semilogarithmic scale for clarity; (b) number-weighted size distributions for the nC_{60} suspensions produced using the four different techniques by SLS (pH) 5.6, (*T*) 20 °C. A refractive index of 2.20 was used for the nC_{60}. The *x*-axis is plotted on a semilogarithmic scale for clarity. Reprinted with permission from Ref. [6]. Copyright (2006) American Chemical Society.

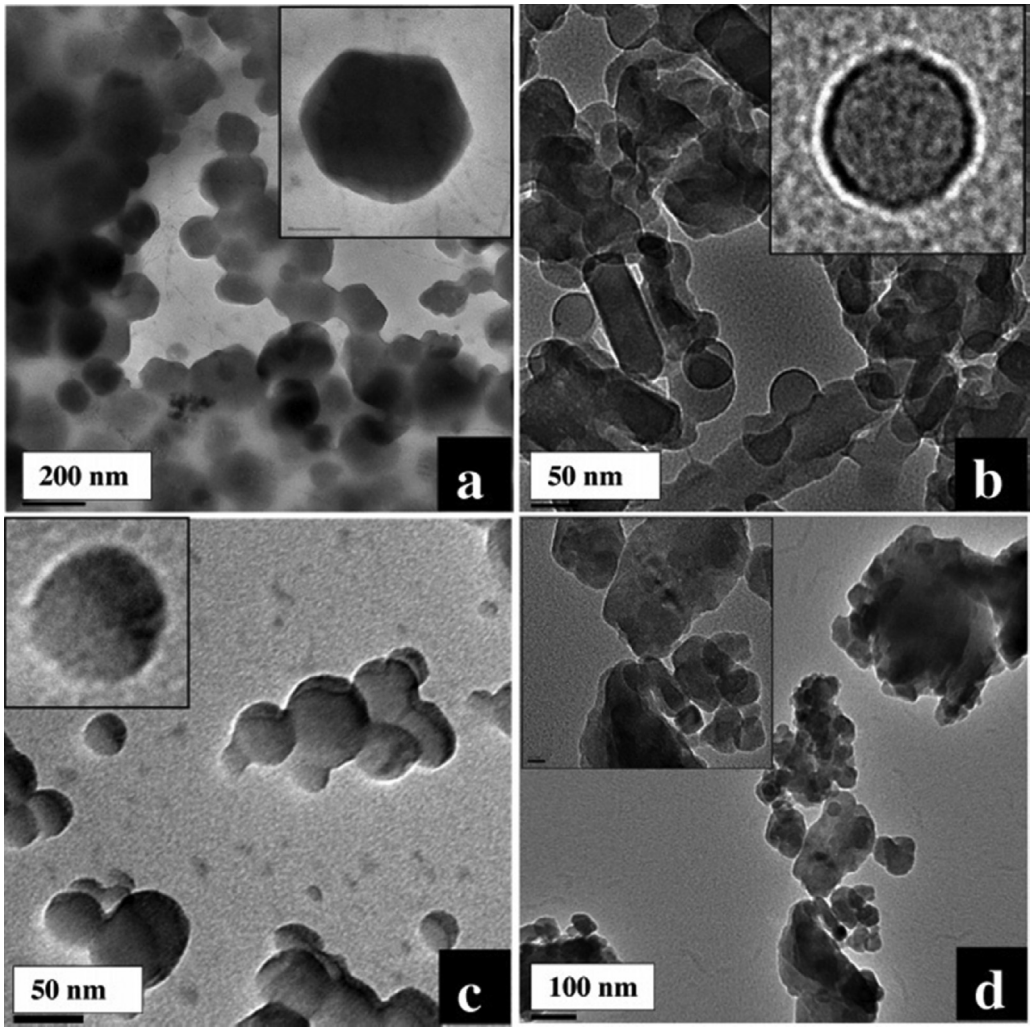

Fig. 3. Representative TEM images of the (a) TTA/nC_{60}, (b) THF/nC_{60}, (c) SON/nC_{60}, and (d) aqu/nC_{60} (pH) 5.6 suspensions. The insets in each figure are magnifications of the respective nC_{60} clusters. Reprinted with permission from Ref. [6]. Copyright (2006) American Chemical Society.

2.2. Effect of the composition and characteristics of the aqueous media on fullerenes aggregation behaviour

The mobility and toxicity of fullerenes in the environment will depend on the colloidal stability of the formed aggregates. To evaluate the health and environmental risks posed by fullerenes, not only the formation of aggregates but also their stability in natural systems needs to be understood in order to predict their sedimentation rate and to be able to find strategies for their removal. The aggregation of these particles into large clusters will reduce their ability to be transported or to come into contact with aquatic organisms. Knowledge of the stability, mobility and aggregation behaviour of fullerenes as a function of matrix composition, pH and ionic strength will allow us to gain an insight into their potential behaviour when released into the environment. Several studies have been carried out for this purpose for aqu/nC_{60} [6,7,10,15,68,84,85,93], aqu/nC_{70} [84] and also for some functionalised fullerenes [80,84].

Independent reports have shown that aqueous fullerene suspensions are negatively charged exhibiting a negative electrophoretic mobility [6,7,10]. Among them, Brant et al. [6] studied the effect of the ionic strength (NaCl solutions from 0.01 to 100 mM) on the surface charge of nC_{60} colloidal solutions prepared by different methods (Table 3). All the nC_{60} colloids obtained displayed negative electrophoretic mobility and negative zeta potentials (ζ) (Table 3) which are similar to the ones of fullerol [7,94]. This indicates that C_{60} acquires a charge through charge transfer from the oxygen atoms of the water and/or the organic solvents and/or hydroxylation of its surface through either adsorption of hydroxyl groups or by "localised hydrolysis" [95].

In general, it is accepted that aqu/nC_{60} will quickly aggregate in natural waters leading to the formation of heteroaggregates settling out of suspension, and as a consequence, reducing its environmental risk [96–98]. However, it has been reported that the presence of natural organic matter (NOM) in waters favours the disaggregation of aqu/nC_{60} causing a significant change in particle size and morphology [85,99,100]. NOM fulvic and humic substances can be attached to the surface of particles in a variety of ways leading to their stabilisation. For instance, Chen and Elimelech [85] reported an effective stabilisation of fullerene nanoparticle suspensions through steric repulsion in the presence of humic acid and at high $CaCl_2$ concentration which lead to a dramatic drop in the rate of aggregation, and to an increase in the critical coagulation concentration (CCC). Moreover, several authors studied the effect of the ionic strength and pH on the degree of aggregation of fullerene in aqueous solutions [7,10,15,80,84,101]. For example, Fortner et al. [15] reported that C_{60} heteroaggregates stay stable for months at low ionic strengths similar to those of most surface waters but the average particle size increased up to 360 nm at an ionic strength of 0.05 and values above 0.1 are high

Table 4
Analysis of fullerenes in complex matrices: chromatographic methods.

Fullerenes	Sample	Extraction, recovery range (%)	Column	Chromatographic conditions	Detection/ quantitation	Detected levels	MLODs/MLOQs	Analysis time	Ref.
C_{60}, C_{70}, PCBM	UPW, surface and ground water (spiked)	LLE with toluene and Mg $(ClO_4)_2$, 89–99%	Cosmosil PYE 150 × 4.6 mm, 5 μm, 120 Å	Toluene:acetonitrile (80:20, v/v) 1.3 mL min^{-1}	UV–vis, 330 and 333 nm External calibration	–	MLODs: 2.9–6.5 μg L^{-1}	6.5 min	[109]
C_{60}	Wastewater, secondary effluent (spiked)	LLE with toluene and NaCl, 88–97%	Cosmosil Buckyprep 250 × 4.6 mm, 5 μm, 120 Å	Toluene (100%) 1 mL min^{-1}	UV–vis, 332 nm Mass spectrometry (−) APCI-MS (single quadrupole) External calibration	–	MLODs (μg L^{-1}): 3–4 (LC–UV); 4–11 (LC–MS).	–	[120]
nC_{60}	UPW, surface water (spiked)	C18-SPE with toluene, 32–42%	Nova-Pak C18 150 × 3.9 mm, 4 μm, 60 Å	Toluene:methanol (50:50, v/v) 1 mL min^{-1} 0.2 mL min^{-1}	UV–vis, 333 nm Mass spectrometry (−) APCI/ESI-MS (LTQ-FT Orbitrap) External calibration	–	MLOD: 5 ng L^{-1}	–	[141]
C_{60}, C_{70}, PCBM, C_{70}-PCBM, bis-PCBM, PCBB, ThCBM, PCBO	UPW, tap water, surface water (spiked)	C18-SPE with toluene and NaCl, >78%	Cosmosil Buckyprep 250 × 2 mm, 5 μm, 120 Å	(A) Toluene; (B) acetonitrile (from 75% to 100% (A)) 0.2 mL min^{-1}	Mass spectrometry (−) ESI-MS (LTQ Orbitrap) External calibration	–	MLODs: 0.17–0.28 ng L^{-1}	30 min	[115]
C_{60}, C_{70}, C_{76}, C_{78},C_{84}	Pond water	UAE with toluene (suspended solids), 80–88%	Hypersil GOLD C18 150 × 2.1 mm, 1.9 μm, 175 Å	Toluene:methanol (45:55, v/v) 0.5 mL min^{-1}	Mass spectrometry (−) APPI-MS (triple quadrupole) Dopant: toluene Matrix-matched calibration	C_{60}: 0.01–0.02 ng L^{-1} C_{70}: 0.01–0.03 ng L^{-1} C_{76}: 1.04 ng L^{-1} C_{84}: 5–19.2 ng L^{-1}	MLOQs: 0.01–5 ng L^{-1}	3.5 min	[144]
C_{60}, C_{70}, PCBO, PCBB, PCBM, bis-PCBM, C_{70}-PCBM, ThCBM	Sewage water	UAE and C18-SPE with toluene, 49–104%	Cosmosil Buckyprep 250 × 2 mm, 5 μm, 120 Å	Toluene (100%) 0.2 mL min^{-1}	Mass spectrometry (−) APPI-MS (LTQ-Orbitrap) External calibration	C_{60}: <0.1–19 ng L^{-1}	MLOQs: 230–1400 pg L^{-1}	–	[154]
C_{60}, C_{70}, C_{60}-pyrr	Wastewater	UAE with toluene (suspended solid), 58–84%	Purospher STAR C18 125 × 2 mm, 5 μm	Toluene:methanol (50:50, v/v) 0.4 mL min^{-1}	Mass spectrometry (−) ESI-MS (QqLIT) External calibration	C_{60}: 0.5–14,400 ng L^{-1} C_{70}: 181–1650 ng L^{-1} C_{60}-pyrr: 60–65,900 ng L^{-1}	MLODs: 1–20 ng L^{-1}	4 min	[143]
C_{60}, C_{70}, PCBM	Surface water, effluent, influent	UAE-LLME with benzyl bromide (extraction solvent), 2 propanol (dispersive solvent) and NaCl, 70–86%	Ascentis Express C18 50 × 2.1 mm, 2.7 μm, 90 Å	Toluene:methanol (50:50, v/v) 0.2 mL min^{-1}	Mass spectrometry (−) APPI-MS/MS (ion trap) Dopant: toluene Standard addition calibration	C_{60}: 56–130 ng L^{-1} C_{70}: 25–83 ng L^{-1}	MLODs: 3–40 ng L^{-1}	2.5 min	[145]
C_{60}, C_{70}, C_{76}, C_{78}, C_{84}, PCBM, PCBB, C_{60}-pyrr	Pond water, sediments	LLE with toluene and NaCl, 83– 96% PLE with toluene, 70–92%	Hypersil GOLD C18 150 × 2.1 mm, 1.9 μm, 175 Å	(A) Toluene; (B) methanol (from 30% to 55% (A)) 0.5 mL min^{-1}	Mass spectrometry (−) APPI-MS (triple	Pond waters (pg L^{-1}): C_{60}: 9–22; C_{70}: 22–330; PCBM: 5.2–8; PCBB: 5; C_{60}-pyrr: 2–8.5 Sediments (ng kg^{-1}): C_{60}: 0.8–1.1;	MLODs: 1.4–1600 pg L^{-1} (pond water), 0.03–	4.3 min	[117]

					quadrupole) Dopant: toluene Matrix-matched calibration	C_{70}: 2.1–7.2; PCBM: 0.15–2.6; PCBB: 0.18–5.1; C_{60}-pyrr: 0.5–2.7	158 ng kg^{-1} (sediments)		
C_{60}, C_{70}	Soils and sediments	UAE with toluene, 72–104%	Luna C18 150 × 4.60 mm, 5 μm, 100 Å	Toluene:acetonitrile (60:40, v/v) 0.75 mL min^{-1}	UV–vis, 334 nm External calibration	Not detected	MLOQs: 0.2–0.3 ng g^{-1}	9 min	[158]
C_{60}, C_{70}	Sediments	UAE with toluene, 80%	Nova-Pak C18 300 × 3.9 mm, 4 μm, 60 Å	Toluene:methanol (40:60, v/v) 2 mL min^{-1}	Uv–vis 310–430 nm External calibration	0.1–11.9 ng g^{-1} C_{60}; C_{70}/C_{60}: 0.2–0.3	MLODs: 0.2–0.3 ng injected	11 min	[155]
C_{60}, C_{70}, C_{60}- pyrr, PCBM, ThCBM	Soils and sediments	UAE with toluene, 35–108%	Purospher STAR RP- 18 125 × 2.0 mm, 5 μm	Toluene:methanol (50:50, v/v) 3 mL min^{-1}	Mass spectrometry (−) ESI-MS (triple quadrupole) External calibration	C_{60}: 0.15–6.83 ng g^{-1}	MLODs: 8.7–290 pg g^{-1}	–	[157]
C_{60}, C_{70}, C_{60}- pyrr, PCBM, ThCBM, C_{70}-PCBM, CPTAE	Soils and sediments	UAE with toluene, 68–106%	Cosmosil Buckyprep, 150 × 2 mm, 120 Å	Toluene (100%) 0.4 mL min^{-1}	Mass spectrometry LC-APPI (−)-HRMS (Q-Orbitrap) Matrix matched calibration	C_{60}, C_{70}: low fg g^{-1}–154 pg g^{-1}	MLODs: 0.02–0.4 pg g^{-1}	10 min	[122]
C_{60}, C_{70}, PCBB, PCMO, PCBM, bis-PCBM,ThCBM, C_{70}-PCBM	Clayish, sandy and lower top-soils (spiked)	UAE and shaking with toluene, 47–71%	Cosmosil Buckyprep 250 × 4.6 mm, 5 μm, 120 Å	(A) Toluene; (B) acetonitrile (from 75% to 100% (A)) 1 mL mmin^{-1}	UV–vis, 305 and 332 nm External calibration	–	MLODs: 6–10 μg L^{-1}	25 min	[124]
C_{60}, C_{70}	Geological materials	UAE and Soxhlet with toluene (demineralisation with HCl and HF), 90%	Nova-Pak C18 3.9 × 300 mm, 4 μm, 60 Å	Toluene:methanol (40:60, v/v) 2 mL min^{-1}	UV–vis, 330 nm External calibration	C_{60}: 2 mg kg^{-1}; C_{70}: 0.68 μg kg^{-1}	–	12 min	[105]
C_{60}, C_{70}, C_{60}- pyrr, CPTAE, PCBM, ThCBM	Airborne particulate	UAE with toluene, 60–71%	Luna C18 (2)-HST 50 × 2.0 mm, 2.5 μm, 100 Å	(A) Toluene; (B) methanol (from 50% to 80% (A)) 0.3 mL min^{-1}	Mass spectrometry (−) ESI-MS (triple quadrupole) Standard addition calibration	C_{60}: 0.03–49.3 ng m^{-3}; C_{70}: 0.08–233.8 ng m^{-3}	MLODs: 5.4–20.9 pg m^{-3}	–	[156]
C_{60}	Plasma (porcine), skin permeable media (bovine serum albumin-BSA)	LLE with toluene, $Mg(ClO_4)_2$ and GAA, 94–100%	Delta Pak C18 150 × 3.9 mm, 5 μm, 300 Å	Toluene:acetonitrile (60:40, v/v) 1 mL min^{-1}	UV–vis, 333 nm External calibration	–	MLOD (ng mL^{-1}): 0.68 (plasma); 0.34 (BSA)	3 min	[150]
C_{60}	Blood, spleen, liver	LLE with toluene, SDS and GAA, 90–103%	LiChrocart C18 20 × 4.6 mm, 5 μm, 100 Å	Toluene:acetonitrile (60:40, v/v) Toluene:acetonitrile (55:45, v/v) Toluene:methanol (55:45, v/v) 1 mL min^{-1}	UV–vis, 333 nm Mass spectrometry (−) APCI-MS (ion trap) Internal standard calibration (C_{70})	–	MLOD: 0.1 ng/injection	6 min	[151]
C_{60}	Embryonic zebrafish homologeate	LLE with toluene (no salt), 90%	Targa C18, 150 × 2 mm, 5 μm, 120 Å	Toluene:methanol (45:55, v/v)	(−) ESI-MS Internal standard calibration ($^{13}C_{60}$)	–	MLOD: 0.02 μg L^{-1}	15 min	[142]
MSAD-C_{60}	Plasma	LLE with ethylacetate, 73–100%	Alltech, Deerfield, Ill C18, 150 × 4.5 mm, 5 μm	5 mM dibasic sodium phosphate–methanol–acetonitrile (35:4:61; v/v), pH 7.5	UV–vis, 270 nm Internal standard calibration (DESD)	7 μg L^{-1} (after 3 h of intravenous administration of 15 mg kg^{-1})	–	15 min	[129]
C_{60}, C_{70}	Cosmetic products	LLE with toluene, $Mg(ClO_4)_2$, and GAA, 96–107% C18-SPE with toluene, 27–42%	Nova-Pak C18 150 × 3.9 mm, 4 μm, 60 Å	Toluene:acetonitrile (55:45, v/v) 1 mL min^{-1}	Mass spectrometry (−) APCI-MS (triple	0.04–1.1 μg g^{-1} (C_{60})	–	6 min	[152]

Table 4 (*Continued*)

Fullerenes	Sample	Extraction, recovery range (%)	Column	Chromatographic conditions	Detection/ quantitation	Detected levels	MLODs/MLOQs	Analysis time	Ref.
					quadrupole) Standard addition calibration				
C_{60}	Cosmetic products	Mechanically mixing with toluene and KCl, 75–86%	Cosmosil Buckyprep 250 × 4.6 mm, 5 μm, 120 Å	Toluene (100%)	UV–vis, 285 nm Standard addition calibration	0.002–0.005% (w/w)	–	–	[121]

UPW: ultra-pure water; DESD: diethylstilbestrol dipropionate.

enough to precipitate the particles after 48–72 h. Moreover, the average particle sizes also depend on the pH, decreasing at high pH values from 120 nm (pH 3.7) to 60 nm (pH 10). Brant et al. [14] also reported the formation of large nC$_{60}$ aggregates with the increase of the ionic strength with average diameters up to 700 nm (0.01 M).

The above mentioned studies combine light scattering techniques with TEM to study the physical and chemical properties of fullerene aggregates. However, as previously mentioned the use of other complementary techniques such as AFM and AF4 has also been reported [77,78,80,99,102]. For instance, AF4 combined with DLS was used to evaluate the effects of sunlight and water composition (NOM) on the size distribution and ζ potential of aqu/C$_{60}$ [99]. The results show that the presence of divalent cations and NOM in the water stabilizes the aqu/nC$_{60}$ nanoparticles leading to sizes lower than the ones observed in deionised water (average sizes of 150–175 nm and 210–230 nm, respectively). Moreover, a decrease in the ζ potential of aqu/nC$_{60}$ with time has been reported under laboratory lighting conditions [84] and under natural sunlight [99]. Thus, the sunlight and the presence of NOM lead to a decrease in the size and zeta potential of aqu/nC$_{60}$ aggregates making them more stable and more available for transport and organism uptake.

Due to the increase in the production and use of functionalised fullerenes their behaviour in aqueous solutions has also been recently evaluated [80,84,94,101]. The studies show that their aggregation is also promoted by the increase of the ionic strength as observed for aqu/nC$_{60}$, but the aggregates present smaller sizes. For instance, Assemi et al. [80] studied by AF4 and AFM the behaviour of a water soluble fullerene compound, C$_{60}$(OH)$_{24}$, in water showing that this compound exist as very small clusters (doublets or triplets) at basic pH and low salt concentration and its ζ potential is not affected by the pH or ionic strength of the solution as usually happens for aqu/nC$_{60}$. However, the size of the particles increased with the ionic strength from 1.2 nm at zero ionic strength up to 6.7 nm at 0.1 M NaCl. These small sizes disagree with the ones previously reported by TEM and DLS techniques (∼100 nm) [94]. This disagreement could be due to the different methodology used for the size measurements of the particles. The above mentioned studies indicate that surface modified fullerenes with polar groups present much smaller particle sizes than pristine fullerenes. Further studies are needed to establish the toxicity of this family of compounds, their fate and transport in the environment.

Although, the source of the negative electrophoretic mobility is not yet well understood, there are evidences that fullerene aggregation behaviour is in agreement with the classic Derjaguin–Landau–Verwey–Overbeek (DLVO) theory of colloidal stability [6,85]. According to this theory, the attractive and repulsive interactions between colloids are dominated by van der Waals forces and electrostatic double layer forces [103]. Ionic strength controls the extent of the radius of the diffuse layer on the surface. At high ionic strength, the electrical double layer is compressed, the van der Waals attractive interactions dominate and particle aggregation is promoted. Dissolved ionic solutes and pH play crucial roles on the aggregation of fullerenes in engineered and natural systems. Seemingly, the factors that will reduce the degree of aggregation of these materials in the environment include a low ionic strength and the presence of humic-like substances. The typical ionic strengths of many natural waters and the presence of polysaccharide-based natural organic matter, which could be produced by algae or bacteria, will tend to favour deposition and reduce the potential for exposure.

The above mentioned studies have demonstrated that the physicochemical transformations acting simultaneously will affect the behaviour of fullerenes in the environment by encountering a multitude of conditions important for aggregation (*e.g.*, pH, ionic strength, NOM). Nevertheless, studies about their aggregation

behaviour and properties in complex matrices are lacking. Further research is needed to gain a full understanding of the aggregation of nanoparticles and how to apply this knowledge for industrial applications and risk assessment.

3. Determination of fullerenes

The current section presents the most commonly used methodologies for the determination of pristine and surface-functionalised fullerenes. For this purpose, the analytical separation and detection techniques are discussed.

3.1. Separation

The separation of fullerenes represents a challenge, especially due to their structure similarities, limited solubility in common solvents and tendency to form aggregates. The most widely employed techniques are liquid chromatography (LC) and capillary electrophoresis (CE) in combination with different on-line detectors (*e.g.*, UV–vis and mass spectrometry). For particle separation, one of the most promising techniques is AF4 coupled to light scattering detection. This technique is suitable for the determination of fullerene aggregate sizes but, to the best of our knowledge, its applicability for the separation of fullerene compounds has not been reported yet.

3.1.1. Liquid chromatography

Among the separation techniques, liquid chromatography (LC) is the most effective and its applicability for the separation of fullerenes has been investigated since the 1990s [104–108]. Table 4 summarizes the LC methods reported in the literature for the analysis of this family of compounds in complex matrices. As can be observed, most of the LC methods are focused on pristine fullerenes, mainly C_{60} and C_{70} although recently, some studies have been published describing the separation of functionalised C_{60}-fullerenes, including some water soluble derivatives [109–114] and that of a C_{70}-functionalised fullerene together with other pristine and hydrophobic C_{60} fullerene derivatives [115]. The most common chromatographic separation conditions for hydrophobic fullerenes are reversed-phase chromatography mainly using octadecylsilica stationary phases and mobile phases containing toluene:methanol or toluene:acetonitrile (Table 4). In most of the works, conventional 3.5–5 μm particle size columns are used, resulting in long analysis times (up to 15 min) although recently, columns with sub-2 μm totally porous particles or core–shell partially porous particles have been used (Table 4). A considerable reduction in the analysis time can be achieved with these columns (2.5–4.3 min), as well as a high column efficiency while maintaining a good chromatographic separation (Fig. 4). The elution order of hydrophobic fullerenes in reversed-phase columns is correlated with the presence and number of functional groups on the fullerene cage (functionalised fullerenes eluting earlier than pristine fullerenes), and with the size of the fullerene cage (the greater the size, the higher their retention). Additionally, the retention of this family of compounds on these columns is controlled by adding a polar solvent (*e.g.*, methanol, acetonitrile) to a non-polar solvent (*i.e.*, toluene) since the interaction of fullerenes with aromatic solvents such as toluene is stronger than with polar solvents [116]. As regards to these two solvents an interesting chromatographic behaviour in C18 columns has been described in the literature. As an example, Fig. 4 shows the chromatograms obtained on a sub-2 μm particle size C18 column for C_{60}–C_{84}, C_{60}, C_{60}-pyrr, PCBM and PCBB, using toluene:methanol and toluene:acetonitrile (40:60 v/v) as mobile phases under isocratic conditions. As can be seen, higher retention times were obtained using toluene:acetonitrile than with toluene:methanol. This seems

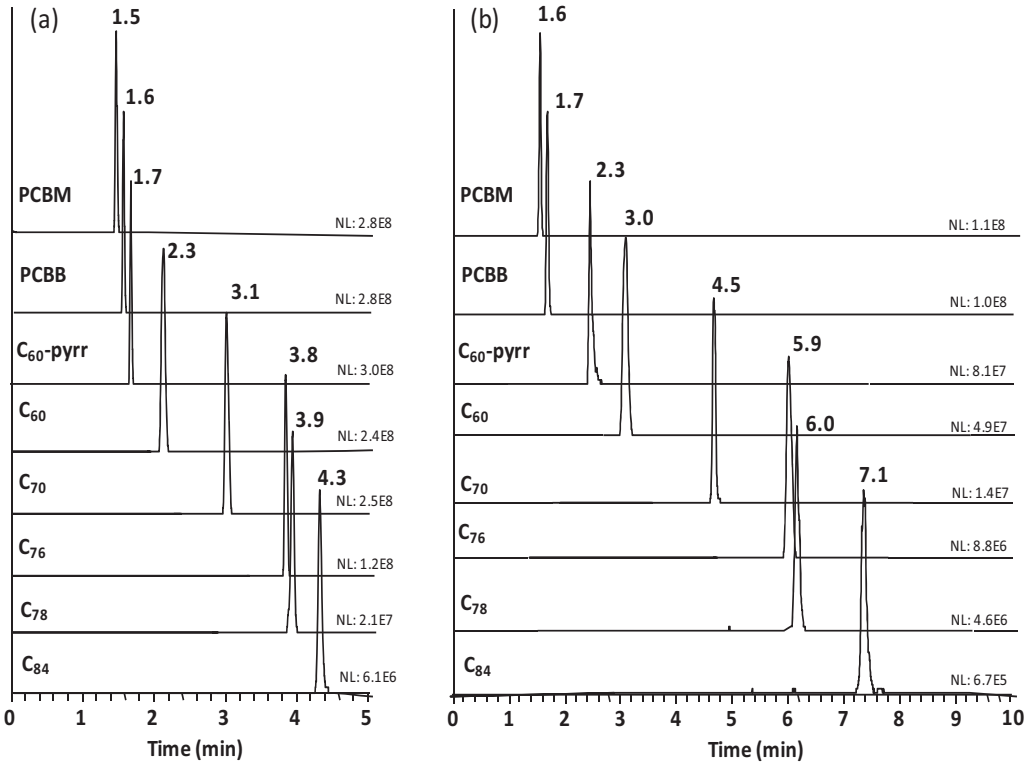

Fig. 4. Chromatographic separation of three C_{60}-fullerene derivatives and five pristine fullerenes in a sub-2 μm C18 Hypersil Gold (150 × 2.1 mm, 1.9 μm particle size) column using (a) toluene:methanol (40:60 v/v) and (b) toluene:acetonitrile (40:60 v/v) as mobile phases under isocratic elution. Flow rate: 500 μL min^{-1}. Acquisition performed by LC-(−)APPI-MS(/MS). Reprinted with permission from Ref. [117]. Copyright (2014) Elsevier.

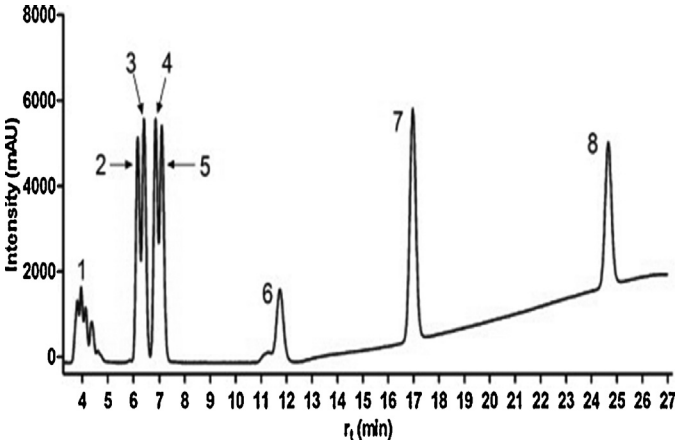

Fig. 5. HPLC-UV chromatogram of fullerenes and functionalised fullerenes in a Cosmosil Buckyprep (250 × 4.6 mm, 5 μm particle size) column. Separation under gradient elution from toluene:acetonitrile (75:25 v/v) to 100% toluene in 6 min, and then isocratic elution at 100% toluene. Peak identification: (1) bis-PCBM; (2) PCMO; (3) PCBB; (4) PCBM; (5) ThCBM; (6) C_{70}-PCBM); (7) C_{60}; and (8) C_{70}. Reprinted with permission from Ref. [124]. Copyright (2014) Elsevier.

counterintuitive, since the eluotropic strength of the mixture toluene:acetonitrile is higher, hence lower retention times should be expected compared with the toluene:methanol mobile phase. The authors [117] explained this behaviour as being related to the size of fullerene aggregates in each solvent mixture. As previously mentioned, fullerenes can form aggregates in binary mixtures of toluene and a second organic solvent and their sizes decrease with the increase in the polarity of the latter [75,76]. Therefore, bigger aggregates will be formed in toluene:acetonitrile than in toluene: methanol and as a consequence higher retention is observed.

Several other reversed-phase columns such as C_{30} and C_8 have also been evaluated for the separation of pristine fullerenes (C_{60}, C_{70}, C_{76}, C_{78}, C_{82} and C_{84}) [118] and the C_{30} chains showed to be very effective for the interaction with fullerene molecules, achieving a strong retention, although with very long analysis times (>40 min). Moreover, several chromatographic columns have been especially designed for the separation of these compounds [119]. Among them, Cosmosil Buckyprep (pyrenylpropyl group) and Cosmosil PYE (pyrenylethyl group) columns are the most commonly used for the analysis of fullerenes. These columns have been employed by several authors for the separation of fullerenes and several derivatives using 100% toluene as mobile phase [120–123], toluene mixtures with acetonitrile [109,115,124] or methanol [78], and acetonitrile–dichlormethane mixtures [106] . For instance, Carboni et al. [124] reported the separation of C_{60}, C_{70} and several functionalised fullerenes (PCMO, bis-PCBM, ThCBM, C_{70}-PCBM, PCBM and PCBB) (Fig. 5). The first eluting compound in the chromatogram (bis-PCBM) presented a jagged peak shape that was attributed to either the presence of different isomers or to the formation of micelles in the solution. As depicted in Fig. 5, long analysis times are usually obtained with the Cosmosil Bulkyprep column (25 min), which is disadvantageous in comparison to the short analysis times that can be achieved with sub-2 μm or core–shell C18 columns, as previously commented. This specially designed column is ideal for preparative-scale separations since it exceeds the injection volume of a standard C18 column by a factor of 35 [119].

Among the other stationary phases reported for the analysis of pristine fullerenes [125,126] the ones based on phenylporphyrin immobilized on silica, such as tetraphenylporphyrin-silica [108] and hydroxyphenyltriphenylporphyrin-silica [127] provide very good selectivity and efficiency. However, the use of these columns is limited by the high cost of phenylporphyrin materials. In addition, chiral columns have been used [110,128] for the enantiomeric separation of chiral fullerene derivatives.

Recently, there is a manifested interest in developing methods for the analysis of water soluble fullerenes with potential industrial, biomedical and cosmetic applications. Different stationary phases and polar solvent combinations (*e.g.*, water, methanol, acetonitrile) are employed for the analysis of water soluble surface-functionalised fullerenes, such as $C_{60}(OH)_{24}$ [111,112], chiral hexakis adducts ($C_{60}(COOEt)_{12}$) [110], (C_3, D_3) tris-dicacrboxymethanofullerene-C_{60} [114], dendritic monoadduct methano [60] fullerene octadeca acid [113] and MSAD-C_{60} [129]. Among them, the chromatographic separation of $C_{60}(OH)_{24}$ is challenging because of the high hydroxylation and the associated negative surface charges that make difficult the use of conventional C18 separation approaches. Despite this, Silion et al. [112] used a Zorbax SB-C18 reversed-phase column and 100% water as the mobile phase for the retention of fullerol (retention time of 2.6 min). In contrast, Chao et al. [111] were not able to retain fullerol in a XBridge C18 column regardless the mobile phase composition used. Therefore, the authors proposed the use of

Table 5
Analysis of fullerenes: capillary electrophoresis techniques.

Compound	Sample	Experimental conditions	Detection	Ref.
C_{60}, C_{70}, C_{84}	Standard solution	(NACE) BGE: 100 mM TDAB, 50 mM TEAB, 6% MeOH, 1% acetic acid in chlorobenzene–acetonitrile 1:1 (v/v), V = +30 kV Capillary: 75 μm × 60 cm	UV: 313 nm	[131]
C_{60}, C_{70}, C_{60}-pyrr and C_{60} COOH	Commercial cosmetic product (C_{60})	(NACE) BGE: 200 mM TDAB, 40 mM TEAB, 6% MeOH, 10% acetic acid in chlorobenzene–acetonitrile 1:1 (v/v), V = +30 kV Capillary: 50 μm × 50 cm	UV: 350 nm	[130]
Open cage fullerenes	Standard solution	(NACE) BGE: 200 mM trifluoroacetic acid, 20 mM sodium acetate in acetonitrile–methanol (90:10, v/v), V = +25 kV Capillary: 75 μm × 60 cm	UV: 200 nm	[132]
C_{60}, C_{70}	Standard solution	(MECC) BGE: 100 mM SDS in 10 mM sodium tetraborate-phosphate, pH 9.5, V = +10 kV Capillary: 75 μm × 28 cm	UV: 254 nm	[133]
Dentro[60]fullerene (DF)	Standard solution	(CZE) BGE: 75 mM phosphate buffer pH 6, V = +25 kV Capillary: 50 μm × 40 cm	UV: 254 nm	[135]
Carboxy fullerene (C_3) and DF	Serum matrix	DF: (CZE) BGE: 40 mM sodium tetraborate, pH 9.2, V = −14 kV C_3: (MECC) BGE: 10 mM sodium tetraborate and 150 mM SDS, pH 9.2, V = +14 kV; (CZE) BGE: 40 mM sodium tetraborate, pH 7.4, V = +14 kV Capillary: 50 μm × 40 cm, dynamic coating	UV: 260 nm	[134]
Th-symmetric hexakis-adduct $C_{66}(COOH)_{12}$	Standard solution	(CZE) BGE: 15 mM sodium tetraborate, pH 9.3, V = +20 kV Capillary: 75 μm × 50 cm	UV: 330 nm	[136]

C_{60} COOH: (1,2-methanofullerene C_{60})-61-carboxylic acid.

hydrophilic interaction liquid chromatography (HILIC) employing a XBridge amide column with water:acetonitrile (10:90 v/v) as mobile phase achieving a good efficiency and a retention time of 3 min for fullerol.

Although advances have been made in the analysis of water soluble fullerenes, there is still a limited number of studies, and most of them have been performed using standard mixtures [46,110–112,114]. In comparison, a significantly higher number of studies have been reported for the analysis of hydrophobic fullerenes, and most of them are applied to complex matrices (*i.e.*, environmental, biomedical, and cosmetic) (Table 4).

3.1.2. Capillary electrophoresis

Capillary electrophoresis (CE) techniques with UV–vis detection have also been proposed to separate fullerene compounds [130–136] although its employment for the analysis of these compounds in real samples is very limited. Table 5 summarises the reported methods and the experimental conditions used.

CE is an analytical technique that separates ions inside a fused-silica capillary according to their differences in electrophoretic mobility under the influence of a strong electric field. The main problems to be addressed when using CE for the separation of hydrophobic fullerenes is their lack of charge and electrophoretic mobility and their low solubility in aqueous buffers currently used as electrophoretic media in CE. To overcome these drawbacks two approaches have been proposed: non aqueous capillary electrophoresis (NACE) by employing charged compounds and organic solvent mixtures as separation medium and micellar electrokinetic capillary chromatography (MECC) by adding a surfactant above the critical micellar concentration to an aqueous electrophoretic buffer in order to form micelles.

The separation of hydrophobic fullerenes by NACE has been studied by several authors [130–132]. Different compounds able to interact with the target analytes to form charged complexes which can migrate under the electric field are added to the background electrolyte to accomplish their separation. For instance, pristine fullerenes (*i.e.*, C_{60}, C_{70}) and several hydrophobic C_{60} derivatives have been separated using tetraalkylammonium (TAA) salts in a solvent mixture containing acetonitrile, chlorobenzene, methanol and acetic acid as background electrolyte (BGE) [130,131]. A long chain TAA salt (tetradecylammonium bromide, TDAB) was used to induce the electrophoretic migration of the analytes *via* solvophobic interactions while the short chain TAA salt (tetraethylammonium bromide, TEAB) reduced the electro-osmotic flow (EOF) improving the separation. Among these studies, Astefanei et al. [130] applied a NACE method for the analysis of C_{60} in a commercial cosmetic product as an alternative to conventional LC methods. NACE has also been proposed for the separation of three open-cage fullerenes using a mixture of acetonitrile and methanol with trifluoroacetic acid and sodium acetate in order to provide the compounds with an overall positive charge *via* protonation [132].

The separation of C_{60} and C_{70} using an aqueous buffer by MECC using sodium dodecylsulphate (SDS) as surfactant has also been reported [133]. To overcome solubility problems, the fullerenes were first solubilised in the aqueous media *via* complexation with SDS. Nevertheless, this involves an additional time-consuming sample preparation step to the analytical procedure. Moreover, the encapsulation process and the sizes of C_{60} and C_{70} aggregates within the SDS micelle are yet to be understood.

CE techniques have also been proposed for the separation of water soluble fullerenes [134–136]. For instance, Chan et al. [134] evaluated the use of capillary zone electrophoresis (CZE) and MECC with SDS micelles, for the analysis of two water soluble fullerene derivatives (dendro[60]fullerene (DF) and carboxy fullerene (C_3)) in human serum samples. For the CZE experiments, bare and dynamically coated fused-silica capillaries were used. Using the coated capillaries, the EOF was suppressed allowing faster

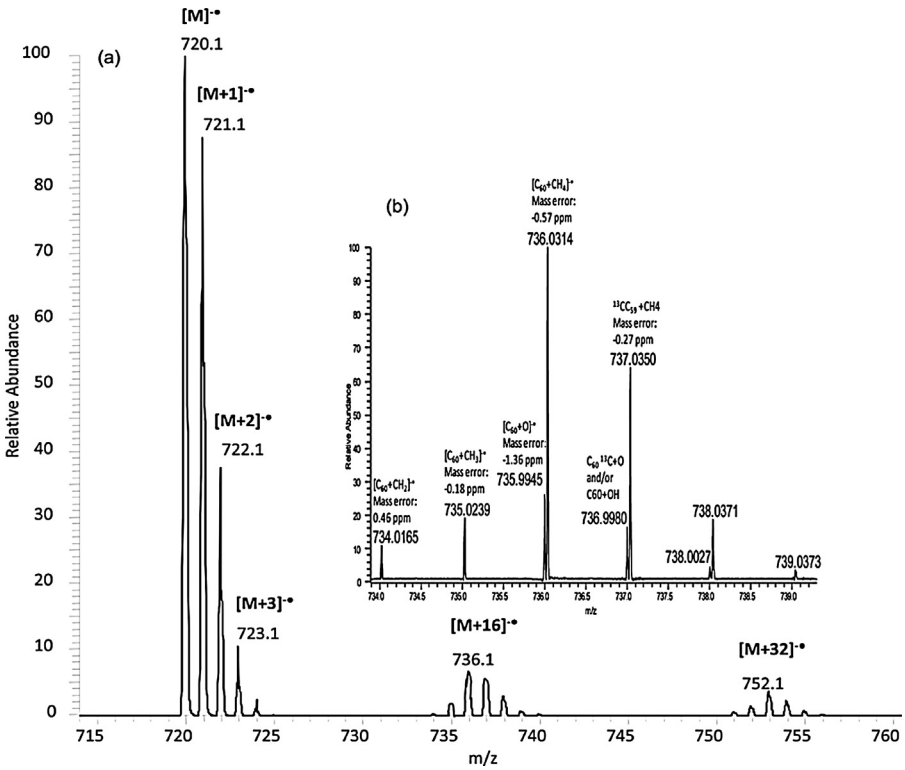

Fig. 6. (a) Full scan MS spectrum of C_{60} (b) HRMS spectrum of C_{60} cluster ion at M + 16 at a resolving power of 100,000 FWHM. Reproduced with permission from Ref. [144]. Copyright (2012) American Chemical Society.

migration times but with a slight decrease in resolution between both nanoparticles. The authors recommend using CZE for the quantitation of both C_3 and DF in human serum because this technique allowed to obtain good results for DF and presented some advantages over MECC for C_3 such as lower analysis time and lower detection limits due to less baseline noise and better reproducibility. However, dilution of the human serum with SDS or addition of SDS to the running buffer to break the interactions between nanoparticles and proteins within the serum sample is required. The behaviour of DF in CZE as a function of pH, ionic strength, solvent amount and concentration of additives to reduce EOF has been also reported [135]. The parameters which showed the most important effect on the migration time and separation efficiency of the analytes were the pH and the ionic strength. The migration time of DF increased with the pH and decreased with the salt concentration.

The above mentioned studies indicated that CE could be a suitable technique for the analysis of both hydrophobic and water soluble fullerenes as an alternative to LC, in samples with relative high concentrations such as cosmetic and pharmaceutical products.

3.2. Detection

For the detection of fullerenes, either UV–vis or mass spectrometry (MS) has been used, due to the excellent response obtained with both techniques. UV–vis detection is commonly used for CE techniques and to the best of our knowledge its coupling to MS has not been described in the literature. Nevertheless, MS provides better selectivity, allows differentiating fullerenes by their molecular weight and provides structural information that can indicate the presence of surface functional groups. Different mass analysers (Table 4) such as single quadrupole (Q), triple quadrupole (QqQ), ion-trap (IT), and quadrupole-linear ion-trap (QqLIT) have been used for their analysis. High-resolution mass spectrometry (HRMS) either using time-of-flight (TOF), hybrid quadrupole-time-of-flight (Q-TOF), and more recently hybrid linear trap-Orbitrap (LTQ-Orbitrap) and hybrid quadrupole Orbitrap (Q-Orbitrap) analysers has also been reported (Table 4).

Among the atmospheric pressure ionisation (API) techniques, electrospray ionisation (ESI) and atmospheric pressure chemical ionisation (APCI) in negative ionisation mode are the sources most frequently used for both pristine and functionalised fullerenes (Table 4). Atmospheric pressure photoionisation (APPI) [137] allowed to expand the application of LC–MS to non-polar compounds and compounds difficult to be ionised by ESI or APCI such as polycyclic aromatic hydrocarbons (PAHs), polybrominated diphenyl ethers, naphtalene, nitropyrenes and lipids [138–140] and it has been also proposed for the LC–MS analysis of fullerene and fullerene derivatives (Table 4). The relatively high number of papers that used APPI for the analysis of fullerenes is related to the use of toluene in the chromatographic mobile phase which favours the formation of fullerene molecular ions through a solvent-mediated ionisation mechanism by electron capture.

Mass spectra of fullerenes in negative mode are simple providing the isotopic pattern of the molecular radical anion $[M]^{-\bullet}$ (Fig. 6a). However, the presence of other radical anions in negative ESI and APPI, such as the oxidized ions $[M+O]^{-\bullet}$ (*i.e.*, *m/z* M + 16 and *m/z* M + 32) [141–144] and solvent adduct ions $[M+CH_3OH-H]^-$ [145,146] has also been reported. Núñez et al. [144] studied and characterised the cluster ions present in the MS spectra of fullerenes at *m/z* M + 16 and *m/z* M + 32 by tandem MS, HRMS and accurate mass measurements using an Orbitrap mass analyser at a mass resolving power of 100,000 full width at half maximum (FWHM). As an example, the spectrum obtained for C_{60} cluster ion *m/z* M + 16 is shown in Fig. 6b where it is shown the presence of two ions, one at *m/z* 735.9945 (mass error −1.36 ppm) due to the addition of oxygen ($[M+O]^{-\bullet}$) [147] and another at *m/z* 736.0314 (mass error −0.57 ppm) assigned to $[M+CH_4]^{-\bullet}$and explained by the gas-phase ion molecule reaction of $[M]^{-\bullet}$ with a radical $^{\bullet}CH_3$ and subsequent stabilization by hydrogen addition.

Several studies compared the ionisation efficiency of pristine fullerenes [144] with that of hydrophobic C_{60}-derivatives [117,145] using different API sources (ESI, heated-ESI (H-ESI), APCI and APPI). Better sensitivity is always reported by using an APPI in negative mode which is, as previously mentioned, related to the use of toluene in the mobile phase that improves ionisation efficiency in APPI [148]. Regarding the other API sources, H-ESI showed better results than ESI for pristine fullerenes, mainly for larger fullerenes,

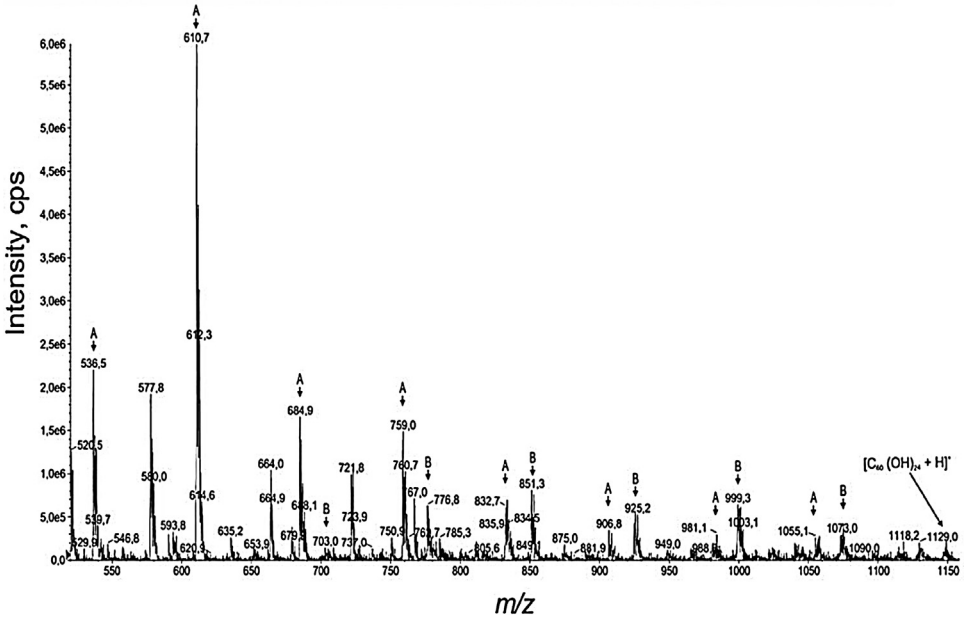

Fig. 7. Overview (Q1) scan spectrum of a fullerol sample. Peaks of the two 74 *m/z* series (A and B) are indicated by the arrows. Reproduced with permission from Ref. [111]. Copyright (2011) American Chemical Society.

while APCI showed worst performance for the ionisation of these compounds [144]. In contrast, for several functionalised C_{60} fullerenes (C_{60}-pyrr, PCBM and PCBB) better results were obtained with APCI in comparison to ESI since for these specific compounds electron capture is favoured in the APCI plasma [117].

Other ionisation techniques such as matrix-assisted laser desorption ionisation (MALDI) have also been proposed for the characterisation of pristine fullerenes [108] and fullerol [111], although the utility of MALDI for quantitative analysis is limited. For instance, Xiao and Meyerhoff [108] used MALDI–TOF-MS to identify several fullerenes, from C_{76} to C_{94} in a pyridine extract of crude soot. More recently, Chao et al. [111] used MALDI–TOF-MS to characterise fullerol using 2,5-dihydrobenzoic acid as matrix. In the MALDI–MS spectra, the authors found a major peak at m/z 720, corresponding to the molecular mass of C_{60} and a peak series from m/z 720 to 576 with a spacing of 24 m/z. These ions have also been observed in early studies of fullerol and have been attributed to sequential C_2 losses [149]. The authors also studied the same sample by LC–ESI-MS(/MS) in positive mode obtaining (Fig. 7) a complex full scan spectrum with a weak peak corresponding to the protonated molecular mass of fullerol $[C_{60}(OH)_{24}+H]^+$ at m/z 1129. In contrast to MALDI-TOF spectra, no C_2 losses were found although a decreasing series spaced by 74 m/z units from m/z 1129 to 537 ($[M-n74+H]^+$, $n=1-8$) was observed, which was explained by subsequent neutral losses of $C_2H_2O_3$ groups.

4. Analysis of complex matrices

This section presents the existing sample treatment strategies (*i.e.*, extraction and preconcentration) and the proposed methods for the identification and quantitation of fullerenes. The reported recoveries, detection/quantitation limits and detected levels in complex matrices (*i.e.*, environmental, cosmetic and biological) are discussed and included in Table 4.

4.1. Sampling and sample treatment

Sampling and sample preparation are always a critical step in an analytical method but in the analysis of fullerenes additional problems arise because nanoparticles physicochemical changes that modify their dispersion state can occur and the presence of other nanoparticles and/or organic matter complicates the sample treatment. Hence, attention should be given to minimize and prevent changes in the aggregation state of the particles [59] especially when the objective of the study is the characterisation of fullerene aggregates in complex samples as undetected changes could lead to incorrect conclusions about their properties. Since the aggregation state of fullerenes is unstable and difficult to be preserved during sample treatment, most of the reported analytical methods quantify the total amount of compounds without taking into account their different aggregation states. Recently, Herrero et al. [79] addressed this problem by coupling AF4 to high resolution mass spectrometry allowing both size and concentration determination of fullerene aggregates.

On the other hand, for the extraction of fullerenes from complex matrices, procedures that fit with the nature of the matrix but also with the characteristics of the particles must be applied. For instance, despite the fact that C_{60} presents a very high solubility in toluene, it cannot be readily extracted from water samples where it is present as stable colloidal aggregates (nC_{60}) without the presence of oxidizing agents or salts to disrupt the stability of the colloidal aggregates and enhance the partitioning into the toluene phase [10,15,150]. Moreover, care must be taken during the analysis to prevent losses. For example, it has been reported that C_{60} in methanol adsorbs to glassware, being 100% adsorbed in few hours [63].

Liquid–liquid extraction (LLE) is the method typically used for C_{60} extraction from environmental [63,109,117,120] biological samples [142,150,151] and cosmetics [152]. The extraction methods and the recoveries reported for fullerenes in complex matrices are included in Table 4. LLE [109,117,120] and solid phase extraction (SPE) [141,153] are the methods most commonly used for the extraction of fullerenes from environmental waters. In LLE, salts are currently added to destabilize the aqueous nC_{60} aggregates and facilitate its transfer into the organic solvent [109,120]. In general, LLE provides higher recoveries than SPE (Table 4) and it can be applied to a wider range of water samples. For instance, Wang et al. [120] reported the use of LLE for the determination of nC_{60} in different wastewater matrices, while SPE required filtration and was only applicable to reclaimed wastewater and effluents with little suspended solids. Some authors only analysed the suspended solids obtained after the filtration of the water samples [143,144]. Nonetheless, taking into account the characteristics and complexity of the aggregates formed in aqueous media, the procedure proposed in these two studies does not seem to be the best approach to ensure that the maximum possible amount of the analytes is extracted. Ultrasound assisted extraction (UAE) has also been used to extract fullerenes from water samples. For example, Emke et al. [154] proposed recently the combined analysis of the water particulate matter by SPE and its aqueous phase by UAE for C_{60} and C_{70} and several functionalised fullerenes in environmental waters. In this context, Chen and Ding [145] reported the use of ultrasound assisted dispersive liquid–liquid micro-extraction (UAE-LLME) with benzyl bromide as the extraction solvent and 2-propanol as the dispersive solvent for the extraction of surface water and wastewater samples (Table 4).

The proposed methods for the extraction of fullerene compounds from environmental solids such as sediments, soils, airborne particulate and water suspended solids used UAE [105,122,124,143,144,155–158], Soxhlet [105], and pressurized liquid extraction (PLE) [117,159] with toluene as extraction solvent. Similar recoveries were reported for these methods (>70%) except for two studies regarding the extraction of fullerenes by UAE from soils and sediments that found lower recoveries [124,157] (Table 4). It was reported that the extraction efficiency may be affected by the adsorption of fullerenes to different soil components (*e.g.*, clay minerals, natural organic matter, etc.) [159,160]. For functionalised fullerenes, Sanchis et al. [157] obtained significantly lower recovery yields (35–59%) which was attributed to their lower affinity to toluene. PLE was also proposed for the extraction of pristine and functionalised fullerenes from sediment samples and allowed to achieve higher recovery values (87–92%) than those reported by UAE (35–59%) for the same functionalised fullerene compounds (Table 4). Regarding the extraction of fullerenes from airborne particulate, recoveries between 60 and 70% were reported by using UAE with toluene [156]. For the extraction of C_{60} and C_{70} from cosmetic samples, Benn et al. [152] obtained recoveries between 96 and 107% by LLE whereas SPE yielded recoveries from 27 to 42% (Table 4). Additionally, mechanical mixing with toluene and salt was reported for the extraction of C_{60} from cosmetics yielding recoveries between 75 and 86% [121].

Regarding the extraction of fullerenes from biological samples, the conventional LLE protocols cannot be used due to the large amounts of proteins, lipids and surfactants commonly present in these kind of samples [150]. Magnesium perchlorate ($Mg(ClO_4)_2$) and/or sodium dodecyl sulfate (SDS) together with the addition of glacial acetic acid (GAA) are usually used as destabilizing agents to solubilise the proteins and surfactants and to eliminate emulsion problems during the LLE with toluene. In general, recoveries higher than 90% are reported [129,142,150,151].

It should be mentioned that although several procedures have been proposed for the extraction of fullerenes from complex

matrices, a robust protocol has not been developed yet, and the extraction mechanisms involved are not fully understood. Moreover, studies related to the extraction of water-soluble fullerenes (*i.e.*, fullerols) in complex matrices are lacking. Currently, there are no reports for the combined extraction of hydrophobic and hydrophilic fullerenes which may be present in some samples. Therefore, the development of an extraction protocol able to extract fullerenes of different polarities is needed. For this purpose, the existing LLE and SPE strategies should be extended by using serial extractions with several solvents of increasing polarity and by combining different SPE sorbents to differentiate and extract all the fullerenes present in the selected samples. Another potential method to separate the fractions of hydrophobic fullerenes from the hydrophilic ones could be the use of porous membranes such as polyethersulphone ones. In the presence of salts, the aggregation of hydrophobic fullerenes will increase enabling their retention on the membrane while the fraction of the hydrophilic ones could be collected after filtration. It has been reported that hydrophobic membranes can induce the adsorption of aromatic compounds (*e.g.*, polycyclic aromatic hydrocarbons, humic substances, aromatic pesticides) onto the surface by hydrophobic and electrostatic interactions [161–163] and this fact has been used for the removal of organic pollutants during water treatment [162].

4.2. Identification, quantitation and detected levels

The necessity to control and analyse fullerene nanoparticles in complex matrices, and the legal requirements for unequivocal identification and confirmation of positive/negative samples posed by the European Union directive 2002/657/EC [164] drives the need to make use of sensitive and reliable analytical methods. Nowadays, the best technique to fulfil these requirements is liquid chromatography coupled to mass spectrometry (LC–MS).

In MS/MS with triple quadrupole instruments the four identification points per analyte required by the EU legislation to guarantee confirmation can be achieved by using two selected reaction monitoring (SRM) transitions. However, pristine fullerenes cannot be fragmented because of their highly stable buckyball structure, thus other strategies need to be used for confirmation purposes. Despite this fact, several authors used a "pseudo" SRM mode by selecting the same ion as both precursor and product ion. For instance, Sanchis et al. [122,157] proposed the monitoring of $[M]^{-\bullet} \rightarrow [M]^{-\bullet}$ (quantitation) and $[M+1]^{-\bullet} \rightarrow [M+1]^{-\bullet}$ (confirmation) SRM transitions for the analysis of pristine fullerenes in river sediments and soils. Alternatively, monitoring the transitions of $[M]^{-\bullet} \rightarrow [M]^{-\bullet}$ for quantitation, and of the oxidized ions $[MO]^{-\bullet} \rightarrow [MO]^{-\bullet}$ for confirmation has been reported for the analysis of pristine fullerenes in wastewater [143], tap and surface water [115] and aerosol [156] samples though in this case the detection limits increased due to the low abundance of the oxidized ions (Fig. 6a). Since no fragmentation occurs in this "pseudo" SRM mode, the four identification points required by the EU legislation are not fulfilled although potential coeluting isobaric interference compounds can be eliminated. The use of HRMS by selecting two ions from the obtained spectra represents a good strategy to guarantee confirmation for this family of compounds. For instance, highly selective-selected ion monitoring (H-SIM) by monitoring two ions of the pristine fullerene isotopic cluster, $[M]^{-\bullet}$ and $[M+1]^{-\bullet}$, has been proposed [117,144]. Nevertheless, to apply this strategy MS instruments with high enough mass resolving power (at least higher than 12,500 FWHM) must be used [144].

In contrast to pristine fullerenes, C_{60}-functionalised fullerenes can be fragmented at relatively high collision energies. In general, the most intense peak of the resulting MS/MS spectra is the ion at m/z 720 corresponding to the buckyball structure (C_{60}) caused by the loss of all the functional groups of these derivatives. In some cases, additional fragments with lower abundances have also been reported, such as the cleavage of the carboxylate ester for fullerenes with large alkyl moieties and the loss of both the propyl acid alkyl ester group $(CH_2)_2COO(CH_x)H$ and the butyl acid alkyl ester group $(CH_2)_3COO(CH_x)H$ for PCBM and PCBB, respectively [115,117,145]. For PCBB, the loss of the butyl group of the carboxylate ester and of the propene group has also been described [117]. Hence, for functionalised fullerenes SRM mode, by monitoring the transition $[M]^{-\bullet} \rightarrow [C_{60}]^{-\bullet}$ for quantitation, and a transition providing a characteristic fragment ion for confirmation is generally used, although the isotopic cluster has also been proposed for confirmation purposes ($[M+1]^{-\bullet} \rightarrow [C_{60}+1]^{-\bullet}$) [117,157].

Most of the LC and LC–MS methods proposed in the literature for the quantitation of fullerenes in complex matrices were developed for the analysis of environmental samples, and only a limited number are addressed to other sample matrices such as cosmetics [121,152] or biological fluids and tissues [142,150,151] (Table 4). Without any doubt, isotope dilution is the best quantitation method for trace level analysis of organic contaminants in complex samples. However, for fullerenes it only exists a single commercially available stable-isotope labelled fullerene, $^{13}C_{60}$ [165] and to the best of our knowledge, there is only one study reporting its use as internal standard in a toxicological assay using *Zebrafish embryos* [142] and one study using it as a surrogate in the extraction of soil samples [122]. This situation is expected to change in the near future since the demand for stable-isotope labeled fullerene standards for the quantitative detection, fate and toxicity studies of these compounds is likely to increase. In general, the quantitation method used in most of the studies is external calibration (Table 4).

As previously mentioned, C_{60} is being considered for drug delivery and recently it has begun to be used in a number of cosmetic products. Hence, methods suitable for the analysis of fullerenes in cosmetic products are needed. For instance, LC–UV has been reported for the quantitation of C_{60} in different commercial creams by standard addition calibration [121]. C_{60} was found at low concentration levels, between 0.002 and 0.005% (w/w), in all the analysed products. Additionally, the ROS production of the cosmetic products was studied under different illumination conditions and the photochemical reactivity of the creams containing C_{60} in deionised water was compared with that of fullerol which is a well-known ROS generator [166]. The results showed that although radical scavenging occurs in the dark, a significant amount of ROS is generated by the aged cosmetic products raising concerns about their effect when released into the environment. However, the relationship between the amount of fullerene present in the product and the ROS generation and their impact on the environment is unknown yet. Recently, Benn et al. [152] analysed C_{60} and C_{70} in anti-aging commercial cosmetic products by LC-(−)APCI-MS after their extraction by LLE with toluene, in order to provide potential exposure levels for future risk assessment of fullerenes. The quantitation was performed by standard addition calibration and C_{60} was found at concentrations ranging from 0.04 to 1.1 $\mu g\,g^{-1}$, while C_{70} was only qualitatively detected in some samples. The authors indicated that a single-use quantity of cosmetic (around 0.5 g) may contain up to 0.6 μg of C_{60}, which can be a pathway for human exposure. In addition, CE with UV detection was reported for the analysis of C_{60} in a cosmetic product (serum) after LLE with toluene [130] and a C_{60} concentration level of 2.10 $mg\,L^{-1}$ in the analysed serum was reported.

Regarding the analysis of biological samples, the number of papers related to the presence of fullerenes in these samples is rather limited. In general, LLE with toluene followed by LC–MS is performed. For instance, this procedure has been reported for the

analysis of C_{60} in blood, tissues [142,150,151] and in protein containing media [150]. Some of these works are devoted to evaluate fullerene's *in vivo* toxicity. For example, Moussa et al. [151] developed an LC-(−)APCI-MS method for the quantitation of C_{60} in blood, liver and spleen samples to evaluate its possible acute toxicity. The method limit of detection was 0.1 ng of C_{60} (injected amount) and the results showed that C_{60} is well absorbed in tissues and its concentration in different organs varied strongly between the animals. As respects functionalised fullerenes, Rajagopalan et al. [129] developed a LC–UV method for the analysis of MSAD-C_{60} in order to perform pharmacokinetic studies in plasma and urine samples of rats. MSAD-C_{60} is a pharmaceutical compound that possess antiviral activity against human immunodeficiency virus types 1 (HIV-1) and 2 (HIV-2) *in vitro* and has virucidal and anti-human immunodeficiency virus protease activities [167]. The study was focused to evaluate the binding of MSAD-C_{60} to plasma proteins (>99%) and the tolerated dose (15 mg kg^{-1}).

With respect to the analysis of environmental samples, LC–UV and LC–MS methods have been used to determine pristine fullerenes and some functionalised fullerenes in geological materials [105], soot extracts [106], soils and sediments [117,122,124,157,158], aerosols [156], and water samples [109,115,117,120,141,143–145,154], although in some of these works only blank matrices spiked with fullerenes have been used. To the best of our knowledge, there are still no LC–UV or LC–MS methods reported for the analysis of water soluble fullerenes such as fullerol in environmental samples. As regards the presence of fullerenes and fullerene derivatives in aerosols, soils and sediments, Sanchis et al. [122,156] reported for the first time the presence of C_{60} and C_{70} in airborne particulate at concentration levels of 0.06 ng m^{-3} and 0.48 ng m^{-3}, respectively. Several fullerene derivatives (C_{60}-pyrr, C_{60} pyrrolidine tris-acid ethyl ester (CPTAE), PCBM, and ThCBM) were not detected in the analysed samples at concentrations higher than the method limits of detection. The same research group [157] also analysed C_{60}, C_{70} and three C_{60}-fullerene derivatives in soils collected from different urban and industrial areas in Saudi Arabia and river sediments from the Llobregat River Basin (Spain). C_{60} was the only fullerene detected and was quantitated in 19% of the soil samples (0.15–6.83 ng g^{-1}) and 33% of the sediments (0.13–0.70 ng g^{-1}). More recently, these authors [122] found C_{60}, C_{70} in sediments and soils from Santa Catarina (Brasil) at concentration levels from low fg g^{-1} up to 154 pg g^{-1} whereas none of the functionalised fullerenes were detected. Astefanei et al. [117] reported the presence of C_{60} and also of three C_{60} fullerene derivatives (C_{60}-pyrr, PCBM and PCBB) in sediment samples collected from several ponds located around Barcelona's Airport (Spain). In this work C_{60} and C_{70} fullerenes were detected in 85% and 71% of the analysed samples, respectively, at levels from 0.8 to 7.2 ng kg^{-1} while the PCBM, PCBB and C_{60}-pyrr were found at levels from 0.14 to 5.1 ng kg^{-1} and the highest concentration was found for PCBB. The presence of fullerenes in sediment and soil samples [117,122,157] could be related to the location of the sampling points which generally are close highly industrial areas or international airports.

The number of publications dealing with the analysis of fullerene compounds in environmental waters is higher than for soils and sediments (Table 4). Most of the works are focused on the analysis of several pristine and functionalised fullerenes simultaneously and one is devoted to the screening of nC_{60} and some of its transformation products in water [141]. The method was able to detect and quantitate concentrations of nC_{60} as low as 5 ng L^{-1} but, despite its high sensitivity no nC_{60} or transformation products were detected in the analysed surface waters. Regarding the simultaneous analysis of pristine and functionalised fullerenes, two recent works reported methods for the determination of up to 8 fullerene compounds. Kolkman et al. [115] used a LC-(−)ESI-Orbitrap system for the analysis of C_{60}, C_{70} and six functionalised fullerenes in spiked tap water after SPE (C18) achieving very low MLODs ranging from 0.17 ng L^{-1} (C_{70}-PCBM) to 0.28 ng L^{-1} (C_{60}). However, the developed method was not applied for the analysis of environmental water samples and its main disadvantage was the long chromatographic analysis time (27 min). Astefanei et al. [117] reported an LC-(−)APPI-MS (/MS) method for the analysis of river water samples achieving MLODs ranging from 0.4 pg L^{-1} for PCBM to 1.6 ng L^{-1} for C_{84}, with a run chromatographic time of only 4.3 min. The method was applied to the analysis of pond water samples collected around the airport of Barcelona (Spain) where C_{60} and C_{70} were found at concentration levels between 9 and 330 pg L^{-1} and three C_{60}-fullerene derivatives (C_{60}-pyrr, PCBM, and PCBB) were detected (50–83% of the samples) at levels between 2 and 8.5 pg L^{-1} (Table 4). This is the first report of the presence of these functionalised fullerenes in water samples, except for C_{60}-pyrr which has been also found in wastewater effluents (Table 4).

The presence of pristine fullerenes in environmental water samples has been reported by several authors being usually present at low ng L^{-1} levels [143,144,157] although in one of these works [143] C_{60} was found in some of the analysed samples at μg L^{-1} levels. To the best of our knowledge, the presence of C_{84} in water samples has only been reported once, and also at low ng L^{-1} levels, when analysing water particulate suspended material using a LC-(−)APPI-MS method [144] meanwhile C_{76} and C_{78} have never been found in environmental samples.

5. Conclusions and future trends

Fullerenes occupy a prominent place among nanomaterials. Furthermore, these particles display a high reactivity potential that has led to their use in a wide array of applications (*i.e.*, biomedicine, cosmetic products, solar cells and catalysts). Their anticipated market growth in combination with the potential for direct human exposure *via* several applications has led to widespread concerns about their potential adverse effects on human health. There are a number of factors that appear to be implicated in fullerene behaviour and toxicity, including chemical structure, surface functionalisation and size distribution. The particle sizes and size distribution are important characteristics of nanoparticles and determine their mobility and deposition in the aquatic environment, *in vivo* distribution, biological fate, and toxicity. Therefore, a thorough physicochemical characterisation of fullerene aggregates in terms of size distribution, shape and ζ potential is required in order to know which attributes are responsible for the observed toxic responses. Moreover, these parameters should be taken into account for health and environmental regulations. To determine these characteristics, a great number of complementary techniques such as TEM, DLS, SLS, flow-FFF, NTA, and AFM should be combined. However, it has been demonstrated that the solubilisation procedures used to prepare the samples affect the physicochemical properties of the fullerenes, thus the measured sizes and shapes would not be totally representative of the actual degree of aggregation of the particles in the aqueous media. The aggregates found in the environment will probably be more similar to those obtained by direct solubilisation in water *via* extended stirring (aqu/nC_{60}) than to those obtained *via* solvent exchange methods. Hence, the solubilisation of fullerenes *via* extended stirring is recommended for the studies devoted to their behaviour and toxicity.

Efforts have been made to investigate the fate of fullerenes under laboratory and environmental conditions and the current literature stresses the physicochemical transformations that occur to fullerenes after being released in the environment. So far, it has been demonstrated that the degree of aggregation is affected by several conditions such as the ionic strength, pH, the presence of

natural organic matter and sunlight but further research is needed to determine how aggregate size and surface charge affect the ability of environmental test organisms to uptake the aggregated forms. While there are a significant number of studies on the biological effects of fullerenes, there are very few attempts to rigorously quantitate them in biological matrices. Due to the potential interaction between fullerenes and organs and tissues, the still unknown incubation time, and the possible DNA damaging, thorough studies are recommended before using them in cosmetic, biomedical and other industrial applications.

Each step involved in the analysis of fullerenes (*i.e.*, extraction, separation, identification and quantitative detection) represents a specific challenge. The extraction procedure used could affect the physicochemical properties of fullerenes. Hence, it is crucial to develop methodologies which preserve their properties and degree of aggregation. Moreover, the analytical methodologies should not only address the characterisation and analysis of hydrophobic fullerenes but must be extended to a broader range of compounds including the water soluble derivatives and related transformation products. To date, most of the reported methods are focused on the analysis of the total amount of fullerene compounds, mainly the hydrophobic ones, without taking into account their different aggregation states. Sample treatment procedures for hydrophobic fullerenes are based on their extraction with toluene (LLE, PLE, SPE and UAE) and disrupt the fullerene aggregates present in the matrix. Moreover, they cannot be applied for the extraction of the water soluble fullerenes. Therefore, combined extraction methods enabling the analysis of the entire family of compounds need to be developed.

Chromatographic separation could also be problematic due to the differences in the mobile and/or stationary phases which must be used to achieve proper separation of a wide range of compounds. In this context, it would be useful to evaluate the applicability of comprehensive two-dimensional liquid–liquid chromatography (normal-phase × reversed-phase). Moreover, in order to cope with the necessity of performing a high number of analyses in complex matrices, a short analysis time is ideal. Therefore, the use of UHPLC column technology either with sub-2 μm particle size totally porous columns or core–shell partially porous columns is recommended.

Finally, the specific detection of a maximum range of fullerenes and transformation products is challenging. Although it has been reported the formation of transformation products *via* oxidation and photochemical reactions generating reactive oxygen species (ROS), very little is known about their chemical identities and there are still no methods for their detection in real samples. Information about the presence of these products is important since they may possess inherent toxicity or may alter that of the fullerenes under investigation. Thus, methodologies for the identification and quantitation of these products are necessary.

LC–MS is without any doubt the best option when dealing with the analysis of this family of compounds, although LC–UV and few CE–UV methods have also been reported and can be used for the analysis of specific fullerenes in samples such as cosmetic and pharmaceutical products. However, these latter methods do not fulfil the requisite for unambiguous detection of fullerenes in complex samples that contain potential interferences. Although fullerenes have been detected in a wide variety of samples, including airborne particulate, sediments, soils, and water, the available data is still limited to correctly asses the occurrence, fate and behaviour of fullerene nanoparticles in the environment. Hence, both the scientific community and stakeholders must address these knowledge gaps and provide tools for the risk assessment legislation.

Although LC–MS methods are a powerful tool for the quantitation of fullerenes in complex samples, these techniques alone cannot provide detailed qualitative information. Therefore, these methods need to be adapted for the identification and quantitation of these particles while preserving the information of their degree of aggregation and cluster size. The hyphenation of techniques able to separate the natural aggregate particles with LC–MS seems to be a suitable approach to overcome this problem. In this context, the recent paper of Herrero et al. [79] reporting the coupling of AF4-MALS to high resolution mass spectrometry for the characterisation and quantitation of aqu/nC$_{60}$ and aqueous functionalised fullerene aggregates can be an example of future research direction. This hyphenation represents a powerful methodology for both characterisation and accurate analysis of fullerene aggregates in aqueous samples at environmentally relevant conditions.

Acknowledgements

The authors gratefully acknowledge for the financial support received from the Spanish Ministry of Economy and Competitiveness under the project CTQ2012-30836, and from the Agency for Administration of University and Research Grants (Generalitat de Catalunya, Spain) under the project 2014 SGR-539. Alina Astefanei thanks the Spanish Ministry of Economy and Competitiveness for a Ph.D. grant (FPI-MICINN).

References

[1] H.W. Kroto, J.R. Heath, S.C. O'Brien, R.F. Curl, R.E. Smalley, C$_{60}$: buckminsterfullerene, Nature 318 (1985) 162–163.
[2] D.J. Burleson, M.D. Driessen, L.R. Penn, On the characterization of environmental nanoparticles, J. Environ. Sci. Health Part A: Tox. Hazard. Subst. Environ. Eng. A 39 (2004) 2707–2753.
[3] K. Tiede, A.B.A. Boxall, S.P. Tear, J. Lewis, H. David, M. Hassellov, Detection and characterization of engineered nanoparticles in food and the environment, Food Addit. Contam. Part A 25 (2008) 795–821.
[4] B. Gulson, H. Wong, Stable isotopic tracing – a way forward for nanotechnology, Environ. Health Perspect. 114 (2006) 1486–1488.
[5] C.T. Jafvert, P.P. Kulkarni, Buckminsterfullerene's (C$_{60}$) octanol–water partition coefficient (K_{ow}) and aqueous solubility, Environ. Sci. Technol. 42 (2008) 5945–5950.
[6] J. Brant, J. Labille, J.Y. Bottero, M.R. Wiesener, Characterizing the impact of preparation method on fullerene clusters structure and chemistry, Langmuir 22 (2006) 3878–3885.
[7] J. Brant, H. Lecoanet, M. Hotze, M. Wiesner, Comparison of electrokinetic properties of colloidal (n-C$_{60}$) formed using two procedures, Environ. Sci. Technol. 39 (2005) 6343–6351.
[8] G.V. Andrievsky, M.V. Kosevich, O.M. Vovk, V.S. Shelkovsky, L.A. Vashchenko, On the production of an aqueous colloidal solution of fullerenes, Chem. Commun. (1995) 1281–1282.
[9] G.V. Andrievsky, V.K. Klochkov, E.L. Karyakina, N.O. Mchedlov-Petrossyan, Studies of aqueous colloidal solutions of fullerene C$_{60}$ by electron microscopy, Chem. Phys. Lett. 300 (1999) 392–396.
[10] S. Deguchi, R.G. Alargova, K. Tsujii, Stable dispersions of fullerenes, C$_{60}$ and C$_{70}$, in water. Preparation and characterization, Langmuir 17 (2001) 6013–6017.
[11] K.L. Chen, M. Elimelech, Aggregation and deposition kinetics of fullerene (C$_{60}$) nanoparticles, Langmuir 22 (2006) 10994–11001.
[12] S. Deguchi, S. Mukai, M. Tsudome, K. Horikoshi, Facile generation of fullerene nanoparticles by hand-grinding, Adv. Mater. 18 (2006) 729–732.
[13] D.Y. Lyon, L.K. Adams, J.C. Falkner, P.J.J. Alvarez, Antibacterial activity of fullerene water suspensions: effects of preparation method and particle size, Environ. Sci. Technol. 40 (2006) 4360–4366.
[14] J. Brant, H. Lecoanet, M.R. Wiesner, Aggregation and deposition characteristics of fullerene nanoparticles in aqueous systems, J. Nanopart. Res. 7 (2005) 545–553.
[15] J.D. Fortner, D.Y. Lyon, C.M. Sayes, A.M. Boyd, J.C. Falkner, E.M. Hotze, L.B. Alemany, Y.J. Tao, W. Guo, K.D. Ausman, V.L. Colvin, J.B. Hughes, C$_{60}$ in water: nanocrystal formation and microbial response, Environ. Sci. Technol. 39 (2005) 4307–4316.
[16] M. Prato, [60] Fullerene chemistry for materials science applications, J. Mater. Chem. 7 (1997) 1097–1109.
[17] M. Prato, Fullerene materials, in: A. Hirsch (Ed.), Fullerenes and Related Structures, Topics in Current Chemistry, vol. 199, Springer, Berlin, 1999, pp. 173–187.
[18] F. Wudl, Fullerene materials, J. Mater. Chem. 12 (2002) 1959–1963.
[19] V. Georgakilas, F. Pellarini, M. Prato, D.M. Guldi, M. Melle-Franco, F. Zerbetto, Supramolecular self-assembled fullerene nanostructures, Proc. Natl. Acad. Sci. U. S. A. 99 (2002) 5075–5080.

[20] D.M. Guldi, M. Nazario, Fullerenes: from synthesis to optoelectronic properties, Developments in Fullerene Science, fourth ed., Springer Science + Business Media, Dordrecht, 2002.
[21] S. Erkoc, Perspectives of fullerene nanotechnology, E. Osawa (Ed.), Mater. Manuf. Process. 17 (2002) 881–883.
[22] Y. Kim, S. Cook, S.M. Tuladhar, S.A. Choulis, J. Nelson, J.R. Durrant, D.D.C. Bradley, M. Giles, I. McCulloch, C.S. Ha, M. Ree, A strong regioregularity effect in self-organizing conjugated polymer films and high-efficiency polythiophene:fullerene solar cells, Nat. Mater. 5 (2006) 197–203.
[23] N. Tagmatarchis, H. Shinohara, Fullerenes in medicinal chemistry and their biological applications, Mini-Rev. Med. Chem. 1 (2001) 339–348.
[24] U. Sagman, Application and commercial prospects of fullerenes in medicine and biology, Perspect. Fullerene Nanotechnol. (2002) 145–153.
[25] T. Mashino, Application of fullerenes to medicine, Farumashia 40 (2004) 1023–1027.
[26] R. Bakry, R.M. Vallant, M. Najam-ul-Haq, M. Rainer, Z. Szabo, C.W. Huck, G.K. Bonn, Medicinal applications of fullerenes, Int. J. Nanomed. 2 (2007) 639–649.
[27] S.M. Moghimi, A.C. Hunter, J.C. Murray, Nanomedicine: current status and future prospects, FASEB J. 19 (2005) 311–330.
[28] L.O. Husebo, B. Sitharaman, K. Furukawa, T. Kato, L.J. Wilson, Fullerenols revisited as stable radical anions, J. Am. Chem. Soc. 126 (2004) 12055–12064.
[29] T. Da Ros, M. Prato, Medicinal chemistry with fullerenes and fullerene derivatives, Chem. Commun. 8 (1999) 663–669.
[30] B.H. Chen, J.P. Huang, L.Y. Wang, J. Shiea, T.L. Chen, L.Y. Chiang, Synthesis of octadecahydroxylated C_{70}, Synth. Commun. 28 (1998) 3515–3525.
[31] J.R. Heath, S.C. O'Brien, Q. Zhang, Y. Liu, R.F. Curl, F.K. Tittel, R.E. Smalley, Lanthanum complexes of spheroidal carbon shells, J. Am. Chem. Soc. 107 (1985) 7779–7780.
[32] T. Zuo, M.M. Olmstead, C.M. Beavers, A.L. Balch, G. Wang, G.T. Yee, C. Shu, L. Xu, B. Elliott, L. Echegoyen, J.C. Duchamp, H.C. Dorn, Preparation and structural characterization of the I_h and the D_{5h} isomers of the endohedral fullerenes $Tm_3N@C_{80}$: icosahedral C_{80} cage encapsulation of a trimetallic nitride magnetic cluster with three uncoupled Tm^{3+} ions, Inorg. Chem. (Washington, D.C., U. S.) 47 (2008) 5234–5244.
[33] C.R. Wang, T. Kai, T. Tomiyama, T. Yoshida, Y. Kobayashi, E. Nishibori, M. Takata, M. Sakata, H. Shinohara, A scandium carbide endohedral metallofullerene: $(Sc_2C_2)@C_{84}$, Angew. Chem. Int. Ed. 40 (2001) 397–399.
[34] N. Chen, M.N. Chaur, C. Moore, J.R. Pinzon, R. Valencia, A. Rodriguez-Fortea, J. M. Poblet, L. Echegoyen, Synthesis of a new endohedral fullerene family, $Sc_2S@C_{2n}$ ($n = 40–50$) by the introduction of SO_2, Chem. Commun. 46 (2010) 4818–4820.
[35] L. Dunsch, S. Yang, L. Zhang, A. Svitova, S. Oswald, A.A. Popov, Metal sulfide in a C_{82} fullerene cage: a new form of endohedral clusterfullerenes, J. Am. Chem. Soc. 132 (2010) 5413–5421.
[36] X. Lu, H. Nikawa, T. Nakahodo, T. Tsuchiya, M.O. Ishitsuka, Y. Maeda, T. Akasaka, M. Toki, H. Sawa, Z. Slanina, N. Mizorogi, S. Nagase, Chemical understanding of a non-IPR metallofullerene: stabilization of encaged metals on fused-pentagon bonds in $La_2@C_{72}$, J. Am. Chem. Soc. 130 (2008) 9129–9136.
[37] S. Yang, L. Dunsch, Di- and tridysprosium endohedral metallofullerenes with cages from C_{94} to C_{100}, Angew. Chem. Int. Ed. 45 (2006) 1299–1302.
[38] E.B. Iezzi, J.C. Duchamp, K.R. Fletcher, T.E. Glass, H.C. Dorn, Lutetium-based trimetallic nitride endohedral metallofullerenes: new contrast agents, Nano Lett. 2 (2002) 1187–1190.
[39] R.B. Ross, C.M. Cardona, D.M. Guldi, S.G. Sankaranarayanan, M.O. Reese, N. Kopidakis, J. Peet, B. Walker, G.C. Bazan, E. Van Keuren, B.C. Holloway, M. Drees, Endohedral fullerenes for organic photovoltaic devices, Nat. Mater. 8 (2009) 208–212.
[40] The European Parliament and the Council Regulation (EC) No 1907/2006 concerning the Registration, Evaluation, Authorisation and Restriction of Chemicals (REACH).
[41] The European Parliament resolution on Regulatory aspects of nanomaterials, 2008/2208(INI).
[42] C.M. Sayes, J.D. Fortner, W. Guo, D. Lyon, A.M. Boyd, K.D. Ausman, Y.J. Tao, B. Sitharaman, L.J. Wilson, J.B. Hughes, J.L. West, V.L. Colvin, The differential cytotoxicity of water-soluble fullerenes, Nano Lett. 4 (2004) 1881–1887.
[43] E. Oberdorster, Manufactured nanomaterials (fullerenes, C_{60}) induce oxidative stress in the brain of juvenile largemouth bass, Environ. Health Perspect. 112 (2004) 1058–1062.
[44] G. Andrievsky, V. Klochkov, L. Derevyanchenko, Is the C_{60} fullerene molecule toxic?!, Fullerenes Nanotubes Carbon Nanostruct. 13 (2005) 363–376.
[45] L. Xiao, H. Takada, K. Maeda, M. Haramoto, N. Miwa, Antioxidant effects of water-soluble fullerene derivatives against ultraviolet ray or peroxylipid through their action of scavenging the reactive oxygen species in human skin keratinocytes, Biomed. Pharmacother. 59 (2005) 351–358.
[46] N. Gharbi, M. Pressac, M. Hadchouel, H. Szwarc, S.R. Wilson, F. Moussa, [60] Fullerene is a powerful antioxidant in vivo with no acute or subacute toxicity, Nano Lett. 5 (2005) 2578–2585.
[47] H.T. Ham, Y.S. Choi, I.J. Chung, An explanation of dispersion states of single-walled carbon nanotubes in solvents and aqueous surfactant solutions using solubility parameters, J. Colloid Interface Sci. 286 (2005) 216–223.
[48] S. Zhu, E. Oberdorster, M.L. Haasch, Toxicity of an engineered nanoparticle (fullerene, C_{60}) in two aquatic species, *Daphnia* and *fathead minnow*, Mar. Environ. Res. 62 (Suppl) (2006) S5–S9.
[49] T.B. Henry, F.M. Menn, J.T. Fleming, J. Wilgus, R.N. Compton, G.S. Sayler, Attributing effects of aqueous C_{60} nano-aggregates to tetrahydrofuran decomposition products in larval zebrafish by assessment of gene expression, Environ. Health Perspect. 115 (2007) 1059–1065.
[50] P. Spohn, C. Hirsch, F. Hasler, A. Bruinink, H.F. Krug, P. Wick, C_{60} fullerene: a powerful antioxidant or a damaging agent? The importance of an in-depth material characterization prior to toxicity assays, Environ. Pollut. (Oxford, U. K.) 157 (2009) 1134–1139.
[51] B.C. Seda, P.C. Ke, A.S. Mount, S.J. Klaine, Toxicity of aqueous C_{70}-gallic acid suspension in *Daphnia magna*, Environ. Toxicol. Chem. 31 (2012) 215–220.
[52] C.M. Sayes, J.D. Fortner, W. Guo, D. Lyon, A.M. Boyd, K.D. Ausman, Y.J. Tao, B. Sitharaman, L.J. Wilson, J.B. Hughes, J.L. West, V.L. Colvin, The differential cytotoxicity of water-soluble fullerenes, Nano Lett. 4 (2004) 1881–1887.
[53] T. Mashino, D. Nishikawa, K. Takahashi, N. Usui, T. Yamori, M. Seki, T. Endo, M. Mochizuki, Antibacterial and antiproliferative activity of cationic fullerene derivatives, Bioorg. Med. Chem. Lett. 15 (2003) 4395–4397.
[54] L.L. Dugan, E.G. Lovett, K.L. Quick, J. Lotharious, T.T. Lin, K.L. O'Malley, Fullerene-based antioxidants and neurodegenerative disorders, Parkinsonism Relat. Disord. 7 (2001) 243–246.
[55] J.P. Kamat, T.P.A. Devasagayam, K.I. Priyadarsini, H. Mohan, Reactive oxygen species mediated membrane damage induced by fullerene derivatives and its possible biological implications, Toxicology 155 (2000) 55–61.
[56] J.E. Roberts, A.R. Wielgus, W.K. Boyes, U. Andley, C.F. Chignell, Phototoxicity and cytotoxicity of fullerol in human lens epithelial cells, Toxicol. Appl. Pharmacol. 228 (2008) 49–58.
[57] S. Yamago, H. Tokuyama, E. Nakamura, K. Kituchi, S. Kananishi, K. Sueki, H. Nakahara, S. Enmoto, F. Ambe, In vivo biological behavior of a water-miscible fullerene: ^{14}C labeling, absorption, distribution, excretion and acute toxicity, Chem. Biol. 2 (1995) 385–389.
[58] M. Hassellov, J.W. Readman, J.F. Ranville, K. Tiede, Nanoparticle analysis and characterization methodologies in environmental risk assessment of engineered nanoparticles, Ecotoxicoloxy 17 (2008) 344–361.
[59] B.M. Simonet, M. Valcarcel, Monitoring nanoparticles in the environment, Anal. Bioanal. Chem. 393 (2009) 17–21.
[60] B. Nowack, T.D. Bucheli, Occurence, behavior and effects of nanoparticles in the environment, Environ. Pollut. 150 (2007) 5–22.
[61] A. Nel, T. Xia, L. Mädler, N. Li, Toxic potential of materials at the nanolevel, Science 311 (2006) 622–627.
[62] V.L. Colvin, The potential environmental impact of engineered nanomaterials, Nat. Biotechnol. 21 (2003) 1166–1170.
[63] C.W. Isaacson, M. Kleber, J.A. Field, Quantitative analysis of fullerene nanomaterials in environmental systems: a critical review, Environ. Sci. Technol. 43 (2009) 6463–6474.
[64] Y. Saito, H. Ohta, K. Jinno, Chromatographic separation of fullerenes, Anal. Chem. 76 (2004) 266A–272A.
[65] A. Astefanei, O. Núñez, M.T. Galceran, Liquid chromatography in the analysis of fullerenes, in: S.B. Ellis (Ed.), Fullerenes, Chemistry, Natural Sources and Technological Applications, Nova Science Publishers, New York, 2014, pp. 35–63.
[66] S.J. Klaine, P.J.J. Alvarez, G.E. Batley, T.F. Fernandes, R.D. Handy, D.Y. Lyon, S. Mahendra, M.J. McLaughlin, J.R. Lead, Nanomaterials in the environment: behavior, fate, bioavailability, and effects, Environ. Toxicol. Chem. 27 (2008) 1825–1851.
[67] R.D. Handy, R. Owen, E. Valsami-Jones, The ecotoxicology of nanoparticles and nanomaterials: current status, knowledge gaps, challenges, and future needs, Ecotoxicology 17 (2008) 315–325.
[68] A. Dhawan, J.S. Taurozzi, A.K. Pandey, W. Shan, S.M. Miller, S.A. Hashsham, V. V. Tarabara, Stable colloidal dispersions of C_{60} fullerenes in water: evidence for genotoxicity, Environ. Eng. Sci. 40 (2006) 7394–7401.
[69] J.T. Quik, I. Velzeboer, M. Wouterse, A.A. Koelmans, D. van de Meent, Heteroaggregation and sedimentation rates for nanomaterials in natural waters, Water Res. 48 (2014) 269–279.
[70] J. Sanchis, C. Bosch-Orea, M. Farre, D. Barcelo, Nanoparticle tracking analysis characterisation and parts-per-quadrilion determination of fullerenes in river samples from Barcelona catchment area, Anal. Bioanal. Chem. (2014) , doi:http://dx.doi.org/10.1007/s00216-014-8273-y.
[71] A. Goel, J.B. Howard, J.B. Vander Sande, Size analysis of single fullerene molecules by electron microscopy, Carbon 42 (2004) 1907–1915.
[72] B.W. Smith, M. Monthioux, D.E. Luzzi, Carbon nanotube encapsulated fullerenes: a unique class of hybrid materials, Chem. Phys. Lett. 315 (1999) 31–36.
[73] J. Sloan, R.E. Dunin-Borkowski, J.L. Hutchison, K.S. Coleman, V. Clifford Williams, J.B. Claridge, A.P.E. York, C. Xu, S.R. Bailey, G. Brown, S. Friedrichs, M. H.L. Greeen, The size distribution, imaging and obstructing properties of C_{60} and higher fullerenes formed within arc-grown single walled carbon nanotubes, Chem. Phys. Lett. 316 (2000) 191–198.
[74] A.P. Burden, J.L. Hutchison, In situ fullerene formation – the evidence presented, Carbon 36 (1998) 1167–1173.
[75] A. Mrzel, A. Mertelj, A. Omerzu, M. Copic, D. Mihailovic, Investigation of encapsulation and solvatochromism of fullerenes in binary solvent mixtures, J. Phys. Chem. B 103 (1999) 11256–11260.
[76] R.G. Alargova, S. Deguchi, K. Tsujii, Stable colloidal dispersions of fullerenes in polar organic solvents, J. Am. Chem. Soc. 123 (43) (2001) 10460–10467.
[77] H. Kato, N. Shinohara, A. Nakamura, M. Horie, K. Fujita, K. Takahashi, H. Iwahashi, S. Endoh, S. Kinugasa, Characterization of fullerene colloidal

suspension in a cell culture medium for in vitro toxicity assessment, Mol. BioSyst. 6 (2010) 1238–1246.
[78] C.W. Isaacson, D. Bouchard, Asymmetric flow field flow fractionation of aqueous C_{60} nanoparticles with size determination by dynamic light scattering and quantification by liquid chromatography atmospheric pressure photo-ionization mass spectrometry, J. Chromatogr. A 1217 (2010) 1506–1512.
[79] P. Herrero, P.S. Bäuerlein, E. Emke, E. Pocurull, P. de Voogt, Asymmetrical flow field-flow fractionation hyphenated to Orbitrap high resolution mass spectrometry for the determination of (functionalised) aqueous fullerene aggregates, J. Chromatogr. A 1356 (2014) 277–282.
[80] S. Assemi, S. Tadjiki, B.C. Donose, A.V. Nguyen, J.D. Miller, Aggregation of fullerol $C_{60}(OH)_{24}$ nanoparticles as revealed using flow field-flow fractionation and atomic force microscopy, Langmuir 26 (2010) 16063–16070.
[81] I.V. Mikheev, D.S. Volkov, M.A. Proskurnin, M.V. Korobov, Monitoring of aqueous fullerene dispersions by thermal-lens spectrometry, Int. J. Thermophys. (2015) , doi:http://dx.doi.org/10.1007/x10765-014-1814-y.
[82] H. Lecoanet, J.Y. Bottero, M.R. Wiesener, Laboratory assessment of the mobility of nanomaterials in porous media, Environ. Eng. Sci. 38 (2004) 5164–5169.
[83] K.L. Chen, M. Elimelech, Relating colloidal stability of fullerene (C_{60}) nanoparticles to nanoparticle charge and electrokinetic properties, Environ. Sci. Technol. 43 (2009) 7270–7276.
[84] X. Ma, D. Bouchard, Formation of aqueous suspensions of fullerenes, Environ. Sci. Technol. 43 (2009) 330–336.
[85] K.L. Chen, M. Elimelech, Influence of humic acid on the aggregation kinetics of fullerene nanoparticles in monovalent and divalent electrolyte solutions, Abstracts of Papers, 234th ACS National Meeting, Boston, MA, United States, August 19–23, 2007 ENVR-092.
[86] W. Zhu, D.E. Miser, W.G. Chan, M.R. Hajaligol, Characterization of combustion fullerene soot, C_{60}, and mixed fullerene, Carbon 42 (2004) 1463–1471.
[87] L. Xiao, H. Takada, X. Gana, N. Miwa, The water-soluble fullerene derivative 'Radical Sponge' exerts cytoprotective action against UVA irradiation but not visible-light-catalyzed cytotoxicity in human skin keratinocytes, Bioorg. Med. Chem. Lett. 16 (2006) 1590–1595.
[88] G. Dadalt Souto, A. Raffin Pohlmann, S. Stanisçuaski Gutteres, Ultraviolet A irradiation increases the permeation of fullerenes into human and porcine skin from C_{60}-poly(vinylpyrrolidone) aggregate dispersions, Skin Pharmacol. Physiol. 28 (2015) 22–30.
[89] DermAsia: P. Skin-background. Available at: http://www.dermasia.com.hk/en/pskin-bg.php.
[90] Envie De Neuf: Fullerene C60 Youth Recruit Complx 3.4 fl. oz (100 mL). Available at: http://shop.enviedeneuf.com/Fullerene-C60-Youth-Recruit-Complex-p/s25.htm.
[91] Dr Brandt Skin-Changing Science: LinelessCream. Available at: http://www.drbrandtskincare.com/p/lineless/lineless-cream.
[92] I. Montes-Burgos, D. Walczyk, P. Hole, J. Smith, I. Lynch, K. Dawson, Characterisation of nanoparticle size and state prior to nanotoxicological studies, J. Nanopart. Res. 12 (2010) 47–53.
[93] J.D. Fortner, D.I. Kim, A.M. Boyd, J.C. Falkner, S. Moran, V.L. Colvin, J.B. Hughes, J.H. Kim, Reaction of water-stable C_{60} aggregates with ozone, Environ. Sci. Technol. 41 (2007) 7497–7502.
[94] J.A. Brant, J. Labille, C.O. Robichaud, M. Wiesner, Fullerol cluster formation in aqueous solutions: implications for environmental release, J. Colloid Interface Sci. 314 (2007) 281–288.
[95] G.V. Andrievsky, V.K. Klochkov, A.B. Bordyuh, G.I. Bovbeshko, Comparative study of two aqueous colloidal solutions of C_{60} fullerene with help of FTIR reflactance and UV–vis spectroscopy, Chem. Phys. Lett. 364 (2002) 8–17.
[96] H. Lecoanet, M.R. Wiesner, Velocity effects on fullerene and oxide nanoparticle deposition in porous media, Environ. Sci. Technol. 38 (2004) 4377–4382.
[97] M.R. Wiesner, G. Lowry, P. Alvarez, D. Dionysiou, P. Biswas, Assessing the risks of manufactured nanomaterial, Environ. Sci. Technol. 40 (2006) 4336–4345.
[98] B. Espinasse, E.M. Hotze, M.R. Wiesener, Transport and retention of colloidal aggregates of C_{60} in porous media: effects of organic macromolecules, ionic composition, and preparation method, Environ. Sci. Technol. 41 (2007) 7396–7402.
[99] C.W. Isaacson, D.C. Bouchard, Effects of humic acid and sunlight on the generation and aggregation state of aqu/C_{60} nanoparticles, Environ. Sci. Technol. 44 (2010) 8971–8976.
[100] B. Xie, Z. Xu, W. Guo, Q. Li, Impact of natural organic matter on the physicochemical properties of aqueous C_{60} nanoparticles, Environ. Sci. Technol. 42 (2008) 2853–2859.
[101] B. Sitharaman, S. Asokan, I. Rusakova, M.S. Wong, L.J. Wilson, Nanoscale aggregation properties of neuroprotective carboxyfullerene (C_3) in aqueous solution, Nano Lett. 4 (2004) 1759–1762.
[102] C.W. Isaacson, X. Ma, B. Wigington, T. Burns, Determining aqueous fullerene particle size distributions by asymmetric flow field-flow fractionation (AF4) without surfactants, Abstract of Papers, 238th ACS National Meeting, Washington, DC, United States, August 16–20, 2009 ANYL-338.
[103] E.M. Hotze, T. Phenrat, G.V. Lowry, Nanoparticle aggregation: challenges to understanding transport and reactivity in the environment, J. Environ. Qual. 39 (2010) 1909–1924.
[104] K. Jinno, Y. Saito, Y.L. Chen, G. Luehr, J. Archer, J.C. Fetzer, W.R. Biggs, Separation of C_{60} and C_{70} fullerenes on methoxyphenylpropyl bonded stationary phases in microcolumn liquid chromatography, J. Microcolumn Sep. 5 (1993) 135–140.
[105] D. Heymann, L.P.F. Chibante, R.E. Smalley, Determination of C_{60} and C_{70} fullerenes in geologic materials by high-performance liquid chromatography, J. Chromatogr. A 689 (1995) 157–163.
[106] J.F. Anacleto, M.A. Quilliam, Liquid chromatography/mass spectrometry investigation of the reversed-phase separation of fullerenes and their derivatives, Anal. Chem. 65 (1993) 2236–2242.
[107] Z. Li, X. Wu, G. Zeng, M. Sakai, Y. Muramatsu, Separation and analysis of fullerenes by high-performance liquid chromatography, Fenxi Kexue Xuebao 12 (1996) 220–222.
[108] J. Xiao, M.E. Meyerhoff, High-performance liquid chromatography of C_{60}, C_{70}, and higher fullerenes on tetraphenylporphyrin-silica stationary phases using strong mobile phase solvents, J. Chromatogr. A 715 (1995) 19–29.
[109] D. Bouchard, X. Ma, Extraction and high-performance liquid chromatographic analysis of C_{60}, C_{70}, and [6,6]-phenyl C_{61}-butyric acid methyl ester in synthetic and natural waters, J. Chromatogr. A 1203 (2008) 153–159.
[110] B. Gross, V. Schurig, I. Lamparth, A. Hirsch, Enantiomer separation of [60] fullerene derivatives by micro-column high-performance liquid chromatography using (*R*)-(−)-2-(2,4,5,7-tetranitro-9-fluorenylideneaminooxy) propionic acid as chiral stationary phase, J. Chromatogr. A 791 (1997) 65–69.
[111] T.C. Chao, G. Song, N. Hansmeier, P. Westerhoff, P. Herckes, R.U. Halden, Characterization and liquid chromatography–MS/MS based quantification of hydroxylated fullerenes, Anal. Chem. 83 (2011) 1777–1783.
[112] M. Silion, A. Dascalu, M. Pinteala, B.C. Simionescu, C. Ungurenasu, A study on electrospray mass spectrometry of fullerenol $C_{60}(OH)_{24}$, Beilstein J. Org. Chem. 9 (2013) 1285–1295.
[113] N. Gharbi, S. Burghadt, M. Brettreich, C. Herrenknecht, S. Tamisier-Karolak, R. V. Bensasson, H. Szwarc, A. Hirsch, S.R. Wilson, F. Moussa, Chromatographic separation and identification of a water-soluble dendritic methano[60] fullerene octadecaacid, Anal. Chem. 75 (2003) 4217–4222.
[114] B. Natalini, V. Capodiferro, L. Mattoli, M. Marinozzi, G. Constantino, R. Pellicciari, Chromatographic separation and evaluation of the lipophilicity by reversed-phase high-performance liquid chromatography of fullerene-C_{60} derivatives, J. Chromatogr. A 847 (1999) 339–343.
[115] A. Kolkman, E. Emke, P.S. Baeuerlein, A. Carboni, D.T. Tran, T.L. ter Laak, A.P. van Wezel, P. de Voogt, Analysis of (functionalized) fullerenes in water samples by liquid chromatography coupled to high-resolution mass spectrometry, Anal. Chem. 85 (2013) 5867–5874.
[116] R.S. Ruoff, D.S. Tse, R. Malhotra, D.C. Lorents, Solubility of fullerene (C_{60}) in a variety of solvents, Phys. Chem. B 97 (1993) 3379–3382.
[117] A. Astefanei, O. Núñez, M.T. Galceran, Analysis of fullerenes and C_{60}-fullerene derivatives in environmental samples by liquid chromatography–atmospheric pressure photoionization–mass spectrometry, J. Chromatogr. A 1365 (2014) 61–71.
[118] H. Ohta, Y. Saito, N. Nagae, J.J. Pesek, M.T. Matyska, K. Jinno, Fullerenes separation with monomeric type C_{30} stationary phase in high-performance liquid chromatography, J. Chromatogr. A 883 (2000) 55–66.
[119] Cosmosil Buckyprep column, Nacalai USA, Inc. Available at: http://www.nacalaiusa.com/product.php?id=22.
[120] C. Wang, C. Shang, P. Westerhoff, Quantification of fullerene aggregate nC_{60} in wastewater by high-performance liquid chromatography with UV–vis spectroscopic and mass spectrometric detection, Chemosphere 80 (2010) 334–339.
[121] S.R. Chae, E.M. Hotze, Y. Xiao, J. Rose, M.R. Wiesner, Comparison of methods for fullerene detection and measurements of reactive oxygen production in cosmetic products, Environ. Eng. Sci. 27 (2010) 797–804.
[122] J. Sanchis, L.F. Oliviera, F.B. Leão, M. Farre, D. Barcelo, Liquid chromatography–atmospheric pressure photoionization–Orbitrap analysis of fullerene aggregates on surface soils and river sediments from Santa Catarina (Brazil), Sci. Total Environ. 505 (2015) 172–179.
[123] K. Kimata, K. Hosoya, T. Araki, N. Tanaka, [2-(1-Pyrenyl)ethyl]silyl silica packing material for liquid chromatographic separation of fullerenes, J. Org. Chem. 58 (1993) 282–283.
[124] A. Carboni, E. Emke, J.R. Parsons, K. Kalbitz, P. de Voogt, An analytical method for determination of fullerenes and functionalized fullerenes in soils with high performance liquid chromatography and UV detection, Anal. Chim. Acta 807 (2014) 159–165.
[125] Q.W. Yu, Z.G. Shi, B. Lin, Y. Wu, Y.Q. Feng, HPLC separation of fullerenes on two charge-transfer stationary phases, J. Sep. Sci. 29 (2006) 837–843.
[126] Q.W. Yu, Y.Q. Feng, Z.G. Shi, J. Yang, HPLC separation of fullerenes on the stationary phases of two Lewis bases modified magnesia–zirconia, Anal. Chim. Acta 536 (2005) 39–48.
[127] D.E. Coutant, S.A. Clarke, A.H. Francis, M.E. Meyerhoff, Selective separation of fullerenes on hydroxyphenyl-triphenylporphyrin-silica stationary phases, J. Chromatogr. A 824 (1998) 147–157.
[128] Y. Wang, D.I. Schuster, S.R. Wilson, Chemoselective synthesis and resolution of chiral [1,9] methanofullerene[70] derivatives, J. Org. Chem. 61 (1996) 5198–5199.
[129] P. Rajagopalan, F. Wudl, R.F. Schinazi, D. Boudinot, Pharmacokinetics of a water-soluble fullerene in rats, Antimicrob. Agents Chemother. 40 (1996) 2262–2265.

[130] A. Astefanei, O. Nunez, M.T. Galceran, Non-aqueous capillary electrophoresis separation of fullerenes and C_{60} fullerene derivatives, Anal. Bioanal. Chem. 404 (2012) 307–313.
[131] T.S.M. Wan, G.N.W. Leung, T.S.C. Tso, K. Komatsu, Y. Murata, Non-aqueous capillary electrophoresis as a new method for the separation of fullerenes, Proc. Electrochem. Soc. 95 (1995) 1474–1487.
[132] H.L. Su, W.C. Kao, C.y. Lee, S.C. Chuang, Y.Z. Hsieh, Separation of open-cage fullerenes using nonaqueous capillary electrophoresis, J. Chromatogr. A 1217 (2010) 4471–4475.
[133] J.M. Treubig, P.R. Brown, Novel approach to the analysis and use of fullerenes in capillary electrophoresis, J. Chromatogr. A 873 (2000) 257–267.
[134] K.C. Chan, A.K. Patri, T.D. Veenstra, S.E. McNeil, H.J. Issaq, Analysis of fullerene-based nanomaterial in serum matrix by CE, Electrophoresis 28 (2007) 1518–1524.
[135] S.L. Tamisier-Karolak, S. Pagliarusco, C. Herrenknecht, M. Brettreich, A. Hirsch, R. Ceolin, R.V. Bensasson, H. Szwarc, F. Moussa, Electrophoretic behavior of a highly water-soluble dendro[60]fullerene, Electrophoresis 22 (2001) 4341–4346.
[136] J. Cerar, M. Pompe, M. Gucek, J. Cerkovnik, J. Skerjanc, Analysis of sample of highly water-soluble Th- symmetric fullerenehexamalonic acid $C_{66}(COOH)_{12}$ by ion-chromatography and capillary electrophoresis, J. Chromatogr. A 1169 (2007) 86–94.
[137] D.B. Robb, T.R. Covey, A.P. Bruins, Atmospheric pressure photoionization: an ionization method for liquid chromatography–mass spectrometry, Anal. Chem. 72 (2000) 3653–3659.
[138] A. Raffaelli, A. Saba, Atmospheric pressure photoionization mass spectrometry, Mass Spectrom. Rev. 22 (2003) 318–331.
[139] I. Marchi, S. Rudaz, J.L. Veuthey, Atmospheric pressure photoionization for coupling liquid-chromatography to mass spectrometry: a review, Talanta 78 (2009) 1–18.
[140] L. Song, A.D. Wellman, H. Yao, J. Adcock, Electron capture atmospheric pressure photoionization mass spectrometry: analysis of fullerenes, perfluorinated compounds, and pentafluorobenzyl derivatives, Rapid Commun. Mass Spectrom. 21 (2007) 1343–1351.
[141] A.P. van Wezel, V. Moriniere, E. Emke, T. ter Laak, A.C. Hogenboom, Quantifying summed fullerene nC_{60} and related transformation products in water using LC LTQ Orbitrap MS and application to environmental samples, Environ. Int. 37 (2011) 1063–1067.
[142] C.W. Isaacson, C.Y. Usenko, R.L. Tanguay, J.A. Field, Quantification of fullerenes by LC/ESI-MS and its application to in vivo toxicity assays, Anal. Chem. 79 (2007) 9091–9097.
[143] M. Farre, S. Perez, K. Gajda- Schrantz, V. Osorio, L. Kantiani, A. Ginebreda, D. Barcelo, First determination of C_{60} and C_{70} fullerenes and *N*-methylfulleropyrrolidine C_{60} on the suspended material of wastewater effluents by liquid chromatography hybrid quadrupole linear ion trap tandem mass spectrometry, J. Hydrol. 383 (2010) 44–51.
[144] O. Núñez, H. Gallart-Ayala, C.P.B. Martins, E. Moyano, M.T. Galceran, Atmospheric pressure photoionization mass spectrometry of fullerenes, Anal. Chem. 84 (2012) 5316–5326.
[145] H.C. Chen, W.H. Ding, Determination of aqueous fullerene aggregates in water by ultrasound-assisted dispersive liquid–liquid microextraction with liquid chromatography–atmospheric pressure photoionization–tandem mass spectrometry, J. Chromatogr. A 1223 (2012) 15–23.
[146] L. Li, S. Huhtala, M. Sillanpaeae, P. Sainio, Liquid chromatography–mass spectrometry for C_{60} fullerene analysis: optimisation and comparison of three ionisation techniques, Anal. Bioanal. Chem. 403 (2012) 1931–1938.
[147] S.i. Kawano, H. Murata, H. Mikami, K. Mukaibatake, H. Waki, Method optimization for analysis of fullerenes by liquid chromatography/atmospheric pressure photoionization mass spectrometry, Rapid Commun. Mass Spectrom. 20 (2006) 2783–2785.
[148] T.J. Kauppila, T. Kotiaho, R. Kostiainen, A.P. Bruins, Negative ion-atmospheric pressure photoionization-mass spectrometry, J. Am. Soc. Mass Spectrom. 15 (2004) 203–211.
[149] L.Y. Chiang, J.B. Bhonsle, L. Wang, S.F. Shu, T.M. Chang, J.R. Hwu, Efficient one-flask synthesis of water-soluble [60]fullerenols, Tetrahedron 52 (1996) 4963–4972.
[150] X.R. Xia, N.A. Monteiro-Riviere, J.E. Riviere, Trace analysis of fullerenes in biological samples by simplified liquid–liquid extraction and high-performance liquid chromatography, J. Chromatogr. A 1129 (2006) 216–222.
[151] F. Moussa, M. Pressac, E. Genin, S. Roux, F. Trivin, A. Rassat, R. Ceolin, H. Szwarc, Quantitative analysis of C_{60} fullerene in blood and tissues by high-performance liquid chromatography with photodiode-array and mass spectrometric detection, J. Chromatogr. B: Biomed. Sci. Appl. 696 (1997) 153–159.
[152] T.M. Benn, P. Westerhoff, P. Herckes, Detection of fullerenes (C_{60} and C_{70}) in commercial cosmetics, Environ. Pollut. 159 (2011) 1334–1342.
[153] A. Kolkman, E. Emke, P.S. Baeuerlein, A. Carboni, D.T. Tran, T.L. ter Laak, A.P. van Wezel, P. de Voogt, Analysis of (functionalized) fullerenes in water samples by liquid chromatography coupled to high-resolution mass spectrometry, Anal. Chem. 85 (2013) 5867–5874.
[154] E. Emke, J. Sanchis, M. Farre, P.S. Bäuerlein, P. de Voogt, Determination of several fullerenes in sewage water by LC HR-MS using atmospheric pressure photoionisation, Environ. Sci. (2015) , doi:http://dx.doi.org/10.1039/C4EN00133H.
[155] D. Heymann, A. Korochantsev, M.A. Nazarov, J. Smit, Search for fullerenes C_{60} and C_{70} in Cretaceous–Tertiary boundary sediments from Turkmenistan, Kazakhstan, Georgia, Austria, and Denmark, Cretaceous Res. 17 (1996) 367–380.
[156] J. Sanchis, N. Berrojalbiz, G. Caballero, J. Dachs, M. Farre, D. Barcelo, Occurrence of aerosol-bound fullerenes in the Mediterranean Sea atmosphere, Environ. Sci. Technol. 46 (2012) 1335–1343.
[157] J. Sanchis, D. Bozovic, N.A. Al-Harbi, L.F. Silva, M. Farre, D. Barcelo, Quantitative trace analysis of fullerenes in river sediment from Spain and soils from Saudi Arabia, Anal. Bioanal. Chem. 405 (2013) 5915–5923.
[158] R.A. Perez, B. Albero, E. Miguel, J.L. Tadeo, C. Sanchez-Brunete, A rapid procedure for the determination of C_{60} and C_{70} fullerenes in soil and sediments by ultrasound-assisted extraction and HPLC-UV, Anal. Sci. 29 (2013) 533–538.
[159] A. Shareef, G. Li, R.S. Kookana, Quantitative determination of fullerene (C_{60}) in soils by high performance liquid chromatography and accelerated solvent extraction technique, Environ. Chem. 7 (2010) 292–297.
[160] J. Jehlicka, O. Frank, V. Hamplova, Z. Pokorna, L. Juha, Z. Bohacek, Z. Weishauptova, Low extraction recovery of fullerene from carbonaceous geological materials spiked with C_{60}, Carbon 43 (2005) 1909–1917.
[161] R.L. Hartmann, R.S.K. Williams, Flow field-flow fractionation as an analytical technique to rapidly quantitate membrane fouling, J. Membrane Sci. 209 (2002) 93–106.
[162] Y. Kiso, Y. Sugiura, T. Kitao, K. Nishimura, Effects of hydrophobicity and molecular size on rejection of aromatic pesticides with nanofiltration membranes, J. Membrane Sci. 192 (2001) 1–10.
[163] J. Cho, G. Amy, J. Pellegrino, Membrane filtration of natural organic matter: factors and mechanisms affecting rejection and flux decline with charged ultrafiltration (UF) membrane, J. Membrane Sci. 164 (2000) 89–110.
[164] European Commission, Commission Decision of 12 August 2002 Implementing Council Directive 96/23/EC Concerning the Performance of Analytical Methods and the Interpretation of Results, European Commission, Brussels, 2002.
[165] Isotope labelled fullerene internal standard, $^{13}C_{60}$. Available at: http://www.nanomaterials.iolitec.de/Nanomaterialien/fullerene.html.
[166] Pickering, M.R. Wiesner, Fullerol-sensitized production of reactive oxygen species in aqueous solution, Environ. Sci. Technol. 39 (2005) 1359–1365.
[167] R. Sijbesma, G. Srdanov, F. Wudl, J.A. Castoro, C.W. Wilkins, S.H. Friedman, D.L. DeCamp, G.L. Kenyol, Synthesis of a fullerene derivative for the inhibition of HIV enzymes, J. Am. Chem. Soc. 115 (1993) 6510–6612.

CHAPTER 2

ANALYSIS OF FULLERENES

2.1. Introduction

Up to now, few quantitative analytical methods, mostly LC and CE with UV detection or coupled to MS, are available for measuring the presence of this family of compounds in natural systems, resulting in a serious lack of information on their occurrence in industrial products and in the environment. Taking into account the increasing use of fullerenes in different sectors (i.e., industrial, biological and cosmetic applications), developing sensitive and reliable analytical methodologies capable of accurately identifying and detecting relevant concentrations of these compounds in complex samples becomes imperative and represents a logical step towards the assessment of the risks posed by them. Moreover, it must be noticed that the most used fullerenes in technical applications are the functionalised ones and despite this fact, most of the reported studies are focused on the analysis of pristine fullerenes that may not be relevant for assessing the presence of fullerenes in commercial products, biological fluids and in the environment. For instance, only few works have been published (Table 4, Section 1.3.1, Chapter 1) about the analysis of functionalised compounds mainly referred to the hydrophobic ones (i.e., C_{60} pyrr, PCBM, C_{70}-PCBM, bis-PCBM, PCBB, ThCBM) and there is a lack of methodologies for the analysis of water soluble fullerene derivatives which present increasing applications especially in the biomedical field.

This chapter describes the development of analytical methodologies using liquid chromatography and capillary electrophoresis for the determination of pristine and surface modified fullerenes in complex samples.

Regarding the analysis of hydrophobic fullerenes by liquid chromatography reversed phase columns, mainly C18 (Núñez et al., 2012; Chen et al., 2012; Perez et al., 2013), have been currently used for their separation. However, some authors proposed the use of specifically developed columns (i.e., Buckyprep) (Wang et al., 2010; Sanchis et al., 2015b) but higher analysis times, up to 30 min, are obtained (Table 4, Section 1.3.1, Chapter 1). As mobile phase, 100% toluene is used in order to solubilise the fullerenes although mixtures of toluene and a polar organic solvent (methanol or acetonitrile) have been also proposed to improve the separation between the compounds. In this thesis, in order to reduce toluene consumption and to obtain short analysis times, while maintaining a good chromatographic separation, a sub-2 μm C18 column was employed following a method previously proposed in our research group for the analysis of pristine fullerenes (Núñez et al., 2012). By using this C18 column, the separation of five pristine fullerenes (C_{60}-C_{84}) was achieved in less than 3.5 min, achieving symmetric and sharp peaks under isocratic elution (toluene/methanol, 45:55 *v/v*).

For the detection of fullerenes, both UV-Vis and MS have been reported. Nowadays, LC-MS is without any doubt the best choice to fulfil the legal requirements for unequivocal identification and confirmation of positive/negative samples posed by the European Union directive 2002/657/EC (European Commission, 2002) and it was selected to be used in our study. As ionisation sources, electrospray (ESI), atmospheric pressure chemical ionization (APCI) and atmospheric pressure photoionization (APPI), have been used (Table 4, Section 1.3.1, Chapter 1). This last interface was proposed in the previous paper published in our research group (Núñez et al., 2012) and presents the advantage of an important increase in sensitivity in front of other ionization sources such as ESI and APCI that is related to the use of toluene in the chromatographic mobile phase. In APPI the liquid sample is vaporised in a heated nebuliser similar to the one in APCI and the photons emitted by a krypton discharge lamp initiate a series of gas-phase reactions that lead to the ionisation of the analytes. A schematic diagram of an APPI source is presented in Figure 1. However, direct ionization of an analyte molecule occurs with a low statistical probability, partly because the solvent depletes the photons emitted by the discharge lamp (Raffaelli et al., 2003). To increase the number of ions, a suitable substance called dopant must be added in larger amounts than the analyte. This dopant is effective if it is photoionisable, possessing an effective ionisation energy (lower than the photon energy of the emitted light) and can act as an intermediate between the photons and the analytes reacting with them by charge exchange or proton transfer (Harrison et al., 1983).

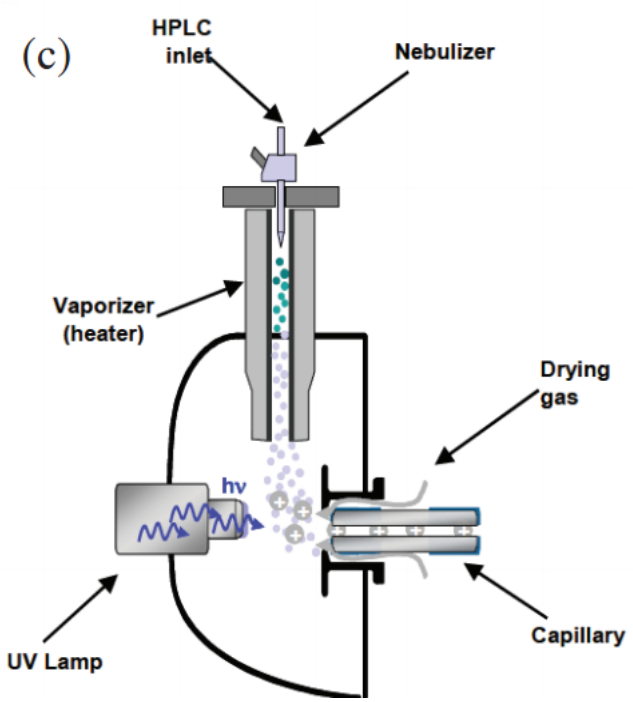

Figure 1. Schematic diagram of APPI source. Photograph used courtesy of Thermo Fisher Scientific; copying prohibited.

Fullerene ionisation in APPI occurs through a solvent mediated (toluene) ionisation mechanism by electron capture yielding the radical molecular ion $[M]^{-\bullet}$ (Kawano et al., 2006). The formation of negative molecular fullerene ions by electron capture is possible for these compounds because they present positive electron affinity (≈ 2.7-3.0 eV for C_{60}-C_{92}) (Botalina et al., 1993; Wang et al., 1999). The ionisation process starts with the formation of toluene cations and electrons, since the ionisation energy of toluene (approx. 8.82) is lower that the photon energy of the APPI source (10 eV), and the electrons are further captured by fullerene molecules (Harrison et al., 1983) as follows:

$$C_7H_8 + h\upsilon \rightarrow C_7H_8^{+} + e^{-}$$
$$[M] + e^{-} \rightarrow [M]^{-\bullet}$$

Among the advantages in using APPI for the ionisation of pristine fullerenes, is that the adduct formation with oxygen, hydrogen, methanol and toluene is reduced dramatically compared to ESI and, consequently, the sensitivity is enhanced (Emke et al., 2015). Moreover, better limits of detection and quantification than those obtained with the other interfaces (Table 4, section 1.3.1., Chapter 1) are reported as well as more reproducible signals and less susceptibility to ion suppression by matrix effects compared to ESI and APCI (Núñez et al., 2012; Emke et al., 2015). Due to the previously proven benefits in using this ionisation source for fullerene analysis, APPI was used in this thesis as ionisation source for the LC-MS study included in this chapter.

In contrast to liquid chromatography, the employment of CE techniques for the separation of fullerenes is very limited. CE separates compounds that differ in charge to hydrodynamic size ratio being an excellent technique for the analysis of polar compounds that easily acquire a charge, but its application to the separation of hydrophobic fullerenes showed important limitations due to their low solubility in the aqueous buffers used as BGE, and their lack of charge. To overcome these drawbacks and induce their electrophoretic mobility, MECC (Treubig et al., 2000) and NACE (Wan et al., 1995; Su et al., 2010) by employing a surfactant above the critical micellar concentration in aqueous buffers and charged compounds (i.e., tetraalkylammonium salts, sodium acetate) able to interact with the analytes to form charged complexes in organic solvent mixtures (i.e., chlorobenzene, acetonitrile, methanol, acetic acid), respectively, have been proposed. As previously mentioned, in NACE the separation medium is comprised totally of one or a mixture of organic solvents representing a major advantage when the objective of the study is the separation of compounds that are not readily soluble in water or that show very similar electrophoretic mobility in aqueous media, such as fullerenes. In NACE,

there are a number of advantages compared to the use of aqueous electrolytes for the separation of small molecules. For instance, the improved homogeneity due to less aggregation and thus better solubility of hydrophobic compounds may account for better resolution (Wan et al., 1995). Additionally, non-aqueous solvents are favourable not only for solubility enhancement but also for separation selectivity. Since a wide range of organic solvents can be used, this represents an additional flexibility for optimisation of the separation and the selectivity can be significantly improved by changing the nature of the organic solvent or by mixing appropriate solvents. The increased selectivity of the separation in organic solvents compared to aqueous systems is due to the fact that the levelling effect of water is eliminated (Hansen et al., 2000). Moreover, the use of non-aqueous BGE in NACE allows for higher voltages to be applied than when using aqueous electrolytes and consequently, the analysis time can be significantly reduced and higher peak efficiencies may be achieved. An important practical consequence of using a non-aqueous separation medium is that the extracts comprising organic solvents resulting from the sample preparation procedure can be injected directly into the system, thereby saving time. One of the main difficulties in NACE is finding a suitable electrolyte due to the low solubility of many electrolytes in organic solvents. For the separation of pristine fullerenes by NACE (C_{60}, C_{70}, C_{84}) the employment of quaternary ammonium salts (TDAB and TEAB) and organic solvent mixtures of acetonitrile, chlorobenzene and acetic acid as BGE was reported (Wan et al., 1995) and these conditions were used in this thesis as initial BGE for the separation of pristine and surface modified fullerenes. Nevertheless, the disadvantage posed by the use of such salts in the BGE makes incompatible the coupling to mass spectrometry which represents a limitation in the application of this technique.

MECC was also used for the analysis of C_{60} and C_{70} using SDS micelles and sodium tetraborate-sodium phosphate buffers, but their separation could not be achieved, because the compounds presented the same electrophoretic mobility (Treubig et al., 2000). Regarding water soluble fullerenes, CZE and MECC have been reported for the separation of carboxy- and dentro-fullerenes employing aqueous buffers and SDS micelles (Tamisier-Karolak et al., 2001; Chan et al., 2007; Cerar et al., 2007). In this thesis, the applicability of both MECC and NACE, has been evaluated for the analysis of hydrophobic and water soluble fullerenes. The results obtained for NACE are included in this chapter while those of MECC which were more related to the characterisation of fullerenes are included in Chapter 3.

One important aspect in the analysis of complex samples is the extraction and separation of the analytes from the matrix. In general, for fullerenes, liquid-liquid extraction (LLE) with toluene is the method mostly used for their extraction from environmental waters (Bouchard et

al., 2008; Isaacson et al., 2009; Wang et al., 2010), biological samples (Moussa et al., 1997; Xia et al., 2006; Isaacson et al., 2007) and cosmetics (Benn et al., 2011). In this context, it is important to remember that in environmental waters fullerenes are present as aggregates and so, the addition of salts is recommended in order to disrupt the stability of the aggregates helping the recovery in the organic solvent. For the extraction of fullerenes from solid samples, generally environmental ones, such as soils, sediments, airborne particulate and water suspended solids, ultrasound assisted extraction (UAE) with toluene is the method currently used (Sanchis et al., 2012; Sanchis et al., 2013; Perez et al., 2013; Carboni et al., 2014; Sanchis et al., 2015b). It is well known that the extraction efficiency in UAE depends on the extraction time, and longer extraction time usually yield higher recoveries of the target analytes (Mitra, 2004) and for this reason some authors used up to 4 hours extraction times (Sanchis et al., 2013). However, low recoveries were reported by using this method, especially for some fullerene derivatives (see Table 4, Section 1.3.1., Chapter 1), and consequently, a different strategy, using pressurized liquid extraction (PLE), is proposed in this thesis. The use of PLE offers several advantages and it is among the most widely used extraction methods of solid and semi-solid samples (Mitra, 2004). PLE is mostly performed at high pressures and temperatures, and consequently the solvents tend to penetrate the solid samples at a high rate and supply a fast and efficient extraction (Mitra, 2004). Temperature is an important factor influencing the extraction efficiency of the analytes in PLE, as it can decrease the viscosity of solvents and promote the diffusion of the analytes to the solvents, which may be strongly bonded to the soil/sediment components as previously reported for PAHs (Saleh et al., 2009). Another advantage is that for packing the sample in the extractor, drying materials (Na_2SO_4) may be used as a desiccant to reduce the moisture and as a disperser to increase the permeation of the solvents into the sample matrices. In addition, to prevent the aggregation of sample particles and to yield an efficient extraction, diatomaceous earth, hydromatrix, silica or acidic alumina can be used (Mitra, 2004). Moreover, faster extraction times and lower solvent consumption may be achieved by PLE compared to UAE. Furthermore, PLE presents some obvious advantages such as high-level automation, high extraction efficiency, improved safety and good environmental compatibility.

Regarding the types of the samples analysed, most of the reported methods are dedicated to the quantitation of pristine fullerenes, in environmental samples, and only a few are devoted to their analysis in cosmetics and biological samples. Specifically, in relation to the analysis of environmental samples, the number of reports dealing with the analysis of fullerenes in environmental waters is significantly higher than those for soils,

sediments and airborne particulates. The fullerenes most frequently studied and most commonly detected are C_{60} and C_{70}, although recently the presence of C_{84} and of a hydrophobic C_{60}-derivative (C_{60}-pyrr) in water samples has been also reported. The concentration of these compounds in environmental samples is low and levels of pg L^{-1} in water samples and from fg g^{-1} to pg g^{-1} in sediments and soils have been reported. With regard to the application of CE techniques for the analysis of fullerenes, there is only one report on the analysis of water soluble fullerenes (carboxy fullerene (C3) and dentro[60]fullerene) in a spiked serum matrix (Chan et al., 2007) and no works dedicated to the analysis of environmental and cosmetic samples have been published. Therefore, there is a need of sensitive and accurate methodologies for the analysis of both pristine and surface modified fullerenes in complex matrices, especially sediments, cosmetics and biological samples.

In order to fill these gaps, in this thesis, a fast and sensitive UHPLC-(-)APPI-MS/MS method for the simultaneously analysis of pristine and surface modified fullerenes was developed and applied to the analysis of both sediments and water samples. Moreover, a NACE-UV method for the quantitation of C_{60} cosmetic products was established. Both methods are included in the next sections of this chapter.

The first section of this chapter includes the paper entitled: "*Analysis of C60-fullerene derivatives and pristine fullerenes in environmental samples by ultrahigh performance liquid chromatography-atmospheric pressure photoionization-mass spectrometry*" published in the Journal of Chromatography A, **1365**: 61-71 (2014). As commented above, this work was based on the LC-MS method previous developed in our research group (Núñez et al., 2012) and was extended including three C_{60}-derivatives with increasing industrial applications (C_{60}-pyrr, PCBB and PCBB). The effect of the chromatographic conditions (i.e., column particle and pore size, mobile phase composition) on the separation of the target analytes was studied. Different API interfaces (ESI, APCI and APPI) were evaluated for the ionisation of the three C_{60}-derivatives and their MS/MS spectra was studied in order to characterise the product ions and to select the most abundant and selective ones for quantitation and confirmation purposes. The developed method was applied to the analysis of environmental water samples and sediments. For the extraction of sediments, a PLE method was established. Finally, the developed methodology was used to evaluate the presence of the selected analytes in environmental samples collected from a highly industrialised area (close to Barcelona's airport).

The last section includes the paper entitled: "*Non-aqueous capillary electrophoresis separation of fullerenes and C60 fullerene derivatives*" published in Analytical and Bioanalytical Chemistry, **404**: 307-

313 (2012). In this work, the effect of the composition of the background electrolyte on the separation of two pristine and two C_{60}-fullerene derivatives was thoroughly studied in order to understand the specific role of each component and the method was successfully applied for the quantitation of C_{60} in a cosmetic product. This sample was selected for two reasons. The first one being the current lack of methodologies for the determination of fullerenes in this kind of samples although, according to the consumer products inventory of nanotechnology, about one third of these products is represented by cosmetics (i.e., skin-care) and sunscreen lotions (Inventory of nanotechnology, 2013). The second reason was the relatively high C_{60} concentration (up to 1.1 $\mu g\ g^{-1}$) present in cosmetic products making it suitable to be quantified by NACE.

CHAPTER 2

ANALYSIS OF FULLERENES

2.2. Scientific article II: Analysis of C60-fullerene derivatives and pristine fullerenes in environmental samples by ultrahigh performance liquid chromatography-atmospheric pressure photoionization-mass spectrometry

A. Astefanei, O. Núñez and M.T. Galceran

Journal of Chromatography A, **1365**: 61-71 (2014).

Journal of Chromatography A, 1365 (2014) 61–71

Contents lists available at ScienceDirect

Journal of Chromatography A

journal homepage: www.elsevier.com/locate/chroma

Analysis of C_{60}-fullerene derivatives and pristine fullerenes in environmental samples by ultrahigh performance liquid chromatography–atmospheric pressure photoionization-mass spectrometry

Alina Astefanei, Oscar Núñez *, Maria Teresa Galceran

Department of Analytical Chemistry, University of Barcelona, Martí i Franquès 1-11, E08028 Barcelona, Spain

ARTICLE INFO

Article history:
Received 24 March 2014
Received in revised form 7 July 2014
Accepted 27 August 2014
Available online 2 September 2014

Keywords:
C_{60}-fullerene derivatives
Pristine fullerene
APPI
Ultrahigh performance liquid chromatography
Mass spectrometry
Environmental samples

ABSTRACT

In this work, a method is proposed for the simultaneous analysis of several pristine fullerenes (C_{60}, C_{70}, C_{76}, C_{78}, and C_{84}) and three C_{60}-fullerene derivatives (N-methyl fulleropyrrolidine, [6,6]-phenyl C_{61} butyric acid methyl ester and [6,6]-phenyl C_{61} butyric acid butyl ester) in environmental samples. The method involves the use of ultrahigh performance liquid chromatography coupled to atmospheric pressure photoionization mass spectrometry (UHPLC–APPI-MS) and allowed the chromatographic separation in less than 4.5 min. The product ions from tandem mass spectrometry studies of fullerene derivatives were characterized and the most abundant one (m/z 720), corresponding to $[C_{60}]^{-\bullet}$, was selected for quantitation. Selected reaction monitoring (SRM at 0.7 m/z FWHM) by acquiring two transitions using both isotopic cluster ions $[M]^{-\bullet}$ and $[M+1]^{-\bullet}$ as precursor ions was proposed for quantitation and confirmation purposes. For pristine fullerenes, highly selective selected ion monitoring (H-SIM) acquisition mode by monitoring the isotopic cluster ions $[M]^{-\bullet}$ and $[M+1]^{-\bullet}$ was used. Pressurized solvent extraction conditions were optimized in order to improve recoveries of the studied fullerene compounds from sediment samples. Values up to 87–92% for C_{60}-fullerene derivatives and lower but still acceptable, 70–80%, for pristine fullerenes were obtained. Method limits of quantitation (MLOQs) ranging from 1.5 pg L^{-1} to 5.5 ng L^{-1} in water samples and from 0.1 ng kg^{-1} to 523 ng kg^{-1} in sediments were obtained with good precision (relative standard deviations always lower than 13%). The applicability of the developed method was evaluated by analyzing several environmental samples such as sediments and pond water and the detected levels for C_{60}-fullerene derivatives were of 0.1–2.7 ng kg^{-1} and 1.5–8.5 pg L^{-1}, respectively. C_{60} and C_{70} were the only pristine fullerenes detected in the analyzed samples (0.1–7.2 ng kg^{-1} in sediments and 9–330 pg L^{-1} in water pond samples).

© 2014 Elsevier B.V. All rights reserved.

1. Introduction

Since their discovery [1], fullerenes have gained a prime role on the scientific scene because of their exceptional properties and versatility. Fullerenes are used in a wide range of applications such as in optical and electronic devices (polymer additives, solar cells, photovoltaic and electro-optical devices) [2], in commercial cosmetic products [3], as well as in biomedicine (antiviral, anticancer, and antioxidant agents, in drug delivery systems, or as gene carriers) [4]. Nevertheless, nowadays surface-functionalized fullerenes are produced in larger quantities than empty fullerenes in an attempt to create more biologically compatible forms [5,6]. The most common modification of fullerenes consists of the addition of esters of the butyric acid as in [6,6]-phenyl C_{61} butyric acid methyl ester (PCBM) and [6,6]-phenyl C_{61} butyric acid butyl ester (PCBB) and also the addition of azomethineylide groups to form N-methylfulleropyrrolidines. N-methyl fulleropyrrolidine (C_{60}-pyrr) is being used as an intermediate for the synthesis of other fullerene compounds with medical and biological applications [7] and PCBM and PCBB are commonly used as electron acceptors in solar cells [8,9]. Pristine fullerenes, mostly C_{60} and C_{70}, are used in cosmetic products due to their antioxidant behavior [10] as well as in organic photovoltaic cells [11]. The industrial scale production (currently exceeding several tones/year) and extensive use of fullerenes and fullerene derivatives [12] would increase human and environmental exposure although it has been reported that they also occur

* Corresponding author. Tel.: +34 93 403 3706; fax: +34 93 402 1233.
E-mail addresses: oscar.nunez@ub.edu, oscarnubu@yahoo.es (O. Núñez).

http://dx.doi.org/10.1016/j.chroma.2014.08.089
0021-9673/© 2014 Elsevier B.V. All rights reserved.

in a variety of natural materials [13]. The potential toxicity of fullerene compounds is an intensely debated issue. Several reports showed that pristine fullerenes are non-toxic and that they have a wide spectrum of positive and unique biological activity while other works are suggesting the possibility of some adversary effects [3,14].

Nowadays, these compounds are being considered emerging contaminants hence, sensitive and reliable methods for their analysis in environmental samples are needed. Chromatographic separation of fullerenes has been studied since the 1990s [15,16] but their detection in environmental samples occurred only recently [17–20]. This partly due to the lack of methodology for the detection and characterization of fullerene compounds, especially functionalized fullerenes, in complex matrices, i.e., water and soil. Among the analytical methods reported in the literature for fullerene determination in environmental samples [17–20], liquid chromatography–mass spectrometry (LC–MS) is the method of choice for the quantification of low concentrations of fullerenes, and the use of MS analyzers of both low [21] and high resolution [22,23], has been described. Regarding ionization sources, electrospray ionization (ESI) and atmospheric pressure chemical ionization (APCI) are the most frequently used [21,24–27] although lately, atmospheric pressure photoionization (APPI) has been proposed for the analysis of fullerenes in water samples [27–29]. Most of the reported studies focus on the analysis of pristine fullerenes, especially C_{60} and C_{70} [18,21,22,28–30] and only few studies describe analytical methodologies for some functionalized fullerenes [21,23,31]. Most of the works dealing with the analysis of environmental samples are devoted to the determination of pristine fullerenes, especially C_{60} and C_{70} in industrial effluents and surface waters [29], although recently their presence has also been reported in airborne samples from the Mediterranean Sea as well as in some soil and sediment samples [32]. Only one paper in the literature [21] reported the presence of a C_{60}-fullerene derivative, C_{60}-pyrr, in wastewater treatment plant effluents.

For the extraction of fullerenes from environmental waters, liquid–liquid extraction (LLE) [18,24,25,30] and solid phase extraction (SPE) [19,22–24] are most commonly used although recently, Chen et al. [29] reported ultrasound assisted dispersive liquid–liquid micro-extraction for the extraction of C_{60}, C_{70} and PCBM. In general LLE provides higher recoveries [20,24,30] and the addition of salts is recommended to destabilize the aqueous nC_{60} aggregates and facilitate its transfer into the organic solvent [30,33]. Ultrasound extraction has been also proposed for the extraction of fullerenes from the water suspended solids [21,28]. Very few reports have been published regarding sediments and soil sample treatment. In general, Soxhlet and ultrasound assisted extraction with toluene [32,34–38] are the most frequently used, although pressurized liquid extraction (PLE) [32,39] has also been proposed. However, most of the works evaluate the extraction of C_{60} or C_{70} fullerene and very few are devoted to functionalized fullerenes [21,23,37] and generally they do not report method performance characteristics.

In the present work, a method based on LLE for water and PLE for sediments and analysis by UHPLC–MS(/MS) of several pristine fullerenes (C_{60}, C_{70}, C_{76}, C_{78}, and C_{84}) and three C_{60}-fullerene derivatives (C_{60}-pyrr, PCBM and PCBB), which present increasing industrial applications, was developed. The behavior of the compounds in different reversed phase columns and mobile phases was studied. Mass spectrometry atmospheric pressure ionization sources (ESI, APCI and APPI) were evaluated for the ionization of C_{60}-fullerene derivatives and the obtained spectra were discussed. Tandem mass spectrometry behavior of the derivatives was studied to characterize the product ions and to select the most abundant and selective ones for quantitation and confirmation. Moreover, PLE conditions for the extraction of the compounds from sediment samples were optimized. Finally the proposed method was applied for the determination of the studied compounds in environmental samples.

2. Experimental

2.1. Chemicals and standard solutions

C_{60} (CAS: 99685-96-8), C_{70} (CAS: 115383-22-7), C_{76} (CAS: 142136-39-8), C_{78} (CAS: 136316-32-0), C_{84} (CAS: 135113-16-5) fullerenes and C_{60} fullerene derivatives: N-methyl fulleropyrrolidine (C_{60}-pyrr) (CAS: 151872-44-5), [6,6]-phenyl C_{61} butyric acid methyl ester (PCBM) (CAS: 160848-22-6), and [6,6]-phenyl C_{61} butyric acid butyl ester (PCBB) (CAS: 571177-66-7) were purchased from Sigma–Aldrich (Steinheim, Germany). The chemical structures and abbreviations of these compounds are given in Fig. 1. Methanol, acetonitrile and toluene, all of them LC–MS grade, were also supplied by Sigma–Aldrich. Sodium chloride (NaCl) was purchased from Merck (Darmstadt, Germany) and diatomaceous earth sorbent (Hydromatrix) from Varian (California, USA). Stock standard solutions of fullerenes (10 mg kg^{-1}) were individually prepared by weight in toluene and stored at 4 °C. Working solutions were prepared weekly by appropriate dilution of the stock standard solution in toluene/methanol (30:70, *v/v*).

Accucore C18 (150 mm × 2.1 mm, 2.6 μm particle size) and Hypersil GOLD C18 (150 mm × 2.1 mm, 1.9 μm particle size) chromatographic columns were both purchased from Thermo Fisher Scientific (San José, CA, USA).

Nitrogen (99.98% pure) supplied by Claind Nitrogen Generator N2 FLO (Lenno, Italy) was used for the API sources, and high purity Argon (Ar1), purchased from Air Liquid (Madrid, Spain), was used as a collision-induced dissociation gas (CID gas) in the triple quadruple instrument.

2.2. Instrumentation

The chromatographic separation was carried-out using an ultra-high performance liquid chromatography (UHPLC) system (Accela system; Thermo Fisher Scientific), equipped with a quaternary pump, autosampler, and column oven. The UHPLC final separation of the studied compounds was performed with a Hypersil GOLD C18 column (150 mm × 2.1 mm, 1.9 μm particle size, Thermo Scientific). Toluene (mobile phase A) and methanol (mobile phase B) at a flow rate of 500 μL min^{-1} (column back pressure ~ 600 bar) was used. Gradient elution was as follows: 1 min at 30% of solvent A, a linear gradient from 30 to 55% in 1 min, then an isocratic step of 3 min at 55%, and returning to initial conditions in 1 min which were maintained for 5 min in order to prepare the column for the next analysis.

Mass spectrometric analysis was performed using a TSQ Quantum Ultra AM (Thermo Fischer Scientific) triple quadrupole instrument, equipped with hyperbolic rods that permit operation in enhanced mass resolution (isolation window: 0.1–0.04 *m/z*, FWHM) and with an Ion Max API source housing device (Thermo Fisher Scientific) equipped with ESI and APCI probes. The working conditions for ESI and heated-electrospray ionization (H-ESI) (Thermo Fisher Scientific) in negative mode were: electrospray voltage −3 kV, capillary temperature 350 °C, vaporizing temperature for H-ESI probe 300 °C. For negative APCI, the discharge current was 10 μA and the vaporizing temperature 300 °C. When operating with negative APPI, the Ion Max source housing was equipped with a Syagen Photo Mate VUV light source (krypton discharge lamp, 10.0 eV) (Syagen Technology Inc., Tustin, CA, USA), and the APCI probe was used as a nebulizer-desolvation device (no corona discharge was applied). For all studies, nitrogen (purity >99.98%) was

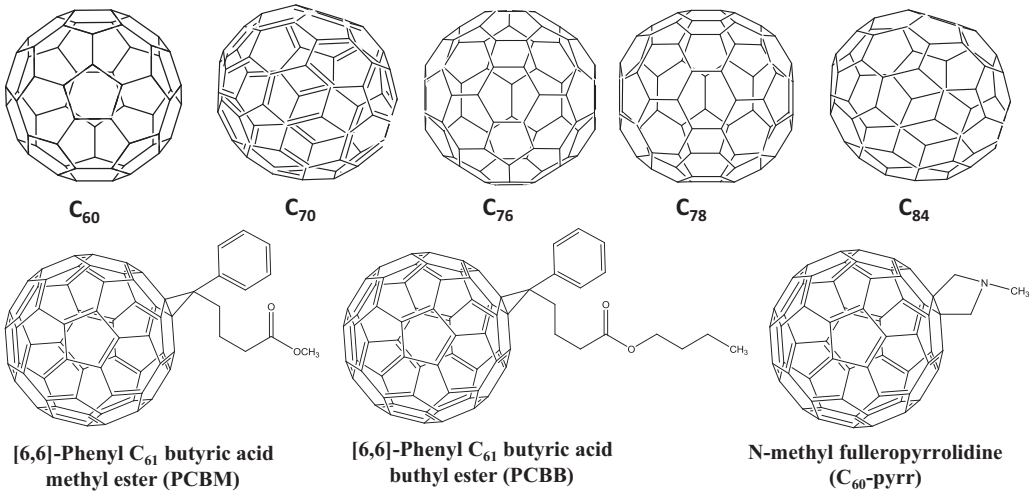

Fig. 1. Pristine fullerenes and C_{60}-fullerene derivatives chemical structures.

employed as sheath gas and auxiliary gas at a flow rate of 30 and 25 a.u. (arbitrary units), respectively. Tube lens offset was 180 V and the ion sweep gas was kept at 0 a.u. Ion transfer tube and the vaporizer temperatures were set at 300 °C. To optimize both API source parameters and mass spectrometry conditions, infusions of fullerene standard solutions prepared in toluene/methanol (40:60, *v/v*) of 1 mg L^{-1}, at a flow rate of 10 μL min^{-1}, were used. Additionally, fullerene solutions of 100 μg L^{-1} were chromatographically analyzed by isocratic elution with toluene-methanol (40:60, *v/v*), at a flow rate of 500 μL min^{-1}, in order to evaluate the purity of the standards used. Both, C_{60}-pyrr and PCBB standards showed a 10% contamination with pristine C_{60} fullerene. This contamination has been taken into account when working with mixed standard solutions for calibration. For instrument control and data processing, Xcalibur v2.0 (Thermo Fisher Scientific) software was used.

For the acquisition, the chromatogram was divided in 2 segments, with different acquisition modes for each one of them. For C_{60}-fullerene derivatives (segment 1: 0–2.8 min), selected reaction monitoring (SRM, Q1 and Q3 at 0.7 *m/z* FWHM) by monitoring two SRM transitions (using the isotopic cluster ions $[M]^{-\bullet}$ and $[M+1]^{-\bullet}$ as precursor ions) was used (Table 1). For the analysis of pristine fullerenes (segment 2: 2.8–5 min) highly selective selected ion monitoring (H-SIM) mode working at enhanced resolution in Q3 (0.06 *m/z* FWHM, with a mass resolving power higher than 12,500), and monitoring the isotopic cluster ions $[M]^{-\bullet}$ and $[M+1]^{-\bullet}$, was used as previously described [28]. For H-SIM mode, the scan width was set at 0.1 *m/z* and a 10 ms scan time (1 μscan) and for SRM mode 0.7 and 10 ms, respectively, were used.

2.3. Sampling and sample treatment

Water and sediment samples were collected from several ponds located around Barcelona's Airport (El Prat de Llobregat, Spain) and were stored at 4 °C and room temperature, respectively, and in the dark for a maximum of 2 weeks.

For method validation, blank water and sediment samples collected from a zone located away from industrialized urban areas were used. Chromatograms of these blank samples are included in Supplementary data (Fig. S1).

Supplementary Fig. S1 related to this article can be found, in the online version, at http://dx.doi.org/10.1016/j.chroma.2014.08.089.

2.4. Water samples

Liquid–liquid extraction (LLE) with toluene following a previously described procedure [30] with some modifications was used. Samples (200 mL) were processed in triplicate, without filtration, as follows: each sample was placed in a separatory funnel and 20% (*w/v*) of NaCl was added prior to the addition of 20 mL of toluene. After shaking the funnel on a shaker (Selecta, Barcelona, Spain) for 10 min, the toluene phase was collected. This procedure was repeated 3 times for each sample. The final toluene extract (60 mL) was then evaporated to approx. 5 mL using nitrogen in a

Table 1
Product ion spectra of C_{60}-fullerene derivatives and selected SRM transitions.

Compound	Precursor ion $[M]^{-\bullet}$	Product ion spectra		Selected reaction monitoring
	(*m/z*)	*m/z* (%Rel. Ab.)	Ion assignment (CE, eV)	Transitions (CE, eV)
PCBM	910	910 (40%)	$[M]^{-\bullet}$, 80	910 → 720 (100)[a]
		823 (5%)	$[M-(CH_2)_2COOCH_3]^{-\bullet}$	911 → 721 (100)[b]
		809 (10%)	$[M-(CH_2)_3COOCH_3]^{-\bullet}$	
		720 (100%)	$[M-C_6H_5C(CH_2)_3COOCH_3]^{-\bullet}$	
PCBB	952	952 (30%)	$[M]^{-\bullet}$, 80	952 → 720 (150)[a]
		896 (5%)	$[M-(CH_2)_3CH_3]^{-\bullet}$	953 → 721 (150)[b]
		823 (5%)	$[M-(CH_2)_2COO(CH_2)_3CH_3]^{-\bullet}$	
		809 (5%)	$[M-(CH_2)_3COO(CH_2)_3CH_3]^{-\bullet}$	
		720 (100%)	$[M-C_6H_5C(CH_2)_3COO(CH_2)_3CH_3]^{-\bullet}$	
C_{60}-pyrr	777	777 (40%)	$[M]^{-\bullet}$, 50	777 → 720 (80)[a]
		720 (100%)	$[M-(CH_2)_2NCH_3]^{-\bullet}$	778 → 721 (80)[b]

[a] Quantitation.
[b] Confirmation.

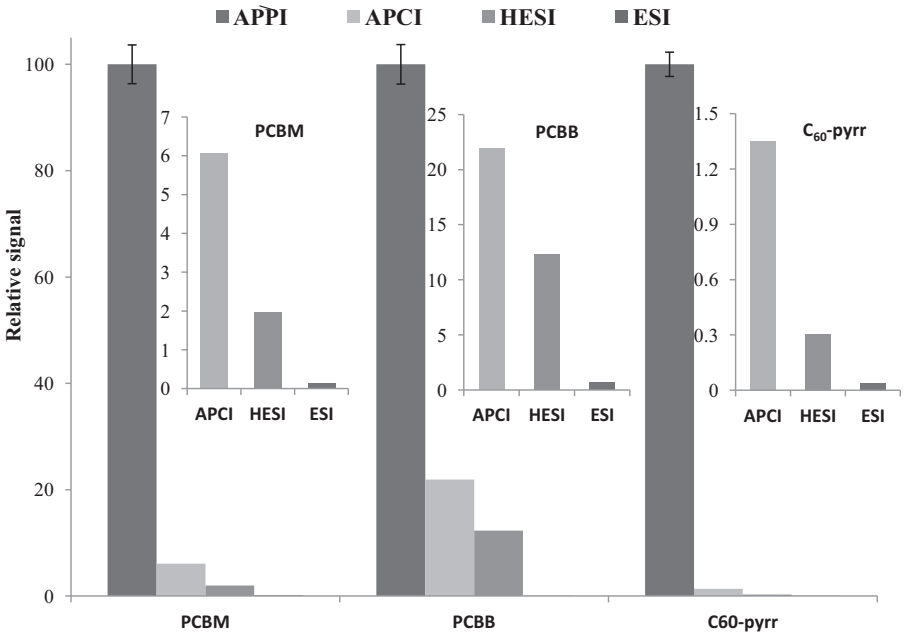

Fig. 2. Signal of the $[M]^{-\bullet}$ ion of C_{60}-fullerene derivatives with different API sources.

Turbovap II Concentration Workstation (Zymark Corporation, Hopkinton, MA, USA), and finally evaporated to almost dryness (0.1 mL) with a Visidry vacuum manifold (Supelco, Bellefonte, PA, USA). The extract was reconstituted in toluene–methanol (30:70, *v/v*) solution to a final volume of 0.5 mL and transferred to an amber-glass injection vial. Finally, 10 μL of this extract was injected into the UHPLC–APPI-MS(/MS) system.

2.5. Sediment samples

Prior to extraction, the samples were air dried for 48 h, and then homogenized using a mortar and pestle and then sieved using a 2 mm sieve. Two different extraction methods were evaluated: ultrasound extraction and pressurized solvent extraction (PLE). For ultrasound extraction, 15 g of homogenized sediment sample was dispersed in 50 mL toluene and sonicated for 1 h in an ultrasound bath. The solution was then centrifuged at 4500 RPM for 10 min using a Selecta Centronic Centrifuge (Barcelona, Spain). The extraction was repeated three times collecting a total toluene extract of 150 mL. PLE extractions were performed on an ASE 100 Accelerated Solvent Extractor system (Dionex, San Jose, CA, USA). Sediment samples were extracted as follows: 15 g of homogenized sample was placed in 34 mL steel cell, filling the remaining cell volume with Hydromatrix (Varian, Harbor City, CA, USA). The cell was sealed at each end by cellulose glass fiber paper circles. Samples were extracted at 150 °C with toluene and working at a pressure of 1300 psi applying one static cycle of 10 min and a flush volume of 100% (100 s of purge with N_2). The solvent was flushed out of the cell by N_2, obtaining a final toluene extract volume of approx. 34 mL.

Finally, toluene extracts obtained by both ultrasound extraction and PLE were evaporated and treated as previously described for the pond water samples.

3. Results and discussion

3.1. Mass spectrometry studies

In a previous study carried out in our research group [28], high ionization efficiency for pristine fullerenes was observed when using solvent-mediated negative-ion APPI, in comparison to other API sources. One of the aims of this work was to analyze three C_{60} fullerene derivatives, whose presence in the environment is expected to rise due to their increasing use, together with the five pristine fullerenes previously studied. For this purpose, different API sources (APPI, ESI, H-ESI, and APCI) were evaluated by infusing individual standard solutions of the C_{60} fullerene derivatives (1 mg L^{-1}) in toluene/methanol (40:60, *v/v*) in both, positive and negative modes. For all the evaluated API sources, higher ionization efficiency was observed in negative mode and the MS spectra was always dominated by the isotope cluster of the molecular ion $[M]^{-\bullet}$, with *m/z* ions at M, M+1, M+2, and M+3, in agreement with previous reports [23,29]. A comparison of the ionization efficiency of the tested API sources (APPI, ESI, H-ESI, and APCI) is shown in Fig. 2 where the signals obtained with each source for the molecular ion $[M]^{-\bullet}$ of the three C_{60}-fullerene derivatives (PCBM, PCBB and C_{60}-pyrr), normalized to the signal observed in APPI, is given. As can be seen, the sensitivity of C_{60}-fullerene derivatives is considerably higher when using solvent-mediated (toluene) APPI as previously reported for pristine fullerenes [28] and also for PCBM [29]. Among the other sources, APCI provided better results than electrospray in both, ESI and H-ESI modes, which can be explained because electron capture is favored in the APCI plasma.

In the full scan MS spectra of some of the fullerene derivatives obtained by infusion of the standard solutions, in addition to the isotope cluster of the molecular ion $[M]^{-\bullet}$, there is another cluster at *m/z* 720 corresponding to the isotopic pattern of the molecular ion $[M]^{-\bullet}$ of the C_{60} buckyball structure. Fig. 3a shows, as an example, the full scan MS spectrum of C_{60}-pyrr in negative APPI mode where both the molecular ions $[M]^{-\bullet}$ (*m/z* 777) and the cluster at *m/z* 720 appeared. This could be due to the presence of C_{60} fullerene residues in the commercial C_{60}-pyrr standard or to the loss of the pyrrolidine functional group by in-source fragmentation. In the LC chromatogram of the C_{60}-pyrr standard two peaks appeared, one at the retention time of C_{60}-pyrr and another one at the retention time of C_{60} fullerene indicating a contamination of C_{60}-pyrr by C_{60} (~10%). PCBB standard also contained a 10% contamination by C_{60} fullerene. Additionally, a minor contribution (5%) of an ion at *m/z* 910 was present in the spectrum of this compound, resulting from the loss of propene (CH_2=CH–CH_3). This ion was caused by thermal

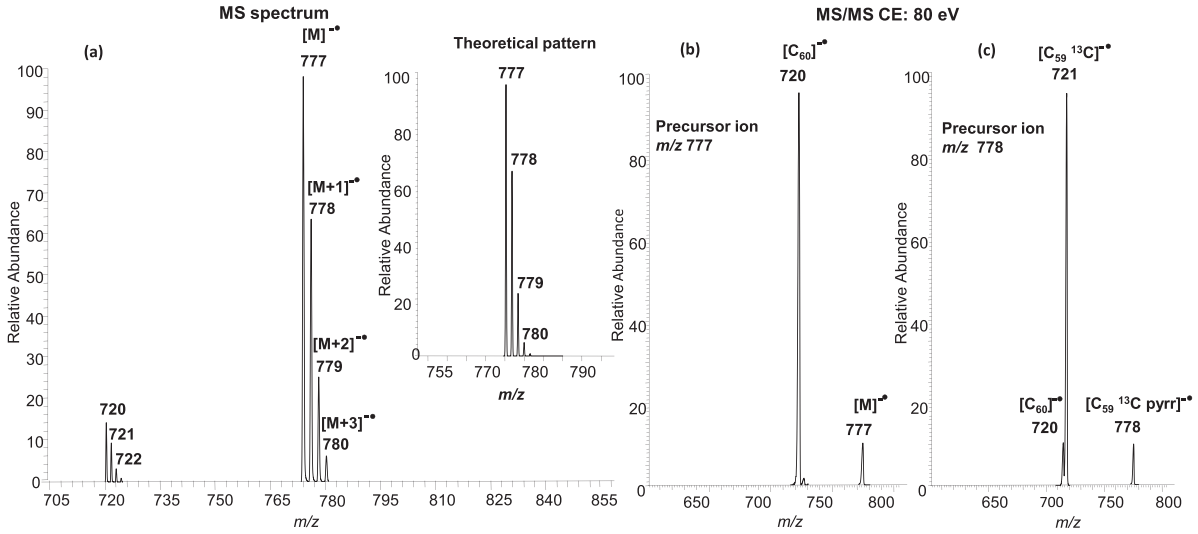

Fig. 3. LC–APPI-MS spectra of C_{60}-pyrr. (a) Full scan MS spectrum, (b) MS/MS spectrum of the precursor ion at *m/z* 777 (CE: 80 eV), and (c) MS/MS spectrum of the precursor ion at *m/z* 778 (CE: 80 eV).

degradation and its intensity increased with the vaporizer temperature. In contrast, no contamination by C_{60} was observed for PCBM standard.

As previously reported [28], pristine fullerenes presented isotopic patterns with relative abundances of *m/z* M+1, M+2, and M+3 higher than the theoretical ones, because of the addition of hydrogen to a double bond of the fullerene structure. In contrast to this behavior, for the C_{60}-fullerene derivatives studied in this work, the isotope patterns obtained using APPI matched with those obtained by H-ESI, APCI, and also with the theoretical ones (Fig. 3a). A possible explanation for this different behavior can be the presence of the functional groups which reduces the tendency of hydrogen addition to the double bonds. In addition, it must be mentioned that when analyzing low concentration levels of C_{60} the isotope cluster matched with the theoretical pattern, in contrast to the previously reported behavior of pristine fullerenes. This fact seems to indicate that addition of hydrogen to the fullerene double bond in the ion source could be related to the fullerene concentration. In order to confirm this assertion, the LC–MS spectra of C_{60} and C_{70} (isocratic elution with toluene-methanol, 40:60, *v/v*) were obtained by injecting standard solutions at several concentrations (0.1–1000 $\mu g\,L^{-1}$), and the variation of the ion ratio (M/M+1) with the concentration was evaluated. The results showed that the isotope pattern matched with the theoretical one at low concentration levels (<100 $\mu g\,L^{-1}$) while at higher concentrations, the ion ratio M/M+1 decreased, showing abundances of M+1, M+2 and M+3 higher than the theoretical ones. A similar behavior with a decrease in the signal of the $[M+1]^{-\bullet}$ ion of the isotopic cluster at low concentrations (<10 $\mu g\,L^{-1}$) was also observed for the fullerenes of higher size.

With the objective of charactering the product ions obtained in tandem mass spectrometry and selecting the most abundant and selective ones for quantitation and confirmation purposes, negative APPI MS/MS spectra of C_{60}-fullerene derivatives were obtained by analyzing individual standard solutions (100 $\mu g\,L^{-1}$) under chromatographic isocratic conditions (toluene/methanol, 40:60, *v/v*). In contrast to the behavior observed for pristine fullerenes which cannot be fragmented [28], C_{60}-fullerene derivatives did show fragmentation. The product ion scan spectra of each compound at different collision energies were acquired. Table 1 shows the product ions obtained for the $[M]^{-\bullet}$ of each compound in the triple quadrupole MS/MS spectrum (relative abundance ≥5%), the collision energies (CE) and the corresponding ion assignment. All the compounds showed a product ion at *m/z* 720 corresponding to the radical $[C_{60}]^{-\bullet}$ which was always the most intense product ion of the spectra and whose intensity increased with the applied collision energy. No additional fragmentation occurred for C_{60}-pyrr at any of the evaluated collision energies (10–100 eV). In contrast, for PCBM and PCBB, with larger functional groups, the loss of both, the propyl acid alkyl ester group, $(CH_2)_2COO(CH)_xH$, and the butyl acid alkyl ester group, $(CH_2)_3COO(CH)_xH$, was observed in the product ion spectra at collision energies lower than 80 eV (*m/z* 823). For PCBB, an additional product ion was observed at *m/z* 896 corresponding to the loss of the butyl group of the carboxylate ester. Moreover, the loss of propene ($CH_2{=}CH{-}CH_3$) was also observed at collision energies lower than 30 eV (*m/z* 910). The cleavage of the carboxylate ester for fullerenes with large alkyl moieties and the loss of the propyl acid alkyl ester group in the MS/MS spectra of PCBM and PCBB have been reported [23,29]. However, no information has been found in the literature about the fragment ion at *m/z* 809 corresponding to the loss of the butyl acid alkyl ester group observed in the MS/MS spectra of PCBM and PCBB, at CE < 80 eV with a relative abundance from 5 to 10%. At high collision energies ($[C_{60}\text{-pyrr}]^{-\bullet}$: 80 eV, $[PCME]^{-\bullet}$: 100 eV, $[PCBE]^{-\bullet}$: 150 eV) only the loss of the functional groups, $(CH_2)_2N\text{-}CH_3$ for C_{60}-pyrr, $C_6H_5(CH_2)_3COOCH_3$ for PCBM and $C_6H_5(CH_2)_3COO(CH_2)_3CH_3$ for PCBB, occurred providing for all the compounds a product ion at *m/z* 720 corresponding to the $[C_{60}]^{-\bullet}$ and this fragment ion was selected for quantitation. Hence, for C_{60}-fullerene derivatives two SRM (Q1 and Q3 at 0.7 *m/z* FWHF) transitions selecting as precursors the ions $[M]^{-\bullet}$ and $[M+1]^{-\bullet}$ of their isotopic cluster, and as product ions $[M]^{-\bullet}$ and $[M+1]^{-\bullet}$ corresponding to the buckyball (C_{60}) (Table 1) is proposed. As an example, Fig. 3b shows the MS/MS spectra with the two SRM transitions selected for C_{60}-pyrr. For pristine fullerenes, H-SIM (Q3 at 0.06 *m/z* FWHM, mass resolving power >12,500 FWHM) acquisition mode by monitoring the two most intense ions of the fullerene isotope clusters ($[M]^{-\bullet}$ and $[M+1]^{-\bullet}$) was used [28].

3.2. Chromatographic separation

For the chromatographic separation of fullerenes C18 reversed-phase chromatography with conventional LC columns (5 μm particle size) [18,21,24,40] and mainly with toluene/methanol or toluene/acetonitrile mixtures as mobile phase are usually used. In a previous work, the separation of pristine fullerenes was achieved

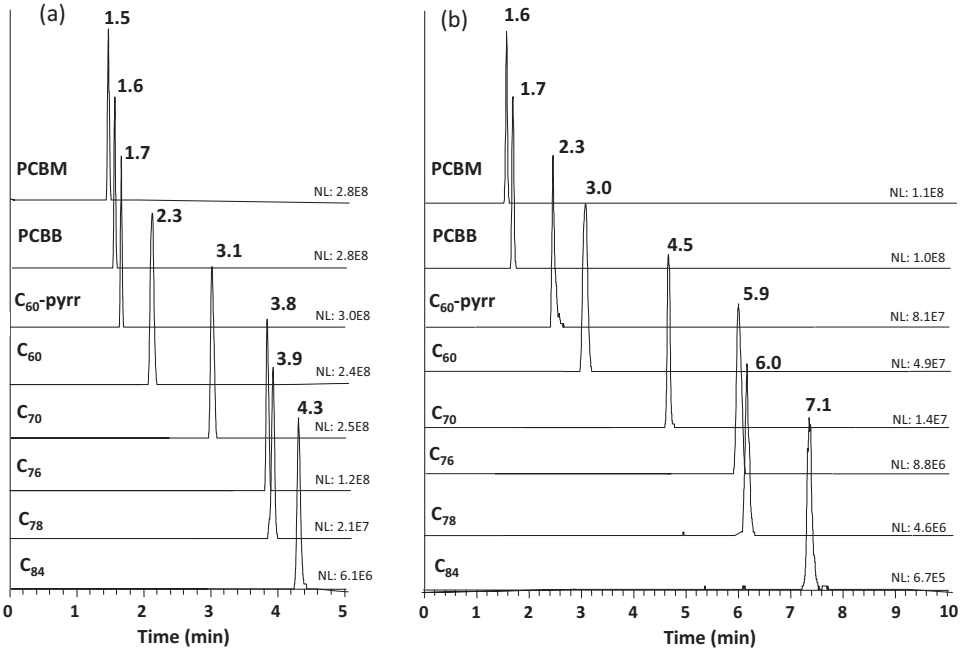

Fig. 4. UHPLC–APPI-MS(/MS) separation of fullerenes in a Hypersil GOLD C18 column (150 mm × 2.1 mm, 1.9 μm) using (a) toluene:methanol (40:60, *v/v*) and (b) toluene:acetonitrile (40:60, *v/v*) as mobile phase, Flow rate: 500 μL min^{-1}.

using a Hypersil GOLD C18 column (150 mm × 2.1 mm, 1.9 μm particle size, 175 Å) and toluene/methanol as mobile phase under isocratic elution conditions [28]. In the present work, in order to optimize the separation of pristine fullerenes and the C_{60}-fullerene derivatives, two columns, the previously used Hypersil GOLD C18 column and a core-shell Accucore C18 column (150 mm × 2.1 mm, 2.6 μm particle size, 80 Å) with superficially porous particles, were evaluated. As expected, C_{60}-fullerene derivatives eluted first in both C18 columns because of their higher polarity, followed by C_{60} and the other pristine fullerenes, their retention time increasing with the number of carbon atoms and, consequently with their hydrophobicity. The analysis time (retention time of C_{84}) was significantly shorter when Hypersil GOLD column was used, 4.3 min instead of 11.2 min in the Accucore C18 column, under isocratic conditions (toluene/methanol, 60:40, *v/v*). This can be due to higher interactions between fullerenes with big size and symmetric shape and the column with the smaller porous size packaging, as previously reported [28]. Among the studied C_{60}-fullerene derivatives, only C_{60}-pyrr presented a slightly higher retention in the Accucore C18 column (1.9 min) than in the Hypersil GOLD one (1.7 min). This could be related to the size of the functional groups of the fullerene derivatives, and therefore, their symmetry. C_{60}-pyrr has the smallest functional group, and therefore its symmetry and retention behavior is more similar to that of pristine fullerenes. The other two C_{60}-fullerene derivatives showed lower retention times in the column with superficially porous particles as currently happens when core-shell columns and columns with totally porous particles (sub-2 μm) are compared [41–43]. Since shorter analysis time and better asymmetry factors were obtained with the Hypersil GOLD column, it was selected for the separation of the studied compounds.

Two mobile phases, toluene/methanol and toluene/acetonitrile were evaluated using the Hypersil GOLD column under isocratic elution conditions (40% toluene and 60% methanol or 60% acetonitrile). Fig. 4 shows the chromatograms obtained in both cases. Although the eluotropic strength of the mixture toluene/acetonitrile is higher than that of toluene/methanol, fullerene compounds presented higher retention times when acetonitrile mixtures were used, behavior that was also observed by Jinno et al. [44]. For instance, the retention time of C_{84} increased from 4.3 min in toluene/methanol to 7.1 min in toluene/acetonitrile. This curious behavior of fullerenes can be related to their ability to form aggregates in polar solvents that explains for instance, their solubility in water [45,46]. It has been reported that stable dispersed colloidal particles are formed when C_{60} and C_{70} dissolved in non-polar solvents such as toluene, are added into polar solvents, like MeOH, ACN, ethanol or THF and that the hydrodynamic diameter of these small particles depends on the properties of both solvents, mainly their miscibility and the dielectric constant of the polar solvent [47,48]. Moreover, it has been suggested that increasing the polarity of the solvent leads to the formation of smaller aggregates [48]. On the bases of this assumption, fullerene clusters in toluene/ACN would be bigger than in toluene/MeOH and as a result, fullerenes will be more retained when toluene/ACN is used compensating the higher eluotropic strength of this mobile phase.

Furthermore, higher responses were observed with LC-APPI-MS when toluene/methanol solutions were used in agreement with the results previously reported by Chen et al. [29] for C_{60}, C_{70}, and PCME. Since lower retention times and better sensitivity were obtained, toluene/methanol was selected as the optimum mobile phase. Finally, gradient elution was optimized to improve the separation of the first two eluting compounds, PCBM and PCBB. Under gradient elution (see Section 2) the resolution between PCBM and PCBB increased from 1.2 (isocratic conditions) to 2.0.

3.3. Sample treatment

In this work, pond water samples were extracted by LLE with toluene after the addition of NaCl to facilitate the transfer to the toluene phase, following a procedure based on the one described by Chen et al. [30] for the analysis of C_{60} in water (see Section 2). Recoveries were evaluated by spiking blank pond water samples (200 mL) with fullerene and fullerene derivatives standard solutions in toluene at 5 concentration levels between 1 and 10 ng L^{-1} for PCBM, PCBB, C_{60}-pyrr, C_{60}, and C_{70}, and between 10 and 100 ng L^{-1} for C_{76}, C_{78} and C_{84} fullerenes. Recoveries were calculated from the slope of the plot of the calculated amount versus the added concentration and the values obtained were always higher

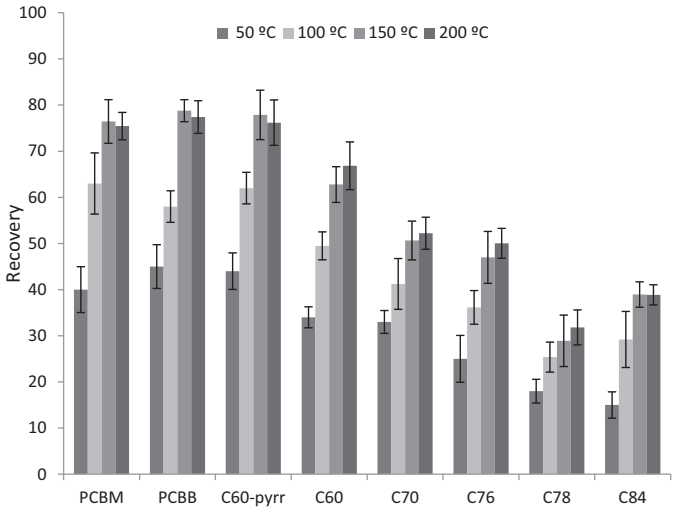

Fig. 5. Effect of the extraction temperature on PLE. Blank sediment samples spiked at 50 ng kg^{-1} for C_{60}, C_{70} and C_{60}-fullerene derivatives, and at 50 μg kg^{-1} for the higher fullerenes (5 extraction cycles of 10 min each).

than 83% and slightly better for C_{60}-fullerene derivatives (93–96%) than for pristine fullerenes (83–89%) (Table 2).

Regarding the extraction of fullerene compounds from sediments, both ultrasound extraction and pressurized liquid extraction (PLE) using toluene as extraction solvent were evaluated. For this purpose, blank sediment samples were spiked with standards prepared in toluene at levels of 50 ng kg^{-1} for PCBM, PCBB, C_{60}-pyrr, C_{60} and C_{70}, and at 50 μg kg^{-1} for the higher fullerenes and kept at room temperature (25 °C) for 24 h before extraction. The extracts obtained in both, ultrasound and PLE extractions were collected, evaporated and analyzed as described in Section 2.

For ultrasound extraction, the recoveries obtained were very low, ranging from <1% to 33% and decreased for the pristine fullerenes of high molecular weight. These values are lower than those reported by Sanchis et al. [32] (35–108%) for the extraction of C_{60}, C_{70} and some fullerene derivatives from sediments. However these authors used a very long extraction time, 2 cycles of 4 h each and the shorter extraction time (1 h) used in our work can explain the lower recoveries obtained.

PLE extractions were initially carried out following a procedure proposed by Shareef et al. [39] for the extraction of C_{60} from soils. In our work, besides C_{60} fullerene, the extraction of C_{70} and higher pristine fullerenes together with three C_{60}-fullerene derivatives (C_{60}-pyrr, PCBM and PCBB) was studied. Sediment samples were extracted with 100% toluene, at 50 °C and applying 5 static cycles of 10 min each. At these conditions, recoveries between 15 and 45% were obtained which were lower than those reported by Shareef et al. [39] (84–107% for C_{60}). However, it is worth mentioning that in the present work the recoveries where calculated in sediments spiked at much lower concentration levels (ng kg^{-1} to μg kg^{-1}) than the soils reported in the Shareef work (mg kg^{-1}) [39]. C_{60}-fullerene derivatives showed higher recoveries (40–45%) than pristine fullerenes (15–34%) and the extraction efficiency decreased with the molecular weight as previously observed by ultrasound extraction.

In order to improve PLE recoveries, several parameters such as the extraction temperature and the number of extraction cycles were optimized. The effect of the extraction temperature, 50–200 °C, was evaluated by maintaining all the other conditions unchanged (5 cycle number of 10 min each) and the recoveries obtained are shown in Fig. 5. As can be seen, an important improvement on recoveries was obtained up to 150 °C. Since no significant increase was observed at higher temperatures, 150 °C was chosen

Table 2
Quality parameters.

Compound	Instrument quality parameters				Method quality parameters									
	ILODs Standard		Ion ratio[a]	Run to run precision[b]	Water					Sediment				
	pg injected	ng L^{-1}			MLODs (pg L^{-1})	MLOQs (pg L^{-1})	Recovery (%)	Day to day precision[c]		MLODs (ng kg^{-1})	MLOQs (ng kg^{-1})	Recovery (%)	Day to day precision[c]	
								Low level[d]	High level[e]				Low level[d]	High level[e]
PCBM	0.004	0.4	1.40 ± 0.07	7	1.4	4.5	93	16	12	0.045	0.15	87	21	13
PCBB	0.002	0.2	1.42 ± 0.07	6	0.9	3.0	94	14	10	0.036	0.12	92	20	11
C_{60}-pyrr	0.001	0.1	1.35 ± 0.06	7	0.4	1.5	96	15	12	0.030	0.10	87	19	12
C60	0.007	0.7	1.28 ± 0.10	5	2.3	7.5	85	14	10	0.23	0.78	80	16	10
C70	0.01	1.0	1.10 ± 0.10	6	3.4	11.2	89	15	11	0.25	0.82	78	18	12
C76	2.0	200	1.07 ± 0.09	7	1200	4090	87	16	12	46	154	76	15	11
C78	1.0	97	0.95 ± 0.07	5	600	1870	83	14	10	31	103	70	17	12
C84	5.5	550	0.98 ± 0.05	6	1600	5460	85	16	12	158	523	73	18	13

[a] (M/M+1) ± S.D.
[b] %RSD (n = 5).
[c] %RSD (n = 3 × 5).
[d] MLOQs.
[e] 10 ng L^{-1} (PCBM, PCBB, C_{60}-pyrr, C_{60}, and C_{70}), 100 ng L^{-1} (C_{76}–C_{84}).

Table 3
Analysis of fullerenes in water and sediment samples by UHPLC–APPI-MS/(MS).

Sample	PCBM		PCBB		C_{60}-pyrr		C_{60}		C_{70}		C_{76}	C_{78}	C_{84}
	Concentration[a]	Ion ratio	Concentration[a]	Ion ratio	Concentration[a]	Ion ratio	Concentration[a]	Ion ratio	Concentration[a]	Ion ratio			
Pond water													
1	5.2 ± 0.5	1.38 ± 0.04	<MLOQ		8.5 ± 0.5	1.32 ± 0.03	15 ± 1	1.30 ± 0.06	330 ± 20		n.d.	n.d.	n.d.
2	8.0 ± 0.9	1.38 ± 0.04	5.0 ± 0.5	1.40 ± 0.04	2.0 ± 0.1	1.34 ± 0.05	25 ± 2	1.20 ± 0.02	31 ± 2	1.11 ± 0.06	n.d.	n.d.	n.d.
3	n.d.		n.d.		MLOD		<MLOQ		22 ± 1	1.15 ± 0.04	n.d.	n.d.	n.d.
4	MLOD		MLOD		5.1 ± 0.6	1.34 ± 0.03	11 ± 1	1.24 ± 0.04	<MLOQ		n.d.	n.d.	n.d.
5	MLOD		<MLOQ		n.d.		9 ± 1	1.27 ± 0.06	n.d.		n.d.	n.d.	n.d.
6	6.1 ± 0.7	1.39 ± 0.05	n.d		n.d.		22 ± 1	1.25 ± 0.03	<MLOQ		n.d.	n.d.	n.d.
Sediment													
1	0.15 ± 0.01	1.36 ± 0.02	2.45 ± 0.04	1.40 ± 0.05	0.36 ± 0.01	1.36 ± 0.03	<MLOQ		<MLOQ		n.d.	n.d.	n.d.
2	MLOQ		0.18 ± 0.01	1.43 ± 0.05	0.140 ± 0.001	1.32 ± 0.01	<MLOQ		MLOD		n.d.	n.d.	n.d.
3	0.16 ± 0.01	1.41 ± 0.04	0.23 ± 0.01	1.43 ± 0.07	0.562 ± 0.003	1.35 ± 0.02	1.0 ± 0.01	1.26 ± 0.08	MLOD		n.d.	n.d.	n.d.
4	<MLOQ		0.91 ± 0.03	1.41 ± 0.06	0.220 ± 0.002	1.32 ± 0.02	n.d.		n.d		n.d.	n.d.	n.d.
5	2.6 ± 0.3	1.37 ± 0.02	5.1 ± 0.3	1.40 ± 0.04	2.7 ± 0.3	1.30 ± 0.01	1.1 ± 0.1	1.21 ± 0.02	2.1 ± 0.1	1.17 ± 0.02	n.d.	n.d.	n.d.
6	<MLOQ		0.18 ± 0.02	1.38 ± 0.02	0.52 ± 0.02		0.82 ± 0.04	1.20 ± 0.02	7.2 ± 0.2	1.13 ± 0.03	n.d.	n.d.	n.d.
7	MLOD		<MLOQ		<MLOQ		MLOD		n.d.		n.d.	n.d.	n.d.

[a] pg L^{-1} (pond waters); ng kg^{-1} (sediments).
Concentrations given as $\bar{X} \pm$ S.D. n.d. = not detected.
Ion ratio values given as (M/M+1) ± S.D.

as optimum temperature for further studies. The effect of the number of extraction cycles was also evaluated and it was observed that the recoveries decreased with the number of cycles mainly for the pristine fullerenes of higher molecular weight, probably due to the co-extraction of interfering compounds from the matrix as the cycle number increased. The highest recoveries were obtained by using only 1 extraction cycle. Thus, one static extraction cycle of 10 min at 150 °C was chosen as optimum conditions for the extraction of the studied fullerenes from sediment samples.

Recovery values were determined by the standard addition method fortifying blank sediment samples at 5 different concentration levels, between 10 and 100 ng kg^{-1} for C_{60}-fullerene derivatives, C_{60} and C_{70} and from 1 to 50 μg kg^{-1} for larger fullerenes. The recoveries were then calculated from the slope obtained by plotting the found concentration versus the added one, and values between 70 and 92% were obtained (Table 2). These recoveries are higher than the ones reported by Sanchis et al. [32] (around 60%) for the extraction of C_{60}, C_{70}, PCBM and C_{60}-pyrr from sediments by using PLE.

3.4. Method performance and application

Both instrumental and method quality parameters were determined, and are given in Table 2. Instrumental limits of detection (ILODs), based on a signal-to-noise ratio of 3:1, calculated using the confirmation ion (for pristine fullerenes) or the confirmation SRM transition (for C_{60}-fullerene derivatives), were obtained by analyzing solutions of the studied compounds at very low concentration levels. ILODs down to 0.001 pg injected were obtained for the C_{60}-fullerene derivatives, while values between 0.007 and 5.5 pg injected were found for pristine fullerenes. Calibration curves based on the peak area of the studied fullerenes at concentrations between ILOQ and 100 μg L^{-1} were obtained, showing good linearity ($r^2 > 0.998$) for all the compounds. To evaluate method detection limits (MLODs), blank pond water and blank sediment samples were spiked at low concentration levels and were subjected to the sample treatments previously described. For water samples, MLODs values between 1.4 and 3.4 pg L^{-1} (PCBM, PCBB, C_{60}-pyrr, C_{60} and C_{70}) and between 0.6 and 1.6 ng L^{-1} (higher fullerenes) were obtained. These values are in agreement with those reported previously for pristine fullerenes [28] and lower than the ones reported by Farre et al. [21] for C_{60}, C_{70} and C_{60}-pyrr. MLOD values for sediment samples, ranged between 45 and 250 pg kg^{-1} for PCBM, PCBB, C_{60}-pyrr, C_{60} and C_{70} and between 31 and 158 ng kg^{-1} for higher fullerenes and were also lower than those reported by Sanchis et al. [32] for C_{60}, C_{70}, C_{60}-pyrr and PCBM (9–21 ng kg^{-1}) in sediment and soil samples. MLOQs, based on a signal-to-noise ratio of 10, were also calculated following the same procedure, and the values are indicated in Table 2.

The matrix effect was evaluated by comparing the peak areas obtained by analyzing a standard solution of target fullerenes (500 ng L^{-1} for PCBM, PCBB, C_{60}-pyrr, C_{60} and C_{70} and 50 μg L^{-1} for C_{76}, C_{78}, and C_{84}) with those of the extracts spiked post extraction treatment at the same concentration level. A reduction of the peak areas, ranging from less than 10% for water samples to 20% in sediments, was observed for large pristine fullerenes (C_{76}–C_{84}). The higher matrix effect observed for sediments compared to water samples which is more pronounced for larger fullerenes is due to the higher content of organic matter. To prevent this effect, matrix matched calibration is proposed for quantitation.

Instrumental run-to-run precision was evaluated by analyzing a total of five replicates of a standard at 100 ng L^{-1} for PCBM, PCBB, C_{60}-pyrr, C_{60}, C_{70}, and 10 μg L^{-1} for higher fullerenes on the same day. The relative standard deviations (RSDs) based on concentration ranged from 5 to 7%. Method day-to-day precision was evaluated by performing 15 replicate determinations on 3

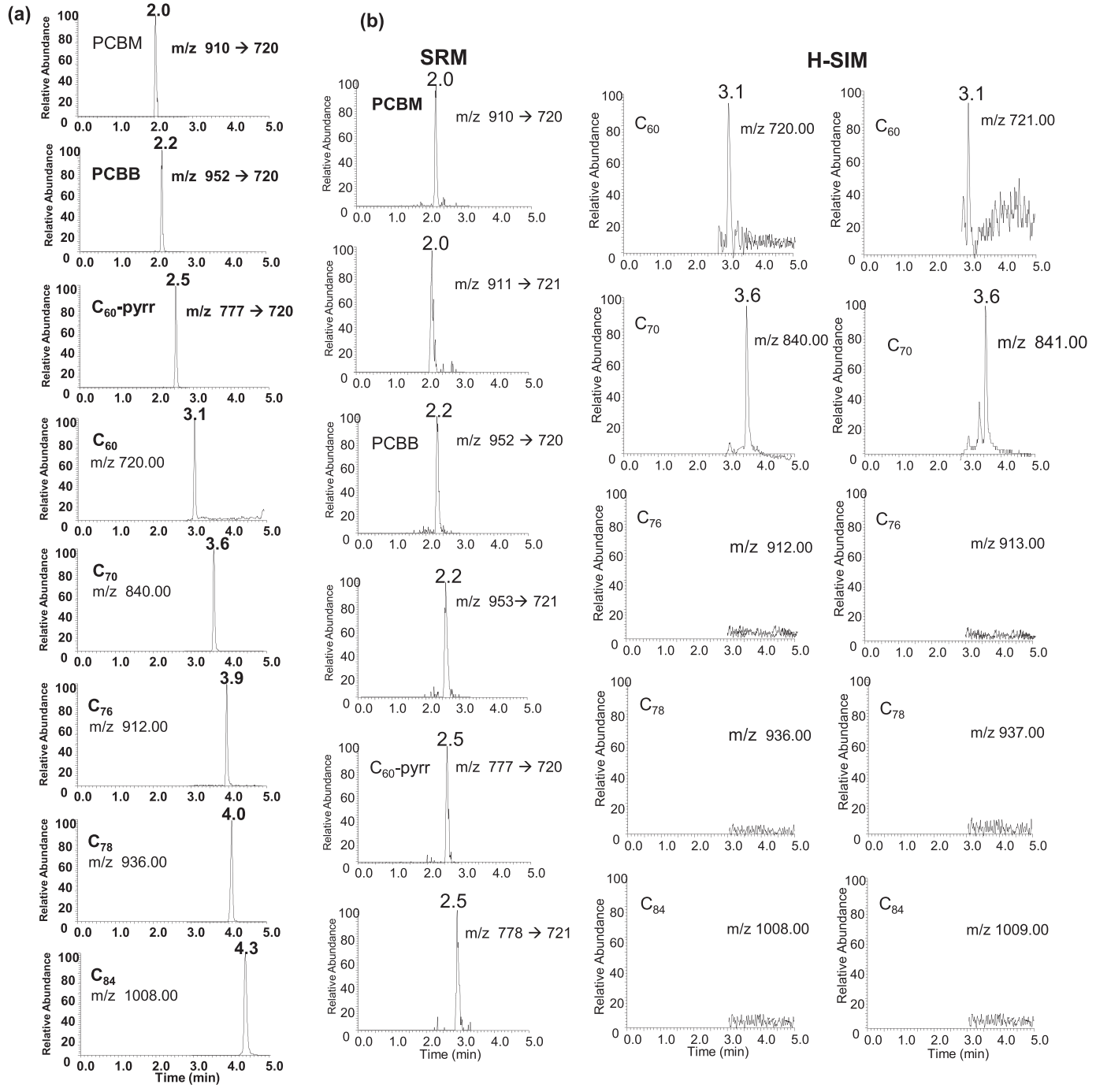

Fig. 6. UHPLC–APPI-MS/(MS) chromatogram of (a) standard mixture (100 ng L^{-1}) and (b) sediment sample.

nonconsecutive days (five replicates per day) of spiked blank water and sediment samples at two concentration levels, a low level (MLOQ values) and a high level (10 ng L^{-1} for PCBM, PCBB, C_{60}-pyrr, C_{60}, and C_{70}, and 100 ng L^{-1} for higher fullerenes in water samples, and 100 ng kg^{-1} for PCBM, PCBB, C_{60}-pyrr, C_{60} and C_{70}, and 50 μg kg^{-1} for C_{76}, C_{78} and C_{84} in sediment samples). Relative standard deviations (RSDs) based on concentration ranged from 10 to 13% (high level) and from 14 to 21% (low level) showing an acceptable performance (Table 2).

In order to evaluate the applicability of the developed method for the analysis of C_{60}-fullerene derivatives and pristine fullerenes in complex matrices, 6 pond water samples and 7 sediment samples collected from different ponds located close to Barcelona's Airport (El Prat de Llobregat, Spain) were analyzed and the results are given in Table 3. Fullerene derivatives were detected in all the analyzed sediment samples at low ng kg^{-1} concentration levels. Fig. 6 shows as an example, the chromatogram obtained for one of the samples. PCBM and C_{60}-pyrr (Table 3) were quantified at levels between 0.14–2.7 ng kg^{-1}, while PCBB was detected at slightly higher concentration levels, up to 5.1 ng kg^{-1}. To the best of our knowledge this is the first report of the presence of PCBM, PCBB and C_{60}-pyrr, compounds in sediment samples. Among pristine fullerenes, C_{60} and C_{70} were detected in most of the samples, but they could only be quantified in some of them, at levels up to 1.1 ng kg^{-1} and 2.1 ng kg^{-1}, respectively, while higher fullerenes were not detected. C_{60} and C_{70} fullerenes have been recently found in sediments and superficial soils [32], also at low ng L^{-1} concentration levels and in samples from highly industrial and urban areas and near

international airports. Thus, their presence in the samples analyzed in this work could be related to the location of the sampling points, close to the landing strips of Barcelona's airport (El Prat de Llobregat, Spain). The C_{60}-fullerene derivatives were also detected in almost all the analyzed water samples at low pg L^{-1} concentration levels (Table 3), and the highest concentration detected was ~8 pg L^{-1} (PCBM and C_{60}-pyrr). There are no previous reports of the presence of these compounds in water samples, except for C_{60}-pyrr that has been found in wastewater effluents [21]. Regarding pristine fullerenes, our results are in agreement with previous reports about the presence of these compounds in environmental water samples, which are detected usually at low ng L^{-1} levels [21,28,32] except in one paper [21] where C_{60} was found at μg L^{-1} levels. As regards larger fullerenes which have not been found in the analyzed samples, the presence of C_{84} in water has been recently reported [28], although C_{76} and C_{78} have not yet been found in environmental samples.

4. Conclusions

A fast and sensitive UHPLC–APPI-MS/(MS) method was developed for the analysis three C_{60}-fullerene derivatives (PCBM, PCBB and C_{60}-pyrr) with increasing industrial applications together with five pristine fullerenes. So far there are no other works describing a comparable analytical method suitable for the simultaneous analysis of all these fullerene compounds, and at the very low detection levels (ng L^{-1}) relevant for environmental analysis. Among the different MS API sources tested, APPI was selected because it showed the best sensitivity. In contrast to pristine fullerenes, the molecular ion $[M]^{-\bullet}$ isotope pattern of the studied C_{60}-fullerene derivatives match with the theoretical ones probably due to a lower tendency of hydrogen addition to the double bonds caused by the presence of their functional groups reducing the carbon cage insaturation. Unlike pristine fullerenes, these compounds did present fragmentation, mainly losing the functional groups and providing the buckyball structure $[C_{60}]^{-\bullet}$. The specific characteristics of fullerene compounds regarding their size, their peculiar solubility behavior and tendency to form aggregates allowed us to explain their retention behavior in different chromatographic columns (totally porous vs core–shell) and mobile phase mixtures (toluene–MeOH and toluene–ACN). C_{60}-fullerene derivatives were detected at low ng kg^{-1} and pg L^{-1} levels, in sediments and water samples collected from highly industrialized areas (near Barcelona's airport). This work is the first report of their presence in these matrices. Among pristine fullerenes, C_{60} and C_{70} were detected in most of the samples, while higher fullerenes were not detected. The results presented in this work demonstrate that the developed method can be proposed for the analysis of fullerene and C_{60}-fullerene derivatives in environmental samples.

Acknowledgements

The authors gratefully acknowledge the financial support received from the Spanish Ministry of Economy and Competitiveness under the project CTQ2012-30836. Alina Astefanei thanks the Spanish Ministry of Economy and Competitiveness for a Ph.D. grant (FPI).

References

[1] H.W. Kroto, J.R. Heath, S.C. O'Brien, R.F. Curl, R.E. Smalley, C_{60}: buckminsterfullerene, Nature 318 (1985) 162–163.
[2] D. Kronholm, J.C. Hummelen, Fullerene-based n-type semiconductors in organic electronics, Mater. Matters 2 (2007) 16–19.
[3] L. Xiao, H. Takada, K. Maeda, M. Haramoto, N. Miwa, Antioxidant effects of water-soluble fullerene derivatives against ultraviolet ray or peroxylipid through their action of scavenging the reactive oxygen species in human skin keratinocytes, Biomed. Pharmacother. 59 (2005) 351–358.
[4] N. Tagmatarchis, H. Shinohara, Fullerenes in medicinal chemistry and their biological applications, Mini-Rev. Med. Chem. 1 (2001) 339–348.
[5] T. Da Ros, M. Prato, Medicinal chemistry with fullerenes and fullerene derivatives, Chem. Commun. (Camb.) (1999) 663–669.
[6] B.H. Chen, J.P. Huang, L.Y. Wang, J. Shiea, T.L. Chen, L.Y. Chiang, Synthesis of octadecahydroxylated C_{70}, Synth. Commun. 28 (1998) 3515–3525.
[7] M. Lens, L. Medenica, U. Citernesi, Antioxidative capacity of C(60)(buckminsterfullerene) and newly synthesized fulleropyrrolidine derivatives encapsulated in liposomes, Biotechnol. Appl. Biochem. 51 (2008) 135–140.
[8] H. Hoppe, M. Drees, W. Schwinger, F. Schaffler, N.S. Sariciftcia, Nanocrystalline fullerene phases in polymer/fullerene bulk-heterojunction solar cells: a transmission electron microscopy study, Synth. Met. 152 (2005) 117–120.
[9] H. Zhu, J. Wei, K. Wang, D. Wu, Applications of carbon materials in photovoltaic solar cells, Sol. Energy Mater. Sol. Cells 93 (2009) 1461–1470.
[10] T.M. Benn, P. Westerhoff, P. Herckes, Detection of fullerenes (C_{60} and C_{70}) in commercial cosmetics, Environ. Pollut. 159 (2011) 1334–1342.
[11] S. Erkoc, in: E. Osawa (Ed.), Perspectives of Fullerene Nanotechnology, Mater. Manuf. Processes, vol. 17, 2002, pp. 881–883.
[12] C.O. Hendren, X. Mesnard, J. Droge, M.R. Wiesner, Estimating production data for five engineered nanomaterials as a basis for exposure assessment, Environ. Sci. Technol. 45 (2011) 4190.
[13] L. Becker, R.J. Poreda, A.G. Hunt, T.E. Bunch, M. Rampino, Impact event at the Permian-Triassic boundary: evidence from extraterrestrial noble gases in fullerenes, Science 291 (2001) 1530–1533.
[14] K. Aschberger, H.J. Johnston, V. Stone, R.J. Aitken, C.L. Tran, S.M. Hankin, S.A.K. Peters, F.M. Christensen, Review of fullerene toxicity and exposure – appraisal of a human health risk assessment, based on open literature, Regul. Toxicol. Pharmacol. 58 (2010) 455–473.
[15] Y. Saito, H. Ohta, K. Jinno, Chromatographic separation of fullerenes, Anal. Chem. 76 (2004) 266A–272A.
[16] K. Jinno, J. Wu, Technical advances in the liquid chromatographic separation of fullerenes, Sep. Fuller. Liq. Chromatogr. (1999) 1–24.
[17] M. Farre, J. Sanchis, D. Barcelo, Analysis and assessment of the occurrence, the fate and the behavior of nanomaterials in the environment, TrAC Trends Anal. Chem. 30 (2011) 517–527.
[18] C.W. Isaacson, M. Kleber, J.A. Field, Quantitative analysis of fullerene nanomaterials in environmental systems: a critical review, Environ. Sci. Technol. 43 (2009) 6463–6474.
[19] B.F.G. Pycke, T.M. Benn, P. Herckes, P. Westerhoff, R.U. Halden, Strategies for quantifying C_{60} fullerenes in environmental and biological samples and implications for studies in environmental health and ecotoxicology, TrAC Trends Anal. Chem. 30 (2011) 44–57.
[20] C. Wang, C. Shang, P. Westerhoff, Quantification of fullerene aggregate nC_{60} in wastewater by high-performance liquid chromatography with UV–vis spectroscopic and mass spectrometric detection, Chemosphere 80 (2010) 334–339.
[21] M. Farre, S. Perez, K. Gajda-Schrantz, V. Osorio, L. Kantiani, A. Ginebreda, D. Barcelo, First determination of C_{60} and C_{70} fullerenes and N-methylfulleropyrrolidine C_{60} on the suspended material of wastewater effluents by liquid chromatography hybrid quadrupole linear ion trap tandem mass spectrometry, J. Hydrol. 383 (2010) 44–51.
[22] A.P. van Wezel, V. Moriniere, E. Emke, T. ter Laak, A.C. Hogenboom, Quantifying summed fullerene nC_{60} and related transformation products in water using LC LTQ Orbitrap MS and application to environmental samples, Environ. Int. 37 (2011) 1063–1067.
[23] A. Kolkman, E. Emke, P.S. Baeuerlein, A. Carboni, D.T. Tran, T.L. ter Laak, A.P. van Wezel, P. de Voogt, Analysis of (functionalized) fullerenes in water samples by liquid chromatography coupled to high-resolution mass spectrometry, Anal. Chem. 85 (2013) 5867–5874.
[24] D. Bouchard, X. Ma, Extraction and high-performance liquid chromatographic analysis of C_{60}, C_{70}, and [6,6]-phenyl C_{61}-butyric acid methyl ester in synthetic and natural waters, J. Chromatogr. A 1203 (2008) 153–159.
[25] C.W. Isaacson, C.Y. Usenko, R.L. Tanguay, J.A. Field, Quantification of fullerenes by LC/ESI-MS and its application to in vivo toxicity assays, Anal. Chem. 79 (2007) 9091–9097.
[26] S.Y. Xie, S.L. Deng, L.J. Yu, R.B. Huang, L.S. Zheng, Separation and identification of perchlorinated polycyclic aromatic hydrocarbons and fullerenes (C_{60}, C_{70}) by coupling high-performance liquid chromatography with ultraviolet absorption spectroscopy and atmospheric pressure chemical ionization mass spectrometry, J. Chromatogr. A 932 (2001) 43–53.
[27] S.i. Kawano, H. Murata, H. Mikami, K. Mukaibatake, H. Waki, Method optimization for analysis of fullerenes by liquid chromatography/atmospheric pressure photoionization mass spectrometry, Rapid Commun. Mass Spectrom. 20 (2006) 2783–2785.
[28] O. Núñez, H. Gallart-Ayala, C.P.B. Martins, E. Moyano, M.T. Galceran, Atmospheric pressure photoionization mass spectrometry of fullerenes, Anal. Chem. 84 (2012) 5316–5326.
[29] H.C. Chen, W.H. Ding, Determination of aqueous fullerene aggregates in water by ultrasound-assisted dispersive liquid–liquid microextraction with liquid chromatography–atmospheric pressure photoionization-tandem mass spectrometry, J. Chromatogr. A 1223 (2012) 15–23.
[30] Z. Chen, P. Westerhoff, P. Herckes, Quantification of C_{60} fullerene concentrations in water, Environ. Toxicol. Chem. 27 (2008) 1852–1859.

[31] J. Sanchis, N. Berrojalbiz, G. Caballero, J. Dachs, M. Farre, D. Barcelo, Occurrence of aerosol-bound fullerenes in the Mediterranean Sea atmosphere, Environ. Sci. Technol. 46 (2012) 1335–1343.
[32] J. Sanchis, D. Bozovic, N.A. Al-Harbi, L.F. Silva, M. Farre, D. Barcelo, Quantitative trace analysis of fullerenes in river sediment from Spain and soils from Saudi Arabia, Anal. Bioanal. Chem. 405 (2013) 5915–5923.
[33] J. Brant, H. Lecoanet, M.R. Wiesner, Aggregation and deposition characteristics of fullerene nanoparticles in aqueous systems, J. Nanopart. Res. 7 (2005) 545–553.
[34] D. Heymann, L.P.F. Chibante, R.R. Brooks, W.S. Wolbach, R.E. Smalley, Fullerenes in the Cretaceous-Tertiary boundary layer, Science 265 (1994) 645–647.
[35] L. Becker, J.L. Bada, R.E. Winans, J.E. Hunt, T.E. Bunch, B.M. French, Fullerenes in the 1.85-billion-year-old Sudbury impact structure, Science 265 (1994) 642–645.
[36] J. Jehlicka, O. Frank, V. Hamplova, Z. Pokorna, L. Juha, Z. Bohacek, Z. Weishauptova, Low extraction recovery of fullerene from carbonaceous geological materials spiked with C_{60}, Carbon 43 (2005) 1909–1917.
[37] A. Carboni, E. Emke, J.R. Parsons, K. Kalbitz, P. de Voogt, An analytical method for determination of fullerenes and functionalized fullerenes in soils with high performance liquid chromatography and UV detection, Anal. Chim. Acta 807 (2014) 159–165.
[38] R.A. Perez, B. Albero, E. Miguel, J.L. Tadeo, C. Sanchez-Brunete, A rapid procedure for the determination of C_{60} and C_{70} fullerenes in soil and sediments by ultrasound-assisted extraction and HPLC–UV, Anal. Sci. 29 (2013) 533–538.
[39] A. Shareef, G. Li, R.S. Kookana, Quantitative determination of fullerene (C_{60}) in soils by high performance liquid chromatography and accelerated solvent extraction technique, Environ. Chem. 7 (2010) 292–297.
[40] F. Moussa, M. Pressac, E. Genin, S. Roux, F. Trivin, A. Rassat, R. Ceolin, H. Szwarc, Quantitative analysis of C_{60} fullerene in blood and tissues by high-performance liquid chromatography with photodiode-array and mass spectrometric detection, J. Chromatogr. B 696 (1997) 153–159.
[41] H. Gallart-Ayala, E. Moyano, M.T. Galceran, Fast liquid chromatography–tandem mass spectrometry for the analysis of bisphenol A-diglycidyl ether, bisphenol F-diglycidyl ether and their derivatives in canned food and beverages, J. Chromatogr. A 1218 (2011) 1603–1610.
[42] A. Staub, D. Zurlino, S. Rudaz, J.L. Veuthey, D. Guillarme, Analysis of peptides and proteins using sub-2 μm fully porous and sub 3-μm shell particles, J. Chromatogr. A 1218 (2011) 8903–8914.
[43] P. Yang, T. McCabe, M. Pursch, Practical comparison of LC columns packed with different superficially porous particles for the separation of small molecules and medium size natural products, J. Sep. Sci. 34 (2011) 2975–2982.
[44] K. Jinno, T. Uemura, H. Ohta, H. Nagashima, K. Itoh, Separation and identification of higher molecular weight fullerenes by high-performance liquid chromatography with monomeric and polymeric octadecylsilica bonded phases, Anal. Chem. 65 (1993) 2650–2654.
[45] C.T. Jafvert, P.P. Kulkarni, Buckminsterfullerene's (C_{60}) octanol–water partition coefficient (K_{ow}) and aqueous solubility, Environ. Sci. Technol. 42 (2008) 5945–5950.
[46] S. Deguchi, R.G. Alargova, K. Tsujii, Stable dispersions of fullerenes, C_{60} and C_{70}, in water. Preparation and characterization, Langmuir 17 (2001) 6013–6017.
[47] A. Mrzel, A. Mertelj, A. Omerzu, M. Copic, D. Mihailovic, Investigation of encapsulation and solvatochromism of fullerenes in binary solvent mixtures, J. Phys. Chem. B 103 (1999) 11256–11260.
[48] R.G. Alargova, S. Deguchi, K. Tsujii, Stable colloidal dispersions of fullerenes in polar organic solvents, J. Am. Chem. Soc. 123 (43) (2001) 10460–10467.

CHAPTER 2

ANALYSIS OF FULLERENES

2.3. Scientific article III: Non-aqueous capillary electrophoresis separation of fullerenes and C60 fullerene derivatives

A. Astefanei, O. Núñez and M.T. Galceran

Analytical and Bioanalytical Chemistry, **404**: 307-313 (2012).

Anal Bioanal Chem (2012) 404:307–313
DOI 10.1007/s00216-012-6041-4

ORIGINAL PAPER

Non-aqueous capillary electrophoresis separation of fullerenes and C60 fullerene derivatives

Alina Astefanei · Oscar Núñez · M. Teresa Galceran

Received: 26 January 2012 / Revised: 28 March 2012 / Accepted: 10 April 2012 / Published online: 24 April 2012
© Springer-Verlag 2012

Abstract As the interest in the use of fullerene compounds in biomedical and cosmetic applications increases, so too does the need to develop methods for their determination and quantitation in such complex matrices. In this work, we studied the behavior of C60 and C70 fullerenes in non-aqueous capillary electrophoresis, as well as two C60 fullerene derivatives not previously reported by any electrophoretic method, *N*-methyl-fulleropyrrolidine and (1,2-methanofullerene C60)-61-carboxylic acid. The separation was performed using fused-silica capillaries with an I.D. of 50 μm and tetraalkylammonium salts, namely tetra-*n*-decylammonium bromide (200 mM) and tetraethylammonium bromide (40 mM), in a solvent mixture containing 6 % methanol and 10 % acetic acid in acetonitrile/chlorobenzene (1:1 *v/v*) as the background electrolyte. Detection limits, based on a signal-to-noise ratio of 3:1, were calculated, and values between 1 and 3.7 mg/L were obtained. Good run-to-run and day-to-day precisions on concentration were achieved with relative standard deviation lower than 15 %. For the first time, an electrophoretic technique has been applied for the analysis of C60 fullerene in a commercial cosmetic cream. A standard addition method was used for quantitation, and the result was compared with that obtained by analyzing the same cream by liquid chromatography coupled to mass spectrometry.

Published in the special paper collection *Progress on Environmental and Bioanalysis in Spain* with guest editors Alfredo Sanz-Medel and Elena Domínguez.

A. Astefanei · O. Núñez (✉) · M. T. Galceran
Department of Analytical Chemistry,
University of Barcelona,
Martí i Franquès 1-11,
08028 Barcelona, Spain
e-mail: oscar.nunez@ub.edu

Keywords Fullerenes · Tetraalkylammonium salts · Non-aqueous capillary electrophoresis · Commercial cosmetic cream

Introduction

Fullerenes are spherical carbon nanoparticles with a unique cage structure. Their presence in the environment is due to both natural and anthropogenic phenomena such as volcanic eruptions, forest fires, and the combustion of carbon-based materials. Since their discovery in 1985, fullerenes have attracted considerable attention in different fields of science. The fullerene family, and especially C60 fullerene, has very appealing photo-, electro-chemical, and physical properties, which can be exploited in many different fields. Their electron double bonds allow pristine fullerenes, which are intrinsically hydrophobic [1], to become readily derivatized and water soluble through the addition of various functional groups. Hence, these molecules are increasingly being investigated for use in biomedical, cosmetic and industrial applications, ranging from drug-delivery systems and anti-aging formulations to electrical components [2]. The size, hydrophobicity, three-dimensionality, and electronic configuration of fullerenes make them an appealing subject in medicinal chemistry. Their unique structure, coupled with their immense scope for derivatization, make them potential therapeutic agents. C60 fullerene is also used in a variety of personal care products, although its widespread usage is a recent development [3]. Among the numerous derivatives of C60 fullerene, fulleropyrrolidines play an important role in the controllable synthesis of new materials and biologically active compounds [4].

Although significant advances have been made in the analysis of fullerenes in the past few years [5], there is still

a need to develop effective, sensitive, and reliable analytical methods for their determination. Reversed-phase liquid chromatography coupled to mass spectrometry (LC-MS) has been the method of choice for analyzing them in different matrices such as environmental waters [6, 7], biological fluids [8, 9], and cosmetics [10, 11]. These studies have focused primarily on the analysis of C60 and C70 fullerenes, although some have also analyzed fullerene derivatives such as *N*-methyl-fulleropyrrolidine (C60 pyrr) [6] and [6,6]-phenyl C61-butyric acid methyl ester [7].

Capillary electrophoresis (CE) techniques have also been used to analyze fullerenes, especially fullerene derivatives [12–18]. For instance, the electrophoretic behavior of a highly water-soluble anionic dendro[60]fullerene derivative in capillary zone electrophoresis (CZE) has been evaluated [13], and this technique has also been proposed for the analysis of Th-symmetric fullerenehexamalonic acid ($C66(COOH)_{12}$) as an alternative to ion-chromatography [14]. Micellar electrokinetic chromatography (MEKC) and CZE have been applied to the analysis of dendro[60]fullerene and carboxyfullerene ($C60(COOH)_6$) in human serum [15], and Treubig and Brown [16] showed that MEKC can be used to analyze C60 and C70 fullerenes in an aqueous buffer using sodium dodecylsulfate as a surfactant. In addition, non-aqueous capillary electrophoresis (NACE) has been reported to separate three open-cage fullerenes using trifluoroacetic acid and sodium acetate in a mixture of acetonitrile and methanol [17], and Wan and Leung presented a communication [18] showing that NACE is also suitable for the separation of C60, C70, and C84 fullerenes and several C60 fullerene derivatives using tetraalkylammonium ions in a solvent mixture containing acetonitrile, chlorobenzene, acetic acid, and methanol as the background electrolyte. Nevertheless, the performance and applicability of the method were not assessed. Moreover, none of the developed NACE methods have been applied to the determination of fullerenes in real samples.

The aim of this work is to study the behavior in non-aqueous capillary electrophoresis of C60 and C70 fullerenes, as well as two C60 fullerene derivatives of relatively high hydrophobicity, C60 pyrr and (1,2-methanofullerene C60)-61-carboxylic acid (C60-COOH), not previously studied by electrophoretic techniques. The composition of the background electrolyte was optimized in order to achieve the best separation of the fullerenes studied. The effect of tetraalkylammonium salts, such as tetra-*n*-decylammonium bromide (TDAB) and tetraethylammonium bromide (TEAB), and organic solvents on the electrophoretic behavior of fullerenes will be discussed in depth. The instrumental quality parameters of the proposed NACE method, such as limits of detection (LODs), limits of quantitation (LOQs), linearity, and run-to-run and day-to-day reproducibility will be assessed, and the method will be applied for the first time to the analysis of C60 fullerene in a commercial cream.

Materials and methods

Chemicals and standard solutions

C60 (CAS, 99685-96-8) and C70 (CAS, 115383-22-7) fullerenes and the C60 fullerene derivatives C60 pyrr (CAS, 151872-44-5) and C60-COOH (CAS, 155116-19-1) were purchased from Sigma-Aldrich (Steinheim, Germany). The chemical structures and abbreviations of these compounds are given in Fig. 1. TDAB (CAS, 14937-42-9), TEAB (CAS, 71-91-0), HPLC-grade chlorobenzene, acetonitrile, and methanol were also purchased from Sigma-Aldrich, and acetic acid (100 %), sodium hydroxide (99 %), and hydrochloric acid (25 %) were obtained from Merck (Darmstadt, Germany). All reagents and chemicals were of analytical grade.

Water was purified using an Elix 3 coupled to a Milli-Q system (Millipore, Bedford, MA, USA) and filtered using a 0.22-μm nylon filter integrated into the Milli-Q system.

Stock standard solutions of C60, C70, C60, pyrr and C60-COOH (~1,000 mg/L) were prepared in chlorobenzene for NACE analysis and in toluene for the LC-MS method and refrigerated at 4 °C. Prior to analysis, each stock solution was diluted using the background electrolyte (BGE) to form the working solution.

Instrumentation

NACE experiments were performed on a Beckman P/ACE MDQ capillary electrophoresis instrument (Fullerton, CA, USA) equipped with a diode array. Electrophoretic separations were carried out using uncoated fused-silica capillaries (Beckman) with a total length of 60 cm (50 cm effective length)×50 μm I.D. (375 μm O.D.) and using a 200-mM TDAB, 40 mM TEAB, 6 % MeOH, and 10 % acetic acid in a solution of acetonitrile and chlorobenzene at 1:1 ratio (*v*/*v*)

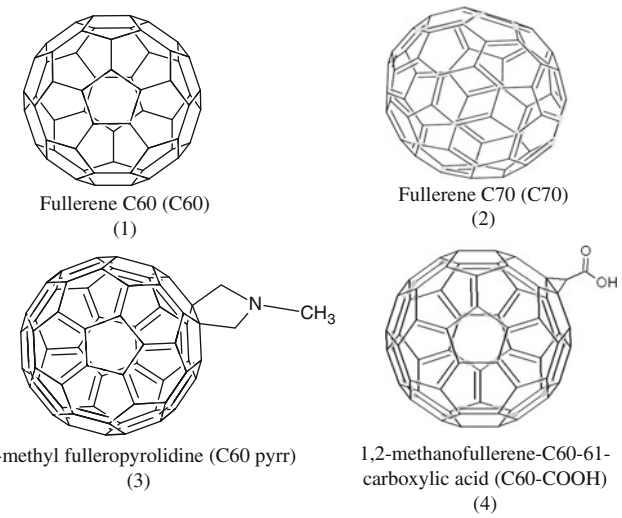

Fig. 1 Fullerene and C60 fullerene derivatives chemical structures

as the BGE. The capillary temperature was held at 25 °C. The BGE was filtered through a 0.45 μm nylon membrane filter before use. A capillary voltage of +30 kV was applied for the separation. Sample introduction was performed by hydrodynamic injection (5 s, 13.5 kPa). Direct UV detection was performed at 350 nm. The CE instrument was controlled using Beckman 32 Karat software version 5.0.

LC-MS experiments for method validation were performed following a previously described method [19]. An ultra-high-performance liquid chromatography (UHPLC) system (Accela system, Thermo Fisher Scientific, San Jose, CA, USA) equipped with a quaternary pump, autosampler, and column was used. The chromatographic separation was performed in a Hypersil GOLD C18 (150 mm×2.1 mm I.D, 1.9 μm particle size) column using a solution of toluene and methanol (45:55, *v/v*) as mobile phase, isocratic elution at a flow rate of 500 μL/min and column temperature of 25 °C. The UHPLC system was coupled to a TSQ Quantum Ultra AM (Thermo Fisher Scientific) triple quadrupole mass spectrometer and a Finnigan Ion Max source (Thermo Fisher Scientific) equipped with a Syagen PhotoMate APPI VUV light source (a krypton discharge lamp, 10 eV; Syagen Technology, Inc., Tustin, CA, USA), and an APCI probe, which was used as nebulization-desolvation device (no corona discharge was applied). Nitrogen (purity, >99.98 %) was used as a sheath gas and an auxiliary gas at a flow rate of 60 and 25 a.u. (arbitrary units). Ion sweep gas was kept at 2 a.u. The temperatures of the ion transfer tube and vaporizer were both set at 350 °C.

Capillary conditioning

New capillaries were pre-treated with 0.1 M HCl for 30 min, water for 30 min, 1 M NaOH for 30 min, and finally washed with water for 30 min. At the beginning of each session, the capillary was rinsed with 0.5 M NaOH for 15 min, water for 15 min, ACN for 5 min, and the BGE for 15 min. The capillary was rinsed with the BGE for 5 min between runs and stored after rinsing with ACN and water at the end of each session. In order to increase migration time reproducibility, the capillary was post-washed with ACN for 5 min, 0.5 M NaOH for 5 min, water for 5 min, ACN for 5 min, and the BGE for 5 min after several runs.

Sample preparation

A previously described method [11], with some modifications, was used to extract fullerene C60 from a personal care product (a cream). Briefly, extraction was performed by sonicating 3 g of cosmetic sample in 20 mL toluene for at least 4 h. The toluene extract was then centrifuged at 4,500 rot/min for 15 min using a Selecta Centronic Centrifuge (Barcelona, Spain). The clear toluene supernatant was then evaporated to dryness and reconstituted with 200 μL chlorobenzene and injected into the CE system.

For the LC-MS method, the same extraction procedure was used but the final extract was reconstituted in toluene and methanol (20:80 *v/v*).

Results and discussion

Optimization of NACE separation

As mentioned in the introduction, only two studies using NACE for the separation of fullerene-based compounds have been published, and only one [18] reported the separation of pristine fullerenes. This last study used tetraalkylammonium salts in an organic solvent mixture containing acetonitrile, chlorobenzene, acetic acid, and methanol. In the present work, the same solution was used as the preliminary BGE (100 mM TDAB, 50 mM TEAB, 6 % MeOH, and 10 % acetic acid in acetonitrile and chlorobenzene at a ratio of 1:1 (*v/v*)), and the effect of its composition on the separation of C60 and C70 fullerenes, together with two C60 fullerene derivatives (C60 pyrr and C60-COOH) was evaluated.

It has been reported that NACE behavior of pristine fullerenes, which are neutral in the organic solvent mixture used, depends on the solvophobic interaction between the fullerenes and the tetraalkylammonium salts, such as TDAB [18]. The charged complexes of the compounds formed by the interaction between the long alkyl chains of TDAB and the fullerenes led to their electrophoretic migration under normal polarity conditions. In this paper, the effect of the background electrolyte TDAB concentration on the separation of the fullerenes studied was evaluated from 90 to 250 mM and the electropherograms obtained for each condition are shown in Fig. 2. As shown, the electrophoretic migration of fullerenes is related to their hydrophobicity. The higher the hydrophobicity of the fullerenes, the stronger the interaction with TDAB, and therefore lower migration times were observed. This explains why pristine C70 fullerene (peak 1) migrate faster than pristine C60 fullerene (peak 2), which is smaller. In contrast, C60 fullerene derivatives, which have a higher polarity, showed lower electrophoretic mobility than pristine fullerenes, with C60-COOH (the most polar compound) showing the highest migration time (peak 4). The increase in TDAB concentration also improved the electrophoretic separation of the fullerenes. A slight improvement in C60 and C70 electrophoretic peak resolution with TDAB concentration was observed (Rs values from 0.9 at 90 mM TDAB to 1.2 at 200 mM TDAB), as was an improvement in peak signal (Table 1). In contrast, the migration behavior of C60 fullerene derivatives was considerably affected by TDAB, which resulted in better separation at high concentrations, although the analysis time increased noticeably. A TDAB concentration of 200 mM was selected as

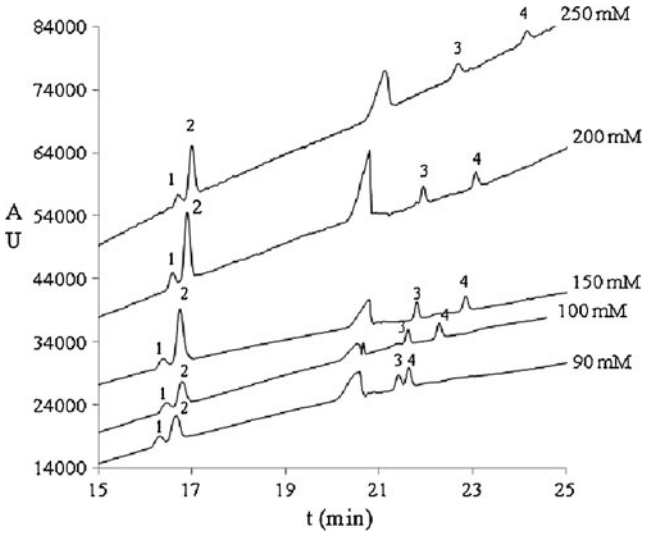

Fig. 2 Electropherograms of a mixture of fullerenes (100 mg/L) at different TDAB concentrations (from 90 to 250 mM). Other BGE conditions: 50 mM TEAB, 6 % MeOH, and 10 % acetic acid in acetonitrile/chlorobenzene 1:1 (*v/v*). Acquisition conditions: capillary voltage, +30 kV; hydrodynamic injection, 5 s (13.5 kPa); and wavelength, λ 350 nm. Peak identification: *1* C60, *2* C70, *3* C60 pyrr, and *4* C60-COOH

optimum for the BGE as a compromise between peak height, electrophoretic separation and analysis time.

The presence of a quaternary ammonium salt with short alkyl chains (TEAB) was needed to improve the resolution of pristine fullerenes. In this study, the effect of TEAB concentration, from 0 to 60 mM, on the fullerene migration time was evaluated and the observed apparent electrophoretic mobility is summarized in Table 2. As shown, the apparent mobility of the fullerenes decreased with TEAB concentration, thus improving electrophoretic separation. This is probably due to a reduction in the EOF caused by the adsorption of this salt on the internal surface of the silica capillary tube by electrostatic interaction reducing its surface charge or zeta potential [20, 21]. As a compromise between analysis time and good electrophoretic separation, a TEAB concentration of 40 mM was selected as optimum for further studies.

The composition of the organic solvent mixture used for the analysis of fullerenes by NACE was also evaluated during this study. It was observed that the volume ratio of

Table 2 Effect of TEAB concentration on the apparent mobilities of the studied fullerenes

TEAB (mM)	$\mu_{app} \times 10^4$ (cm^2/Vs)			
	C70	C60	C60 pyrr	C60-COOH
0	1.75	1.75	1.5	1.5
20	1.22	1.2	1.02	1.01
40	1.0	0.98	0.76	0.72
50	0.96	0.94	0.68	0.65
60	0.9	0.89	0.62	0.59

acetonitrile and chlorobenzene exerted a certain effect on the separation. For instance, increasing the acetonitrile content (acetonitrile/chlorobenzene, 3:2, *v/v*) reduced the migration time of all compounds because of the increase in EOF, which impaired the separation. For a mixture of ACN and chlorobenzene at a ratio of 2:3 (*v/v*), the migration times of the compounds increased considerably (27 and 35 min for C60 and C60-COOH, respectively). For this reason, a solution of acetonitrile and chlorobenzene at a ratio of 1:1 (*v/v*) was maintained for further studies.

The effect of acetic acid content, from 6 to 20 % in the organic solvent mixture, on the separation of fullerene compounds was studied. It was observed that migration times increased considerably with acetic acid as its high viscosity led to a reduction in EOF (Table 3). An improvement on C60 and C70 resolution from 6 to 10 % was observed. However, the separation of the two C60 derivatives worsened with the acetic acid content and was completely lost when 20 % was used. As a compromise between analysis time and separation, an acetic acid content of 10 % was chosen as the optimum value for further studies.

In this work, MeOH was used in order to reduce analysis time. The effect of MeOH content in the BGE on fullerene separation is given in Table 3. As it can be seen, migration times of C60-COOH decreased with the MeOH which can be explained by hydrogen bonding interactions, reducing its polarity and so improving the interaction with TDAB. A content of 6 % methanol in the BGE was chosen as optimum value providing good peak resolution and reducing the analysis time.

Table 1 Effect of TDAB concentration on the separation of the studied fullerenes

TDAB (mM)	Height				Rs	
	C70	C60	C60 pyrr	C60-COOH	C70–C60	C60 pyrr–C60-COOH
90	1,373	3,936	2,220	2,601	0.9	0.6
100	1,400	3,980	2,409	2,056	1.1	2.6
150	1,471	8,132	2,737	2,340	1.2	4.5
200	1,625	10,858	2,820	2,573	1.2	5.1
250	1,502	8,058	2,076	1,823	1.1	5.9

Table 3 Effect of acetic acid and methanol content in the BGE on the separation of the studied fullerenes

	t_m (min)				Rs	
	C70	C60	C60 pyrr	C60-COOH	C70-C60	C60 pyrr–C60-COOH
Acetic acid (%)[a]						
6	14.9	15.0	17.9	22.8	0.7	24
10	16.6	16.9	22.3	25.0	1.2	13
16	19.3	19.6	27.4	28.1	1.3	2.8
20	23.1	23.5	34.3	34.3	1.3	0
MeOH (%)[b]						
0	16.6	16.9	22.3	25.0	1.2	13
4	16.7	17.0	22.2	24.0	1.2	8.6
6	16.7	17.0	22.2	23.3	1.2	5.1
8	16.7	17.0	22.1	22.2	1.2	0.9

[a] Other BGE conditions: 200 mM TDAB and 40 mM TEAB in acetonitrile–chlorobenzene 1:1 (*v/v*)

[b] Other BGE conditions: 200 mM TDAB, 40 mM TEAB, and 10 % acetic acid in acetonitrile–chlorobenzene 1:1 (*v/v*)

In summary, 200 mM TDAB, 40 mM TEAB, 6 % methanol, and 10 % acetic acid in a solvent mixture of acetonitrile and chlorobenzene at a ratio of 1:1 (*v/v*) was selected as the optimum BGE solution for the NACE separation of the four fullerenes studied in this work. The electrophoretic separation achieved under the optimal conditions is shown in Fig. 3a.

Method performance

Instrumental quality parameters of the proposed NACE method were determined and the figures of merit are given in Table 4. LODs, based on a signal-to-noise ratio of 3:1, were calculated using standard solutions prepared in chlorobenzene at low concentration levels. The LODs of the compounds ranged from 1 to 3.7 mg/L, while LOQs, based on a signal-to-noise ration of 10:1, were between 3.0 and 11.1 mg/L.

Calibration curves based on peak areas at a working range of between 3.7 and 100 mg/L were obtained and good linearity with correlation coefficients (r^2) higher than 0.98 was achieved. Run-to-run and day-to-day precisions for the fullerenes studied were calculated at two concentration levels, a low level (LOQ) and a medium level (50 mg/L), and the results, expressed as relative standard deviation (%RSD), are also given in Table 4. To obtain the run-to-run precision, a total of five replicate determinations for each concentration level were carried out on the same day ($n=5$). The day-to-day precision was calculated by performing five replicate determinations of each concentration level on three non-consecutive days (five replicates each day, $n=15$). As can be seen, acceptable run-to-run and day-to-day precisions (with RSD values lower than 14.5 %) were achieved. Run-to-run and day-to-day precisions of the migration times for all fullerenes studied were also calculated, and RSD values lower than 1.8 % were obtained.

In summary, the performance achieved with the optimized NACE method is adequate in terms of repeatability and reproducibility for the analysis of the fullerenes studied.

Application

In order to evaluate the applicability of the optimized NACE method, the analysis of real samples was considered. Due to the limits of detection of the NACE method, real samples with relatively high fullerene concentrations were needed. Recently, the analysis of fullerene C60 in personal care products by LC-MS was described and fullerene concentrations between 1 and 6.8 mg/L for C60 [10, 11] were found. For this reason, we evaluated the applicability of the proposed NACE method by analyzing C60 in a commercial cosmetic cream.

Sample extraction was performed following a previously described procedure [11], as indicated in the "Sample preparation" section. After sample extraction, extracts were submitted to the proposed NACE method and the electropherogram obtained is shown in Fig. 3b. As shown, only one peak was observed, and this was identified as C60 fullerene by

Table 4 Instrumental-quality parameters

	LODs (mg/L)	LOQs (mg/L)	Run to run precision (% RSD; $n=5$)			Day-to-day precision (% RSD; $n=5\times3$)		
			Migration time	Concentration (low level)[a]	Concentration (medium level)[b]	Migration time	Concentration (low level)[a]	Concentration (medium level)[b]
C70	3.7	11.1	0.4	6.2	3.7	1.2	8.1	6.3
C60	1.0	3.0	0.3	5.8	2.5	1.3	10.1	5.8
C60 pyrr	1.3	3.9	1.0	8.0	1.5	1.2	14.5	4.1
C60-COOH	2.8	8.4	0.5	5.7	1.7	1.6	10.1	1.9

[a] LOQ

[b] Fifty milligrams per liter

comparison of UV spectra and the addition of C60 standard to a cream also submitted to the extraction procedure (Fig. 3b). Sample quantitation was carried out by triplicate using a standard addition method (since no blank cream samples were available), and the concentration found was 2.10±0.20 mg/L. In order to validate the NACE method for the analysis of C60 in creams, the result was compared with that obtained by analyzing the same cream sample by LC-MS. C60 extraction from the cream was performed using the same extraction procedure, but the final extract was reconstituted in toluene and methanol at a ratio of 20:80 (*v/v*). Quantitation was also performed by triplicate and the concentration found was 1.93±0.15 mg/L. The LC-MS chromatogram obtained for the quantitation of C60 in a commercial cometic cream is shown in Fig. 3c. A statistical paired-sample comparison analysis was performed based on the quantitation results obtained in both the NACE and LC-MS methods. For a 95 % confidence level, the results were not significantly different (p value of 0.30). The results obtained showed that the NACE method proposed in this work is suitable for the analysis of C60 in commercial cosmetic creams. This method is less expensive and less contaminant, because of the use of much lower amount of solvents, than LC-MS methods which for this kind of application require the use of high amount of toluene in the mobile phases.

Concluding remarks

The behavior of hydrophobic fullerene compounds, C60, C70, C60 pyrr, and C60-COOH, in non-aqueous capillary electrophoresis was studied in depth. The use of a long-chain alkyl ammonium salt (TDAB) at a high concentration to generate a fullerene-TDAB charged complex and a short-chain alkyl ammonium salt (TEAB) at a lower concentration to reduce EOF was needed in order to achieve good electrophoretic performance for all fullerenes studied. The organic solvent composition of the

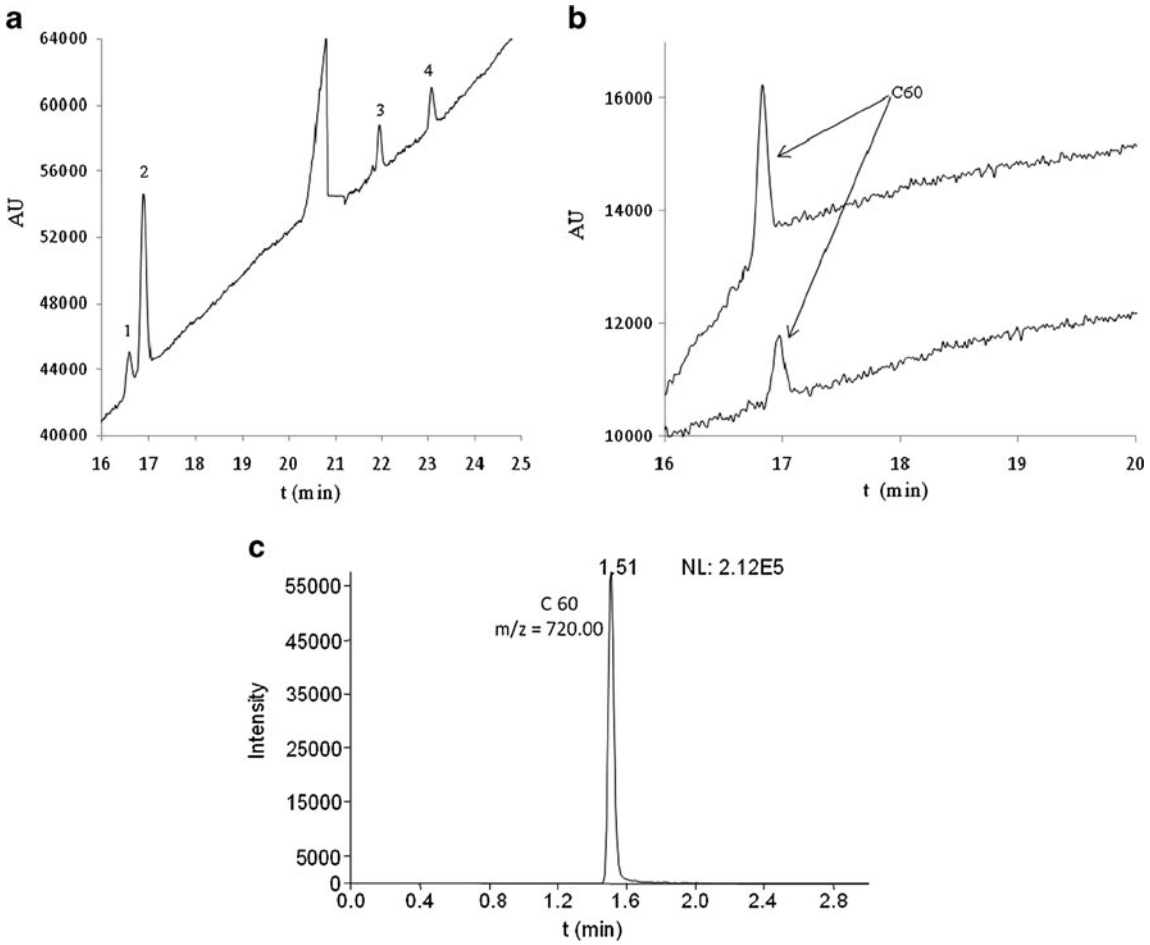

Fig. 3 **a** Separation of fullerenes by NACE under optimum conditions. **b** Electropherogram obtained for a commercial cosmetic cream and the same product fortified with 5 mg/L of C60. **c** LC-MS chromatogram of C60 in a commercial cosmetic cream BGE: 200 mM TDAB, 40 mM TEAB, 6 % MeOH, and 10 % acetic acid in acetonitrile:chlorobenzene 1:1 (*v/v*). Acquisition conditions: capillary voltage, +30 kV; hydrodynamic injection, 5 s (13.5 kPa); and acquisition wavelength, λ 350 nm. LC-MS conditions as indicated in "Instrumentation" section. Peak identification: *1* C60, *2* C70, *3* C60 pyrr, and *4* C60-COOH

BGE had a significant effect on resolutions and migration times of the fullerenes.

It was observed that acetic acid is needed in order to obtain the separation of the studied compounds. The migration times of the compounds increased considerably with acetic acid content due to its high viscosity. The addition of MeOH to the BGE shortened the analysis time by reducing the migration time of C60-COOH because of interactions between MeOH and the functional group of this compound.

Acceptable instrumental limits of detection at parts per million level (as expected with this kind of methodology) were obtained, with good run-to-run and day-to-day precisions at two concentration levels and RSD values lower than 15 %, which made it possible to use the method to analyze these compounds in samples with a high enough concentration. The developed method was applied to the determination of C60 in a commercial cosmetic cream. The results obtained in this work showed that NACE is an inexpensive, and low solvent consumption method, that can be proposed as alternative to conventional LC for the analysis of C60 in commercial cosmetic creams.

Acknowledgments The authors gratefully acknowledge the financial support received from Spanish Ministry of Science and Innovation under the project CTQ2009-09253. Alina Astefanei thanks the Spanish Ministry of Science and Innovation for a Ph.D. grant (FPI).

References

1. Jafvert CT, Kulkarni PP (2008) Buckminsterfullerene's (C60) octanol–water partition coefficient (K_{ow}) and aqueous solubility. Environ Sci Technol 42:5945–5950
2. Pycke BFG, Benn TM, Herckes P, Westerhoff P, Halden RU (2011) Strategies for quantifying C60 fullerenes in environmental and biological samples and implications for studies in environmental health and ecotoxicology. TrAC-Trends Anal Chem 30:44–57
3. Murayama H, Tomonoh S, Alford JM, Karpuk ME (2004) Fullerene production in tons and more: from science to industry. Fullerenes, Nanotubes, Carbon Nanostruct 12:1–9
4. Maralikova B, Weinmann W (2004) Confirmatory analysis for drugs of abuse in plasma and urine by high-performance liquid chromatography-tandem mass spectrometry with respect to criteria for compound identification. J Chromatogr B: Anal Technol Biomed Life Sci 811:21–30
5. Isaacson CW, Kleber M, Field JA (2009) Quantitative analysis of fullerene nanomaterials in environmental systems: a critical review. Environ Sci Technol 43:6463–6474
6. Farre M, Perez S, Gajda-Schrantz K, Osorio V, Kantiani L, Ginebreda A, Barcelo D (2010) First determination of C60 and C70 fullerenes and *N*-methylfulleropyrrolidine C60 on the suspended material of wastewater effluents by liquid chromatography hybrid quadrupole linear ion trap tandem mass spectrometry. J Hydrol 383:44–51
7. Bouchard D, Ma X (2008) Extraction and high-performance liquid chromatographic analysis of C60, C70, and [6,6]-phenyl C61-butyric acid methyl ester in synthetic and natural waters. J Chromatogr A 1203:153–159
8. Moussa F, Pressac M, Genin E, Roux S, Trivin F, Rassat A, Ceolin R, Szwarc H (1997) Quantitative analysis of C60 fullerene in blood and tissues by high-performance liquid chromatography with photodiode-array and mass spectrometric detection. J Chromatogr B: Biomed Sci Appl 696:153–159
9. Xia XR, Monteiro-Riviere NA, Riviere JE (2006) Trace analysis of fullerenes in biological samples by simplified liquid-liquid extraction and high-performance liquid chromatography. J Chromatogr A 1129:216–222
10. Chae SR, Hotze EM, Xiao Y, Rose J, Wiesner MR (2010) Comparison of methods for fullerene detection and measurements of reactive oxygen production in cosmetic products. Environ Eng Sci 27:797–804
11. Benn TM, Westerhoff P, Herckes P (2011) Detection of fullerenes (C60 and C70) in commercial cosmetics. Environ Pollut 159:1334–1342
12. Cottet H, Simo C, Vayaboury W, Cifuentes A (2005) Nonaqueous and aqueous capillary electrophoresis of synthetic polymers. J Chromatogr A 1068:59–73
13. Tamisier-Karolak SL, Pagliarusco S, Herrenknecht C, Brettreich M, Hirsch A, Ceolin R, Bensasson RV, Szwarc H, Moussa F (2001) Electrophoretic behavior of a highly water-soluble dendro [60]fullerene. Electrophoresis 22:4341–4346
14. Cerar J, Pompe M, Gucek M, Cerkovnik J, Skerjanc J (2007) Analysis of sample of highly water-soluble Th-symmetric fullerenehexamalonic acid C66(COOH)12 by ion-chromatography and capillary electrophoresis. J Chromatogr A 1169:86–94
15. Chan KC, Patri AK, Veenstra TD, McNeil SE, Issaq HJ (2007) Analysis of fullerene-based nanomaterial in serum matrix by CE. Electrophoresis 28:1518–1524
16. Treubig JM, Brown PR (2000) Novel approach to the analysis and use of fullerenes in capillary electrophoresis. J Chromatogr A 873:257–267
17. Su HL, Kao WC, Cy L, Chuang SC, Hsieh YZ (2010) Separation of open-cage fullerenes using nonaqueous capillary electrophoresis. J Chromatogr A 1217:4471–4475
18. Wan TSM, Leung GNW, Tso TSC, Komatsu K, Murata Y (1995) Non-aqueous capillary electrophoresis as a new method for the separation of fullerenes. Proc - Electrochem Soc 95–10:1474–1487
19. Núñez ON, Astefanei A, Gallart-Ayala H, Moyano E, Galceran MT (2011) Analysis of fullerenes (C60 to C84) and C60-fullerene derivatives by liquid chromatography-atmospheric pressure photoionization/mass spectrometry. In: Oral communication, 13th Instrumental Analysis Conference, Barcelona, Spain, 14th to 16th November
20. Takayanagi T, Wada E, Motomizu S (1997) Electrophoretic mobility study of ion association between aromatic anions and quaternary ammonium ions in aqueous solution. Analyst 122:57–62
21. Wang H, Hu H, Ding T, Gu J, Dai R, Fu R (1998) Study on the enantiomeric separation of adrenalines by capillary zone electrophoresis. Sepu 16:22–25

CHAPTER 2

ANALYSIS OF FULLERENES

2.4. Discussion of results

2.4. Discussion of results

The current section presents and discusses the most important aspects of the results obtained in the studies herein included related to the establishment and application of separation techniques for the determination of pristine and surface modified fullerenes in environmental and cosmetic samples. The fullerenes considered in these studies were selected for two reasons. On the one hand because their presence in the environment and/or commercial products such as cosmetics is expected to increase considerably in the future due to their increasing applications in different sectors, and on the other hand because of the lack of suitable methods for the analysis of both prisitine and surface modified fullerenes in complex samples.

Separation

Among the current challenges facing the analysis of fullerenes there is the need to separate and distinguish between the very hydrophobic pristine fullerenes of varying sizes, and also differentiate them from those that present surface-functional groups of different type, size and number. In this thesis, two techniques (LC and NACE) have been used for this purpose.

To accomplish the chromatographic separation of pristine (C_{60}-C_{84}) and surface modified fullerenes (PCBM, PCBB and C_{60}-pyrr) we evaluated two types of C18 columns, one with totally porous particles (Hypersil GOLD) and the other with superficial porous (core-shell) particles (Accucore C18) using isocratic elution (tolune:methanol, 60:40, v/v). In both columns (Figure 2.1), the C_{60}-fullerene derivatives eluted before C_{60}, due to their higher polarity, and the retention times increased with the cage size being higher for large fullerenes (C_{76}-C_{84}). As commonly reported for relatively small molecules, PCBM and PCBB were less retained in the core shell Accucore C18 column (Figure 2.1b) than in the column with totally porous particles (Hypersil GOLD) (Figure 2.1a) because of their smaller particle surface area (thin porous shell) than that of totally porous particles (Staub et al., 2011; Gallart-Ayala et al., 2011; Yang et al., 2011; Destefano et al., 2012). In contrast, C_{60}-pyrr and pristine fullerenes presented a higher retention in the Accucore C18 column. This behaviour can be related to the fullerenes size and column's packing pore size since fullerenes with symmetrical shape and relatively big size (~10 Å for C_{60}) would present higher interaction with smaller porous size packing (80 Å, Accucore C18) than with the totally porous ones of higher porosity (175 Å, Hypersil GOLD). The different behaviour shown by C_{60}-pyrr compared to the other two fullerene derivatives could be related to the size

of the functional groups attached to the buckyball structure, and consequently to its geometry. Among the three evaluated compounds, C_{60}-pyrr has the smallest functional group, and therefore its symmetry and retention behaviour is more similar to that of C_{60} than the other fullerene derivatives.

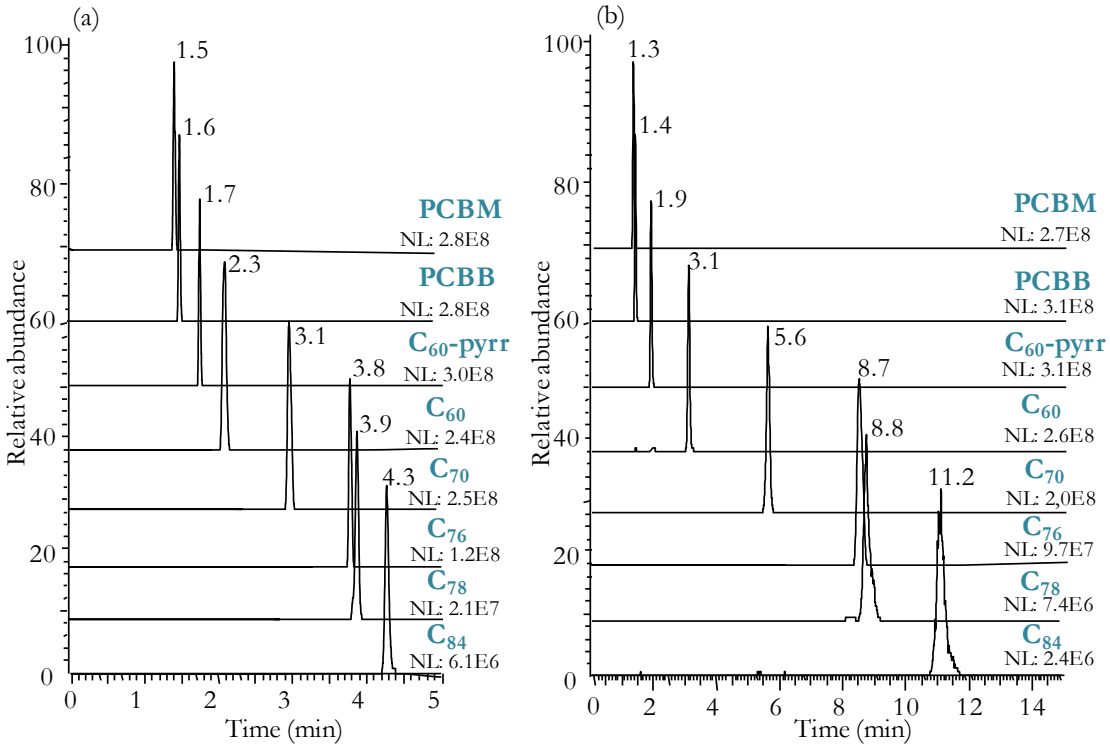

Figure 2.1. UHPLC–APPI-MS(/MS) separation of fullerenes in (a) Hypersil GOLD C18 column (150 mm × 2.1 mm, 1.9 μm) and (b) Accucore C18 column (150 x 2.1 mm, 2,6 μm) using toluene:methanol (40:60, v/v) as mobile phase, Flow rate: 500 μL min^{-1}.

The chromatographic behaviour of fullerenes in toluene:methanol and toluene:acetonitrile mixtures under the same proportion was one of the most relevant aspects noticed during the optimisation of the chromatographic separation of the selected fullerenes. Surprisingly, higher retention times (up to 1.65 times higher for C_{84}) were obtained by using toluene:acetonitrile than toluene:methanol (see Figure 4 Section 2.2., Chapter 2). In theory, the opposite should occur since the eluotropic strength of the first mixture is higher, and consequently, lower retention times should be obtained. In reversed phase chromatography the retention of fullerenes depends on their size and the greater the size, the higher their retention. Hence, the unexpected retention behaviour observed in these solvent mixtures could be related to their particle sizes. As mentioned in the introduction (see Section 1.3.1., Chapter 1), fullerenes aggregate in aqueous media forming stable colloidal complexes that explain their dispersion in

water. Despite the high solubility of fullerenes in nonpolar solvents, their aggregation has also been reported in both neat nonpolar solvents (e.g. toluene, benzene, etc.) (Nath et al., 1998; Rudalevige et al., 1998), and in binary mixtures with a weak fullerene solvent (e.g. toluene-methanol, toluene-acetonitrile, etc.) (Sun et al., 1995; Rudalevige et al., 1998; Mrzel et al., 1999; Alargova et al., 2001). Regarding the aggregation mechanism in binary solvent mixtures, it has been proposed (Ghosh et al., 1996; Mrzel et al., 1999; Alargova et al., 2001) that the presence of the weak solvent forces the fullerene molecules to surround themselves by a strong solvent's shell which holds these entities together like emulsion droplets, and when the fullerene concentration reaches the saturation point, the formation of fullerene clusters occurs (Figure 2.2). Moreover, it has been found that the sizes of the clusters formed decrease when increasing the polarity of the weak solvent (Mrzel et al., 1999; Alargova et al., 2001). Hence, the higher retention times observed in toluene:acetonitrile compared to toluene:methanol mobile phase could be due to the formation of bigger aggregates in the first mixture.

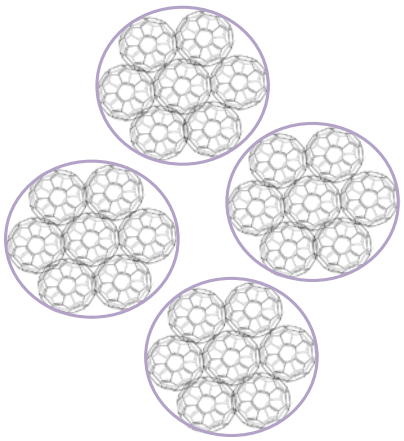

Figure 2.2. Schematic representation of encapsulated fullerene aggregates. Based on (Mrzel et al., 1999).

The separation of fullerenes by capillary electrophoresis was also studied. In a first attempt, NACE was used to evaluate the capability of this technique for the analysis two pristine compounds (C_{60} and C_{70}) and two C_{60}-derivatives (C_{60}-pyrr and C_{60}CHCOOH) of relatively high hydrophobicity. Since these compounds are neutral in organic solvents, the use of charged salts able to interact with the target analytes providing them charge and, consequently, electrophoretic mobility was required. For this purpose a long alkyl chain length tetraalkylammonium salt (tetra-*n*-decylammonium bromide (TDAB)) that forms positively charged complexes with fullerenes by solvophobic interactions, as recommended by Wan et al. (Wan et al., 1995), was employed. Under these conditions the compounds migrated towards the cathode under positive polarity and the separation was related to their hydrophobicity as in reversed phase LC.

Some similarities can be drawn between this technique and reversed phase liquid chromatography. The solvophobic interaction between the compounds and TDA+ ion is similar to that occurring with a reverse phase stationary phase. In NACE, the larger nonpolar compounds present higher interaction with TDA+ ion than the smaller or more polar solutes. Similarly, in reversed phase LC, the larger, more hydrophobic solutes would be more retained in the stationary phase than the smaller ones. However, in NACE the order of elution is exactly the opposite than in LC. The greater the interaction of the compounds with the tetraalkylammonium cations, the higher their electrophoretic mobility, and lower their migration times. Therefore, C_{70} migrated faster than C_{60} followed by C_{60}-pyrr and lastly by C_{60}CHCOOH (see Figure 2, Section 2.3., Chapter 2).

The addition of a short alkyl chain length tetraalkylammonium salt (TEAB) to the running BGE was needed in order to improve the resolution between the compounds, especially between prisitine fullerenes. The resolution (Table 2.1) increased with salt concentrations; from 0.5 (0 mM) up to 1.3 (60 mM). However, concentration values higher than 40 mM led to a significant decrease in the electrophoretic mobility of the compounds (see Table 2, Section 2.3., Chapter 2), and consequently to an increase in the analysis time. This was probably caused by the adsorption of this salt to the capillary wall reducing the zeta potential at high concentrations. On the other hand, the increase in the amount of TDAB in the running electrolyte showed a major effect on the Rs between C_{60}-fullerene derivatives that improved from 0.6 at 90 mM up to 5.9 at 250 mM (see Table 2.1). However, for pristine fullerenes, a slight decrease in resolution was found at 250 mM (1.1) and additionally, at this concentration the peak heights (see Table 1, Section 2.3., Chapter 2) also decreased. Hence, the best results in terms of resolution and peak signals were found a TDAB concentration of 200 mM. The solvophobic interaction mechanism between neutral (hydrophobic) organic molecules and tetraalkylammonium cations involves a dynamic equilibrium between the associated and the dissociated forms of the solutes with the cations. Therefore, an increase in the concentration of TDAB would increase the number of solute molecules associated with TDA^+ cations producing an enhancement in the peaks signal.

Table 2.1. Effect of TEAB and TDAB concentration on the separation of fullerenes

TEAB [mM]	Rs		TDAB [mM]	Rs	
	C_{60}-C_{70}	C_{60}-pyrr-C_{60}CHCOOH		C_{60}-C_{70}	C_{60}-pyrr-C_{60}CHCOOH
0	0.5	3.2	90	0.9	0.6
20	0.5	3.6	100	1.1	2.6
40	1.2	5.1	150	1.2	4.5
50	1.2	5.1	200	1.2	5.1
60	1.3	6	250	1.1	5.9

The use of such high salt concentrations (200 mM TDAB and 40 mM TEAB) and the high voltage applied (30 kV) required for the separation of the compounds caused a baseline drift in the electropherograms obtained with a Beckman P/ACE MDQ CE system. The separation of the compounds was reproduced by using the same NACE method with a different CE system (Agilent 7100) to assure its validity. The electropherogram obtained with both instruments for a standard mixture are shown in Figure 2.3. As can be seen, by using the Agilent system (Figure 2.3a) the baseline drift did not appear in the electropherogram, probably due to a more efficient cooling system which removed the Joule heating effect. A low intensity peak was observed in the electropherograms obtained with both instruments (migration time 17.5 min) which also appeared when injecting the electrolyte mixture.

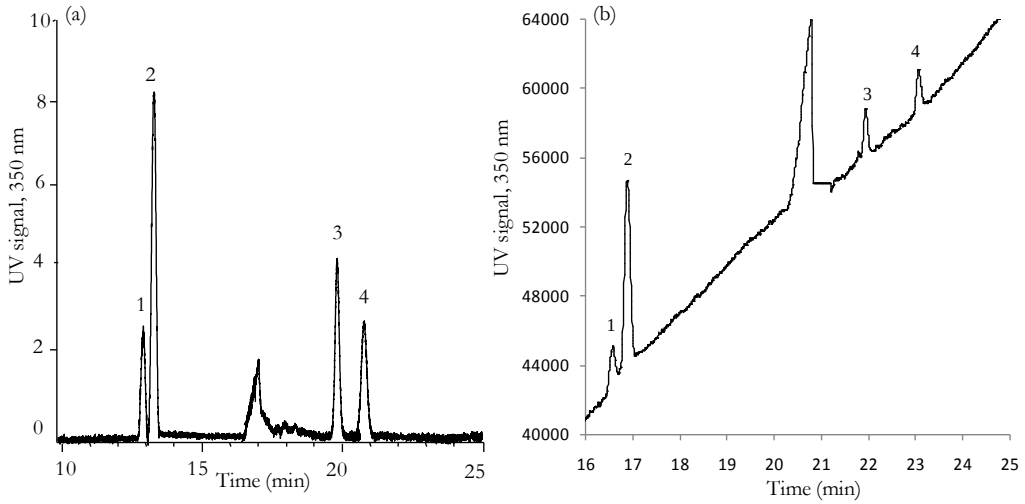

Figure 2.3. Separation of fullerenes by NACE in (a) Agilent 7100 CE system and (b) Beckman P/ACE MDQ CE system; 1: C_{70}; 2: C_{60}; 3: C_{60}-pyrr; 4: C_{60}CHCOOH; BGE: 200 mM TDAB, 40 mM TEAB, 6% methanol, 10 % acetic acid and acetonitrile:chlorobenzene 1:1 (v/v); V= +30 kV; hydrodynamic injection, 5 s (50 mbar), λ= 350 nm.

The selectivity of the separation was further improved by adjusting the solvent composition in the BGE (i.e., chlorobenzene/acetonitrile ratio and methanol and acetic acid percentage). An interesting effect was observed when optimising the amount of acetic acid and methanol. The augment of the acetic acid percentage changed the BGE viscosity leading to a significant increase in the migration times of the selected compounds by reducing the EOF and improving the resolution between C_{60} and C_{70} (Figure 2.4a). In contrast, the separation between the two C_{60}-derivatives worsened and it was completely lost when 20 % acetic acid was used, exerting a major effect on C_{60}-pyrr than on C_{60}CHCOOH. This could be due to the presence of a nitrogen atom with unpaired electrons in the functional group of this compound that can act as proton acceptor favouring the interaction with the acetic acid.

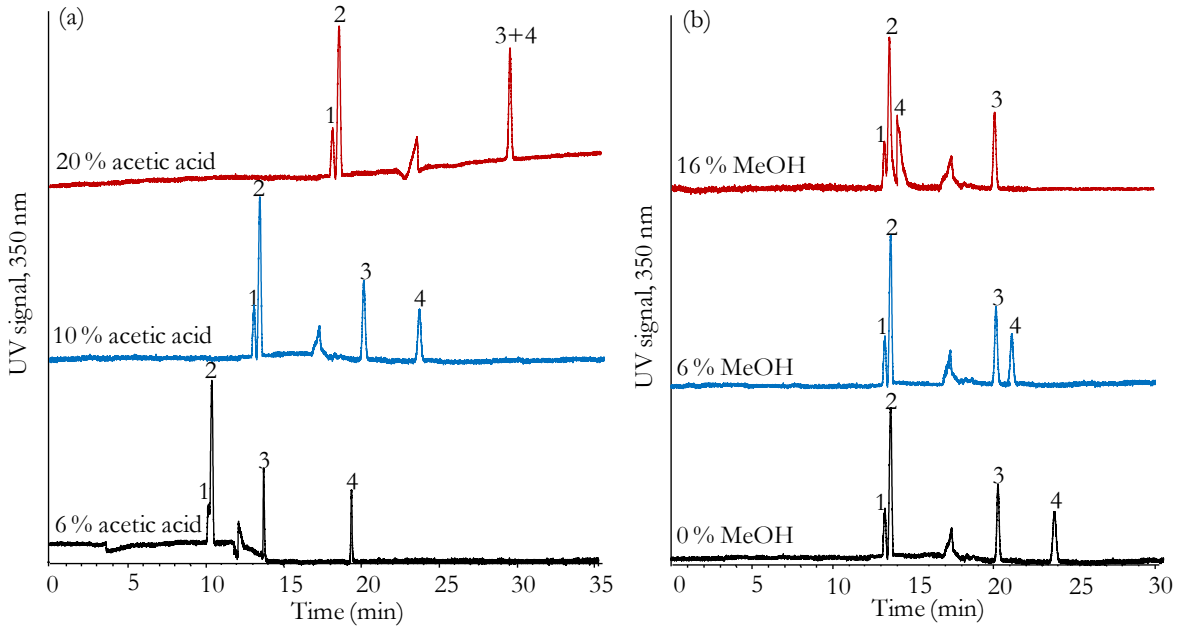

Figure 2.4. Electropherograms of a mixture (100 mg L^{-1}) of fullerenes 1: C_{70}; 2: C_{60}; 3: C_{60}-pyrr; 4: C_{60}CHCOOH at (a) different acetic acid percentages (6-20 %) and 200 mM TDAB, 40 mM TEAB, acetonitrile:chlorobenzene 1:1 (v/v) (b) different MeOH percentages (0-16 %) and 200 mM TDAB, 40 mM TEAB, 10 % acetic acid, acetonitrile:chlorobenzene 1:1 (v/v); V= +30 kV; hydrodynamic injection, 5 s (50 mbar), λ= 350 nm.

Contrary to this behaviour, the addition of MeOH to the BGE resulted in a decrease in the analysis time (Figure 2.4b) due to the reduction of the C_{60}CHCOOH (peak 4) migration time. At 16 % MeOH, its migration time increased significantly eluting right after C_{60} and the separation of the compounds worsened. This behaviour could be caused by hydrogen bonding interactions between the functional group of C_{60}CHCOOH and MeOH, which reduced its

polarity and consequently improved its interaction with the TDAB. Instead, the migration times of the C_{60}, C_{70} and C_{60}-pyrr were not affected by the change in the amount of MeOH. The optimum separation conditions were 200 mM TDAB, 40 mM TEAB, chorobenzene:acetonitrile 1:1 (v/v), 6% MeOH and 10 % acetic acid.

Detection

As previously mentioned, both UV-vis and MS provide good response for the detection of fullerenes. In this thesis, the coupling of the developed NACE method to MS was not possible because of the presence of a high amount of salts required for the separation of the selected fullerenes, thus, UV detection was used.

With regard to LC-MS coupling, different ionization sources were evaluated (Heated-ESI, APCI and APPI) and an extensive optimisation was performed in terms of ionisation performance. Moreover fragmentation studies of the surface modified fullerenes, for which very little information is available in the literature, were carried out. Depending on the ionisation source used, the ionisation mode (positive and negative) and the specific operating ionisation conditions (e.g., source temperature, applied voltage, discharge current, etc.) different results in terms of selectivity and sensitivity were obtained. However, regardless of the source, a higher ionisation efficiency was always observed in negative mode and the MS spectra were dominated by the isotope cluster of the molecular anion $[M]^{-\bullet}$, with m/z ions at M, M+1, M +2, and M+3 (see Figure 2.5). Among the evaluated ionisation sources, APCI provided better results than both ESI and H-ESI, which can be related to the fact that electron capture is favoured in the APCI plasma. Nevertheless, the best sensitivity was obtained by APPI (see Figure 2, Section 2.2., Chapter 2), in agreement with the results formerly reported for pristine compounds (Núñez et al., 2012). This is related, as previously mentioned, to the use of toluene in the mobile phase that improves the ionisation efficiency of these compounds.

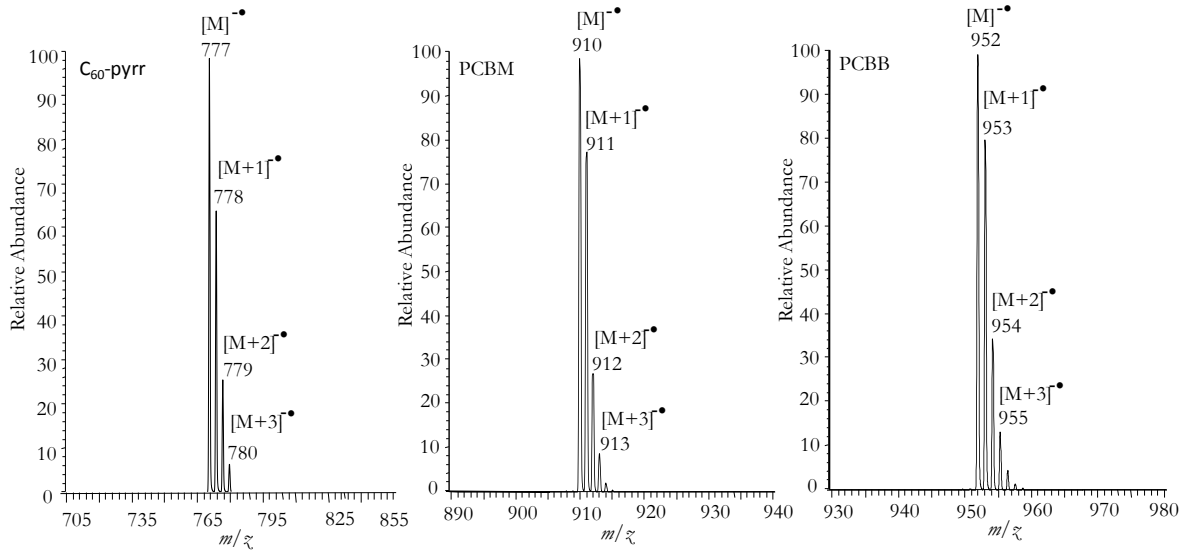

Figure 2.5. UHPLC(-)APPI-MS spectra of C_{60}-fullerene derivatives; Toluene:methanol (45:55, v/v).

In contrast to the behaviour observed for pristine fullerenes which cannot be fragmented due to the high stability of the buckyball structure, the studied C_{60}-fullerene derivatives showed fragmentation at high collision energies (CE) (> 80 eV) loosing the entire functional group and providing a major product ion at *m/z* 720 corresponding to $[C_{60}]^{-\bullet}$. This fragment ion was selected for quantitation purposes. Additionally, for PCBB and PCBM, the loss of the butyl acid alkyl-ester group was observed in its MS/MS spectra at CE < 80 eV for which, to the best of our knowledge, no information is available in the literature. To fulfil EU legislation, two SRM transitions must be used for each fullerene derivative. In this case, since the isotopic cluster of these compounds showed a high abundance of the ^{13}C ion (see Figure 2.5) due to the high number of carbon atoms in the molecules, the transitions, $[M]^{-\bullet} \rightarrow [C_{60}]^{-\bullet}$ for quantification and $[M+1]^{-\bullet} \rightarrow [C_{60}+1]^{-\bullet}$ for confirmation were selected.

One relevant aspect which required special attention for the establishment of the analytical method presented in this section was the evaluation of the matching between the observed isotope pattern and the theoretical one, since this was being used for quantitation and confirmation purposes. It was previously reported that pristine fullerenes present isotopic patterns with relative abundances of *m/z* M+1, M+2, and M+3 higher than the theoretical ones, and the increase of the signal was explained by the addition of hydrogen to a double bond of the fullerene structure (Núñez et al., 2012). In this thesis, the spectra obtained by LC-MS showed that the *m/z* M/M+1 abundance ratio depends on fullerene concentration, and the isotope pattern matches with the theoretical one at concentrations lower than 100 μg L^{-1} for C_{60} (Figure 2.5) and C_{70}, and lower than 10 μg L^{-1} for higher fullerenes. Contrary to this behaviour, the

isotope pattern of the studied fullerene derivatives obtained using APPI matched to those obtained by H-ESI and APCI and also with the theoretical ones regardless of the injected concentration. This could be caused by the presence of functional groups that may reduce the tendency of hydrogen addition to the double bonds.

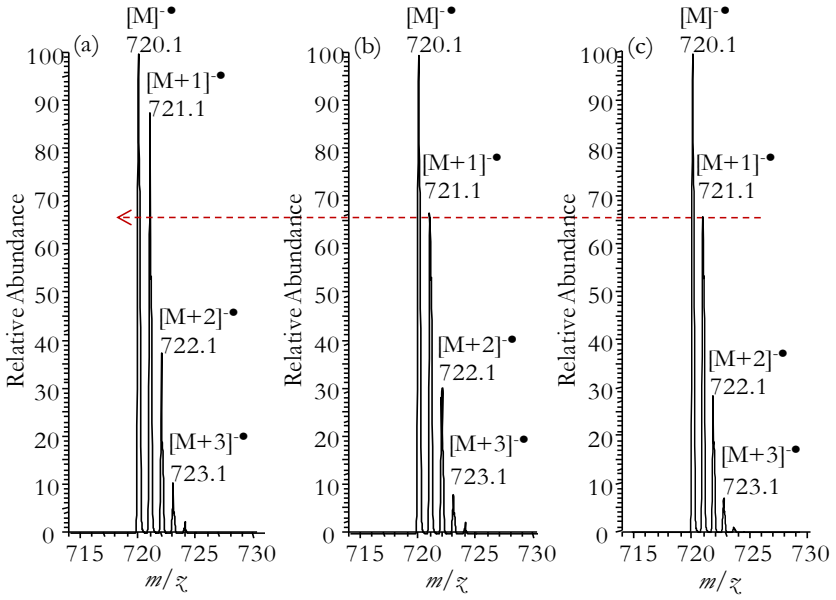

Figure 2.5. UHPLC-(-)APPI-MS spectra of C_{60} at different concentrations: (a) 500 μg L^{-1} (b) 50 μg L^{-1}. (c) Theoretical isotopic patter of C_{60}; Toluene:methanol (45:55, v/v).

Another relevant result of this study is related to the contamination of the standards. The full scan MS obtained by infusion of two C_{60}-derivatives (C_{60}-pyrr and PCBB) showed the cluster of the $[C_{60}]^{-\bullet}$ ion which, as demonstrated by LC, was due to a ≈ 10% contamination of the standard with C_{60}. This is something that must be taken into account in the preparation of the standard solutions for calibration. Since the purity of these nanoparticles may be unreliable and the degree of contamination, especially with other fullerene compounds, can change with the batch, it is recommended to evaluate it in order to prevent inaccurate results.

Analysis of complex matrices

For the extraction of fullerenes from complex matrices, procedures that fit with the nature of the matrix but also with the characteristics of the particles must be applied. In this work, the pond water samples were extracted by LLE with toluene after the addition of NaCl. Despite their high solubility in toluene, the addition of salts is required to disrupt fullerene aggregates in aqueous media (Deguchi et al., 2001; Brant et al., 2005) and facilitate the partition

in the toluene phase. Using this extraction method, slightly higher recoveries were obtained for fullerene derivatives (93-96 %) than for pristine fullerenes (83-89 %), values that are similar to the ones previously reported by LLE for some of these compounds (Wang et al., 2010; Bouchard and Ma, 2013) (see Table 4, Section 1.31., Chapter 1). The advantage of the LLE method used in this thesis is that both suspended and dissolved fullerene aggregates are extracted in only one step. In contrast, when using UAE (Farre et al., 2010; Núñez et al., 2012; Sanchis et al., 2015a) and SPE (van Weezel at al., 2011; Kolkman et al., 2013) only the suspended solids or the aqueous phase that remains after filtration, are currently extracted, and consequently, part of the compounds may be not be analysed. Hence, to improve extraction efficiency the combination of the extracts obtained by UAE (suspended solids) and of the ones obtained by SPE must be considered. Concerning the extraction of pristine and surface modified fullerenes from sediment samples, UAE with toluene has been proposed but low recoveries especially for surface modified fullerenes (see Table 4, Section 1.3.1., Chapter 1) were obtained. In this thesis, PLE is proposed as this method offers several advantages over UAE such as the use of high pressure and extraction temperatures, desiccants and drying materials (see Section 2.1, Chapter 2). The PLE method used in this thesis showed good recoveries (70-92 %) and was performed at high extraction temperature (150 °C) and using only one extraction cycle of 10 min. Higher recoveries were obtained for the fullerene derivatives compared to pristine fullerenes although the extraction efficiency decreased with fullerenes molecular weight. The recoveries obtained in this thesis by PLE for fullerene derivatives are higher (87-92 %) than the ones reported by UAE in the literature (35-59 %) (Sanchis et al., 2013) for the same compounds (i.e., C_{60}-pyrr, PCBM). This could be due to the fact that in such samples fullerenes may be strongly adsorbed to the natural organic matter and their extraction is being improved in PLE probably because a high extraction temperature and mixing the sample with a desiccant (i.e., hydromatrix) prior to the extraction to prevent the aggregation of the particles were used. Moreover, besides de higher recoveries obtained, this method is faster and involves lower solvent consumption than the previously reported UAE methods which require several extraction hours and higher toluene amount.

The limits of detection (MLODs) obtained in this thesis by the proposed methodology for water samples (PCBM, PCBB, C_{60}-pyrr, C_{60} and C_{70}: 1.4 - 3.4 pg L^{-1}; C_{76}-C_{84}: 0.6 - 1.6 ng L^{-1}) and for sediment samples, the MLODs values (PCBM, PCBB, C_{60}-pyrr, C_{60} and C_{70} : 45-250 pg Kg^{-1}; C_{76}-C_{84}: 31-158 ng Kg^{-1}) are lower than most of the data reported in the literature (see Table 4, Section 1.3.1., Chapter 1) mainly because of the use of APPI as ionisation source. The

authors that have also used this ionisation source found similar MLODs (Núñez et al., 2012; Emke et al., 2015; Sanchis et al., 2015b).

The application of the methodology developed in this thesis for the analysis of hydrophobic fullerenes in environmental samples generated new data on the presence of some of these compounds in the environment. For instance, the fullerene derivatives were detected in all the analysed sediments and most of the water samples (Table 3, Section 2.3., Chapter 2), the highest concentrations found being 5 ng Kg^{-1} (PCBB) and 8 pg L^{-1} (PCBM and C_{60}-pyrr), respectively. To the best of our knowledge, this is the first report of the presence of these compounds in environmental samples, except for C_{60}-pyrr which has been found in wastewater effluents at concentration levels up to 66 μg L^{-1} (Farre et al., 2010). Among pristine fullerenes, C_{60} and C_{70} were detected in most of the analysed samples but they could only be quantified in some of them, at levels up to 1 ng kg^{-1} and 7 ng kg^{-1} (sediments), respectively and up to 25 ng L^{-1} and 330 ng L^{-1} (water samples), respectively, while higher fullerenes were not detected in any of the analysed samples. These results are in agreement with previous studies reporting the presence of C_{60} and C_{70} (Heymann et al., 1996; Sanchis et al., 2013) in sediments and superficial soils, at concentration levels up to ng g^{-1} (Sanchis et al., 2015b), and in water samples at low ng L^{-1} levels (Farre et al., 2010; Núñez et al., 2012; Sanchis et al., 2013). With regard to larger pristine fullerenes, the presence of C_{84} in water samples has been recently reported at low ng L^{-1} levels (Núñez et al., 2012) and there are no reports for the presence of other fullerene compounds.

The presence of fullerenes in the environmental samples analysed in this thesis and in the ones reported in the literature seem to be related to the location of the sampling points (highly industrial and urban areas and near international airports) since incidental emissions by different combustion processes (i.e., automobile traffic, wood combustion, coal-burning power plants) are one of most prominent sources of fullerenes (Utsumomya et al., 2002; Laitinena et al., 2014). However, due to the increasing applications of these compounds in different sectors, high amounts may reach the environment through wastewater discharge, landfills, factories, and deposition from the atmosphere (Wiesner et al., 2006). Another application of the methodologies established in this thesis has been the quantitation of C_{60} in a cosmetic product that was performed by both NACE-UV and LC-MS. The good precision obtained by the NACE method and also the agreement of the results obtained by LC-MS (2.10 ± 0.20 mg L^{-1} (NACE) and 1.93 ± 0.15 mg L^{-1} (LC-MS)) allowed to propose the developed NACE method as an alternative to conventional LC for the determination of C_{60} in cosmetic samples where this compound is present at a relatively high concentration with the advantages of being less expensive and involving less solvent consumption.

CHAPTER 2

ANALYSIS OF FULLERENES

2.5. Conclusions

2.5. Conclusions

The studies included in this chapter concerning the development of methodologies for the analysis of fullerenes by UHPLC-(-)APPI-MS(/MS) and NACE-UV in environmental and cosmetic samples allowed us to reach the following conclusions:

With regard to the analysis of environmental samples by LC-MS:

- UHPLC using a 1.9 μm particle size C18 column and toluene-methanol as a mobile phase allowed the fast separation (< 4.5 min) of the eight studied fullerene compounds with a good resolution. The retention of surface modified fullerenes is related to both the polarity and the size of the functional groups attached to the C_{60} buckyball structure. The compounds with ester functional groups eluted according to their polarity (PCBM followed by PCBB), while the fullerene with amine-functional group (C_{60}-pyrr) was the last to elute having the smallest group (and a more symmetric molecule geometry), leaving a higher surface of the buckyball uncovered, which may explain its higher retention.
- The aggregation behaviour of fullerenes in binary organic solvent mixtures with toluene and a weak fullerene solvent (i.e., methanol and acetonitrile) allowed us to justify their retention behaviour in the evaluated mobile phase mixtures (toluene-methanol and toluene-acetonitrile). Higher retention times were obtained by using acetonitrile as a second solvent compared to methanol due to the formation of larger clusters in toluene-acetonitrile than in toluene-methanol mixture.
- APPI showed significantly better sensitivity (improvement >75 %) than H-ESI and APCI for the ionisation of the studied fullerene derivatives. Unlike pristine fullerenes, the experimental isotopic patterns of the molecular ion $[M]^{-\bullet}$ of the fullerene derivatives matched with the theoretical ones, regardless on the injected concentration, probably because of the presence of the functional groups which may reduce the tendency of hydrogen addition to the double bonds.
- Fullerene derivatives presented fragmentation at high collision energies (> 80 eV), losing the entire functional group and providing in the MS/MS spectra a major ion at m/z 720 corresponding to the buckyball structure $[C_{60}]^{-\bullet}$. Collision energies below 80 eV revealed an additional fragment for PCBB and PCBM (m/z 823), corresponding to the

loss o the butyl and propyl acid alkyl ester groups, respectively, that were not previously reported in the literature. Two SRM (Q1 and Q3 at 0.7 *m/z* FWHF) transitions selecting as precursors the ions $[M]^{-\bullet}$ and $[M+1]^{-\bullet}$ of their isotopic cluster, and as product ions [M]−• and [M+1]−• corresponding to C_{60}, were used for the acquisition of these compounds.

- The use of APPI, H-SIM mode for pristine fullerenes working at a mass resolving power > 12,500 FWHM, and SRM mode for fullerene derivatives, allowed achieving MLODs lower than most of those previously reported in the literature being in the order of low pg L^{-1} (water samples) and pg Kg^{-1} (sediments) for PCBM, PCBB, C_{60}-pyrr, C_{60} and C_{70}, and of low ng L^{-1} (water samples) and ng Kg^{-1} (sediments) for higher fullerenes.

- A PLE method using a high extraction temperature (150 °C) and only one extraction cycle is proposed for the extraction of sediments. The method yielded good recoveries (70-92 %), especially for fullerene derivatives (87-92 %) which are significantly higher than the ones previously reported for the same compounds by UAE. This method is faster (10 min) and involves lower solvent consumption than UAE and Soxhlet methods (which requires up to 4 h and higher toluene amounts).

- Using the developed methodology we reported for the first time the presence of three surface modified fullerenes (C_{60}-pyrr, PCBM and PCBB) in sediments (0.1 - 5.1 ng Kg^{-1} levels) and in pond water samples (2.0 - 8.5 pg L^{-1} levels), except for C_{60}-pyrr that was previously found in wastewater samples. Among pristine fullerenes, C_{60} and C_{70} were detected in most of the analysed samples at levels up to 1 ng kg^{-1} and 7 ng kg^{-1} (sediments), respectively and up to 25 ng L^{-1} and 330 ng L^{-1} (water samples), respectively, while higher fullerenes were not detected in any of the analysed samples.

Concerning the analysis of fullerenes by NACE:

- For the separation of hydrophobic fullerenes by NACE, a high concentration of a long alkyl chain length tetraalkylammonium salt (i.e., TDAB) was needed to interact with the compounds providing a positive charge. The addition of short alkyl chain length salts (i.e., TEAB) able to interact with the capillary wall reducing EOF and, consequently improving the separation of the compounds was also required.

- The separation in NACE was strongly affected by the proportion of the organic solvents employed in the running BGE. An increase in the percentage of acetonitrile in the

BGE decreased the analysis time by reducing the EOF and consequently, worsened the separation. The use of acetic acid was needed to improve the separation between pristine fullerenes while the addition of small amounts of MeOH which shortened the analysis time by decreasing the migration time of the last eluting compound (C_{60}CHCOOH) probably because of hydrogen bonding interactions.

- The developed NACE method using 200 mM TDAB, 40 mM TEAB in acetonitrile:chlorobenzene (1:1, v/v), 6% MeOH and 10 % acetic acid as BGE was successfully applied for the quantitation of C_{60} in a commercial product obtaining results comparable to those achieved by analysing the same product by LC-MS (2.10 ± 0.20 mg L^{-1} (NACE) and 1.93 ± 0.15 mg L^{-1} (LC-MS)). Therefore, this method can be proposed as an alternative to LC-MS, showing a good performance, being less expensive and involving significantly less solvent consumption.

CHAPTER 3

CHARACTERISATION OF FULLERENES

3.1. Introduction

The evaluation of the presence of the total amount of fullerenes in environmental samples, as performed in the previous chapter, is not sufficient to allow a realistic risk assessment of these compounds. With respect to nanoparticles safety there are other parameters of interest such as aggregation degree, size distribution, surface morphology, specific surface area and chemical structure that must be taken into account. It is known that the mobility and toxicity of fullerenes in the environment is related to the particle size distribution and colloidal stability of the aggregates formed which depend on the pH, the ionic strength and the presence of natural organic matter (Lead and Wilkinson, 2006). Depending on these factors and the physicochemical properties of fullerene nanoparticles, increased aggregation and thus sedimentation or enhanced dispersion may occur. For example, C_{60} forms negatively charged colloids whose aggregate sizes increase at high ionic strength and low pH values (Fortner et al., 2005; Ma and Bouchard, 2009). Surface modification of nanoparticles, both intentional functionalisation and modifications resulting from natural processes, can influence the environmental fate and behaviour. For instance, pristine fullerenes are known to be highly hydrophobic, with a tendency to aggregate, and they would be expected to settle in the natural environment (Chen and Elimelech, 2006). In contrast, surface modifications such as hydroxylation and carboxylation, improve the dispersion capability and increase stability in the water system presenting lower settling rate, especially in combination with natural organic matter (Brant et al., 2007; Assemi et al., 2010). Moreover, functionalisation has influence on their bioavailability and determines their biological uptake. Nevertheless, most of the reported studies regarding the characterisation of fullerenes nanoparticles are focused on C_{60}, and there is a lack of studies performed on surface modified fullerenes which are nowadays produced in higher quantities and find increasing applications especially in the biomedical field (see Section 1.3.1., Chapter 1). Therefore, the physicochemical characterisation (particle size, size distribution, particle morphology, surface area, surface chemistry and also purity) of surface modified fullerenes is important (Warheit, 2008) in order to assess which attributes can be related to their toxicity.

In terms of techniques for nanoparticles characterisation, there are several measuring approaches that can be applied, including microscopic methods (i.e., transmission electron microscopy (TEM), scanning electron microscopy (SEM), atomic force microscopy (AFM)), light scattering (i.e., dynamic light scattering (DLS), (static) multi-angle light scattering (MALS)), asymmetrical flow-field flow fractionation (AF4) and capillary electrophoretic techniques. Such methods enable the investigation of properties at the level of individual particles as well as

aggregates. However, assessing which technique is most appropriate and relevant to use is challenging.

In this thesis, TEM and AF4-MALS have been used to study the morphology, aggregation degree, size distribution and aggregation behaviour of fullerene derivatives in aqueous solutions as a function of pH and ionic strength. In addition, the aggregation behaviour of these compounds by CE has been evaluated.

With regard to CE, although it is mainly a separation technique, it has been also applied to study the aggregation behaviour of low and high molecular weight species by monitoring changes in charge to size ratio and in the electrophoretic pattern of the peaks (presence of multiple and/or broad peaks) (Bermudez and Forcitini, 2004; Sabella et al., 2004; Pryor et al., 2011). CE techniques can be useful when the objective of the study is the monitorisation of changes in the aggregation behaviour of the compounds, but this technique alone cannot provide size information. Thus, CE must be used in combination with techniques that can provide size information. For instance, the coupling of CE to laser-light scattering and laser induced fluorescence has been reported for the separation, detection and size characterisation of (individual) submicron particles (Duffy et al., 2002; Gunasekera et al., 2002; Rezenom et al., 2007). However, these techniques have not been used yet for the study of the aggregation behaviour of fullerenes. In this thesis, the aggregation of surface modified fullerenes was observed in CE (i.e., in MECC using sodium dodecyl sulfate (SDS) as surfactant, and in CZE) and the effect of the running background electrolyte (BGE) composition, such as buffer and SDS concentration and pH, on their aggregation behaviour was evaluated. Moreover, the sizes and shapes of the aggregates formed in the tested BGE conditions were determined by AF4 and TEM.

Concerning microscopic techniques, they are suitable for elucidating particle shape and to some degree, aggregate structures but they cannot provide information about the size distribution of the aggregates. In addition, the integrity of the particles and aggregates is not always guaranteed since imaging in air induces aggregation due to partial drying of the sample prior to analysis. Furthermore, if the particles are strongly aggregated forming polycrystalline structures, the determination of their sizes is not possible by this technique. Nevertheless, microscopic techniques help in visualising the morphology of aggregates and the results can be compared to the aggregate sizes determined by a more suitable technique. In this context, light scattering techniques offer the advantage of determining the average size of the particles (DLS) and their size distribution (MALS). TEM and DLS techniques have been combined to study the aggregation of aqu/nC_{60} (Lyon et al., 2006) and of aqu/nC_{60}, aqu/nC_{70}, and aqu/nPCBM in

aqueous solutions of different pH and ionic strength values (Ma and Bouchard, 2009), and the results obtained by the two techniques were in general consistent. However, one restriction with simple DLS instruments is that they measure at a fixed angle and provide the average diameter of the total population of particles present in the solution (in a limited size range) rather than a characterisation of individual particles. If the sample is polidisperse, DLS sizes are not an accurate representation for all the particle sizes present in the sample as it will skew the measured sizes towards the larger particles. This can be particularly problematic when aggregation is present. To determine the size distribution, multi-angle light scattering is a better option. In fact, MALS is more popular than DLS for on-line detection since in addition to size distribution it also provides the radius of gyration (r_G) which can be used for absolute molar mass determination.

For the size separation of large molecules and (sub)micron particles field-flow fractionation (FFF), an open channel flow-based separation technique, has been recognised as an ideal option. In FFF, the fractionation is performed by applying a perpendicular field to a main flow across a channel. This field drives the components into the different stream laminae of the flow that travels across the channel at unequal velocities allowing the separation. The normal mode of separation (based on Brownian motion of the analyte in the channel), in which diffusion plays an important role in controlling component distribution across the channel, is the most widely used mechanism for the separation of analytes with sizes smaller than 1 μm. Smaller component populations accumulate in regions of faster streams of the parabolic velocity profile and elute earlier than larger components. Since the first experiments of FFF were conducted by Giddings et al. in 1976 (Giddings et al, 1976), a range of different sub-techniques have been developed to date. These sub-techniques are named according to the nature of the perpendicular field applied. Flow field-flow fractionation (FlFFF) where the field is a cross-flow perpendicular to the channel flow, sedimentation field-flow fractionation (Sed-FFF) and thermal field-flow fractionation (Thermal-FFF) are several examples. Still, there are some other fields that can be applied, such as magnetic, dielectrophoretic and acoustic. However, instrumentation based on these latter ones, has not yet been commercialised. Nowadays, the most frequently used sub-technique is a variation of FlFFF, named asymmetrical FlFFF (AF4). A relatively new variant is the hollow fibre FlFFF (HF5); its channel geometry is based on a ceramic/polymeric hollow fibre having a porous cylindrical wall. The main difference between (symmetric) FlFFF and AF4 consists in the channel design. The former one used two permeable walls (porous ceramic frits) (at the top and the bottom of the channel) and the latter only has one permeable wall (at the bottom, the accumulation wall) and the upper porous wall is replaced by a solid wall that is

impermeable to the carrier liquid. Due to the obvious differences between upper and bottom wall, "asymmetrical" was prefixed to the term AF4. This offers the advantage of a simpler channel construction and the ability to visualize the sample through a transparent upper wall (Messaud et al., 2009). The initial channel geometry was rectangular but it was shortly replaced by a trapezoidal channel which proved to be superior to the traditional one because higher sensitivity is obtained. This is due to a decrease of the flow rate at the channel outlet by at least a factor of four and so, a less diluted sample enters into the detector than in a rectangular channel. Today trapezoidal channels are currently used (Litzén and Wahlund, 1993; Wahlund, 2014).

The principles of both FlFFF and AF4 are well described in the literature (Wahlund and Giddings et al., 1987; Schimpf, 2000; Baalousha et al., 2011; Wahlund, 2014). AF4 is a non-destructive, one-phase separation mechanism able to characterise molecules, macromolecules and particles in solution. As in classic chromatography, the sample components elute at given retention times which are related to a range of physiochemical properties of the retained species. However, in contrast to classic chromatography, an AF4 separation works only on hydrodynamic properties and does not involve interaction with a stationary phase. Figure 1 illustrates the separation principle of AF4. As indicated above, two dimensional forces are used for the separation, an axial flow that carries the analytes across the channel and a second flow (cross-flow), perpendicular to the direction of the main flow, which creates the field for separating the analyte particles according to their hydrodynamic size. During sample introduction, the carrier solution flows in from both inlet and outlet of the channel and meets on a point called the focusing point (see Figure 1) where a "relaxation" step takes place and then starts eluting with the axial flow. The cross-flow drives analytes to the accumulation wall, which is covered by an ultrafiltration membrane through which the carrier solution passes while retaining analyte molecules and particles. Sample components, concentrated by the cross-flow in a thin layer on top of the membrane, are all flushed with the channel flow towards the detector. The velocity of a sample band depends on the thickness of the layer into which the particles are concentrated: the smaller the layer thickness, the lower its velocity in the axial direction. The layer thickness of an analyte depends on the cross-flow velocity and on the molecular diffusion of the analyte. Since the cross-flow is an instrumental parameter, the retention time differences between the particles are purely based on differences in their diffusion coefficients, and consequently in their molecular size. The small analyte particles with higher diffusion coefficients are localised in the higher velocity zone of the parabolic flow profile and as a consequence they are the first to elute, followed by the large particles which are entrained in the lowest laminar flow velocity. This separation mechanism is referred to as normal-mode and it is valid for sample

species between 1 and 1,000 nm. For bigger particles other fractionation mechanisms appear: steric/hyperlayer mode, where the elution order is reversed.

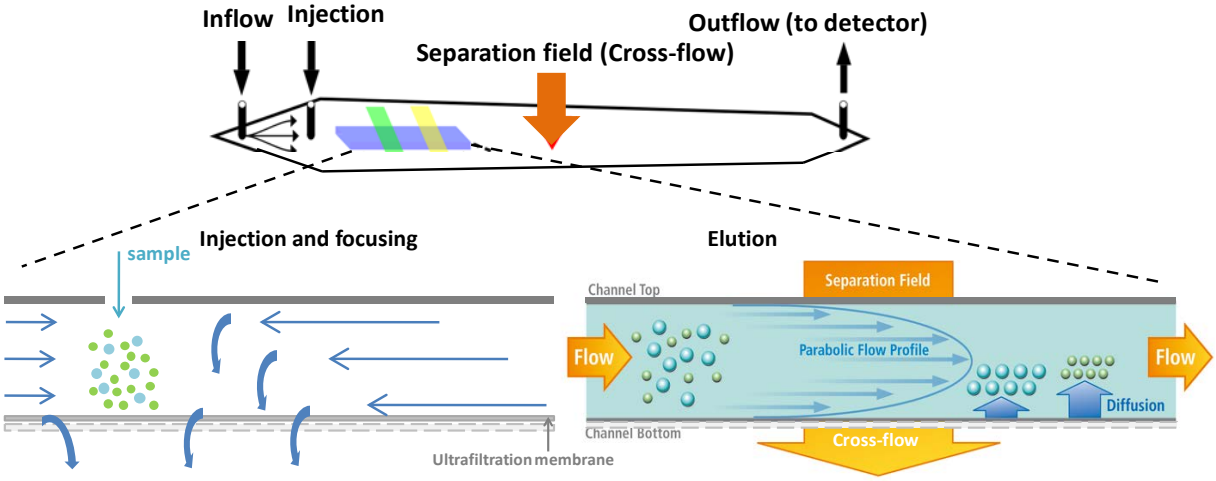

Figure 1. Separation principle of AF4.

With some approximations and simplifications of the original treatment (Wahlund and Giddings, 1987), the elution time of a compound can be given by:

$$t_R = \frac{w^2}{6D} ln\left(1 + \frac{F_{cr}}{F_{ch}}\right) \qquad \text{(Eq. 1)}$$

where w is the height of the channel, F_{cr} and F_{ch} are the flow rates of the cross flow and channel flow, respectively, and D is the translational diffusion coefficient of the analyte particle.

D can be related to the size through the well-known Stokes Einstein equation:

$$D = \frac{kT}{6\pi\eta r_H} \qquad \text{(Eq. 2)}$$

where k is the Boltzmann constant, T the absolute temperature, η the viscosity of the solvent and r_H the hydrodynamic radius of the particle.

Hence, the hydrodynamic radii of the particles can be calculated from the retention time.

One of the characteristics of AF4 is that it can separate particles over a wide size range, from those retained by an ultrafiltration membrane to micrometer-sized solid particles but this technique also presents other advantages. For instance, the experimental conditions can be easily adapted to fit the expected size of the analytes. This is useful when dealing with very polidisperse

samples and a constant cross-flow separation may not be adequate to resolve the smallest and the largest components in one single experiment. In this case, flow-programming (i.e., time delayed exponential decay (TDE) function) can be used. Using TDE programming, the retention time for well retained components can be given by:

$$t_R = \tau(1 - \ln\tau + \ln t_R^*) \qquad \text{(Eq. 3)}$$

where τ is the delay/decay time constant and t_R^* the retention time of the component at a constant flow rate.

With TDE programming, the retention increases linearly with the logarithm of the size of the particle. Another advantage of AF4 is that it can be easily coupled on-line to a suitable detection method (e.g., MALS) to determine the molar masses and shapes of the particles. Moreover, the hyphenation of AF4 and MALS allows determining particle's shape factor by dividing the scattering radii obtained from MALS, which incorporates structural and shape properties, by the r_H calculated from the AF4 results. The shape factor of a sphere is 0.755 and it increases as the particle deviates from a sphere.

With regard to MALS, its basic principle is the same as that of static light scattering at one single angle where a beam of polarized light is focused onto the sample molecule and the scattered light is detected with a photo detector. In MALS the scattered light is detected at several angles at the same time. For small molecules with no angular dependence of the scattered light, the detection on one single angle is enough, but when the sample molecules are large it is assumed that each molecule is made up of several small elements, each one of them scattering independently of another. In this case, it is absolutely necessary to detect the scattered light at multiple angles at the same time. The intensity of the scattered light at each angle carries information about the molar mass, while the angular dependence provides information about the size (mean square radius) of the molecules under investigation. MALS allows determining experimentally the root mean square radius, also known as radius of gyration (r_G). This radius represents the distribution of mass within the molecule, being defined as the mass weighted average distance from the centre of mass of a molecule to each mass element in that molecule. If the macromolecule of mass M is made up of elements m_i (see Figure 2), the radius of gyration may be given by:

$$< r_G^{\,2} >= \sum \frac{r_i^2 m_i}{M} \qquad \text{(Eq. 4)}$$

where r_i is the distance of element m_i from the centre of mass of the molecule of total mass M.

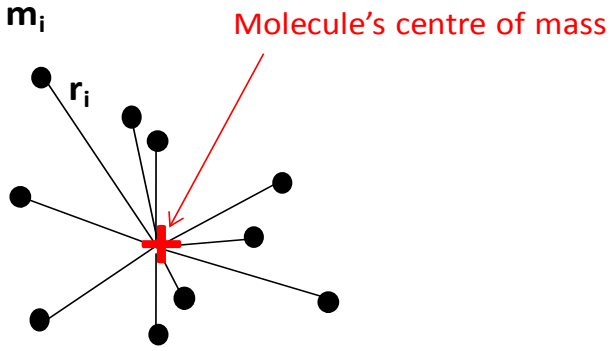

Figure 2. Schematic representation of the mean square radius $<r_G^2>$

The light scattering equation (Eq. 2) based on Zimm's formalism of the Rayleigh-Debye-Ganss theory (Wyatt, 1993) includes both intermolecular and intramolecular effects.

$$\frac{K^* c}{R_\theta} = \frac{1}{M_w P_\theta} + \frac{2A_2 c}{P_\theta} + \ldots \qquad \text{(Eq. 5)}$$

where:

- K^* is an optical constant, $4\pi^2 n_0^{\,2} (dn/dc)^2/(\lambda_o^{\,4} N_A)$, that depends on the refractive index of the solvent (n_0) and the vacuum wavelength of the incident light
- c is the concentration of the solute molecules (g cm^{-3})
- R_θ is the Rayleigh ratio (cm^{-1}).
- M_w is the weight-averaged solute molar mass (g mol^{-1})
- A_2 is the second virial coefficient in the virial expansion of the osmotic pressure
- P_θ is the particle scattering factor which is related to the mean square radius of gyration $<r_G^{\,2}>$. The larger $<r_G^{\,2}>$, the greater the angular variation.

$$\frac{1}{P_\theta} = 1 + \frac{16\pi}{3\lambda_0} < r_G^{\,2} > \sin^2\left(\frac{\theta}{2}\right) + \ldots \qquad \text{(Eq. 6)}$$

So, $<r_G^2>$ can be determined from the plot:

$$\frac{1}{P_\theta} = f\left((sin^2\left(\frac{\theta}{2}\right)\right) \qquad \text{(Eq. 7)}$$

Although since the 1990s AF4 has been very popular for nanoparticle separation and characterisation (Baalousha, 2011), there are very few studies regarding the characterisation of fullerenes in terms of aggregate shape and size distribution. Most of the reported studies have been performed by AF4 coupled either to DLS (Isaacson and Bouchard, 2010), for the determination of hydrodynamic sizes, or to MALS (Kato et al., 2010; Herrero et al., 2014) which enables the determination of the size distribution (r_G) of each fraction. Isaacson and Bouchard, 2010 used AF4 coupled to DLS to determine the aggregate sizes of aqu/nC_{60} in deionised water and reported hydrodynamic diameters between 80 and 260 nm. Regarding AF4-MALS, Herrero et al., 2014 studied the size distribution of aqu/nC_{60}, aqu/PCBM and aqu/bis-PCBM aggregates in Milli-Q water and reported r_G values between 20 and 80 nm. The size distribution of C_{60} and C_{70} in a cell culture medium was also studied, and the authors found similar average r_G values: 256 ± 90 nm and 257 ± 90 nm, respectively (Kato et al., 2010). With regard to water soluble fullerenes, there is only one paper (Assemi et al., 2010) using AF4 combined with atomic force microscopy (AFM) to study the aggregate sizes and morphology of fullerol at different pH and ionic strength values reporting hydrodynamic radii < 5 nm (Milli-Q water) which increased at high ionic strength values. However, the size distribution of the particles cannot be determined by this approach. In this thesis, AF4-MALS was used to study the size distribution and shape of four water soluble surface modified fullerenes with polyhydroxyl and carboxyl groups at different pH and ionic strength values and TEM was employed to visualise the morphology of the particles.

Summarizing, in this thesis several techniques (TEM, AF4-MALS, CE) have been used to obtain a picture of the morphology, aggregation state and size distribution of fullerenes in aqueous solutions.

The first section of this chapter includes the paper entitled "*Aggregation behavior of fullerenes in aqueous solutions: a capillary electrophoresis and asymmetric flow-field flow fractionation study*", sent for publication to Analytical and Bioanalytical Chemistry. In this work, the aggregation behaviour of highly and moderate water soluble fullerenes by CE techniques (i.e., MECC and CZE) at

different SDS concentrations, ionic strength and pH values is studied. The effect of these parameters on the electrophoretic pattern of the peaks is evaluated and the observed changes are discussed. Electrophoretic peak profiles are correlated with particle sizes determined by AF4 at the evaluated CE conditions and the morphology of the samples is studied by TEM. Additionally, MECC is proposed as a suitable method for the analysis of individual hydrophobic fullerenes in cosmetic products.

The second section of this chapter includes the paper entitled "*Characterization of aggregates of surface modified fullerenes by asymmetrical flow field-flow fractionation with multi angle light scattering detection*" which was accepted for publication in Journal of Chromatography A (2015). The study focuses on the development of an analytical method for the particle separation and size distribution determination of aggregates of surface modified fullerene by AF4 hyphenated with MALS in aqueous solutions. This work was carried out at the University of Amsterdam and in collaboration with the KWR Watercycle Research Institute in The Netherlands, during an internship conducted in the course of this thesis. The experimental parameters (cross-flow, focus-flow, focus time and type of membrane) have been optimised for the fractionation of the selected fullerenes and their size distribution in aqueous solutions of different pH and ionic strength values, of environmental relevance, has been determined.

CHAPTER 3

CHARACTERISARION OF FULLERENES

3.2. Scientific article IV: Aggregation behavior of fullerenes in aqueous solutions: a capillary electrophoresis and asymmetric flow-field flow fractionation study

A. Astefanei, O. Núñez[a], M. T. Galceran[a], W. Th. Kok and P. J. Schoenmakers

Analytical and Bioanalytical Chemistry (2015) (sent for publication).

Aggregation behavior of fullerenes in aqueous solutions: a capillary electrophoresis and asymmetric flow-field flow fractionation study

Alina Astefanei[a], Oscar Núñez[a,b,*], Maria Teresa Galceran[a], Wim Th. Kok[c], Peter J. Schoenmakers[c]

[a]Department of Analytical Chemistry, University of Barcelona.Martí i Franquès 1-11, E08028 Barcelona, Spain.

[b] Serra Húnter Fellow, Generalitat de Catalunya, Spain.

[c]Analytical Chemistry Group-HIMS, University of Amsterdam, PO Box 94157, 1090 GD, Amsterdam, The Netherlands

* Corresponding author

Abstract

In this work the electrophoretic behaviour of hydrophobic fullerenes (C_{60}, C_{70} and C_{60}-pyrr) and water soluble fullerenes ($C_{60}(OH)_{24}$, $C_{120}(OH)_{30}$, C_{60}-pyrr tris acid and $C_{60}CHCOOH$) in micellar electrokinetic capillary chromatography (MECC) was evaluated. The aggregation behavior of the water soluble compounds in MECC at different buffer and SDS concentrations and pH values of the background electrolyte (BGE) was studied by monitoring the changes observed in the electrophoretic pattern of the peaks. Broad and distorted peaks that can be attributed to fullerene aggregation were obtained in MECC which became narrower and more symmetric by working at low buffer and SDS concentrations (below the critical micelle concentration, capillary zone electrophoresis (CZE) conditions). For the characterization of the suspected aggregates formed (size and shape), asymmetrical flow field-flow fractionation (AF4) and transmission electron microscopy (TEM) were used. The results showed that the increase in the buffer concentration promoted the aggregation of the particles while the presence of SDS micelles revealed multiple peaks corresponding to particles of different aggregation degree. Furthermore, MECC has been applied for the first time for the analysis of C_{60} in two different cosmetic products (*i.e.,* anti-aging serum and facial mask).

Keywords: Capillary Zone Electrophoresis; Cosmetic products; Micellar Electrokinetic Capillary Chromatography; Asymmetric flow-field flow fracitonation; Fullerene aggregates.

Abbreviations: Fullerol ($C_{60}(OH)_{24}$), Polyhydroxy small gap fullerene, hydrated ($C_{120}(OH)_{30}$), N-methyl-fulleropyrrolidine (C_{60}-pyrr), C_{60} pyrrolidine tris acid (C_{60}-pyrr tris acid), (1,2-Methanofullerene C60)-61-carboxylic acid ($C_{60}CHCOOH$).

1. Introduction

Since the discovery of buckminsterfullerene (C_{60}) [1] fullerene nanoparticles have been widely investigated for their exploitation within biological systems [2], cosmetic products [3], electronics and photovoltaics [4]. The unique physicochemical properties of pristine and especially of surface modified fullerenes make them promising therapeutic and diagnostic agents showing surprising properties and biocompatibility [5-7]. In particular, fullerols which are surface modified C_{60} -fullerenes with (poly)hydroxy functional groups can be ideal candidates for the treatment of neuro-degenerative disorders (*e.g.* Parkinson's and Alzheimer's disease) [6]. Carboxy-fullerene derivatives have potential use in photodynamic therapy [8] and as inhibitors of the HIV-1 protease [9]. However, it was reported that fullerenes are retained in the body for long periods [10] raising concerns about their potential chronic toxic effects. At nanoscale level, even subtle changes in their physicochemical properties can significantly alter their biocompatibility and application [11].

Pristine and surface modified fullerene aggregate in aqueous media leading to the formation of structures of various shapes and sizes depending on the type and number of the functional groups attached to the carbon cage [12-15]. These physicochemical properties impact their mobility, fate, bioavailability and toxicity [16,17]. Nevertheless, there is a significant lack of knowledge on fullerene exposure, and there are conflicting reports on their potential risks. To determine their behavior and distribution, analytical methods adequate for their separation and quantitation have to be developed. Liquid chromatography coupled to mass spectrometry (LC-MS) is the most frequently method used for the analysis of fullerenes in complex matrices but most of the reported studies are focused on hydrophobic compounds [15,18] and only few have been dedicated to the analysis of water soluble fullerenes such as fullerols [19,20].

Capillary electrophoretic (CE) techniques have also been used to analyze fullerenes. For the separation of hydrophobic fullerenes, nonaqueous capillary electrophoresis (NACE) [21-23] by employing charged salts and organic solvent mixtures as separation medium has been reported. The behavior of C_{60} and of a C_{60}-C_{70} mixture in micellar electrokinetic capillary chromatography (MECC) has also been evaluated [24]. This last work also studied the use of C_{60} and C_{70} encapsulated in sodium docecylsulfate (SDS) micelles as pseudostationary phase for the separation of polyaromatic hydrocarbons (PAHs) by MECC. Regarding water soluble fullerene derivatives, both capillary zone electrophoresis (CZE) and MECC with SDS micelles were reported [25-27]. Among these studies, only two addressed the analysis of some carboxy-fullerene derivatives [25,27] and to the best of our knowledge there are no reports about the analysis of fullerols. In this context, Chan *et al.* [27] evaluated the use of CZE and MECC for the

analysis of two water soluble fullerene derivatives (carboxy-fullerene (C3) and dendro[60]fullerene (DF)) in human serum samples and recommended using CZE for the quantitation of both compounds, presenting some advantages over MECC such as lower analysis time, better reproducibility and lower detection limits. Moreover, the presence of SDS micelles increased the number of electrophoretic peaks of DF complicating its analysis in the real samples. The behavior of DF in CZE as a function of pH, ionic strength, solvent amount and concentration of additives has been also reported [26]. The parameters which showed the most important effect on the migration time and electrophoretic peak profile were the pH and the ionic strength. The migration time of DF increased with the pH and decreased with the salt concentration in reversed polarity.

Although CE is mainly a separation technique, it has also been applied for the study of the aggregation behavior of low and high molecular weight species by monitoring changes in the electrophoretic pattern of the peaks (presence of multiple and/or broad peaks) [28-30] although there are no studies involving fullerene compounds.

Asymmetrical flow field-flow fractionation (AF4) is an open channel separation technique able to characterize (macro) molecules and particles in solution and to calculate the hydrodynamic radius (r_H) of the particles from the retention time [31,32]. Although this technique is increasingly used for nanoparticles characterization [33], the number of studies devoted to fullerenes characterization is limited and most of the reports are focused on hydrophobic compounds [15,34-36]. Concerning water soluble fullerenes, there is only one study [37] that used AF4 combined with atomic force microscopy (AFM) to evaluate the aggregate sizes and morphology of fullerol reporting r_H of ≈ 2 nm in Milli-Q water which increased at higher ionic strength.

The aim of this work is to study the aggregation behavior of several surface modified fullerenes, two polyhydrody-fullerenes ($C_{60}(OH)_{24}$, $C_{120}(OH)_{30}$) and two carboxy-fullerene derivatives (C_{60}CHCOOH and C_{60}-pyrr tris acid) not previously reported, at varying buffer and SDS concentrations by CE and to characterize the aggregates by asymmetrical flow-field flow fractionation (AF4). For this purpose, the effect of the BGE composition (*i.e.*, buffer and SDS concentration and pH) on the electrophoretic migration time and peak profile was evaluated and AF4 was used to determine the aggregate sizes of the selected fullerenes in the tested CE conditions. In addition, TEM was employed to visualize the morphology of the selected compounds in the conditions employed for the electrophoretic studies.

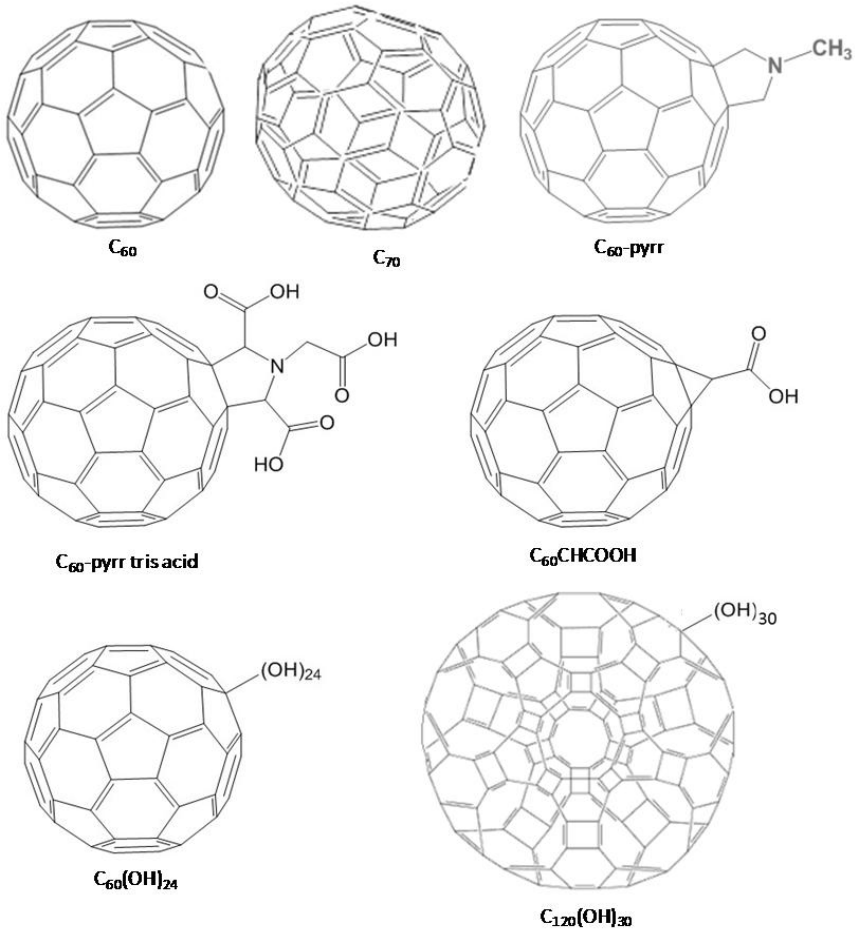

Figure 1. Structures and abbreviations of the studied fullerenes.

2. Materials and methods

2.1. Chemicals and standard solutions

C_{60}, C_{70}, C_{60}-pyrr, $C_{120}(OH)_{30}$, C_{60}CHCOOH and C_{60}-pyrr tris acid were purchased from Sigma-Aldrich (Steinheim, Germany). $C_{60}(OH)_{24}$ was supplied by Materials & Electrochemical Research M.E.R. Corporation (Tucson, Arizona, USA). The chemical structures and abbreviations of these compounds are given in Figure 1.

Sodium phosphate, sodium chloride, sodium tetraborate, and SDS were purchased from Sigma-Aldrich (Steinheim, Germany). Sudan III, sodium hydroxide, hydrochloric acid were obtained from Merck (Darmstadt, Germany).

Water was purified using an Elix 3 coupled to a Milli-Q system (Millipore, Bedford, MA, USA) and filtered using a 0.22 μm nylon filter integrated into the Milli-Q system.

For the preparation of C_{60}-SDS, C_{70}-SDS and C_{60}-pyrr-SDS, individual stock solutions in toluene (~1000 mg Kg^{-1}) and SDS aqueous solutions (100 mM) were used. The stock solutions

in 100 mM SDS (~ 30 mg L^{-1} C_{60}-SDS and C_{60}-pyrr-SDS and ~ 10 mg L^{-1} C_{70}-SDS) were obtained by mixing the exact amounts of each solution in individual amber vials and treated in an ultrasonic bath until the toluene was completely evaporated and the aqueous phase became transparent brownish-yellow (C_{60}-SDS, C_{60}-pyrr) and dark-purple (C_{70}-SDS). The working solutions were diluted with the appropriate amount of SDS 100 mM prior to analysis.

Stock standard solutions of $C_{120}(OH)_{30}$ and $C_{60}(OH)_{24}$(~1000 mg Kg^{-1}) were individually prepared by weight in Milli-Q water and stored at 4°C. The aqueous suspensions of the carboxy-fullerene derivatives were obtained first by dissolving the solid powder in tetrahydrofuran (Merck, Darmstadt, Germany), and the appropriate amount of Milli-Q water (depending on the final fullerene concentration) was added to the solution. Next, the solution was sonicated until the tetrahydrofuran was completely evaporated to obtain stock solutions of approximately 500 mg Kg^{-1}. Prior to analysis, each stock solution was diluted with the appropriate amount of Milli-Q water to obtain the working solution.

2.2. Instrumentation

2.2.1. Capillary electrophoresis(CE)

CE experiments were performed on a Beckman P/ACE MDQ capillary electrophoresis instrument (Fullerton, CA, USA) equipped with a diode array detector. CE separations were carried out using uncoated fused-silica capillaries (Beckman) with a total length of 50 cm (45 cm effective length) x 75 μm I.D. (375 μm O.D.). CZE and MECC analysis were performed by using 2 mM SDS in 1 mM sodium tetraborate and 100 mM SDS in 10 mM sodium phosphate-10 mM sodium tetraborate solutions, respectively, as BGEs. The capillary temperature was held at 25 °C. The BGE was filtered through a 0.45 μm nylon membrane filter before use. A capillary voltage of + 20 kV was applied for the separations. Sample introduction was performed by hydrodynamic injection (10 s, 13.5 kPa). Direct UV detection was performed at 254 nm. The CE instrument was controlled using Beckman 32 Karat software version 5.0.

New capillaries were pre-treated with 0.1 M HCl for 30 min, water for 30 min, 1 M NaOH for 30 min, and finally washed with water for 30 min. At the beginning of each session, the capillary was rinsed with 0.5 M NaOH for 10 min, with water for 10 min, and with the BGE for 15 min. The capillary was rinsed with the BGE for 5 min between runs and stored after rinsing with water at the end of each session.

2.2.2. Asymmetrical flow-field flow Fractionation (AF4)

The fractionation was carried out with an Eclipse Dualtec AF4 separation system (Wyatt Technology Europe GmbH, Dernbach, Germany) equipped with a programmable pump (Isocratic 1100, Agilent Technologies), an Agilent 1100 series degasser and an Agilent 1200 series auto sampler/injector. A mini-channel (11cm in length, 22 mm in width at the injection point and 3 mm close to the end) was equipped with a 480 μm spacer of trapezoidal shape and Millipore regenerated cellulose (RC) membrane of 10 kDa nominal molar mass cut-off (Superon GmbH, Dernbach, Germany). On-line detection was performed with a UV detector (Applied Biosystems, Foster City, California, USA).

The samples were injected in Milli-Q water with an injection flow of 0.1 mL min^{-1}. The relaxation and focusing were carried out during a specific time (3 min for the carboxy-fullerenes and 10 min for polyhydroxy-fullerene derivatives) at a cross flow rate of 2 mL min^{-1}. Time-delayed exponential (TDE) mode was used for the elution step with a delay/decay time of 3 min (carboxy-fullerenes) and 7 min (polyhydroxy-fullerene derivatives), an initial cross flow of 2 mL min^{-1} and a channel flow of 1 mL min^{-1}. The eluted samples were monitored by the UV detector at 254 nm.

2.2.3. Transmission electron microscopy (TEM)

For TEM measurements, one drop of the aqueous fullerene solutions prepared in 100 mM SDS and 10 mM sodium tetraborate-10 mM sodium phosphate was placed on a TEM grid (carbon-coated copper grid 200 mesh (All Carbon)) and stained with a drop of uranyl formate (1% aqueous solution). After air drying of the grid (2 h), TEM images were taken.

2.3. Sample preparation

The extraction of C_{60} from the cosmetic products (*i.e.,* anti- aging serum and a facial mask) was performed by following a procedure previously described [21] with few modifications. Briefly, for the extraction approx. 3 g of cosmetic sample were added to 20 mL toluene and sonicated for 4 h. The toluene extract was then centrifuged at 4500 rot/min for 15 min using a Selecta Centronic Centrifuge (Barcelona, Spain). The clear toluene supernatant was then evaporated to almost dryness, and reconstituted in 200 μL of 100 mM SDS aqueous solution, and the residual toluene was completely evaporated via sonication prior to be injected into the CE system.

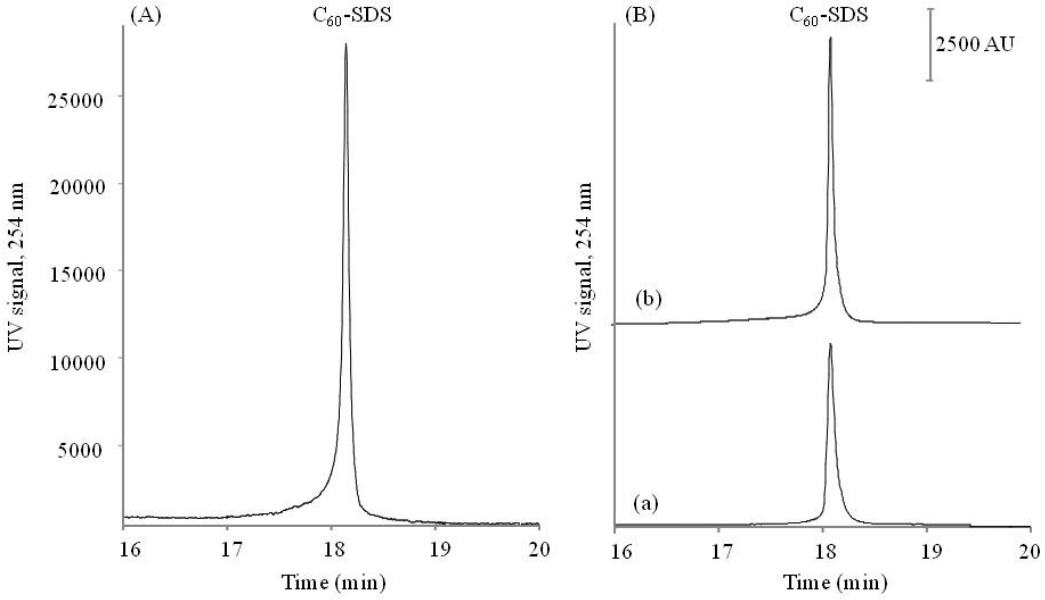

Figure 2. MECC electropherograms of (A) C_{60}-SDS (25 mg L^{-1}), (B) facial mask product (a), the same product fortified with 3 mg L^{-1} of C_{60} (b); BGE: 100 mM SDS, 10 mM sodium tetraborate-10 mM sodium phosphate (pH=9.4); voltage: + 20 kV.

3. Results

3.1. Hydrophobic fullerenes

In this work, the performance of MECC for the analysis of hydrophobic fullerenes (C_{60}, C_{70} and C_{60}-pyrr) using as BGE 100 mM SDS in 10 mM sodium phosphate-10mM sodium tetraborate (pH=9.4), previously proposed by Treubig and Brown [24] was evaluated. The compounds were first solubilized in aqueous media via interaction with SDS micelles following the procedure included in the *Materials and methods* Section. Figure 2A shows as an example the electropherogram obtained for the analysis of C_{60}-SDS appearing as a sharp peak at the migration time of approx. 18 min. Electropherograms with the same migration time indicating identical electrophoretic mobility were also obtained for C_{70} and C_{60}-pyrr. The instrumental quality parameters such as limits of detection (LOD), limits of quantitation (LOQs) based on signal-to-noise ratio of 3:1 and 10:1 respectively, linearity and precision were evaluated for each compound using standard fullerene solutions prepared in SDS (100 mM) and are given in Table 1. The LODs ranged from 0.6 to 2.2 mg L^{-1}, and the calibration curves based on peak areas at concentration ranges between 0.8 and 30 mg L^{-1} (C_{60}-SDS and C_{60}-pyrr-SDS) and between 2.2 and 10 mg L^{-1} (C_{70}-SDS) showed good linearity with correlation coefficients (r^2) of 0.991 (C_{60}),

0.994 (C_{60}-pyrr) and 0.988 (C_{70}). Run-to-run and day-to-day precisions were calculated at two concentration levels, at low level (LOQ) and a medium level (15 mg L^{-1} for C_{60}-SDS and C_{60}-pyrr-SDS and 5 mg L^{-1} for C_{70}-SDS), and the results expressed as relative standard deviation (% RSD), are given in Table 1. As can be seen, acceptable run-to-run and day-to-day precisions were achieved with RSD values lower than 14.3 %.

This MECC method was used to determine C_{60} in two commercial cosmetic products (face mask and anti-aging serum) that contain this compound. Sample extractions were performed as indicated in the *Sample preparation* section and the extracts were analyzed using the proposed MECC method. As an example, the obtained electropherogram for one of the analyzed samples and of the same product fortified with C_{60} is shown in Figure 2B. Since no blank samples were available, quantitation was carried out by triplicate using a standard addition method, and C_{60} was quantitated at 1.86 ± 0.07 mg L^{-1} (anti-aging serum) and 2.77 ± 0.16 mg kg^{-1} (face mask) concentration levels.

Table 1. Instrumental quality parameters

	LODs (mg L^{-1})	LOQs (mg L^{-1})	run-to-run precision (% RSD; n=5)			day-to-day precision (% RSD; n=5 x 3)		
			t_m (min)	Concentration (low level)[a]	Concentration (medium level)[b]	t_m (min)	Concentration (low level)[a]	Concentration (medium level)[b]
C_{60}	0.8	2.4	0.2	5.1	2.4	1.2	6.5	2.1
C_{70}	2.2	6.6	0.4	7.8	4.6	1.3	14.3	9.2
C_{60}-pyrr	0.6	1.8	0.3	4.3	2.3	1.0	5.7	2.0

[a]LOQ

[b] 10 mg L^{-1} (C_{60} and C_{60} pyrr) and 5 mg L^{-1} (C_{70})

3.2. Polyhydroxy- and carboxy-fullerene derivatives

In a first step, polyhydroxy- and carboxy-fullerene derivatives were analyzed by MECC using the BGE employed for the analysis of hydrophobic fullerenes (100 mM SDS, 10 mM sodium phosphate-10mM sodium tetraborate, pH=9.4 solution). Figure 3 shows the electropherograms obtained for each of the studied compounds ($C_{60}(OH)_{24}$, $C_{120}(OH)_{30}$, C_{60}-pyrr tris acid and C_{60}CHCOOH). Under these conditions, broad and distorted peaks were obtained for all the fullerenes. $C_{60}(OH)_{24}$ and C_{60}CHCOOH presented peak tailing and fronting, respectively and the electropherograms of $C_{120}(OH)_{30}$ and C_{60}-pyrr tris acid revealed broad and multiple peaks. Subsequently, the effect of the buffer and SDS concentration and pH value on the migration time and electrophoretic peak profile of the selected analytes was evaluated.

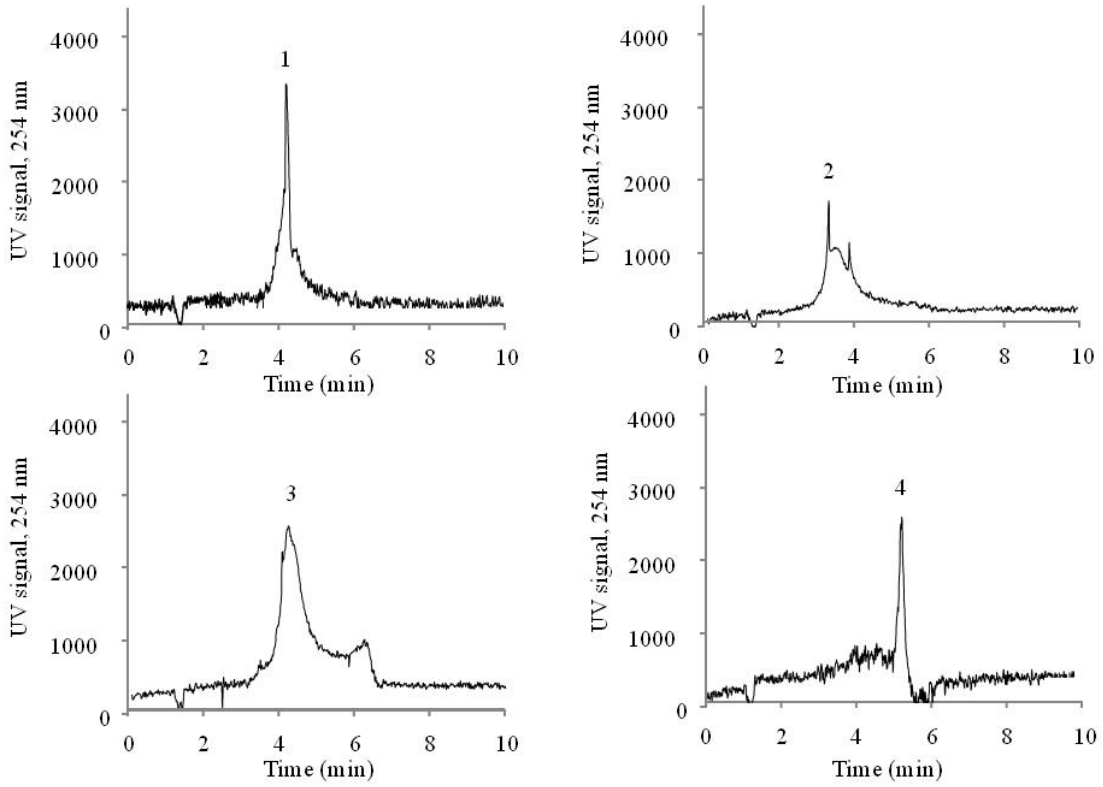

Figure 3. MECC electropherograms of: 1: $C_{60}(OH)_{24}$ (25 mg L^{-1}); 2: $C_{120}(OH)_{30}$ (25 mg L^{-1}); 3: C_{60}-pyrr tris acid (25 mg L^{-1}); 4: $C_{60}CHCOOH$ (25 mg L^{-1}); BGE: 100 mM SDS, 10 mM sodium tetraborate-10 mM sodium phosphate (pH=9.4); voltage: + 20 kV; λ= 254 nm.

The effect of the buffer composition and concentration was studied by keeping constant the SDS concentration (100 mM) and pH value (≈ 9.4). Figure 4 shows the electropherograms obtained for the studied compounds at different buffer composition and concentrations. As can be seen, highly broad and distorted peaks were obtained for all the fullerenes at high buffer concentration values (above 10 mM sodium tetraborate-10 mM sodium phosphate) and for some of the compounds multiple peaks were observed. For instance, the electropherograms of C_{60}-pyrr tris acid revealed two unresolved peaks and the tail of the first one increased so much that at 15 mM sodium tetraborate-15mM sodium phosphate, it embraced migration times from 4 to 11 min. For all the compounds, the migration times decreased with a decrease in the buffer concentration and their electrophoretic pattern changed, revealing sharper peaks at 2.5 mM sodium tetraborate-2.5 mM sodium phosphate buffer concentration. A further improvement in peak shapes was obtained by using only sodium tetraborate as buffer at a concentration of 1 mM (Figure 4).

The changes in the electrophoretic profile of the peaks were further monitored at SDS concentration values between 2 and 100 mM (Figure 5) using 1 mM sodium phosphate as buffer. In general, lower migration times and narrower peaks were obtained by reducing the SDS

concentration in the running BGE and in some cases, changes in the peak profile were observed. For instance, the electropherogram of C_{60}-pyrr tris acid, at SDS concentrations ≥ 40 mM, showed two peaks and bellow this value only one peak was observed although its symmetry worsened showing front tailing. In contrast, for $C_{60}CHCOOH$ a more symmetrical peak is obtained at low SDS concentration. Regarding the studied polyhydroxy-fullerene derivatives in addition to a reduction of the retention times, the number of distinguishable peaks decreased with the SDS concentration (see as an example the electropherograms obtained for $C_{120}(OH)_{30}$ in Fig. 5). Moreover, when working in CZE conditions, using SDS concentrations bellow the critical micellar concentration (CMC, 8 mM) and a low buffer concentration narrower peaks than those found in MECC were obtained.

4. Discussion

4.1. Hydrophobic fullerenes

It has been reported that C_{60} forms aggregates within SDS micelles [24,38,39] but despite this fact, MECC has not been proposed for the analysis of this compound. Therefore, the capability of this electrophoretic method for the analysis of C_{60} but also of C_{70} and C_{60}-pyrr for which there is no information in the literature was evaluated in this work. The MECC electropherograms obtained for the resulting fullerene-SDS complexes analyzed individually indicated that interaction occurred and the three compounds were completely entrapped in the hydrophobic core of the micelles. The migration time of the three compounds was that of the micelles which was measured using Sudan III. Therefore, this technique can only be applied for the analysis of individual hydrophobic fullerenes in quality control analysis where only one of these compounds is present. The quality parameters were evaluated in order to use the method for the determination of the individual compounds in samples where the other fullerenes are not expected. The results showed good repeatability and reproducibility and the obtained LOQs (Table 1) allowed us to propose the MECC method for the analysis of samples with sufficiently high fullerene concentration. Since the presence of C_{60} in cosmetic products was previously reported [40,41] at concentration levels up to 1.1 mg kg^{-1}, and in these samples no other fullerenes are applied, two cosmetic products containing this compound were selected to evaluate the applicability of MECC. C_{60} was found at 1.86 ± 0.07 mg L^{-1} (anti-aging serum) and 2.77 ± 0.16 mg kg^{-1} (face mask) concentration levels. The same anti-aging serum sample was analyzed in our previous work by LC-MS [21], reporting C_{60} at a concentration 1.93 ± 0.15 mg L^{-1} confirming the result obtained by MECC. Since no organic solvents are used in MECC, the

proposed method is less contaminant than the LC-MS method which requires the use of a high amount of toluene in the mobile phase. Nevertheless, MECC implies 2 time-consuming steps, the solubilization of fullerenes in the SDS aqueous solution and the sample preparation.

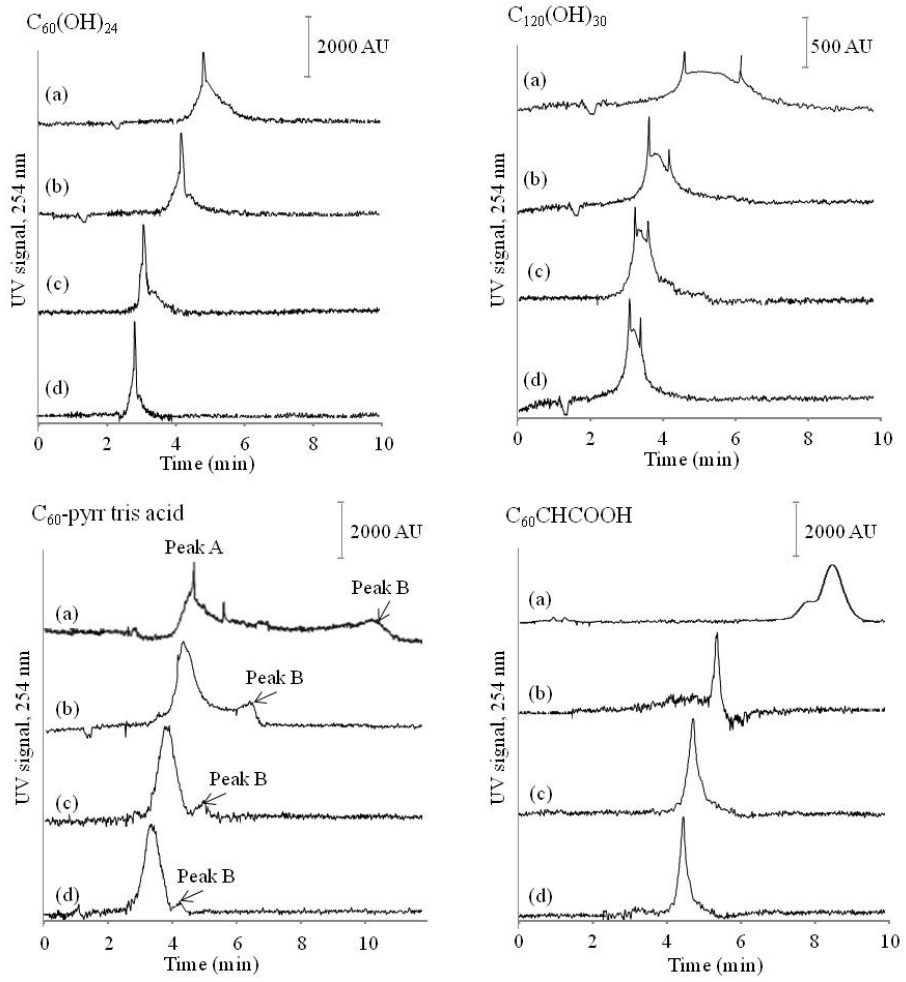

Figure 4. MECC electropherograms of the studied fullerenes at different buffer concentrations: (a) 15 mM sodium tetraborate-15 mM sodium phosphate; (b) 10 mM sodium tetraborate-10 mM sodium phosphate; (c) 2.5 mM sodium tetraborate-2.5 mM sodium phosphate and (d) 1 mM sodium tetraborate; other BGE conditions: 100 mM SDS; voltage: + 20 kV.

4.2. Polyhydroxy- and carboxy-fullerene derivatives

In MECC, the buffer composition and concentration showed a significant influence on the electrophoretic pattern of the peaks of polyhydroxy- and carboxy-fullerene derivatives (Figure 4). As expected, the decrease in the EOF produced an increase in the migration times of the compounds which was very significant at high buffer concentrations (~ 50 % increase). For instance, for C_{60}CHCOOH and C_{60}-pyrr tris acid (peak B) an increase from 4.3 min and 4.2 min,

respectively at 1 mM sodium tetraborate up to 8.5 min and 10.3 min, respectively at 15 mM sodium tetraborate-15 mM sodium phosphate was observed. Moreover, for concentrations higher than 5 mM sodium tetraborate- 5mM sodium phosphate, highly broad and distorted peaks were obtained. The highly skewed peaks with long tails obtained for the compounds, as the ones observed for C_{60}-pyrr tris acid at 15 mM sodium tetraborate-15mM sodium phosphate for example (Figure 4), prompted the thought that several species with different sizes or charges that migrate with slightly different velocities were present. The observed behavior suggests that large aggregates are formed at high buffer concentration values. As a first step to understand the behavior of these compounds in MECC, the morphology and aggregation degree of the analytes was studied using TEM. As an example, Figure 6 shows the micrographs obtained for C_{60}-pyrr tris acid and $C_{60}(OH)_{24}$ in 100 mM SDS and 10 mM sodium tetraborate-10 mM sodium phosphate. The images show some differences between the aggregate structures and shapes of these compounds and the presence of polidisperse aggregates can be observed in both cases. The carboxy-fullerene derivatives presented large aggregates and spherical and irregular shaped structures of various sizes whereas the polyhydroxy-fullerene derivatives presented mainly polycrystalline structures. As shown, complex branched structures were formed in these conditions which were so strongly aggregated that it was difficult to obtain an average particle size.

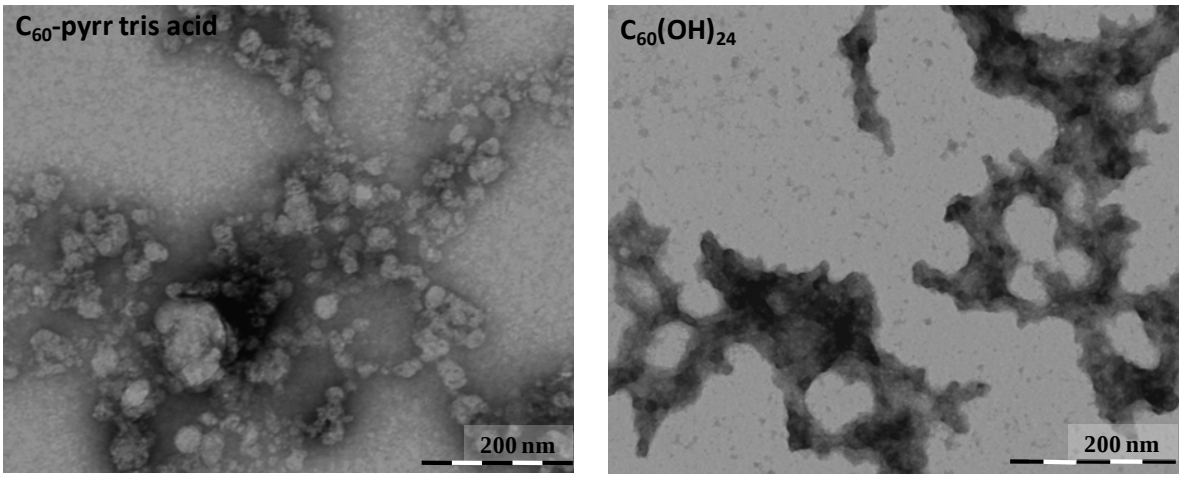

Figure 6: TEM pictures of C_{60}-pyrr tris acid and $C_{60}(OH)_{24}$ aggregates.

The aggregate sizes of the compounds at different buffer composition and concentrations (1 mM sodium tetraborate and sodium tetraborate- sodium phosphate from 2.5 mM to 10 mM of each salt component) and SDS concentrations (from 2 mM to 30 mM) were determined by AF4 with UV detection. The hydrodynamic radii (r_H) of the particles were calculated from the retention time at the maximum of the peak height using standard AF4 theory [32].

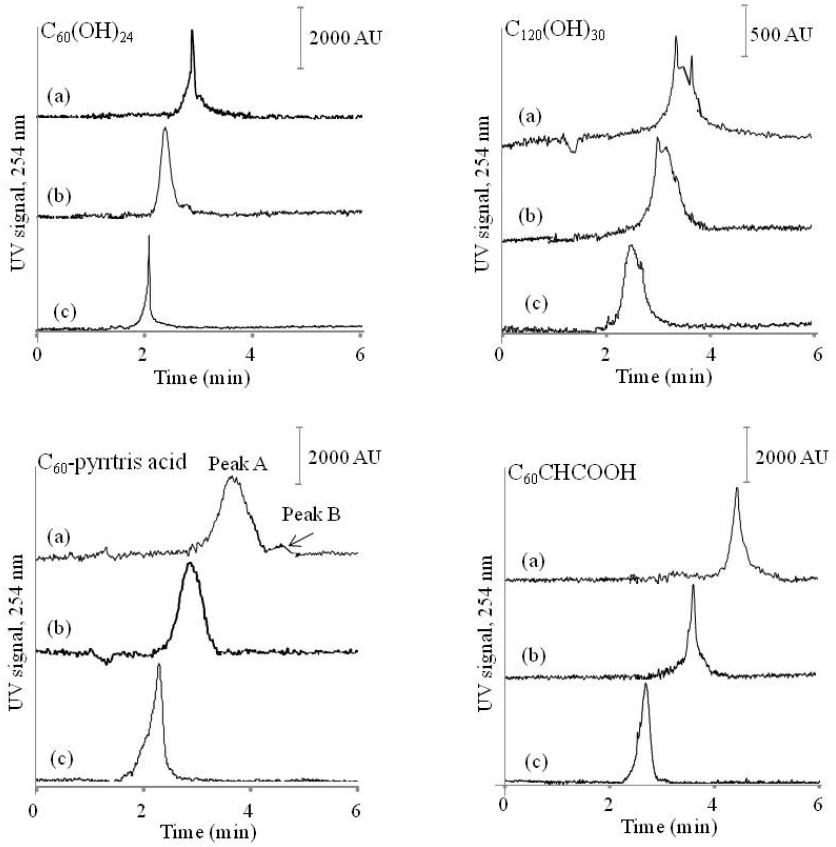

Figure 5. Electropherograms of the selected fullerenes at different SDS concentrations: (a) 100 mM SDS; (b) 40 mM SDS; (c) 2 mM SDS; other BGE conditions: 1 mM sodium tetraborate; voltage: + 20 kV.

Figure 7A shows as an example the fractograms obtained for C_{60}-pyrr tris acid and $C_{60}(OH)_{24}$ using 2 mM SDS and 1 mM sodium tetraborate as carrier solution. At these conditions, the carboxy-fullerene derivatives eluted in fractions of different aggregation degree and presented at least 2 separated peaks, one corresponding to small particles (≈ 10 nm) and a major peak corresponding to big aggregates with a calculated r_H up to 55 nm. The fractograms obtained for $C_{120}(OH)_{30}$ and $C_{60}(OH)_{24}$ revealed in each case one tailed peak presenting smaller particles sizes than the carboxy-fullerene derivatives, with a r_H calculated at the maximum of the peak height of approx 6 nm and 7 nm, respectively. An increase of the buffer concentration in the carrier solution produced a significant decrease of the peak areas of the carboxy-fullerenes which was caused by an enhanced adsorption of these particles to the AF4 membrane as they settled out of suspension. In contrast, this effect was not observed for the polyhydroxy-fullerene derivatives, due to their higher water solubility and significantly smaller sizes than the carboxy-derivatives. Figure 7B shows, as an example, the fractograms obtained for $C_{60}(OH)_{24}$ using 2 mM SDS and different buffer type and concentrations. As shown, tailing peaks were observed as in the CE experiments probably due to the presence of unresolved higher order aggregates. The change in

the elution profile of the polyhydroxy-fullerene derivatives (*i.e.,* retention time shift, broader peaks) at higher buffer concentrations was accompanied by an increase in the calculated r_H at the maximum of the peak height, from approx. 6 nm $(C_{120}OH)_{30}$) and 7 nm $(C_{60}OH)_{24}$) (1 mM sodium tetraborate) up to 18 nm $(C_{120}OH)_{30}$) and 25 nm $(C_{60}OH)_{24}$) (10 mM sodium tetraborate-10 mM sodium phosphate). Therefore, the broad and distorted peaks obtained for the studied compounds by capillary electrophoresis at high buffer concentrations seem to be due to increased aggregation and to the presence of fractions of different aggregation degree.

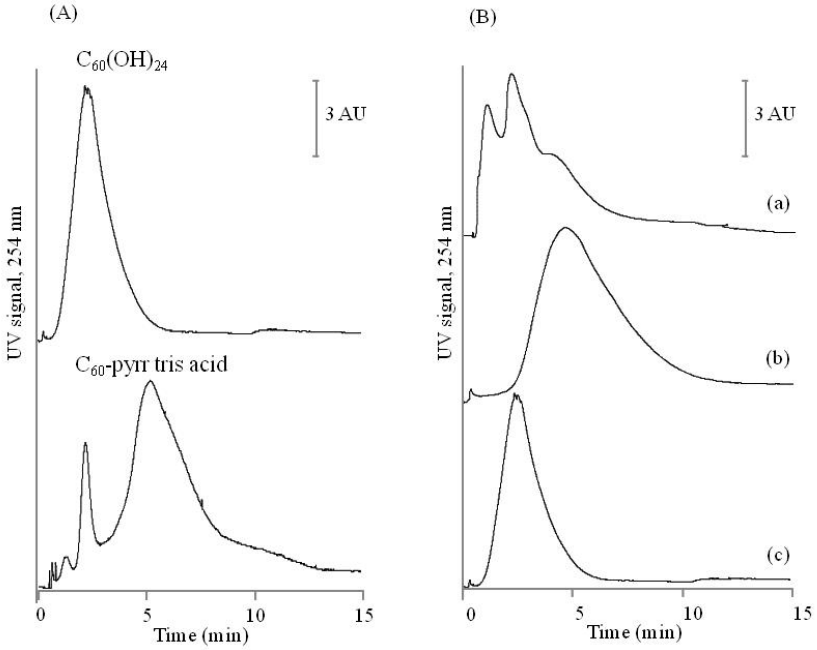

Figure 7. (A) Fractograms of $C_{60}(OH)_{24}$ and C_{60}-pyrr tris acid; carrier solution: 2 mM SDS and 1mM sodium tetraborate, pH=9.2 and (B) Fractograms of $C_{60}(OH)_{24}$; carrier solution: (a) 30 mM SDS and 1 mM sodium tetraborate, (b) 2 mM SDS and 10 mM sodium tetraborate-10 mM sodium phosphate, and (c) 2 mM SDS and 1 mM sodium tetraborate. TDE flow programming with a delay/decay time of 3 min (C_{60}-pyrr tris acid) and 7 min $C_{60}(OH)_{24}$. For the experimental conditions used see text.

The AF4 results showed that the presence of SDS micelles does not seem to increase the aggregation of fullerenes but favors the separation of particles of different aggregate sizes. Figure 7B shows the fractograms obtained for $C_{60}(OH)_{24}$ in the presence (30 mM SDS) and absence (2 mM SDS) of micelles. As can be seen, in the presence of micelles, 3 unresolved peaks were obtained, corresponding to particles with different aggregation degree with an average r_H of 4 nm, 6 nm and 10 nm. Similar behavior was observed for the other studied fullerenes indicating that the presence of micelles allows distinguishing between aggregates of different sizes in the samples probably due to their different partition/complexation with the micelles. This could explain the multiple and broad peaks observed in MECC and the improvement in peak shape with the decrease of SDS concentration (Table 3).

Over the studied pH range (3-12.5), the studied compounds maintained a substantial charge and were detected in normal polarity. These results are in agreement with previous studies reporting that fullerols present negative surface charge over a wide pH range (pH >3), implying a certain proportion of deprotonated surface sites, even at acidic conditions [37,42]. However, to the best of our knowledge, the pKa values of these compounds are not known accurately. As expected, lower migration times were obtained when decreasing the pH because of a slower EOF (Figure S1). Under acidic conditions, broad and distorted peaks with high migration times were obtained.

5. Conclusions

Complementary information about the aggregation of four surface modified fullerenes in aqueous solutions of different buffer and SDS concentrations was obtained by using three different techniques (CE, AF4 and TEM). The observed significant differences in the electrophoretic peak profiles of the studied compounds revealed that CE techniques are able to capture the changes in their aggregation state. The broad, multiple and distorted peaks obtained in MECC (at high buffer and SDS concentrations) can be related to the increased aggregation that generated particles of different sizes, whereas by working in CZE conditions sharper peaks were obtained. AF4 provided information about the changes in the aggregate sizes of the selected fullerenes at the tested conditions. The calculated particle hydrodynamic radii values showed that high buffer concentration values promote the aggregation of the particles while the presence of micelles allows distinguishing between aggregates of different sizes. Regarding the aggregate structures, the obtained TEM images revealed the formation of highly branched and complex aggregates in the evaluated MECC conditions. Therefore, the combination of these techniques offers a wide picture of the aggregation of fullerenes in aqueous solutions.

Acknowledgments

The authors gratefully acknowledge for the financial support received from the Spanish Ministry of Economy and Competitiveness under the project CTQ2012-30836, and from the Agency for Administration of University and Research Grants (Generalitat de Catalunya, Spain) under the project 2014 SGR-539. Alina Astefanei acknowledges the Spanish Ministry of Economy and Competitiveness for a Ph.D. grant (FPI-MICINN) which enabled her to carry out this research at the University of Barcelona and as a visiting scientist at the University of

Amsterdam. We also thank Carmen Lopez and Nieves Hernandez (CCiTUB, University of Barcelona) for help with the TEM analysis.

References

1. Kroto HW, Heath JR, O'Brien SC, Curl RF, Smalley RE (1985) C60: buckminsterfullerene. Nature 318:162-163

2. Tagmatarchis N, Shinohara H (2001) Fullerenes in medicinal chemistry and their biological applications. Mini-Rev Med Chem 1:339-348

3. Xiao L, Takada H, Gana X, Miwa N (2006) The water-soluble fullerene derivative 'Radical Sponge' exerts cytoprotective action against UVA irradiation but not visible-light-catalyzed cytotoxicity in human skin keratinocytes. Bioorg Med Chem Lett 16:1590-1595

4. Kronholm D, Hummelen JC (2007) Fullerene-based n-type semiconductors in organic electronics. Mater Matters (Milwaukee, WI, U S) 2:16-19

5. Meng H, Xing GM, Sun BY, Zhao F, Lei.H., Li W (2010) Potent angiogenesis inhibition by the particulate form of fullerene derivatives. ACS Nano 4:2773-2783

6. Dugan LL, Lovett EG, Quick KL, Lotharious J, Lin TT, O'Malley KL (2001) Fullerene-based antioxidants and neurodegenerative disorders. Parkinson Relat Disord 7:243-246

7. Bosi S, Da Ros T, Spalluto G, Prato M (2003) Fullerene derivatives: an attractive tool for biological applications. Eur J Med Chem 38:913-923

8. Sitharaman B, Asokan S, Rusakova I, Wong MS, Wilson LJ (2004) Nanoscale Aggregation Properties of Neuroprotective Carboxyfullerene (C3) in Aqueous Solution. Nano Lett 4:1759-1762

9. Friedman SH, DeCamp DL, Sijbesma RP, Srdanov G, Wudl F, Kenyon GL (1993) Inhibition of the HIV-1 protease by fullerene derivatives: model building studies and experimental verification. J Am Chem Soc 115:6506-6509

10. Yamago S, Tokuyama H, Nakamura E, Kituchi K, Kananishi S, Sueki K, Nakahara H, Enmoto S, Ambe F (1995) In vivo biological behavior of a water-miscible fullerene: 14C labeling, absorption, distribution, excretion and acute toxicity. Chem Biol 2:385-389

11. Nel AE, Madler L, Velegol D, Xia T, Hoek EMV, Somasundaran P (2009) Understanding biophysicochemical interactions at the nano-bio interface. Nano Mater 8:543-547

12. Vileno B, Marcoux PR, Lekka M, Sienkiewicz A, Feher T, Forro L (2006) Spectroscopic and Photophysical Properties of a Highly Derivatized C60 Fullerol. Adv Funct Mater 16:120-128

13. Pickering KD, Wiesner MR (2005) Fullerol-sensitized production of reactive oxygen species in aqueous solution. Environ Sci Technol 39:1359-1365

14. Sayes CM, Fortner JD, Guo W, Lyon D, Boyd AM, Ausman KD, Tao YJ, Sitharaman B, Wilson LJ, Hughes JB, West JL, Colvin VL (2004) The Differential Cytotoxicity of Water-Soluble Fullerenes. Nano Lett 4:1881-1887

15. Astefanei A, Núñez O, Galceran MT (2015) Characterisation and analysis of fullerenes: A critical review. Anal Chim Acta 828: 1-21

16. Handy RD, Owen R, Valsami-Jones E (2008) The ecotoxicology of nanoparticles and nanomaterials: current status, knowledge gaps, challenges, and future needs. Ecotoxicology 17:315-325

17. Klaine SJ, Alvarez PJJ, Batley GE, Fernandes TF, Handy RD, Lyon DY, Mahendra S, McLaughlin MJ, Lead JR (2008) Nanomaterials in the environment: behavior, fate, bioavailability, and effects. Environ Toxicol Chem 27:1825-1851

18. A. Astefanei, O. Núñez, M.T. Galceran, Liquid Chromatography in the Analysis of Fullerenes, in: S.B. Ellis (Ed.), Fullerenes, Chemistry, Natural Sources and Technological Applications, Nova Science Publishers, New York, 2014, pp. 35-63.

19. Chao TC, Song G, Hansmeier N, Westerhoff P, Herckes P, Halden RU (2011) Characterization and Liquid Chromatography-MS/MS Based Quantification of Hydroxylated Fullerenes. Anal Chem 83:1777-1783

20. Silion M, Dascalu A, Pinteala M, Simionescu BC, Ungurenasu C (2013) A study on electrospray mass spectrometry of fullerenol C60(OH)24. Beilstein J Org Chem 9:1285-1295

21. Astefanei A, Núñez O, Galceran MT (2012) Non-aqueous capillary electrophoresis separation of fullerenes and C60 fullerene derivatives. Anal Bioanal Chem 404:307-313

22. Wan TSM, Leung GNW, Tso TSC, Komatsu K, Murata Y (1995) Non-aqueous capillary electrophoresis as a new method for the separation of fullerenes. Proc - Electrochem Soc 95:1474-1487

23. Su HL, Kao WC, Lee Cy, Chuang SC, Hsieh YZ (2010) Separation of open-cage fullerenes using nonaqueous capillary electrophoresis. J Chromatogr A 1217:4471-4475

24. Treubig JM, Brown PR (2000) Novel approach to the analysis and use of fullerenes in capillary electrophoresis. J Chromatogr A 873:257-267

25. Cerar J, Pompe M, Gucek M, Cerkovnik J, Skerjanc J (2007) Analysis of sample of highly water-soluble Th-symmetric fullerenehexamalonic acid C66(COOH)12 by ion-chromatography and capillary electrophoresis. J Chromatogr A 1169:86-94

26. Tamisier-Karolak SL, Pagliarusco S, Herrenknecht C, Brettreich M, Hirsch A, Ceolin R, Bensasson RV, Szwarc H, Moussa F (2001) Electrophoretic behavior of a highly water-soluble dendro[60]fullerene. Electrophoresis 22:4341-4346

27. Chan KC, Patri AK, Veenstra TD, McNeil SE, Issaq HJ (2007) Analysis of fullerene-based nanomaterial in serum matrix by CE. Electrophoresis 28:1518-1524

28. Bermudez O, Forciniti D (2004) Aggregation and denaturation of antibodies: a capillary electrophoresis, dynamic light scattering, and aqueous two-phase partitioning study. J Chromatogr B: 807:17-24

29. Sabella S, Quaglia M, Lanni C, Racchi M, Govoni S, Caccacialanza G, Calligaro A, Belloti V, De Lorenzi E (2004) Capillary electrophoresis studies on the aggregation process of -amyloid 1-42 and 1-40 peptides. Electrophoresis 25:3186-3194

30. Pryor E, Kotarek JA, Moss M, Hestekin CN (2011) Monitoring Insulin Aggregation via Capillary Electrophoresis. Int J Mol Sci 12:9369-9388

31. Wahlund KG, Giddings JC (1987) Properties of an asymmetrical flow field-flow fractionation channel having one permeable wall. Anal Chem 59:1332-1339

32. Schimph, M.E., Caldwell, K. and Giddings, J.C (2000), Field flow-field fractionation handbook, John Wiley & Sons, Inc., New York.

33. Baalousha M, Stolpe B, Lead JR (2011) Flow field-flow fractionation for the analysis and characterization of natural colloids and manufactured nanoparticles in environmental systems: a critical review. J Chromatogr A 1218:4078-4103

34. Isaacson CW, Bouchard D (2010) Asymmetric flow field flow fractionation of aqueous C60 nanoparticles with size determination by dynamic light scattering and quantification by liquid

chromatography atmospheric pressure photo-ionization mass spectrometry. J Chromatogr A 1217:1506-1512

35. Herrero P, Bäuerlein PS, Emke E, Pocurull E, de Voogt P (2014) Asymmetrical flow field-flow fractionation hyphenated to Orbitrap high resolution mass spectrometry for the determination of (functionalised) aqueous fullerene aggregates. J Chromatogr A 1356:277-282

36. Kato H, Shinohara N, Nakamura A, Horie M, Fujita K, Takahashi K, Iwahashi H, Endoh S, Kinugasa S (2010) Characterization of fullerene colloidal suspension in a cell culture medium for in vitro toxicity assessment. Mol BioSyst 6:1238-1246

37. Assemi S, Tadjiki S, Donose BC, Nguyen AV, Miller JD (2010) Aggregation of Fullerol C60(OH)24 Nanoparticles as Revealed Using Flow Field-Flow Fractionation and Atomic Force Microscopy. Langmuir 26:16063-16070

38. Bensasson RV, Bienvenue E, Dellinger M, Leach S, Seta P (1994) C60 in Model Biological Systems. A Visible-UV Absorption Study of Solvent-Dependent Parameters and Solute Aggregation. J Phys Chem 98:3492-3500

39. Torres VM, Posa M, Srdjenovic B, Simplicio AL (2011) Solubilization of fullerene C60 in micellar solutions of different solubilizers. Colloids Surf , B 82:46-53

40. Chae SR, Hotze EM, Xiao Y, Rose J, Wiesner MR (2010) Comparison of methods for fullerene detection and measurements of reactive oxygen production in cosmetic products. Environ Eng Sci 27:797-804

41. Benn TM, Westerhoff P, Herckes P (2011) Detection of fullerenes (C60 and C70) in commercial cosmetics. Environ Pollut 159:1334-1342

42. Brant JA, Labille J, Robichaud CO, Wiesner M (2007) Fullerol cluster formation in aqueous solutions: Implications for environmental release. J Colloid Interface Sci 314:281-288

Supplementary material

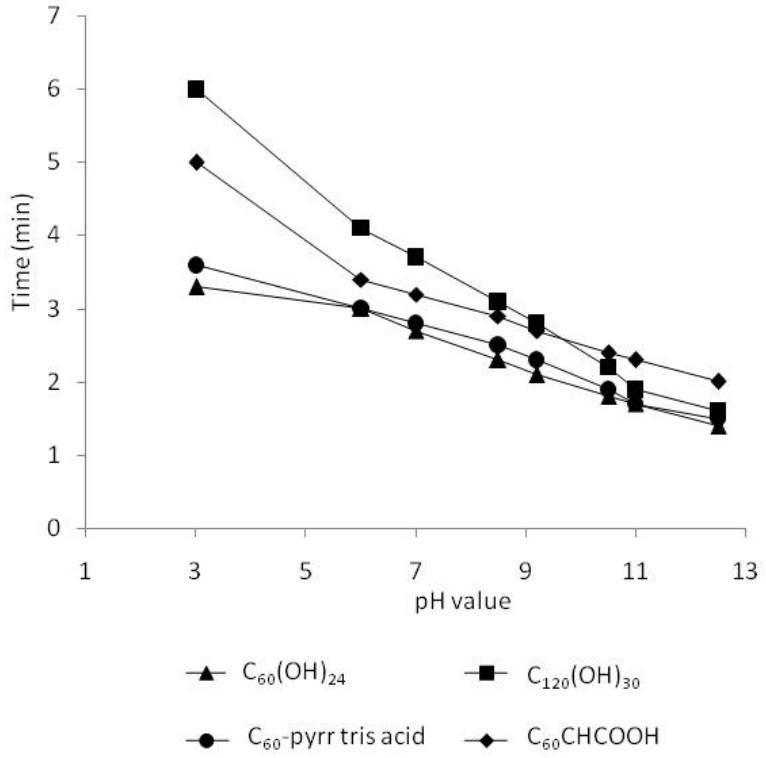

Figure S1. pH effect (3-12.5) on the migration times of 1: $C_{60}(OH)_{24}$; 2: $C_{120}(OH)_{30}$; 3: C_{60}-pyrr tris acid; 4: C_{60}CHCOOH; BGE: 2 mM SDS in 1 mM sodium tetraborate; voltage: + 20 kV; λ= 254 nm.

CHAPTER 3

CHARACTERISARION OF FULLERENES

3.3. Scientific article V: Characterization of aggregates of surface modified fullerenes by asymmetrical flow field-flow fractionation with multi angle light scattering detection

A. Astefanei, W. Th. Kok, P. Bäuerlein, O. Núñez, M. T. Galceran[a], P. de Voogt and P. J. Schoenmakers

Journal of Chromatography A (2015) (accepted for publication).

Characterization of aggregates of surface modified fullerenes by asymmetrical flow field-flow fractionation with multi angle light scattering detection

Alina Astefanei[a *], Wim Th. Kok[b], Patrick Bäuerlein[c], Oscar Núñez[a,d], Maria Teresa Galceran[a], Pim de Voogt[e], Peter J. Schoenmakers[b]

[a]Analytical Chemistry Department, University of Barcelona. Martí i Franquès 1-11, E08028 Barcelona, Spain

[b]Analytical Chemistry Department-HIMS, University of Amsterdam, PO Box 94157, 1090 GD, Amsterdam, The Netherlands

[c] KWR Watercycle Research Institute, Groningenhaven 7, P.O. Box 1072, 3430 BB, Nieuwegein, The Netherlands

[d] Serra Hunter Fellow, Generalitat de Catalunya, Spain.

[e] IBED, University of Amsterdam, PO Box 94248, 1090 GE Amsterdam, The Netherlands

* Corresponding author

Abstract

Fullerenes are carbon nanoparticles with widespread biomedical, commercial and industrial applications. Attributes such as their tendency to aggregate and aggregate size and shape impact their ability to be transported into and through the environment and living tissues. Knowledge of these properties is therefore valuable for their human and environmental risk assessment as well as to control their synthesis and manufacture. In this work, asymmetrical flow-field flow fractionation (AF4) coupled to multi-angle light scattering (MALS) was used for the first time to study the size distribution of surface modified fullerenes with both polyhydroxyl and carboxyl functional groups in aqueous solutions having different pH (6.5-11) and ionic strength values (0-200 mM) of environmental relevance. Fractionation key parameters such as flow rates, flow programming, and membrane material were optimized for the selected fullerenes. The aggregation of the compounds studied appeared to be indifferent to changes in solution pH, but was affected by changes in the ionic strength. Polyhydroxy-fullerenes were found to be present mostly as 4 nm aggregates in water without added salt, but showed more aggregation at high ionic strength, with an up to 10-fold increase in their mean hydrodynamic radii (200 mM), due to a decrease in the electrostatic repulsion between the nanoparticles. Carboxy-fullerenes showed a much stronger aggregation degree in water (50–100 nm). Their average size and recoveries decreased with the increase in the salt concentration. This behavior can be due to enhanced adsorption of the large particles to the membrane at high ionic strength, because of their higher hydrophobicity and much larger particle sizes compared to polyhydroxy-fullerenes. The method performance was evaluated by calculating the run-to-run precision of the retention time (hydrodynamic radii), and the obtained RSD values were lower than 1 %. MALS measurements showed aggregate sizes that were in good agreement with the AF4 data. A comparison of the scattering radii from the MALS with the hydrodynamic radii obtained from the retention times in AF4 indicated that the aggregate shapes are far from spherical. TEM images of the fullerenes in the dry state also showed branched and irregular clusters.

Keywords: Asymmetrical flow field-flow fractionation; Multi angle light scattering; Fullerene aggregates.

1. Introduction

Fullerenes, the third carbon allotrope discovered by Kroto *et al.* in 1985 [1], are hollow-sphere nanoparticles composed entirely of carbon. Due to their unique physical and chemical properties they find widespread application in diverse fields, such as in photovoltaics [2], cosmetics [3], and biomedicine [4]. Nowadays, fullerenes functionalized with polar groups are produced in higher quantities than native fullerenes due to their increasing number of biomedical applications [5]. For instance, polyhydroxy-fullerenes have attracted attention for their good water solubility and biological compatibility [6], and have been demonstrated to be radical scavengers against superoxide anions and hydroxyl radicals [7,8]. Among these compounds, fullerol ($C_{60}(OH)_{24}$) holds a special place, being investigated for clinical application as drug carrier, tumor inhibitor [9] and mitochondrial protective antioxidant [10]. Moreover, it is being considered as starting material for synthesis of fullerene containing polymers [11] and as coating for solid-phase microextraction [12]. Carboxyl C_{60}-derivatives have potential use for photodynamic therapy [13,14] and as inhibitors of the HIV-1 protease [15].

The anticipated market growth of surface modified fullerenes, in combination with the risk of direct human exposure via several applications, has led to concerns about their potential to cause adverse effects on the environment and human health. However, there is a significant lack of knowledge on fullerene exposure, as well as of data on their inherent properties and toxicity. Fullerenes aggregate in aqueous media leading to the formation of structures with various shapes and sizes. It was recently found that the size and shape of the nanoparticles formed dictate their *in vitro* toxicity [16-18] as well as their mobility, fate, bioavailability and toxicity in the environment [19,20]. However, the lack of adequate methods for their characterization and analysis in environmental samples is currently a bottleneck in this field. Currently, the prediction of the fate and behavior of fullerenes is mostly focused on pristine compounds and is being based on laboratory experiments. A direct comparison of the data is not possible because of variations in the experimental conditions which are not consistent among studies. The data gained from the existing studies in not nearly enough to create a detailed prediction model of the behavior and fate of these nanoparticles in the environment, but represent a good starting point for their risk assessment. Therefore, it is crucial to develop reliable methods for the characterization of fullerene aggregates in terms of size distribution and shape, at variant key environmental parameters (e.g., pH, ionic strength natural organic matter) especially for the water soluble compounds for which there is a lack of studies.

The most commonly used techniques for particle sizing are microscopy, *e.g.,* transmission electron microscopy (TEM) or scanning electron microscopy (SEM), optical spectroscopy (UV-

Vis) and light scattering techniques [21]. Nonetheless, with microscopic methods the integrity of the particles and aggregates is not always guaranteed, and light-scattering methods (*e.g.*, static (MALS) and dynamic light scattering (DLS)) give average size values and are less suited to obtain information on the particle size distributions [22]. Therefore, these methods alone are often not conclusive when applied to nanoparticles and they must be combined with separation techniques for more accurate sizing or aggregation determination [23].

FlFFF is a separation technique introduced by J. Calvin Giddings in the late seventies [24] and has become the most commonly employed mode of FFF. This is a versatile analytical tool for the separation and characterization of macromolecules and particles over a wide size range. Asymmetrical flow-field flow fractionation (AF4), including its hollow fiber format (HF5), have been the completely dominating FlFFF techniques generally used during the last decade [25]. The principles of both AF4 and FlFFF have been reviewed elsewhere [26-29]. Briefly, the fractionation principle is based on applying a perpendicular field (cross-flow) to main parabolic flow in an open flat channel. The retention of sample components of different sizes can be controlled by tuning the cross-flow rates and the separation is based on differences in the diffusion coefficients of eluting particles. The particles with larger diffusion coefficients or smaller sizes diffuse faster to upper layers inside the channel and, therefore, reach to the detector faster than the bigger ones. This is is the most widely used mechanism for analytes smaller than 1 μm referred to as normal-mode separation mechanism [30]. When the particle size exceeds approximately 1 μm, the steric/hyperlayer mode prevails, and the elution order is reversed in that larger particles elute before smaller particles [31,32]. The relation between the retention time and diffusion coefficient helps in calculating hydrodynamic radii using standard AF4 theory [28,29]. Recently, AF4 was reported as a method for the size measurement of some fullerene aggregates [16,33-36]. Because of its versatility, this technique is used in a wide range of research and quality control applications, including nanotechnology, molecular biology and environmental analysis. Moreover, when combined with online light-scattering detection, AF4 is a powerful tool for the determination of the size distribution of particles. For instance, Kato *et al.* [16] studied the size distribution of aqueous C_{60} and C_{70} fullerene in a cell culture medium for *in vitro* toxicity assessment by AF4 coupled to MALS, and reported values of 256 ± 90 nm (C_{60}) and 257 ± 90 nm (C_{70}) for their diameters. Isaacson and Bouchard [33] used AF4 coupled to dynamic light scattering (DLS) for the characterization of C_{60} fullerene aggregates in deionized water and reported hydrodynamic diameters between 80 and 260 nm. Recently, Herrero *et al.* [35] described a method for the fractionation and online identification of C_{60} and two hydrophobic C_{60}-derivatives by coupling AF4 to high resolution mass spectrometry and to MALS. The authors

reported very similar size distribution for the three fullerenes, with particle radii of gyration (r_G) ranging between 20 and 80 nm. Regarding water soluble functionalized fullerenes, there are limited studies on their size distribution and aggregation behavior. AF4 with offline atomic force microscopy (AFM) was proposed for the characterization of $C_{60}(OH)_{24}$ [34] as a function of pH and ionic strength. The authors found that fullerol present aggregate sizes of only few nanometers in size (≈2 nm) at basic pH and low ionic strength. Fullerol aggregate size increased with the salt concentration from 1.8 nm at zero ionic strength up to 6.7 nm at 0.1 M NaCl, but was not affected by the pH of the solutions. These results disagree with a previous study [37] reporting sizes on the order of 100 nm for this compound as found by dynamic light scattering and TEM. This could be due to the different methodology used for the size measurements of the particles since imaging in air induces aggregation due to partial drying of the sample before analysis.

In the present paper we describe the development and optimization of a separation method for the characterization of four surface modified fullerenes (polyhydroxy-and carboxy-derivatives) that find increasing biomedical application, in aqueous solutions by AF4 on-line coupled to UV and MALS detectors. The effect of the fractionation parameters such as carrier liquid composition, membrane material, cross flow and focus flow rate, focusing time and flow programming were evaluated. Additionally, TEM was employed to visualize the morphology and aggregate structures of the compounds studied. This research provides relevant information regarding the effect of the aqueous solution chemistry on the aggregate sizes and shapes of surface modified fullerenes.

2. Experimental Section

2.1 Chemicals and solutions

Fullerol ($C_{60}(OH)_{24}$) was purchased from Materials & Electrochemical Research M.E.R. Corporation (Tucson, Arizona, USA). Polyhydroxy small gap fullerene, hydrated ($C_{120}(OH)_{30}$), (1,2-Methanofullerene C_{60})-61-carboxylic acid ($C_{60}CHCOOH$) and C_{60}-pyrrolidine tris acid (C_{60}-pyrr tris acid) were purchased from Sigma-Aldrich (Steinheim, Germany). The chemical structures and abbreviations of these compounds are given in Figure 1.

Bovine serum albumin (BSA, molecular weight ≈ 66 kDa) was purchased from Sigma-Aldrich (Steinheim, Germany). NaCl and phosphate buffered saline (PBS) were purchased from Merck (Darmstadt, Germany).

Water was purified using an Elix 3 coupled to a Milli-Q system (Millipore, Bedford, MA, USA) and filtered using a 0.22 μm nylon filter integrated into the Milli-Q system.

Stock standard solutions of polyhydroxy-fullerenes (≈1000 mg kg^{-1}) were individually prepared by weight in Milli Q water and stored at 4°C. The aqueous suspensions of both carboxy-fullerenes were obtained following the procedure proposed by Andrievsky et al., [38] with some modifications as follows: first the solid powder was dissolved in tetrahydrofuran (Merck, Darmstadt, Germany), and then an exact volume of Milli Q water was added to the solution to the solution. Next, the solution was sonicated in a high power ultrasonic bath (Transonic Digital S, Elma, 40 kHz, 130 W) (Singen (Hohentwiel), Germany) until the tetrahydrofuran was completely evaporated to obtain stock solutions of approximately 500 mg kg^{-1}. Working solutions of 1 mg/mL (polyhydroxy-fullerenes) and 0.4 mg/mL (carboxy-fullerenes) were prepared weekly by appropriate dilution of the stock standard solution with Milli Q water.

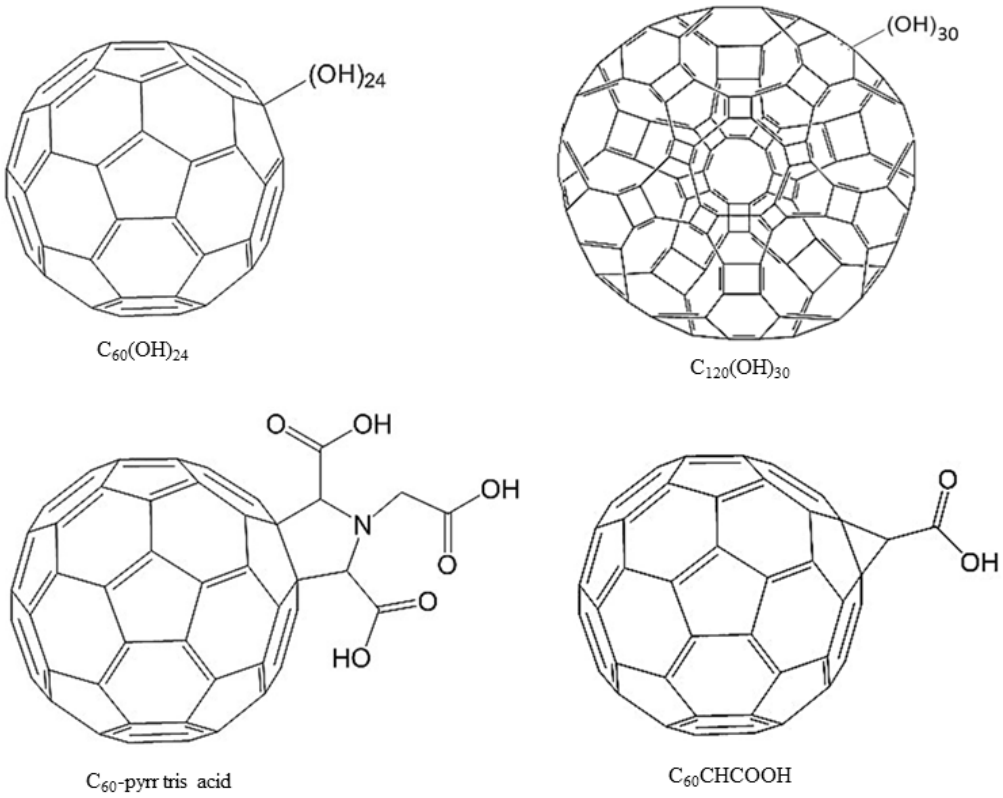

Figure 1. Structure of the surface modified fullerenes studied.

2.2 Instrumentation

The optimization of the fractionation was carried out with an Eclipse Dualtec AF4 separation system (Wyatt Technology Europe GmbH, Dernbach, Germany) equipped with a programmable pump (Isocratic 1100, Agilent Technologies, Waldbronn, Germany), an Agilent

1100 series degasser and an Agilent 1200 series auto sampler/injector. A mini-channel (11cm in length, 22 mm in width at the injection point and 3 mm close to the end) was equipped with a 480 μm spacer of trapezoidal shape and Millipore regenerated cellulose (RC) membrane of 10 kDa nominal molar mass cut-off (Superon GmbH, Dernbach, Germany). Additional experiments were conducted with Millipore 3 kDa RC and 3 and 10 kDa polyethersulfone (PES) membranes (Superon GmbH, Dernbach, Germany). Online detection was performed with a UV detector (Applied Biosystems, Foster City, California, USA). For the measurement of the r_G radii by MALS, a DAWN-DSP MALS detector (Wyatt Technology Europe GmbH, Dernbach, Germany) coupled in series to the UV detector was used. ASTRA software (Wyatt Technology) version 4.9 was used to process the data.

For TEM measurements a Jeol 1010 TEM instrument (Jeol, Japan) was used, applying an accelerating voltage of 80 kV.

2.3 Procedures:

The calibration of FFF channel was performed by injecting 1 mg/ mL of bovine serum albumin (BSA) and using as carrier solution phosphate buffer saline (PBS) of 0.15 M at pH 7.4. From the retention data, determined from the UV signal at 280 nm, the exact channel thickness (*w*) was calculated according to the procedure described by Litzén *et al.* [39].

The fractionations were performed in 3 steps. First, 1 μL of samples were injected in Milli Q water with an injection flow of 0.1 mL/min. Then relaxation and focusing was carried out during a specific time (3 min for the carboxy-fullerenes and 10 min for polyhydroxy-fullerenes) at a cross flow rate of 2 mL/min. Time-delayed exponential (TDE) mode was used for the elution step with a delay/decay time of 3 min (carboxy-fullerenes) and 7 min (polyhydroxy-fullerenes), an initial cross flow of 2 mL/min and a channel flow of 1 mL/min.

The eluted samples were monitored by the UV detector at 254 nm and the MALS detector. The signals from the MALS detector were measured simultaneously at 12 different angles (channels no. 6-17) for the calculation of the radii of gyration. Angle-dependent measurements revealed a Berry model to be appropriate for evaluation of the measured values. For the normalization of the MALS channels, and to determine the inter-detector delay, a standard solution of BSA was injected. In the normalization procedure, the Stokes radius of BSA was assumed to be 3.5 nm. The experiments were conducted in a temperature controlled room (23 ± 2 °C).

Carrier solutions with different ionic strengths (0 to 200 mM NaCl) and pH values (6.5-11) were tested to study the aggregation behavior of the fullerenes. Each carrier solution was

filtered through a 0.45 μm nylon membrane filter before use.

Diffusion coefficients and hydrodynamic radii were calculated from the observed retention times using Equation (1) and (2).

$$t_R = \frac{w^2}{6D} \ln\left(1 + \frac{F_{cr}}{F_{ch}}\right) \qquad (1)$$

where w is the height of the channel, F_{cr} and F_{ch} are the flow rates of the cross flow and channel flow, respectively, and D is the diffusion coefficient of the analyte particle.

The (translational) diffusion coefficient can be related to the hard-sphere equivalent size of the particle via the Stokes Einstein equation for spherical particles:

$$D = \frac{kT}{6\pi\eta r_H} \qquad (2)$$

where k is the Boltzmann constant, T the absolute temperature, η the viscosity of the solvent and r_H the hydrodynamic radius of the particle,

The recovery from an AF4 run, *i.*e., the ratio between the recovered mass after analysis and injected mass, was expressed as:

$$R(\%) = \frac{A}{A_0} \times 100 \qquad (3)$$

where A and A_0 are the peak areas obtained with and without applying cross-flow, respectively. Recovery was calculated from both UV and MALS signals.

For TEM measurements, one drop of the aqueous fullerene solutions was placed on a TEM grid (carbon-coated copper grid 200 mesh (All Carbon)) and stained with a drop of uranyl formiate (1 % aqueous solution). After air drying of the grid (2 h), TEM images were taken.

3. Results and Discussion

3.1 AF4 separations

The fractionation of fullerenes was optimized in terms of flow rates, flow programming, and focusing procedure. First, methods with a constant cross flow were conducted to determine flow rates that would ensure reasonable sample retention and thus the fractionation of the fullerenes studied. With a 1 mL/min channel flow, cross flow rates from 0.3 to 2.5 mL/min were tested. For the polyhydroxy-fullerenes, poor separation from the void peak at cross flow rates between 0.3 and 1.5 mL/min was observed, while with cross flows of 2 mL/min or higher, part

of the fullerenes eluted only when the cross flow was stopped. Regarding the carboxy-fullerenes, their fractions could not be separated within a reasonable run time with any of the isocratic cross flow conditions tested. Therefore, flow programming was evaluated. Applying a cross flow program, with a decrease of the cross flow during the run, is a valuable tool in the AF4 separation of polydisperse samples and a simple way to expand the size window of AF4 [40]. TDE programming was used and the effect of the flow conditions (initial cross flow rate, delay/decay times) was established. Poor separation from the void peak was obtained for polyhydroxy-fullerenes in the TDE mode with initial cross flow values of 1.5 mL/min or lower, as previously observed by using the constant cross flow elution mode. Hence, a TDE program with an initial cross flow and a focus flow of 2 mL/min was used for further experiments. The best results (i.e., fractionation of the particles in a reasonable run time, and a good separation from the void peak) were obtained with a delay/decay time of 7 min (see Figure 2). The hydrodynamic radii of the particles at the maximum of the peak height (peak-top values) were estimated from the retention time of the peaks using standard AF4 theory and the Stokes formula (Eq. 2).

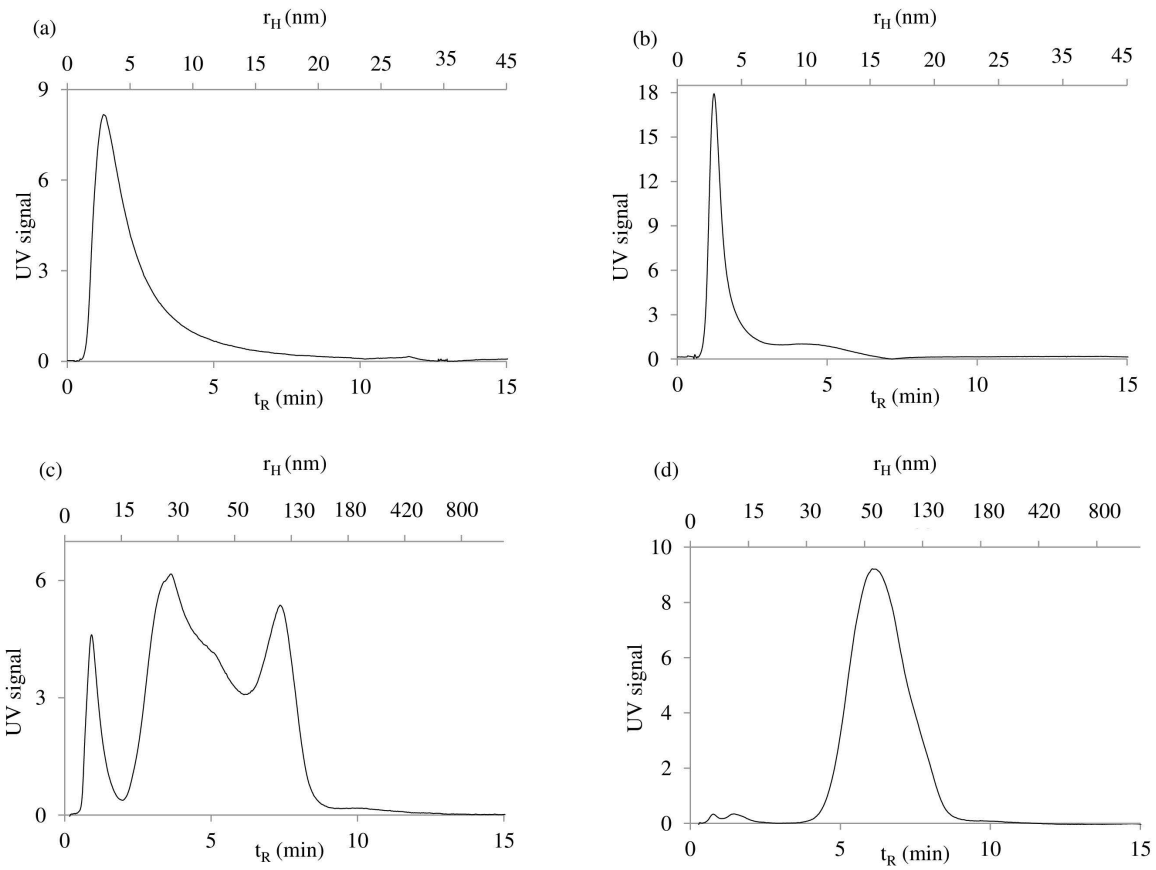

Figure 2. AF4-UV fractograms of the surface modified fullerenes. TDE flow programming with a delay/decay time of 7 min (a and b) or 3 min (c and d). For experimental conditions see text. (a) $C_{60}(OH)_{24}$; (b) $C_{120}(OH)_{30}$; (c) C_{60}-pyrr tris acid; (d) $C_{60}CHCOOH$.

For $C_{60}(OH)_{24}$ tailing peaks were observed in the fractograms obtained using UV detection, with r_H values between 3 and 30 nm and an average r_H at the maximum of the peak of approx. 4 nm (see Figure 2). The peak tailing may indicate the presence of unresolved higher order aggregates. The fractogram of $C_{120}(OH)_{30}$ showed a major peak corresponding to small particles with an average r_H of 4 nm and a second peak at 5 min corresponding to particles with higher degree of aggregation, with an average r_H of 12 nm. However, the retention time and the apparent size of the fullerenes in the first peak depended on the initial cross flow rate. As can be seen in Figure 3, the calculated radii of $C_{60}(OH)_{24}$ and $C_{120}(OH)_{30}$ increased from 4 nm, for cross flow values of 1.5 and 2 mL/min, to 10 nm for 2.5 mL/min. Similar behavior was observed when increasing the focus flow rate above 2 mL/min, or when increasing the focusing time. The focusing time was varied from 3 to 15 min while the other parameters (flow rates, amount of sample) were kept the same. For a good separation from the void peak for the polyhydroxy-fullerenes a minimum 10 min focusing time was required, while the r_H value found remained constant (≈ 4 nm). However, when using a 15 min focusing time, the r_H value increased to 20 nm. The observed increase in the size of the particles with the cross flow and focus flow could have its origin in particle-particle interactions, as during focusing the particles are strongly concentrated near the wall, and particle-particle interactions may be more prominent during this step, leading to more aggregation. Although these fullerenes display elevated water solubility due to the high number of hydroxyl groups covalently bound to the C_{60} structure, they aggregate in water since the spheres tend to stick together in micelle-like aggregates [41].

For the carboxy-fullerenes the optimal fractionation conditions were a 3 min focusing time and a TDE program with an initial cross flow of 2 mL/min and a delay/decay time of 3 min. The C_{60}-pyrr tris acid fullerene eluted in at least three discernable fractions, with radii in the order of approx. 10, 30 and 95 nm, respectively (see Figure 2). For $C_{60}CHCOOH$ a small peak close to the void time was observed in the fractograms corresponding to small particles with average r_H values of 10 nm and a major peak at 7 min corresponding to larger aggregates with average r_H of 55 nm. The effect of the flow conditions (cross flow, focus flow) and focusing time on the carboxy-fullerenes was negligible, and their average radii were not affected by these experimental parameters. The effect of the cross flow on the observed r_H values of these particles is shown in Figure 3. For C_{60}-pyrr tris acid, the plotted r_H values correspond to the largest aggregates, the third peak in the fractogram (see Figure 2). Apparently, induced aggregation by the fractionation method itself does not play a major role for carboxy-fullerenes.

Table 1. Recoveries of surface modified fullerenes from the AF4 channel using different membrane materials.

Membrane, cutoff	Recovery± S.D. (%)			
	$C_{60}(OH)_{24}$	$C_{120}(OH)_{30}$	C_{60}-pyrr tris acid	C_{60}CHCOOH
RC, 10 kDa	85 ± 4.1	87 ± 3.5	83 ± 5.0	79 ± 3.6
PES, 10 kDa	88 ± 3.0	85 ± 4.5	76 ± 5.7	73 ± 4.0
RC, 3 kDa	83 ± 3.7	85 ± 4.0	79 ± 3.3	76 ± 4.8
PES, 3 kDa	83 ± 5.3	87 ± 2.4	75 ± 3.1	70 ± 6.8

Membranes with different chemistries, regenerate cellulose (RC) and polyethersulphone (PES), with a molar mass cut-off of 3 and 10 kDa, were evaluated for the fractionation of the fullerenes. The relative recoveries obtained using each membrane were calculated from the total peak areas obtained with and without applying a cross flow. As can be seen in Table 1, similar relative recoveries (values between 83 and 88 %) were obtained for the polyhydroxy-fullerenes with all membranes. Slightly lower values were obtained for the carboxyl-fullerenes when using PES membranes compared to RC membranes. PES membranes are relatively hydrophobic (as measured by the water droplet contact angle) and they have a high negative surface charge (measured by the zeta potential), while RC membranes are more hydrophilic and have a lower negative surface charge [42,43].

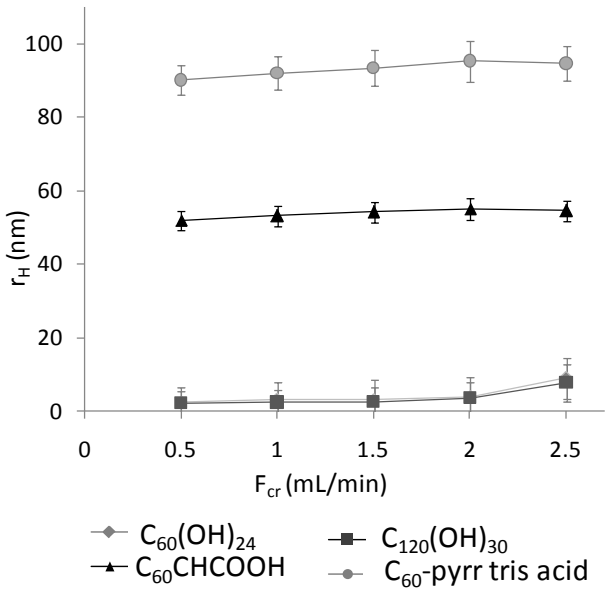

Figure 3. Influence of the cross flow rate on the apparent size of fullerene aggregates.

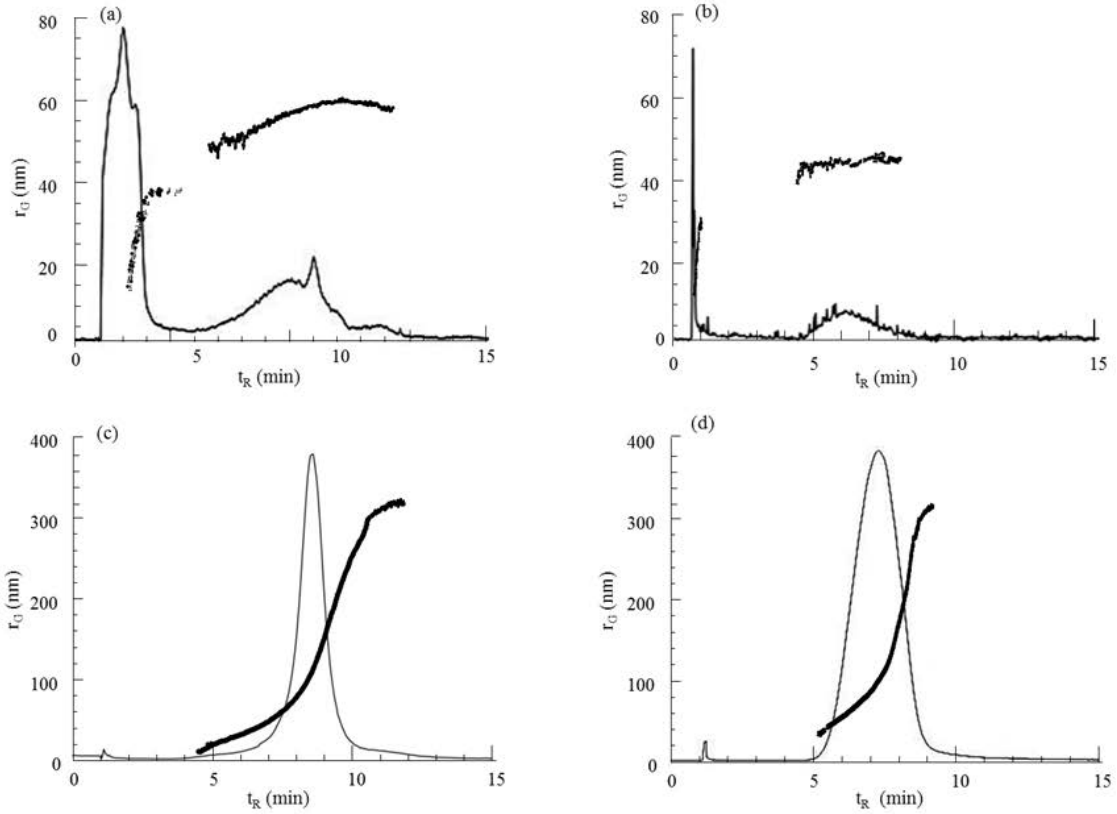

Figure 4. AF4-MALS fractograms of surface modified fullerenes. The line shows the 90° scattering intensity, the marks the values of the r_G. For experimental conditions see text. (a) $C_{60}(OH)_{24}$; (b) $C_{120}(OH)_{30}$; (c) C_{60}-pyrr tris acid; (d) $C_{60}CHCOOH$.

It was previously reported that hydrophobic aromatic compounds (*e.g.,* polycyclic aromatic hydrocarbons, humic substances, aromatic pesticides) adsorb strongly on PES membranes and that the adsorption properties depend on both the hydrophobicity and molecular shape of the solutes [43-47]. For instance, Thang *et al.* obtained a higher recovery of isolated humic acid with a 5 kDa RC membrane than with a 2 kDa PES membrane, and found the losses to be due to adsorption of humic substances to the PES membrane [46].

The method reproducibility was tested by calculating the run-to-run precision. For this purpose, a total of five replicate determinations for each compound at concentration levels of 1 mg/mL were carried out on the same day (n=5). The calculated relative standard deviation (% RSD) values of the retention time at the maximum of the peak height and of the r_H were between 0.3 and 0.9 %.

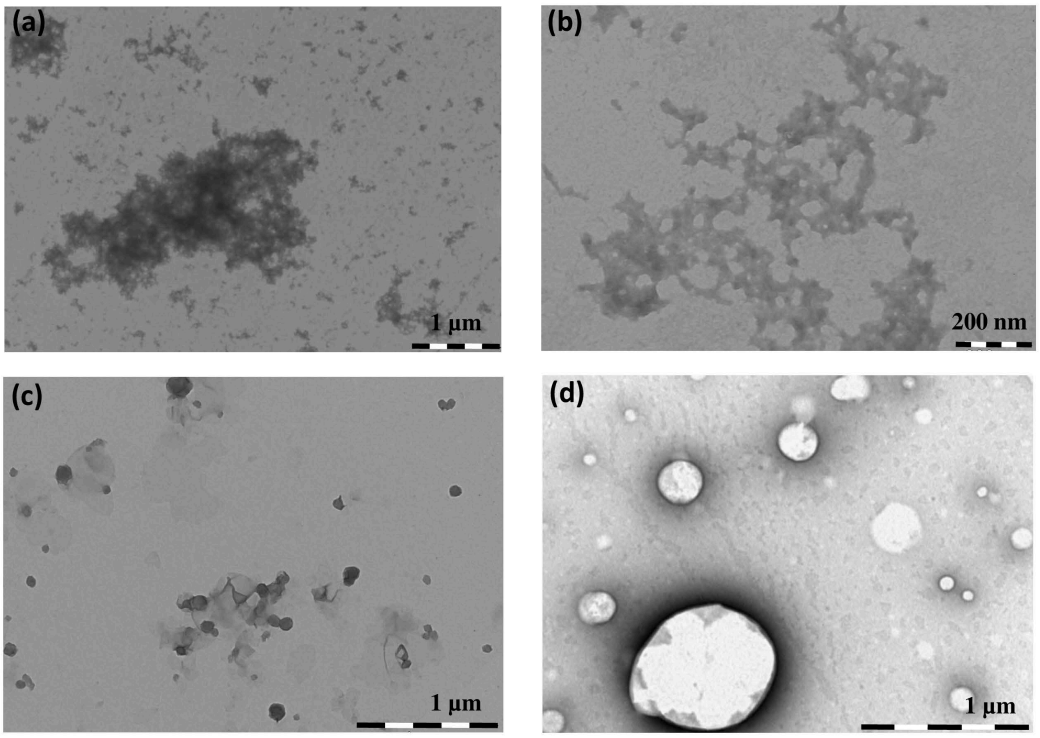

Figure 5. TEM pictures of fullerene aggregates. (a) $C_{60}(OH)_{24}$; (b) $C_{120}(OH)_{30}$; (c) C_{60}-pyrr tris acid; (d) $C_{60}CHCOOH$.

3.2. AF4-MALS and TEM measurements

AF4-MALS hyphenation can offer a further insight into particle properties and can provide information on the particle size distributions as well as of the particle shape. MALS measurements can provide the radius of gyration or rms radius of particles (r_G). The r_G is defined as the mass weighted average distance from the center of mass of a molecule to each mass element in the molecule and incorporates structural and shape properties of the particles. The AF4 retention time, on the other hand, provides the hydrodynamic radius r_H of a particle, which is related to its friction factor in solution. By combining the retention data from AF4 with the scattering data from the MALS detector information on the shape or architecture of particles can be obtained, by calculating a shape factor ϱ, which is defined as the ratio between the scattering radii and the hydrodynamic radii. This shape factor has a value of 0.775 for spherical particles and increases as particles deviate from the spherical shape ($\varrho \approx 0.8$ for coils and $\varrho \approx 1.7$ for rods) [49,50].

In the present work, the AF4 instrument was coupled to MALS detection and used for the determination of the size distribution of the surface modified fullerenes and to study their shapes in aqueous solutions. Figure 4 shows the AF4-MALS fractograms obtained and the size distributions of the fullerenes studied. The 90^0 scattering signal shown in the figure was

monitored for quantification. It should be noted that the scattering intensity of particles increases strongly with their size, so that the presence of larger aggregates is much emphasized in the fractograms with the light scattering signal compared to the UV signals shown in Figure 2. As can be seen in the plot, the fractionation of polyhydroxy-fullerenes revealed two resolved peaks, indicating the presence of fractions with different degree of aggregation. For $C_{60}(OH)_{24}$, the first peak close to the void time, corresponds to small aggregates with r_G of 10-40 nm and the second peak to larger aggregates with r_G of 50-60 nm. $C_{120}(OH)_{30}$ showed slightly smaller r_G with values between 10 and 30 nm (first peak) and around 40 nm (second peak). The separation of these two entities was not clear in the AF4-UV fractograms except for the peak tailing observed (Figure 2). The AF4-MALS fractograms obtained for the carboxy-fullerenes revealed in both cases a small peak corresponding to small particles with sizes lower than 20 nm and one intense and broad peak corresponding to aggregates presenting r_G ranging from 15 to 310 nm (C_{60}-pyrr tris acid) and from 20 to 310 nm (C_{60}CHCOOH), respectively.

To obtain information regarding the shapes of the aggregates, the peak-top radius values obtained by MALS measurements were correlated with the r_H values calculated for each peak in the fractograms at the maximum of the peak height. It can be noticed that the r_G values obtained for polyhydroxy-fullerenes are systematically higher than their r_H values. This could indicate that the aggregate shape of these fullerenes is far from spherical. For the carboxy-fullerenes this was not obvious, as the fractograms obtained by AF4-UV revealed several distinguishable peaks corresponding to particles of different aggregate sizes. Additionally, the morphology and aggregate structures of the surface modified fullerenes in water was studied by TEM and the micrographs obtained are presented in Figure 5. The images show clear differences between their aggregate structure and particle shape. In agreement with the results obtained by AF4-MALS, the images show complex branched aggregates with polycrystalline snow flake-like structures for the polyhydroxy-fullerenes which were so strongly aggregated that it was difficult to obtain an average particle size. Mostly spherical clusters and some irregular shaped structures were observed for the carboxy-fullerenes. Moreover, the TEM images confirmed the polydispersity and the wide size distribution of the aggregates formed by the carboxy-fullerenes as previously observed by AF4. The micrographs revealed particles with estimated sizes between 20 and 160 nm and between 20 and 410 nm, for C_{60}-pyrr tris acid and C_{60}CHCOOH, respectively. The somewhat higher size values obtained by TEM can be due to the fact that the grids must be dried prior to imaging, and that the particles are likely to aggregate further to some degree. Nevertheless, the TEM images do provide a basis for comparison and for elucidating particle shapes and structure.

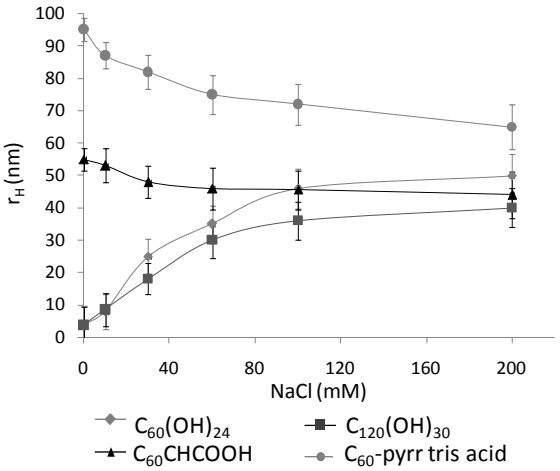

Figure 6. Effect of the salt concentration of the carrier solution on the aggregate sizes as measured by AF4-UV.

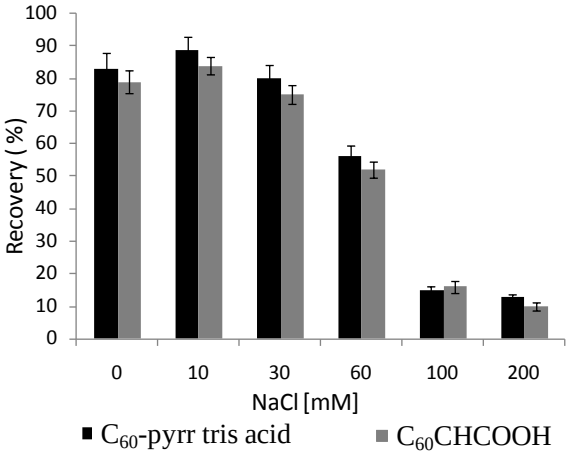

Figure 8. Effect of the salt concentration of the carrier solution on the recovery of carboxy-fullerenes.

3.3. Influence of pH and ionic strength

The mobility and toxicity of fullerenes released to the environment will depend on the colloidal stability of the aggregates formed. The aggregation of these particles into larger clusters will reduce their ability to be transported or to come into contact with aquatic organisms. Knowledge of the aggregation behavior of fullerenes as a function pH and ionic strength will allow gaining an insight into their potential behavior when released in the environment. It has been reported that high ionic strength and low pH values lead to an increase in the aggregate size of C_{60} fullerene [50,51]. Regarding surface modified fullerenes, previous studies have shown that fullerol aggregation is also promoted by an increase in the ionic strength and that it is not affected by the pH variation [34,51]. In this work, the behavior of the fullerenes studied was evaluated at different ionic strength (0-200 mM) and pH values (6.5-11). These values were chosen as they include the normal range of the pH of surface and sea waters (6.5-8.5) and their usual salt concentration (1-500 mM). No significant changes in the size of the particles were observed when varying the pH between 6.5 and 11. Apparently, within this pH range fullerene clusters maintain a substantial charge, which is in agreement with previous reports [34,37]. In Figure 6 the influence of the ionic strength on the average hydrodynamic radii of the particles is shown. The hydrodynamic radius of polyhydroxy-fullerene aggregates increases significantly with the ionic strength. The mean radius of $C_{120}(OH)_{30}$ and $C_{60}(OH)_{24}$ increased from approximately 4 nm at zero ionic strength up to 40 nm and 50 nm, respectively, in 200 mM salt concentration.

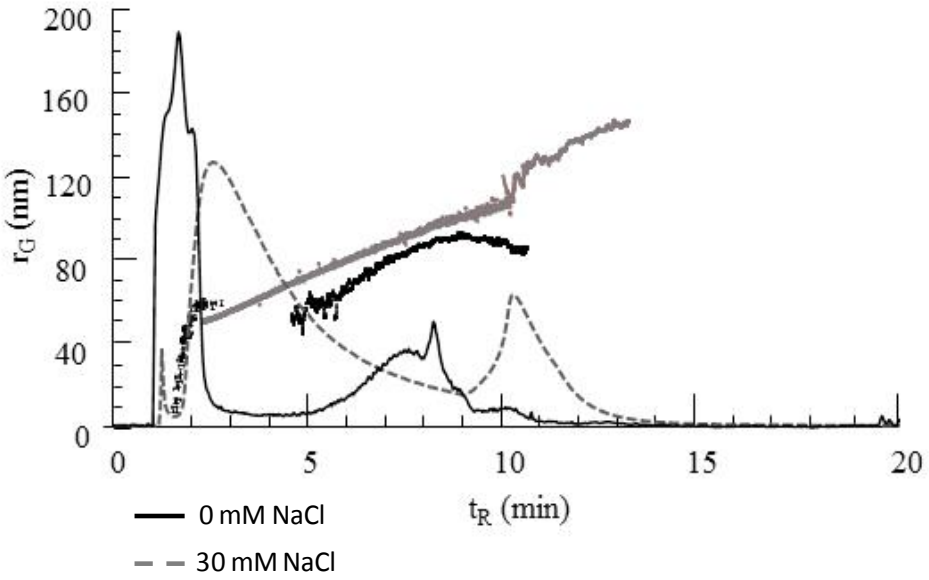

Figure 7. Effect of the salt concentration of the carrier solution on the aggregate sizes of $C_{60}(OH)_{24}$ as measured by AF4-MALS.

At the same time, an increase in their r_G with the ionic strength was observed in AF4-MALS measurements. As an example, Figure 7 shows the fractograms and size distribution obtained by MALS for $C_{60}(OH)_{24}$ at 0 and 30 mM salt concentrations. The change in the elution profile (retention time shift) with higher salt concentration is accompanied by an increase in r_G, up to 160 nm in a solution containing 30 mM NaCl. This behavior is in agreement with the findings in previous studies [34,37] and with the Derjaguin–Landau–Verwey–Overbeek (DLVO) theory which is commonly used to describe interactions of charged surfaces across liquids [52]. The increase in the ionic strength showed a different effect for the carboxy-fullerenes. A slight decrease in the average hydrodynamic radii of both C_{60}CHCOOH and C_{60}-pyrr tris acid with an increase in NaCl concentration was observed, from 55 and 95 nm, respectively, at zero ionic strength to 45 and 65 nm, respectively, in 200 mM NaCl (Figure 6). In agreement with these results, their r_G as obtained by MALS also slightly decreased. Moreover, the increase in the ionic strength of the solution caused a significant decrease in the peak areas of the carboxy-fullerenes. Figure 8 shows the relative recoveries of these compounds from the channel at different salt concentrations. A possible explanation for the low recovery of the carboxy-fullerenes at high salt concentration (less than 20 % for 200 mM NaCl) could be an enhanced adsorption of these particles to the membrane. Due to their higher hydrophobicity and larger size, membrane adsorption of carboxy fullerenes is more likely compared to the polydroxy-fullerenes. This assumption was further confirmed by the appearance of a brown spot in the focusing area of the AF4 membrane after repeated injections. Particle adsorption on the accumulation wall in

AF4 is governed by the attractive van der Waals forces and the electrostatic repulsion between particles and the membrane surface, which will decrease with increasing salt concentration [53-55]. In other studies it has been reported that the increase in the salt content reduces the zeta potential of RC membrane which lowers the electrostatic forces between nanoparticles and the RC membrane, leading to increased adsorption [56,57].

4. Conclusions:

The chemical derivatization of fullerenes with different polar functional groups has an effect on the agglomeration state of the particles in aqueous solutions and therefore could affect their environmental behavior. In this study, AF4-MALS was used to determine the aggregate sizes of surface modified fullerenes. With a 10 kDa cut-off RC membrane in the AF4 channel good relative recovery values (79-85 %) were obtained for the fullerenes studied. The application of TDE cross flow programming enabled the separation of aggregates with sizes (hydrodynamic radii) from approximately 4 nm to well over 100 nm. It was found that polyhydroxy-fullerenes are present in pure water as small aggregates with hydrodynamic radii in the order of 4–15 nm. Only a small fraction of these fullerenes is present in larger agglomerates. Experiments with high cross flows and/or long focusing times indicated that the aggregation as found experimentally may be partly induced by the focusing process, in which the fullerenes are strongly concentrated. The pH of the solution did not affect their aggregation. On the other hand, the ionic strength of the solution was found to be an important factor. In the presence of sodium chloride (30–200 mM) a much larger fraction of the polyhydroxy-fullerenes was found in aggregates with radii in the order of 40–60 nm. The carboxy-fullerenes studied showed a much stronger tendency to aggregate than the polyhydroxy-fullerenes. Even in water without added salt, their aggregation radius was around 55 nm and 95 nm. With the addition of salt to the solution a small decrease of their average aggregate size was found. However, at higher ionic strength the recovery of the carboxy-fullerenes from the AF4 channel was strongly decreased. This can possibly be attributed to an increased adsorption of the (fairly hydrophobic) fullerenes to the membrane material. When this adsorption would be size-dependent, the observed decrease of the average aggregate size could be related to this. Data obtained from the MALS detector coupled on-line to the AF4 instrument largely confirmed the aggregate size distributions as calculated from the fractograms. The shape factors for the aggregates, obtained by comparing the scattering radii from the MALS data with the hydrodynamic radii from the elution times, indicate that the aggregates of polyhydroxy-fullerenes are not spherical but strongly branched. TEM measurements confirmed this observation.

The methodology developed in this study can guide future work for the characterization of fullerenes, to study their aggregation behavior in aqueous media and hence to improve the understanding of the fate of these particles in the environment.

Acknowledgments

The authors gratefully acknowledge for the financial support received from the Spanish Ministry of Economy and Competitiveness under the project CTQ2012-30836, and from the Agency for Administration of University and Research Grants (Generalitat de Catalunya, Spain) under the project 2014 SGR-539. Alina Astefanei acknowledges the Spanish Ministry of Economy and Competitiveness for a Ph.D. grant (FPI-MICINN) which enabled her to carry out this research as a visiting scientist at the University of Amsterdam. The authors also want to thank the Joint Research Program of the Dutch Water Utilities (BTO); NanoNextNL, a micro- and nanotechnology consortium of the Government of The Netherlands and 130 partners. We also thank Carmen Lopez and Nieves Hernandez (CCiTUB, University of Barcelona) for help with the TEM analysis.

References:

[1] H.W. Kroto, J.R. Heath, S.C. O'Brien, R.F. Curl, R.E. Smalley, C60: buckminsterfullerene, Nature 318 (1985) 162-163.

[2] D. Kronholm, J.C. Hummelen, Fullerene-based n-type semiconductors in organic electronics, Mater. Matters 2 (2007) 16-19.

[3] L. Xiao, H. Takada, K. Maeda, M. Haramoto, N. Miwa, Antioxidant effects of water-soluble fullerene derivatives against ultraviolet ray or peroxylipid through their action of scavenging the reactive oxygen species in human skin keratinocytes, Biomed. Pharmacother. 59 (2005) 351-358.

[4] N. Tagmatarchis, H. Shinohara, Fullerenes in medicinal chemistry and their biological applications, Mini-Rev. Med. Chem. 1 (2001) 339-348.

[5] R. Partha, J.L. Conyers, Biomedical applications of functionalized fullerene-based nanomaterials, Int. J. Nanomed. 4 (2009) 261-275.

[6] J. Li, A. Takeuchi, M. Ozawa, X. Li, K. Saigo, K. Kitazawa, C60 fullerol formation catalyzed by quaternary ammonium hydroxides, J. Chem. Soc., Chem. Commun. (1993) 1784-1785.

[7] L.L. Dugan, J.K. Gabrielsen, S.P. Yu, T.S. Lin, D.W. Choi, Buckminsterfullerenol free radical scavengers reduce excitotoxic and apoptotic death of cultured cortical neurons, Neurobiol. Dis. 3 (1996) 129-135.

[8] D.M. Guldi, K.D. Asmus, Activity of water-soluble fullerenes towards Â·OH-radicals and molecular oxygen, Radiat. Phys. Chem. 56 (1999) 449-456.

[9] M. Prato, [60]Fullerene chemistry for materials science applications, J. Mater. Chem. 7 (1997)

1097-1109.

[10] X. Cai, H. Jia, Z. Liu, B. Hou, C. Luo, Z. Feng, W. Li, J. Liu, Polyhydroxylated fullerene derivative C60(OH)24 prevents mitochondrial dysfunction and oxidative damage in an MPP+-induced cellular model of Parkinson's disease, Journal of Neuroscience Research 86 (2008) 3622-3634.

[11] L. Dai, A.W.H. Mau, A facile route to fullerol-containing polymers, Synthetic Metals 86 (1997) 2277-2278.

[12] J. Yu, L. Dong, C. Wu, L. Wu, J. Xing, Hydroxyfullerene as a novel coating for solid-phase microextraction fiber with sol–gel technology, Journal of Chromatography A 978 (2002) 37-48.

[13] B. Sitharaman, S. Asokan, I. Rusakova, M.S. Wong, L.J. Wilson, Nanoscale Aggregation Properties of Neuroprotective Carboxyfullerene (C3) in Aqueous Solution, Nano Lett. 4 (2004) 1759-1762.

[14] H. Tokuyama, S. Yamago, E. Nakamura, T. Shiraki, Y. Sugiura, Photoinduced biochemical activity of fullerene carboxylic acid, J. Am. Chem. Soc. 115 (1993) 7918-7919.

[15] S.H. Friedman, D.L. DeCamp, R.P. Sijbesma, G. Srdanov, F. Wudl, G.L. Kenyon, Inhibition of the HIV-1 protease by fullerene derivatives: model building studies and experimental verification, J. Am. Chem. Soc. 115 (1993) 6506-6509.

[16] H. Kato, N. Shinohara, A. Nakamura, M. Horie, K. Fujita, K. Takahashi, H. Iwahashi, S. Endoh, S. Kinugasa, Characterization of fullerene colloidal suspension in a cell culture medium for in vitro toxicity assessment, Mol. BioSyst. 6 (2010) 1238-1246.

[17] K.W. Powers, M. Palazuelos, B.M. Moudgil, S.M. Roberts, Characterization of the size, shape, and state of dispersion of nanoparticles for toxicological studies, Nanotoxicoloxy 1 (2007) 42-51.

[18] D.Y. Lyon, L.K. Adams, J.C. Falkner, P.J.J. Alvarez, Antibacterial activity of fullerene water suspensions: Effects of preparation method and particle size, Environ. Sci. Technol. 40 (2006) 4360-4366.

[19] R.D. Handy, R. Owen, E. Valsami-Jones, The ecotoxicology of nanoparticles and nanomaterials: current status, knowledge gaps, challenges, and future needs, Ecotoxicology 17 (2008) 315-325.

[20] S.J. Klaine, P.J.J. Alvarez, G.E. Batley, T.F. Fernandes, R.D. Handy, D.Y. Lyon, S. Mahendra, M.J. McLaughlin, J.R. Lead, Nanomaterials in the environment: behavior, fate, bioavailability, and effects, Environ. Toxicol. Chem. 27 (2008) 1825-1851.

[21] C.F. Jones, D.W. Grainger, In vitro assessments of nanomaterial toxicity, Adv. Drug Delivery Rev. 61 (2009) 438-456.

[22] J. Demeester, S.S. De Smedt, N.N. Sanders, J.Haustraete, Light scattering, in: W. Jiskoot, D.J. Crommelin (Eds.), Methods for structural analysis of protein pharmaceuticals, AAPS Press, Arlington, 2005, pp. 245-275

[23] S.M. Brar, M. Verma, Measurement of nanoparticles by light-scattering techniques, TrAC 30 (2011) doi:10.1016/j.trac.2010.08.008-

[24] J.C. Giddings, F.J. Yang, M.N. Mayers, Theoretical and experimental characterization of flow field-flow fractionation, Anal. Chem. 48 (1976) 1126 1132.

[25] K.G. Wahlund, Flow field-flow fractionation: Critical overview, J. Chromatogr. A 1287 (2013) 97-112.

[26] K.G. Wahlund, J.C. Giddings, Properties of an asymmetrical flow field-flow fractionation channel having one permeable wall, Anal. Chem. 59 (1987) 1332-1339.

[27] M. E. Schimpf, C.K. Caldwell, J.C. Giddings, Field Flow Fractionation Handbook, John Wiley & Sons, New York, 2000

[28] K.G. Wahlund, Improved terminology for experimental field-flow fractionation, Anal. Bioanal. Chem. 406 (2014) 1579-1583.

[29] M. Baalousha, B. Stolpe, J.R. Lead, Flow field-flow fractionation for the analysis and characterization of natural colloids and manufactured nanoparticles in environmental systems: a critical review., J. Chromatogr. A 1218 (2011) 4078-4103.

[30] C.J. Giddings, Field-flow fractionation: analysis of macromolecular, colloidal, and particulate materials, Science 260 (1993) 1456-1466.

[31] C.J. Giddings, M.N. Myres, Steric field-flow fractionation: a new method for separating 1-100 um particles, Separat. Sci. Technol. 13 (1978) 637-645.

[32] M.N. Myres, C.J. Giddings, Properties of the transition from normal to steric field-flow fractionation, Anal. Chem. 54 (1982) 2284-2289.

[33] C.W. Isaacson, D. Bouchard, Asymmetric flow field flow fractionation of aqueous C60 nanoparticles with size determination by dynamic light scattering and quantification by liquid chromatography atmospheric pressure photo-ionization mass spectrometry, J. Chromatogr. , A 1217 (2010) 1506-1512.

[34] S. Assemi, S. Tadjiki, B.C. Donose, A.V. Nguyen, J.D. Miller, Aggregation of Fullerol C60(OH)24 Nanoparticles as Revealed Using Flow Field-Flow Fractionation and Atomic Force Microscopy, Langmuir 26 (2010) 16063-16070.

[35] P. Herrero, P.S. Baeuerlein, E. Emke, E. Pocurull, P. de Voogt, Asymmetrical flow field-flow fractionation hyphenated to Orbitrap high resolution mass spectrometry for the determination of (functionalised) aqueous fullerene aggregates, J. Chromatogr. A 1356 (2014) 277-282.

[36] P. Herrero, P.S. Baeuerlein, E. Emke, R.M. Marcé, P. de Voogt, Size and concentration determination of (functionalised) fullerenes in surface and sewage water matrices using field flow fractionation coupled to an online accurate mass spectrometer: Method development and validation, Anal. Chim. Acta 851 (2015) 77-84.

[37] J.A. Brant, J. Labille, C.O. Robichaud, M. Wiesner, Fullerol cluster formation in aqueous solutions: Implications for environmental release, J. Colloid Interface Sci. 314 (2007) 281-288.

[38] G.V. Andrievsky, M.V. Kosevich, O.M. Vovk, V.S. Shelkovsky, L.A. Vashchenko, On the production of an aqueous colloidal solution of fullerenes, J. Chem. Soc. , Chem. Commun. (1995) 1281-1282.

[39] A. Litzén, Separation Speed, Retention, and Dispersion in Asymmetrical Flow Field-Flow Fractionation as Functions of Channel, Dimensions and Flow rates, Anal. Chem. 65 (1993) 461-470.

[40] K.G. Wahlund, H.S. Winegarner, K.D. Caldwell, J.C. Giddings, Improved flow field-flow fractionation system applied to water-soluble polymers: programming, outlet stream splitting, and flow optimization, Anal. Chem. 58 (1986) 573-578.

[41] V. Georgakilas, F. Pellarini, M. Prato, D.M. Guldi, M. Melle-Franco, F. Zerbetto, Supramolecular

self-assembled fullerene nanostructures, Proc. Natl. Acad. Sci. U. S. A. 99 (2002) 5075-5080.

[42] J. Cho, G. Amy, J. Pellegrino, Membrane filtration of natural organic matter: initial comparison of rejection and flux decline characteristics with ultrafiltration and nanofiltration membranes, Water Res. 33 (1999) 2517-2526.

[43] J. Cho, G. Amy, J. Pellegrino, Membrane filtration of natural organic matter: factors and mechanisms affecting rejection and flux decline with charged ultrafiltration (UF) membrane, J. Membrane Sci. 164 (2000) 89-110.

[44] R.L. Hartmann, R.S.K. Williams, Flow field-flow fractionation as an analytical technique to rapidly quantitate membrane fouling, J. Membrane Sci. 209 (2002) 93-106.

[45] Y. Kiso, Y. Sugiura, T. Kitao, K. Nishimura, Effects of hydrophobicity and molecular size on rejection of aromatic pesticides with nanofiltration membranes, Journal of Membrane Science 192 (2001) 1-10.

[46] M.N. Thang, H. Geckeisa, J.I. Kim, H.P. Beck, Application of the flow field flow fractionation (FFFF) to the characterization of aquatic humic colloids: evaluation and optimization of the method, Colloids and Surfaces A: Physicochemical and Engineering Aspects 181 (2001) 289-301.

[47] J.F. Blanco, J. Sublet, Q.T. Nguyen, P. Schaetzel, Formation and morphology studies of different polysulfone-based membranes made by wet phase inversion process, Journal of Membrane Science 283 (2006) 27-37.

[48] M. Baalousha, M. Motelica-Heino, P. Le Coustumera, Conformation and size of humic substances: Effects of major cation concentration and type, pH, salinity, and residence time, Colloids and Surfaces A: Physicochemical and Engineering Aspects 272 (2006) 48-55.

[49] M.R. Schure, S.A. Palkar, Accuracy estimation of multiangle light scattering detectors utilized for polydisperse particle characterization with field-flow fractionation techniques: a simulation study, Anal. Chem. 74 (2002) 684-695.

[50] J.D. Fortner, D.Y. Lyon, C.M. Sayes, A.M. Boyd, J.C. Falkner, E.M. Hotze, L.B. Alemany, Y.J. Tao, W. Guo, K.D. Ausman, V.L. Colvin, J.B. Hughes, C60 in Water: Nanocrystal Formation and Microbial Response, Environ. Sci. Technol. 39 (2005) 4307-4316.

[51] J. Brant, H. Lecoanet, M.R. Wiesner, Aggregation and deposition characteristics of fullerene nanoparticles in aqueous systems, J. Nanopart. Res. 7 (2005) 545-553.

[52] B. Derjaguin, L. Landau, Theory of the stability of strongly charged lyophobic sols and of the adhesion of strongly charged particles in solutions of electrolytes, Acta Physicochim. URSS 14 (1941) 633-662.

[53] G. Karaiskakis, M. Douma, I. Katsipou, A. Koliadima, L. Farmakis, Study of the recovery of colloidal particles in potential barrier sedimentation field-flow fractionation, J. Liq. Chromatogr. & Relat. Technol. 23 (2000) 1953-1959.

[54] N. Lioris, A. Farmakis, A. Koliadima, G. Karaiskakis, Estimation of the particle-wall interaction energy in sedimentation field-flow fractionation, J. Chromatogr. A 1087 (2005) 13-19.

[55] L. Pasol, M. Martin, M.L. Ekiel-Jezwska, E. Wajnryb, J. Blawzdziewicz, F. Feullebois, Motion of a sphere parallel to plane walls in a Poiseuille flow. Application to field-flow fractionation and hydrodynamic chromatography, Chem. Eng. Sci. 66 (2011) 4078-4089.

[56] A. Ulrich, S. Losert, N. Bendixen, A. Al-Kattan, H. Hagendorfer, B. Nowack, C. Adlhart, J. Ebert,

M. Lattuadae, K. Hungerbuhler, Critical aspects of sample handling for direct nanoparticle analysis and analytical challenges using asymmetric field flow fractionation in a multi-detector approach, J. Anal. At. Spectrom. 27 (2012) 1120-1130.

[57] S. Schachermeyer, J. Ashby, M. Kwon, W. Zhong, Impact of Carrier Fluid Composition on Recovery of Nanoparticles and Proteins in Flow Field Flow Fractionation, J. Chromatogr. , A 1264 (2012) 72-79.

CHAPTER 3

CHARACTERISARION OF FULLERENES

3.4. Discussion of results

3.4. Discussion of results

The current section presents and discusses the most relevant results obtained in the studies included in this chapter regarding the characterisation of fullerenes in terms of aggregation behaviour, size distribution and shapes in aqueous solutions of different characteristics (i.e., ionic strength, surfactant concentration). In order to obtain a complete picture of the aggregates formed and to increase the amount of information on their characteristics, several techniques were used and combined (i.e., CE, AF4-UV-MALS, TEM). The compounds selected for these studies are highly and moderate water soluble surface modified fullerenes (polyhydroxy- and carboxy-fullerenes) presenting increasing applications especially in the biomedical field and for which very little or no information is available in the literature.

Aggregation behaviour in CE

The first step of the study was to evaluate the capability of MECC for the analysis of hydrophobic fullerenes (C_{60}, C_{70} and C_{60}-pyrr) and although these compounds could not be separated, a method using 100 mM SDS and 10 mM sodium tetraborate-10 mM sodium phosphate as background electrolyte (BGE) was proposed for the analysis of C_{60} in cosmetic products. This method can be used in quality control analysis showing results comparable to those obtained by LC-MS without requiring the use of high amounts of toluene needed in the LC mobile phase. The same BGE was used as the initial electrolyte for the analysis of two polyhydroxy-fullerenes ($C_{60}(OH)_{24}$, $C_{120}(OH)_{30}$) and two carboxy-fullerene derivatives ($C_{60}CHCOOH$, C_{60}-pyrr tris acid). Under these conditions, broad, multiple and distorted peaks were obtained, thus hindering the application of the method for the analysis of these compounds. At this point, the aim of this study was to investigate the reason why these peaks appeared, and moreover, to evaluate to which extent their presence was related to the high buffer concentration and to the presence of micelles in the running BGE. To this end, the effect of buffer's composition and concentration (sodium tetraborate-sodium phosphate between 2.5 and 15 mM of each component and 1 mM sodium tetraborate) on the electrophoretic pattern of the selected fullerene derivatives was evaluated while maintaining the SDS concentration constant (100 mM).

The use of high sodium tetraborate-sodium phosphate buffer concentration (> 5 mM each) produced striking differences in their electrophoretic pattern showing highly broad, distorted and multiple peaks. As an example, the electropherograms obtained for C_{60}-pyrr tris acid in MECC using 100 mM SDS, and the above mentioned buffers at varying concentrations are illustrated in Figure 3.1. As shown, two unresolved broad and tailed peaks were observed when using 15 mM sodium tetraborate-15 mM sodium phosphate (peak A, t_m: 4.8 min; peak B, t_m: 10.3 min) (Figure 3.1a). Considering the high aggregation tendency of fullerenes, it is reasonable to think that these peaks could be related to the presence of particles of different aggregation degree that have different equilibrium distribution constants with the micellar pseudostationary phase. The decrease in the buffer concentration led to a reduction in peaks migration times and peak tailing improving their shapes. For instance, for C_{60}-pyrr tris (Figure 3.1) the area of the second peak (peak B) decreased considerably, especially when using 1 mM of sodium tetraborate (Figure 3.1d). This can be due to a reduction of the micellar phase at lower electrolyte concentration and also to a decrease in the aggregation degree of the fullerenes which is affected by the presence of electrolytes.

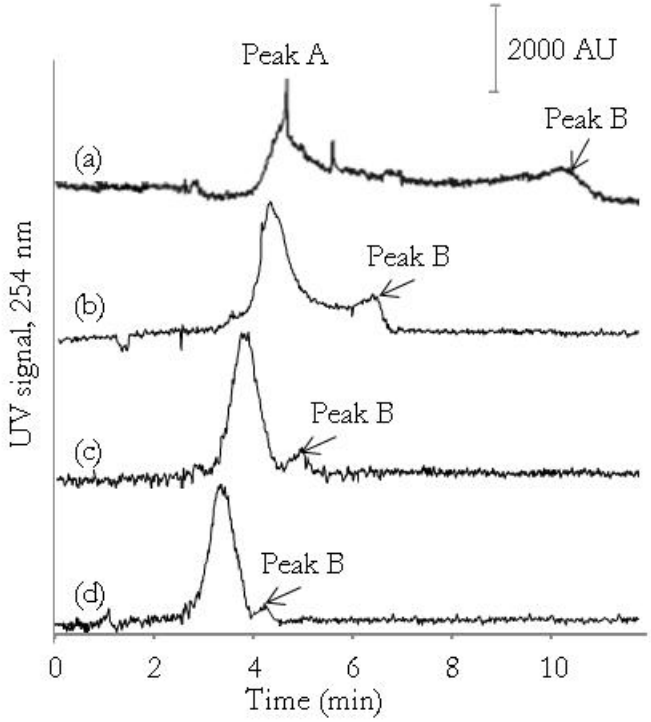

Figure 3.1. MECC electropherograms of C_{60}-pyrr tris acid using as BGE: (a) 100 mM SDS and 15 mM sodium tetraborate-15 mM sodium phosphate (pH 9.4); (b) 100 mM SDS and 10 mM sodium tetraborate-10 mM sodium phosphate (pH 9.4), (c) BGE: 100 mM SDS and 2.5 mM sodium tetraborate-2.5 mM sodium phosphate (pH 9.4) and (d) BGE: 100 mM SDS and 1 mM sodium tetraborate (pH 9.2); V= +20 kV; hydrodynamic injection (5 psi).

As regards the effect of the SDS concentration on the electrophoretic peaks, in general, narrower peaks and lower migration times were obtained when reducing its concentration in the running BGE, and in some cases the peak profiles also changed. For instance, in Figure 3.2 it can be observed that the second peak of C_{60}-pyrr tris acid was no longer visible at SDS concentration values lower than 40 mM. This fact can be probably related to the total ion strength of the BGE that at these conditions is not high enough to favour the aggregation of fullerenes. Moreover, the aggregation of micelles at high SDS concentrations, enhance their interaction with fullerenes which allows distinguishing between particles of different aggregation degree which could be present in the sample. A similar behaviour has been reported for another fullerene derivative (dendro-fullerene) which also presented a high number of peaks when increasing the SDS concentration in the BGE that were not observed by working in CZE conditions (Chan et al., 2007). The authors attributed the appearance of several peaks at high SDS concentration to the heterogeneity of the sample (presence of different particle sizes) as a result of the synthesis process.

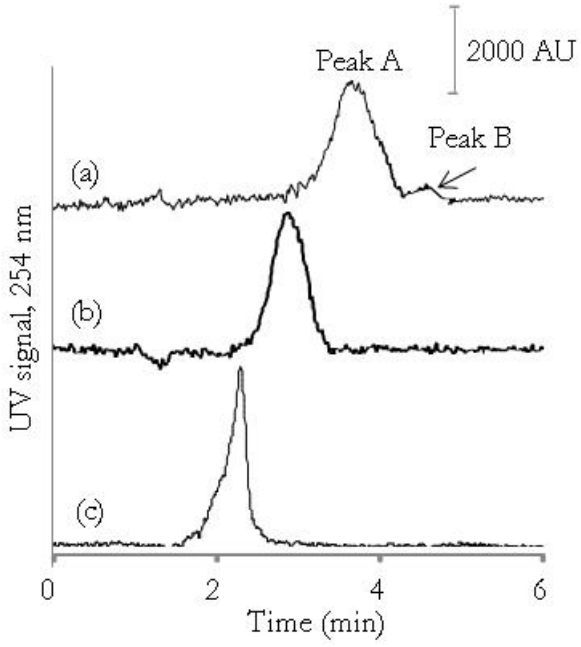

Figure 3.2. Electropherograms of C_{60}-pyrr tris acid at different SDS concentrations: (a) 100 mM SDS; (b) 40 mM SDS; (c) 2 mM SDS; other BGE conditions: 1 mM sodium tetraborate; V= + 20 kV; hydrodynamic injection (5psi).

The peak shapes of the other studied compounds also improved when working in CZE conditions. For comparison, Figure 3.3 shows the electropherograms obtained for the studied compounds in MECC (100 mM SDS in 10 mM sodium tetraborate-10 mM sodium phosphate) and CZE conditions at low buffer and SDS concentration (2 mM SDS and 1 mM sodium tetraborate). As previously mentioned, the broader peaks observed in MECC could indicate the formation of larger aggregates in the evaluated conditions and that the multiple peaks observed for some of the compounds (C_{60}-pyrr tris acid and $C_{120}(OH)_{30}$) could be due to the presence of different aggregates which migrate at different velocities. Nevertheless, although the peak shapes improved in CZE compared to MECC, tailing peaks for polyhydroxy-fullerenes and fronting peaks for the carboxy-fullerenes were still observed.

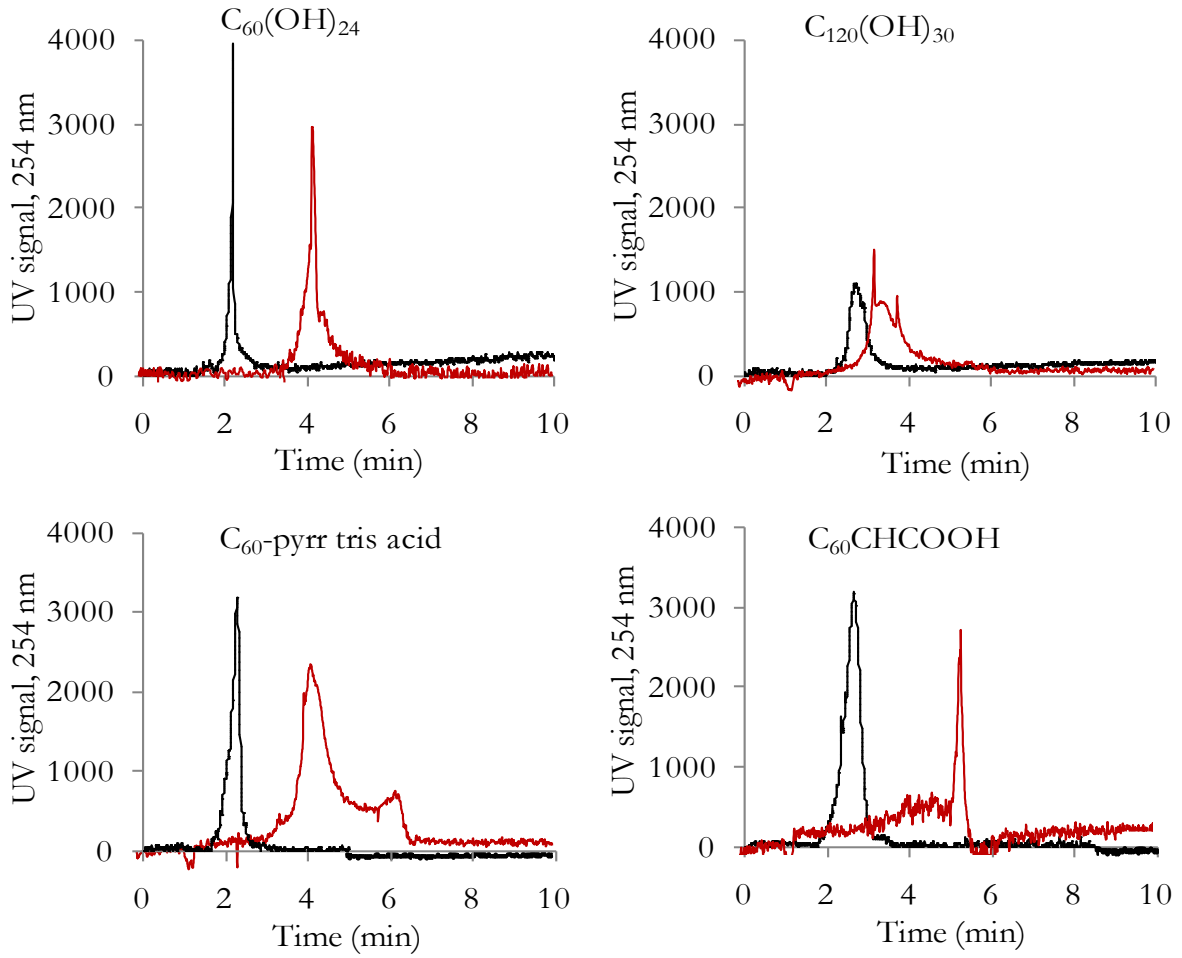

Figure 3.3. Electropherograms of the studied compounds obtained in MECC (red line), BGE: 100 mM SDS, 10 mM sodium tetraborate-10 mM sodium phosphate (pH 9.4) and CZE (black line), BGE: 2 mM SDS, 1 mM sodium tetraborate (pH 9.2); V= +20 kV, hydrodynamic injection (5 psi).

TEM

Although the drying step during sample preparation in TEM could induce more aggregation of particles which may lead to inaccurate conclusions regarding their sizes, this technique was used in this thesis in order to visualise the morphology and aggregate structures of the studied fullerenes in aqueous solutions. As an example, Figure 3.4 shows the micrographs obtained for C_{60}-pyrr tris acid in Milli-Q water (pH 6.5) (Figure 3.4a) and in the running BGE employed in MECC (100 mM SDS and 10 mM sodium tetraborate-10 mM sodium phosphate (pH 9.4)) (Figure 3.4b). The images showed differences between the aggregate structures formed in water and in the BGE used in MECC. The more complex and branched crystalline structures observed for both polyhydroxy- and carboxy-fullerene derivatives in the BGE confirmed an increased aggregation in the latter (Figure 3.4b) and may explain the broad and multiple peaks observed in MECC. However, due to the complexity of their structures, the average size of the aggregates formed cannot be determined by this technique.

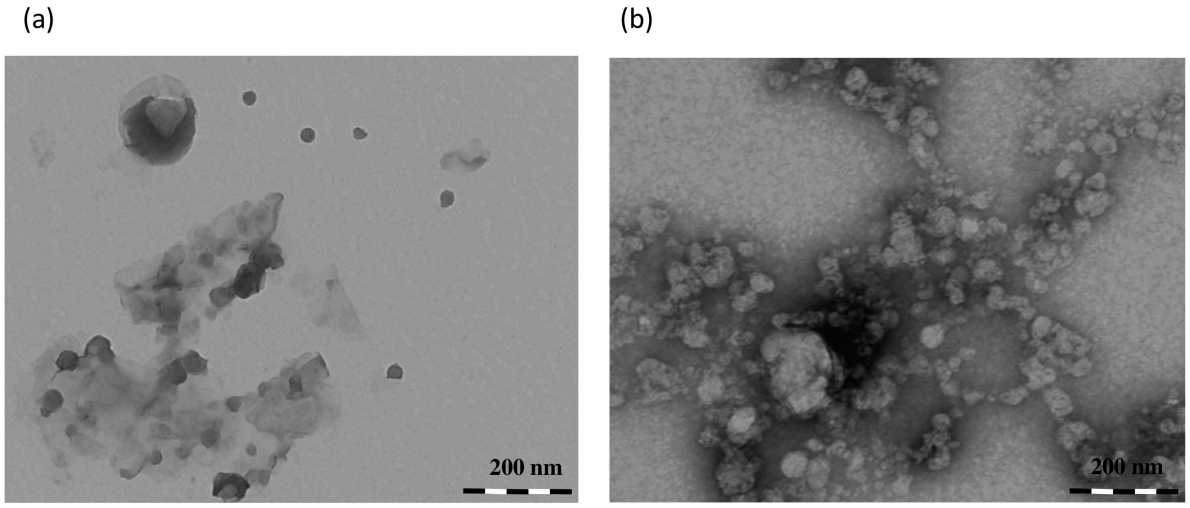

Figure 3.4. TEM micrograms of C_{60}-pyrr tris acid in (a) Milli-Q water and (b) 100 mM SDS and 10 mM sodium tetraborate-10 mM sodium phosphate.

Aggregate sizes and size distribution (AF4-UV, AF4-MALS)

By using AF4 we were able to separate particles of different aggregation degree present in the samples and to calculate their sizes (hydrodynamic radius (r_H)) in aqueous solutions of different ionic strengths, pH and SDS concentration. Furthermore, by coupling the AF4 to MALS, the size distribution of the particles in the evaluated conditions was also determined.

One of the main difficulties encountered when optimising the fractionation of the particles by AF4 was finding the optimal cross-flow rate for the separation of the fractions. Due to the high polydispersity of these samples, isocratic elution could not be used since none of the tested cross-flow values was found to be optimal to achieve an efficient separation of the fractions present in each sample in a reasonable time. This problem was solved by using cross-flow programming (time delayed exponential, TDE). The optimised TDE programs used for the fractionation of the studied analytes, applying an initial cross-flow and focus-flow of 2 mL/min, and the calculated r_H values are shown in Figure 3.5. At the beginning of the program, the cross-flow was kept constant for a certain time and then it was decreased exponentially with a time constant equal to the delay time (the time the cross-flow was kept constant). For polyhydroxy-fullerenes, a delay/decay time of 7 min, and a minimum 10 min focusing time were required to achieve a good separation from the void peak and the fractionation of the particles in a reasonable run time. Focusing time values higher than 10 min produced an increase in the r_H of the particles, due to induced aggregation as during focusing the particles are strongly concentrated near the wall, and particle-particle interactions may be more prominent. Similar behaviour was observed when increasing the cross-flow and focus-flow rate above 2 mL/min. For the carboxy-fullerenes, the effect of the flow conditions (i.e., cross-flow, focus-flow) and focusing time was negligible, and in contrast to polyhydroxy-fullerenes, their r_H values were not affected by these experimental parameters. For these compounds, the optimal fractionation conditions were 3 min focusing time and a delay/decay time of 3 min and using an initial cross-flow and focus-flow of 2 mL/min as for the polyhydroxy-fullerenes. With regard to the membrane type, regenerated cellulose (RC) membrane of 10 kDa nominal mass cut-off was employed for the fractionation, achieving recoveries higher than 79 %. Under the above mentioned conditions, the separation of several fractions (see Figure 2, Section 3.3., Chapter 3) was achieved which allowed determining the r_H of the particles present in these samples (Table 3.2) and also their size distribution by coupling the AF4-UV to MALS.

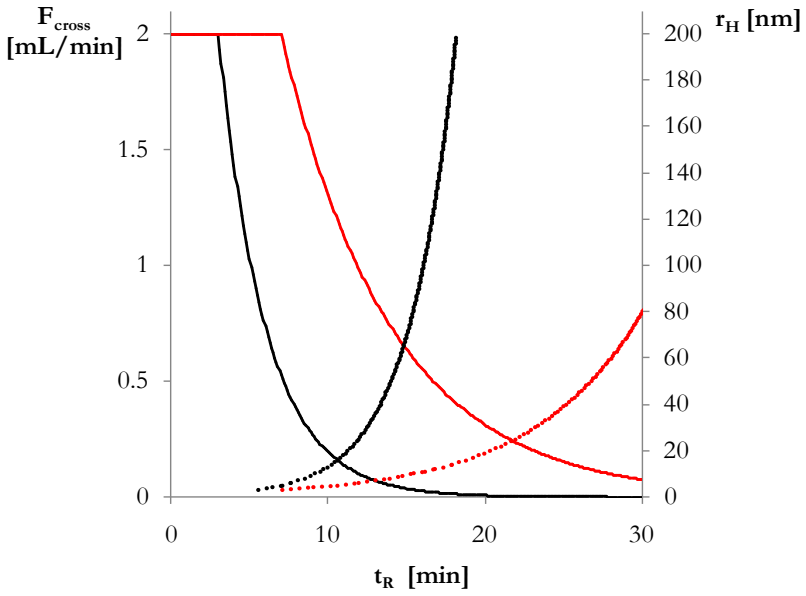

Figure 3.5. Time-delayed exponential decay (TDE) programmes used for the fractionation of polyhydroxy- and carboxy-fullerenes with delay/decay times of 3 min (black) and 7 min (red), respectively, and the calculated hydrodynamic radii (r_H) (dashed lines), black: polyhydroxy-fullerenes; red: carboxy-fullerenes.

In Milli-Q water, the AF4-UV fractograms of $C_{60}(OH)_{24}$ and $C_{120}(OH)_{30}$ showed the presence of an intense peak at a low retention time showing that these compounds are mostly present as small aggregates (r_H approx. 4 nm). In addition, an important peak tailing can be observed for these compounds by using UV detection that could indicate the presence of unresolved particles of higher aggregation degree. This can be clearly observed when using MALS hyphenated to AF4. As an example, Figure 3.6 shows the fractograms obtained for $C_{60}(OH)_{24}$ by AF4 with both, UV and MALS detection. The presence of two peaks corresponding to particles of slightly different aggregation degree (r_G: 1st peak: up to 40 nm, 2nd peak: up to 60 nm) are observed. The detection of the peak corresponding to larger aggregates (peak 2) with MALS, which was not observed with UV except for the peak tailing, can be explained because the scattering intensity is strongly increased for bigger particles enhancing the response compared to the smaller ones. The presence of different aggregated particles for fullerene derivatives in aqueous solutions could explain the broad and tailed peaks observed for these compounds in the CE experiments.

Table 3.1. Fullerene particle sizes in aqueous solutions of different ionic strength determined by AF4-UV and AF4-MALS

	$C_{60}(OH)_{24}$		$C_{120}(OH)_{30}$		C_{60}-pyrr tris acid		$C_{60}CHCOOH$	
Ionic strength (M)	Average r_H (nm)	r_G (nm)	Average r_H (nm)	r_G (nm)	Average r_H (nm)	r_G (nm)	Average r_H (nm)	r_G (nm)
0 (Milli-Q water)	4	1st peak: 10-40 2nd peak: 50-60	4 nm	1st peak: 10 -30 2nd peak: ≈ 40	1st peak: 10 2nd peak: 30 3rd peak: 95	1st peak: < 10 2nd peak: 15-310	1st peak: 10 2nd peak: 55	1st peak: < 10 2nd peak: 20-310
0.100	1st peak: 9 2nd peak: 30	80-160	1st peak: 8 2nd peak: 20	70-100	1st peak: 10 2nd peak: 35 3rd peak: 180	1st peak: < 10 2nd peak: 15-325	1st peak: 10 2nd peak: 65	1st peak: < 10 2nd peak: 20-315
0.150	1st peak: 13 2nd peak: 48	120-180	1st peak: 11 2nd peak: 34	100-150	1st peak: 10 2nd peak: 66 3rd peak: -	1st peak: < 10 2nd peak: 15-280	1st peak: 10 2nd peak: 45	1st peak: < 10 2nd peak: 20-290
0.200	1st peak: 14 2nd peak: 50	140-180	1st peak: 12 2nd peak: 40	120-160	1st peak: 10 2nd peak: 65 3rd peak: -	1st peak: < 10 2nd peak: 15-280	1st peak: 10 2nd peak: 45	1st peak: < 10 2nd peak: 20-290

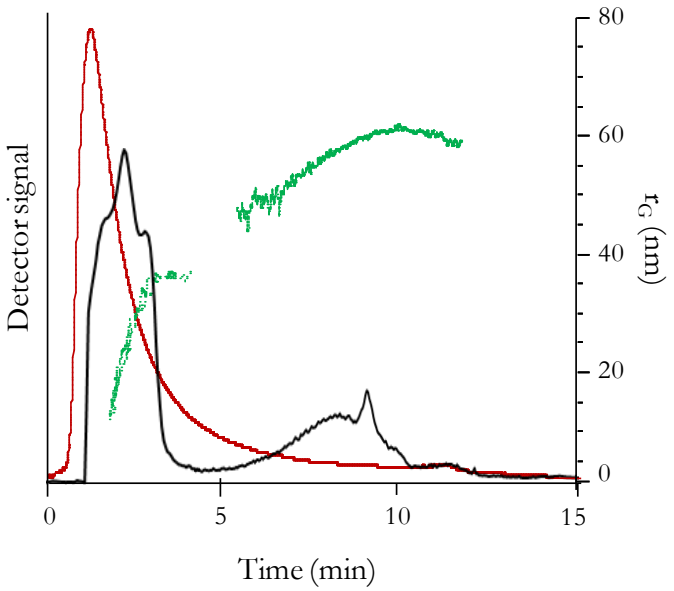

Figure 3.6. Fractograms obtained for $C_{60}(OH)_{24}$. Red line: UV response at 254 nm; black line: light scattering response at 90° angle; green dashed lines: scattering radii (r_G).

The r_H values calculated at the maximum peak heights and the r_G values determined by MALS for the studied fullerenes are included in Table 3.1. The results obtained for C_{60}-pyrr tris acid and C_{60}CHCOOH in Milli-Q water indicated that they present particles of higher aggregation degree (r_H: 10-95 nm) and with a broader size distribution (up to 310 nm (r_G)) than those of the studied polyhydroxy-fullerenes. The bigger aggregate sizes obtained for these compounds can be related to their lower water solubility and consequently higher tendency to aggregate in aqueous media. These two compounds eluted in several discernible fractions (see Figure 2, Section 3.3., Chapter 3), at least three for C_{60}-pyrr tris acid and two for C_{60}CHCOOH, corresponding to particles of significantly different aggregation degree (see Table 3.1).

As previously mentioned, information about the particle sizes of fullerene derivatives is very scarce. In fact, only the sizes of $C_{60}(OH)_{24}$ have been reported. Sizes (1.2 nm) lower that those obtained in this thesis (Table 3.2) were found when using AF4 and AFM (Assemi et al., 2010) and significantly higher values (100 nm) were reported by TEM and DLS (Brant et al., 2007). This incongruence could be due to the different methodology used for the measurements. The smaller sizes reported by AF4 for this compound, could be related to the differences in the cross-flow program (mode) and value used for the fractionation. The authors (Assemi et al., 2010) used a constant cross-flow during the elution step and a significantly higher cross-flow value (3 mL/min) than the one used in this thesis (TDE programming, 2 mL/min) which may have caused the elution of the bigger particles when the cross flow stopped and so, only the

small fractions eluted inside the AF4 size window (during the elution step). Regarding the other paper (Brant et al., 2007), as previously mentioned, the drying of the samples required for the TEM measurements induce aggregation of the particles and the sizes measured by DLS are skewed towards the larger particles when the sample is polidisperse, two reasons that can explain the larger sizes reported in this last study using these techniques.

In this thesis, besides TEM, another approach was evaluated to study the shapes of the aggregates of the surface modified fullerenes. Specifically, by calculating a shape factor, dividing the scattering radii values at the peak top obtained from the MALS measurements by the hydrodynamic radii values calculated from the retention times in AF4 at the maximum of the peak height. As can be seen in Table 3.2 the r_G values of the polyhydroxy-fullerenes where significantly higher than the rH values indicating that the shapes of these particles are far from spherical. For the studied carboxy-fullerenes, which presented particles of different aggregation degree, the results suggested the presence of both spherical and irregular shaped particles. These results are in agreement with those obtained by TEM which also showed highly branched structures for polyhydroxy-fullerenes and the presence of both spherical and irregular clusters for the carboxy-fullerene derivatives. Figure 3.7 shows as an example the TEM micrographs obtained for $C_{60}(OH)_{24}$ and C_{60}-pyrr tris acid in Milli-Q water. This is the first study of the morphology of polyhydroxy- and carboxy-fullerenes aggregates, except for $C_{60}(OH)_{24}$ for which similar structures were reported by TEM (Brant et al., 2007).

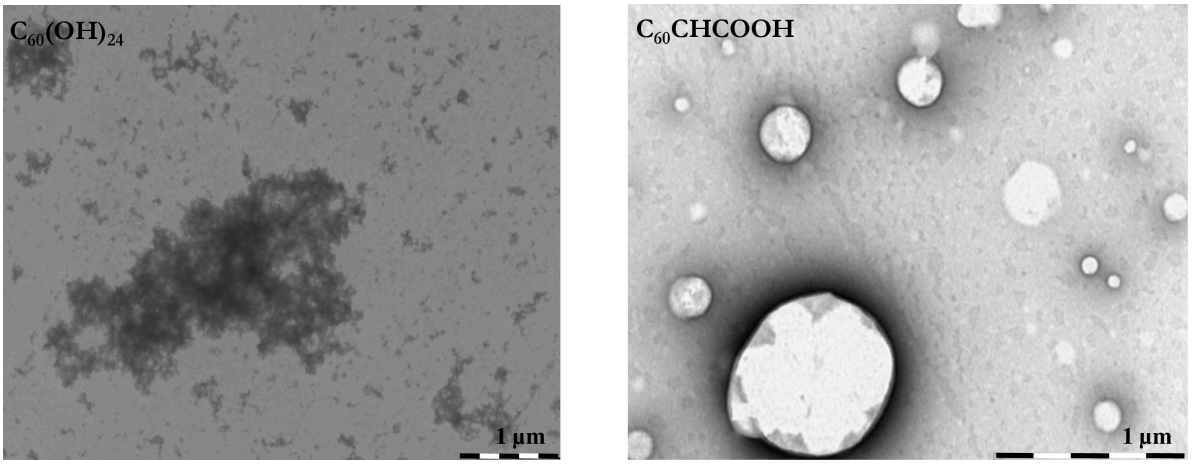

Figure 3.7. TEM micrographs of $C_{60}(OH)_{24}$ and C_{60}CHCOOH in Milli-Q water

As happened in CE, an increase in the ionic strength of the mobile phase produced an important change in the AF4 elution profile of the compounds revealing shifted and broader peaks. Figure 3.8 shows as an example the fractograms obtained for $C_{60}(OH)_{24}$ and for C_{60}-pyrr tris acid at different NaCl concentrations (from 0 to 200 mM). For polyhydroxy-fullerenes, at

ionic strength values ≥ 0.100 M an additional peak appeared in the fractograms at higher retention times that corresponds to bigger aggregates. Moreover, the area of this peak increased when raising the ionic strength since aggregation is favoured at high salt concentration. For instance, an important increase in the calculated r_H value (peak-top) of $C_{60}(OH)_{24}$, from ≈ 4 nm up to 14 nm (peak 1) was observed when the ionic strength raised from 0 to 0.200 M. Accordingly, an increase in their r_G was also observed in the AF4-MALS measurements, reaching r_G values up to 180 nm at high ionic strength (0.200 M). The studied carboxy-fullerenes also showed a change in the elution profile and higher aggregation by increasing the ionic strength. For instance, at an ionic strength value of 0.100 M, their r_H augmented up to 180 nm for C_{60}-pyrr tris acid (3rd peak) and 65 nm for C_{60}-CHCOOH (2nd peak), respectively (see Table 3.1). However, in this case both their peak areas (Figure 3.8b) and recoveries from the AF4 channel strongly decreased after fractionation. As shown in Figure 3.8b, for ionic strength values higher than 0.100 M the third peak observed for C_{60}-pyrr tris acid in Milli-Q water (green line), corresponding to big aggregates, was no longer visible. Moreover, recoveries lower than 10 % were found at 0.200 M NaCl for both carboxy-fullerene derivatives. This can be explained by the adsorption of the particles on the membrane material, due to the significantly higher aggregate sizes of these compounds compared to polyhydroxy-fullerenes. The presence of a brown residue in the focusing area of the AF4 membrane at the end of the measurements was an indicator that the adsorption of these compounds occurred.

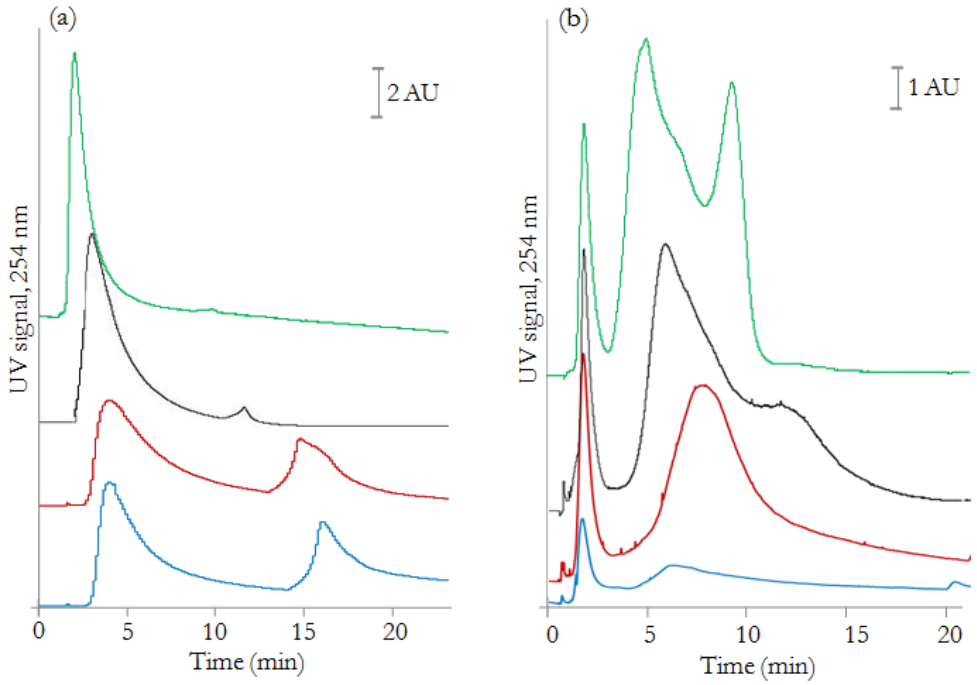

Figure 3.8. AF4-UV fractograms of (a) $C_{60}(OH)_{24}$ and (b) C_{60}-pyrr tris acid at different ionic strength values: 0 (Milli-Q water) (green line), 0.100 (black), 0.150 (red), 0.200 (blue).

The increased aggregation of pristine and surface modified fullerenes at high ionic strength values has also been reported in previous studies (Assemi et al. 2010, Brant et al., 2006, Brant et al. 2005, Brant et al. 2007, Fortner et al., 2005) and it is in agreement with the Derjaguin–Landau–Verwey–Overbeek (DLVO) theory that is commonly used to describe interactions of charged surfaces across liquids (Derjaguin et al., 1941). According to DLVO theory, the colloidal stability of charged particles dispersed in aqueous solutions is controlled by the van der Waals and electrostatic double layer interactions which are being affected by changes in particle shapes. The increase in the ionic strength compresses the electrostatic double layer, the van de Waals attractive forces dominate and thus the aggregation is promoted. As previously mentioned, the fate and transport of fullerenes after being released in the environment are strongly dependent on their aggregation behaviour. Specifically, the rate of aggregation will influence their rate of sedimentation and thus their removal from the aqueous phase. The results obtained in this thesis indicate that in environmental waters of high ionic strength the aggregates of the studied carboxy-fullerenes may have limited mobility as they form large aggregates that will most likely settle out of suspension allowing their deposition, while the polyhydroxy-fullerenes may present a higher mobility and stability.

In addition to the effect of the ionic strength on the aggregation of fullerene derivatives, the effect of the concentration of SDS was also evaluated in order to have a deeper understanding of the behaviour of these compounds in MECC. For all the studied compounds, the number of peaks increased in the presence of micelles. As an example in Fig. 3.9 presents the fractograms obtained for $C_{60}(OH)_{24}$ in the presence and in the absence of micelles where it can be observed that the former conditions allowed the separation of particles of different aggregate sizes. The calculated r_H values at the maxium of the peak height for the studied fullerenes derivatives in aqueous buffers with (30 mM) and without (2 mM) SDS micelles are included in Table 3.2. As can be seen, the peak-top r_H values did not increase as occurred at high ionic strength values. The presence of micelles revealed at least 2 and 3 unresolved peaks for polyhydroxy-fullerenes (e.g. r_H: 4 and 7 nm ($C_{60}(OH)_{24}$)) and carboxy-fullerenes (e.g., r_H: 7, 40 and 47 (C_{60}-pyrr tris acid)), respectively. These results explain the presence of distorted and multiple peaks in MECC, and the improvement in peak shapes and symmetry when working in CZE conditions.

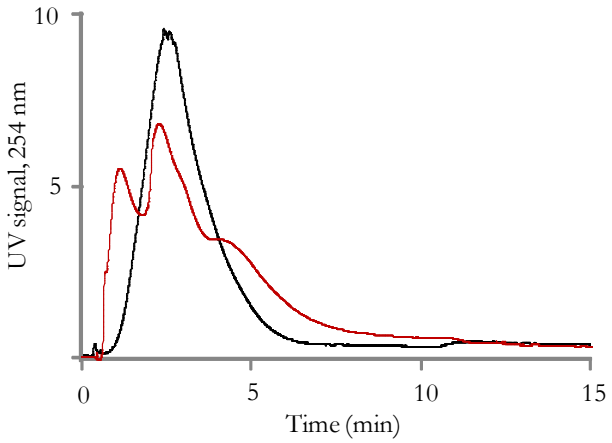

Figure 3.9. AF4-UV fractograms of $C_{60}(OH)_{24}$ using 2 mM SDS and 1 mM sodium tetraborate (black line) and 30 mM SDS and 1 mM sodium tetraborate (red line) as carrier solutions.

Table 3.2. Hydrodynamic radii (r_H) of fullerenes in buffer solutions with and without SDS micelles.

Carrier solution	r_H (nm)			
	$C_{60}(OH)_{24}$	$C_{120}(OH)_{30}$	C_{60}-pyrr tris acid	C_{60}CHCOOH
2 mM SDS and 1 mM sodium tetraborate, pH=9.2	7	6	1st peak: 10 2nd peak: 50	1st peak: 10 2nd peak: 55
30 mM SDS and 1 mM sodium tetraborate, pH=9.2	1st peak: 4 2nd peak: 7	1st peak: 4 2nd peak: 6	1st peak: 7 2nd peak: 40 3rd peak: 46	1st peak: 7 2nd peak: 15 3rd peak: 52

Furthermore, for polyhydroxy fullerenes, in addition to aggregation, the presence of several products in the samples can be the cause of the multiple and/or distorted peaks observed.

Our preliminary results using high resolution MS (Q-Exactive mass analyser (Thermo Fisher, San José, LA, USA), mass resolution: 140,000 full width half maximum (FWHM) at m/z 200 and ESI in negative mode (capillary votlage: 4 kV, capillary temperature 320 °C, S-lens 100) revealed complex spectra with a wide range of characteristic ions at m/z between 100 and 1500. Figure 3.10a shows the ESI(-)MS spectrum obtained for this compound (m/z 600-1500). As can be seen, (at least) 3 sections (dotted lines) in which a pattern corresponding to distinct structures, containing a different number of Na atoms, is repeated. Moreover, in most cases, the observed experimental clusters do not match with the simulated theoretical ones (see as an example Figure 3.10b). This may indicate that the experimental pattern is a sum (mixture) of ions corresponding to different structures.

In order to be able to differentiate between these entities and for their accurate identification, a higher mass resolving power is needed.

These results are in agreement with previous studies reporting that fullerols are not pure $C_{60(}OH)n$ but a complex multi-component mixture of products forming different structures (Chen et al., 2001; Husebo et al., 2004; Semenov et al., 2010; Bobylev et al., 2011; Charkin et al., 2011; Silion et al., 2013). However, an accurate structural identification of fullerols has not been reported yet.

The presence of different products and the contamination of this compound with Na^+ atoms is relevant since they can present different physicochemical and aggregation properties and also reactivity. Further studies are needed for the accurate structural characterisation of fullerols.

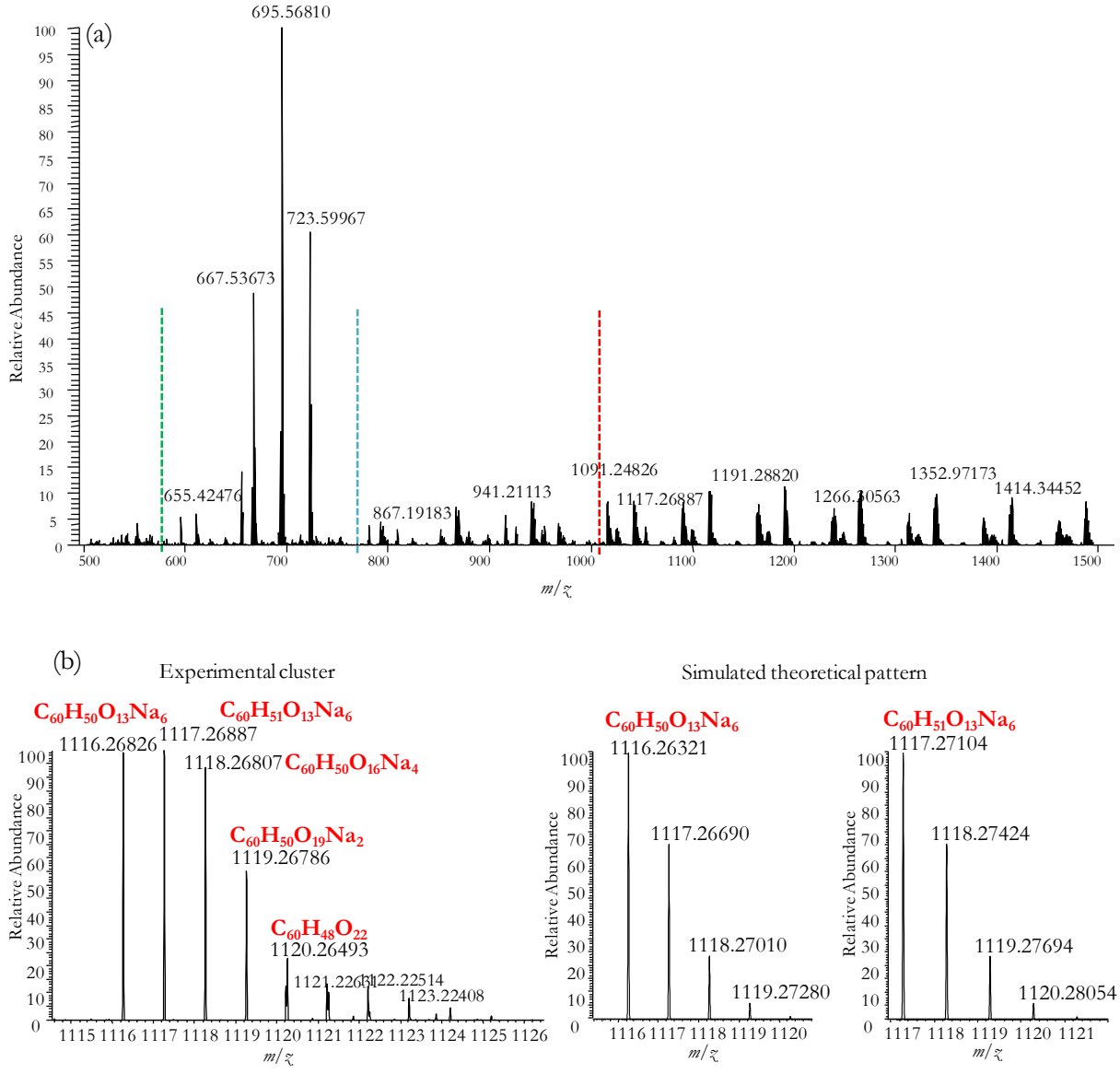

Figure 3.10. ESI(-)HRMS spectrum of $C_{60}(OH)_{24}$ (100 μg L^{-1}); flow injection analysis, mobile phase: acetonitrile:H_2O.

CHAPTER 3

CHARACTERISARION OF FULLERENES

3.5. Conclusions

3.5. Conclusions

The use of CE techniques, AF4-UV/MALS and TEM for the characterisation of fullerene aggregates in aqueous solutions allowed us to reach the following conclusions:

Concerning the aggregation behaviour of surface modified fullerenes:

- The observed changes in the peak electrophoretic profiles of the studied compounds can be due to modifications in their aggregation state. For instance, broad, distorted and multiple peaks were obtained in MECC at high buffer and SDS concentration in the running background electrolyte (100 mM SDS and 10 mM sodium tetraborate-10 mM sodium phosphate) and narrower peaks were observed by working in CZE conditions at low buffer and SDS concentration (2 mM SDS and 1 mM sodium tetraborate). This behaviour indicates an increased aggregation of the particles in MECC and as a consequence, the presence of particles of different aggregation degree that present slightly different interaction with the micelles.
- The TEM micrographs obtained in Milli-Q water and in the background electrolyte used for the MECC experiments showed that higher aggregation and the formation of complex and branched aggregate structures occurred at high ionic strengths and SDS concentrations for all the compounds.
- Both AF4 and TEM results have shown that both the nature and number of the functional groups attached to the buckyball structure have a significant effect on the aggregate sizes and shapes of the compounds. The surface modification with polyhydroxyl groups ($C_{60}(OH)_{24}$ and $C_{120}(OH)_{30}$) leads to the formation of small aggregate sizes in water ($r_H \approx 4$ nm) that present branched and polycrystalline structures while the carboxy-fullerenes (C_{60}CHCOOH and C_{60}-pyrr tris acid) are characterised by particles of higher aggregation degree, ranging from 10 up to 95 nm, and presenting both spherical and irregular shapes in pure water.
- The hyphenation of AF4 to MALS allowed the determination of the size distribution and provided information about the particle shapes of the studied fullerenes in aqueous solutions. For polyhydroxy-fullerenes two distinct entities with different aggregation degree, which were not visible in the AF4-UV fractograms, were separated (e.g. r_G: 10 - 40 nm (1st peak) and 50 - 60 nm (2nd peak) for $C_{60}(OH)_{24}$ in Milli-Q water). The carboxy-

fullerenes present a higher polydispersity and bigger particle sizes (r_G: 10 - 310 nm) than the polyhydroxy fullerenes. The correlation between the r_G values obtained by MALS and the r_H calculated from the retention times in AF4 indicated that the particles of $C_{60}(OH)_{24}$ and $C_{120}(OH)_{30}$ are far from spherical and the presence of different particle shapes for C_{60}CHCOOH and C_{60}-pyrr tris acid (i.e., spherical particles and non-spherical shapes), in agreement with the results obtained by TEM.

- Experiments carried out by AF4 at high ionic strength values have shown a significant increase in particle sizes due to increased aggregation. The polyhydroxy-fullerenes showed up to a 10-fold increase in their r_H values at 0.2 ionic strength. The sizes of the carboxy-fullerene derivatives also increased when enhancing the ionic strength (up to 180 nm at 0.1 M, for C_{60}-pyr tris acid) but for values higher than 0.1 M their peak areas and recoveries decreased significantly (down to ≈ 10 % at 0.2 ionic strength) due to adsorption on the AF4 membrane preventing the determination of the aggregate sizes at high ionic strengths. The increase in the SDS concentration favors the separation of the different aggregated entities. These results explain the presence of multiple and distorted peaks observed in MECC, and the improvement in peak shapes when working in CZE conditions.

With regard to the analysis of hydrophobic fullerenes by MECC:

- The analysis of C_{60}, C_{70} and C_{60}-pyrr –SDS complexes by MECC revealed in each case one sharp peak presenting the same migration time (≈ 18 min) as that of the SDS micelles (measured by Sudan III) indicating that the three compounds were completely entrapped in the hydrophobic core of the micelles. Therefore, this technique can only be applied for the analysis of individual hydrophobic fullerenes and it is proposed to be used in quality control analysis where only one of these compounds is present.
- By using this method, LOQs ranging from 1.8 to 6.6 mg L^{-1} and run-to-run and day-to-day precisions with RSD values lower than 14.3 % were achieved. The results obtained when applying the proposed method for the analysis of C_{60} in cosmetic products (1.86 ± 0.07 mg L^{-1} in an anti-aging serum and 2.77 ± 0.16 mg kg^{-1} in a facial mask), are in agreement with those found by LC-MS indicating that the method can be proposed for this application.

CHAPTER 4

CONCLUDING REMARKS

4. Concluding remarks

The use of the analytical methods established in this thesis for the determination of pristine and surface modified fullerenes in complex matrices has yielded new data on the presence and distribution of these compounds in the environment. In addition, the characterisation of the aggregates of surface modified fullerenes (i.e., polyhydroxy- and carboxy-fullerenes), in terms of size and shape distribution, at variant ionic strength and pH values by combining different techniques, represents a significant contribution for a better understanding of the behaviour of these nanoparticles.

The main conclusions drawn from the studies presented in this thesis can be summarised as follows:

With regard to the analysis of fullerenes in environmental samples:

- The use of a sub-2 μm C18 column, toluene-methanol as a mobile phase and of APPI ionisation source allowed to develop a UHPLC method coupled to MS/(MS) for the analysis of five pristine (C_{60}-C_{84}) and three surface modified fullerenes (PCBM, PCBB and C_{60}-pyrr) in less than 4.5 min showing high sensitivity and selectivity. Furthermore, the employment of H-SIM mode for pristine fullerenes (mass resolving power > 12,500 FWHM), and SRM mode for fullerene derivatives, allowed achieving MLODs lower than most of those previously reported in the literature.
- For the extraction of sediment samples we propose PLE at 150°C using one extraction cycle (10 min) which allowed achieving higher recoveries for fullerene derivatives than the ones reported in the literature by UAE, in a significantly shorter extraction time and involving less toluene consumption.
- The developed UHPLC-(-)APPI/MS(MS) methodology allowed us to report for the first time the presence of C_{60}-pyrr, PCBM and PCBB in sediments (2.0 - 8.5 ng Kg^{-1} levels) and of PCBM and PCBB in pond water samples (0.1- 5.1 pg L^{-1} levels). Since the presence of these surface modified fullerenes, in addition to the occurrence of pristine fullerenes (C_{60} and C_{70}) also found in the analysed samples, may have negative effects in the environment, it would be advisable to include these emerging contaminants in a watching list in order to gather information about the real risks posed by them.

Concerning the analysis of fullerenes in cosmetic products:

- Two CE methods, a non-aqueous (NACE) and a micellar (MECC) one, have been developed. LOQs at mg L^{-1} levels were obtained with both methods making possible their application for the analysis of cosmetic products where fullerenes are present at these concentration levels.
- In NACE, the use of a complex BGE, containing several ammonium salts (TDAB (200 mM) and TEAB (40 mM)) and a solvent mixture of acetonitrile/chlorobenzene (1:1, v/v), MeOH (6%) and acetic acid (10 %), was needed to achieve the separation of two pristine (C_{60} and C_{70}) and two surface modified fullerenes (C_{60}CHCOOH and C_{60}-pyrr). In MECC, the separation of the hydrophobic fullerenes was not possible because of their high interaction with the micelles while the water soluble fullerenes provided broad and distorted peaks that prevent their quantitation (using 100 mM SDS and sodium tetraborate-sodium phosphate buffers (10 mM of each component) as BGE).
- Both methods (NACE and MECC) were applied for the quantitation of C_{60} in cosmetic products and the results are comparable to those obtained by LC-MS (in an anti-aging serum). Hence, NACE and MECC can be used as an alternative to LC-MS for the analysis of cosmetic products. Since MECC provided lower LODs and it is less contaminant than NACE and LC-MS as it does not involve the use of organic solvents, it is proposed as a good alternative for the analysis of individual fullerenes in cosmetic samples.

With respect to the characterisation of fullerene aggregates:

- The hyphenation of AF4 to MALS demonstrated that fullerene aqueous solutions contain particles of different aggregation degree. For instance, in pure water, surface modified fullerenes with polyhydroxyl functional groups showed two groups of agglomerates, one with small particle sizes and the other of higher aggregation degree (e.g. $r_H \approx 4$ nm; r_G: 10-40 nm and 50-60 nm, respectively for $C_{60}(OH)_{24}$), whereas carboxy-fullerenes (C_{60}CHCOOH and C_{60}-pyrr tris acid) present bigger aggregate sizes and a broader size distribution (r_H up to 95 nm; r_G: 10-310 nm for C_{60}-pyrr tris acid). These results are in agreement with TEM micrographs that confirmed the higher polydispersity and broader size distribution for the carboxy-fullerenes aggregates.

- The size determination of the studied compounds by AF4 at different salt concentrations demonstrated that the enhanced aggregation of fullerenes with the increase in the ionic strength explains the broad, multiple and distorted peaks obtained in MECC which were more obvious at high buffer concentration. The hydrodynamic radii of polyhydroxy-fullerenes increased more than 5 times and those of the carboxy-fullerene derivatives up to 180 nm (for C_{60}-pyrr tric acid) for 0.1M NaCl. At higher salt concentrations, a further increase in sizes was observed for polyhydroxy-fullerenes while for carboxy-fullerenes the deposition of particles on the AF4 membrane occurred as they settled out of suspension.
- The increase in the SDS concentration in the carrier solution allowed distinguishing between particles of different aggregation degree present in the samples revealing a higher number of peaks in the obtained fractograms. These findings also explain the multiple and distorted peaks observed in MECC.
- The propensity of fullerenes to aggregate in both aqueous solutions and organic solvent mixtures exmplains the electrophoretic peak profiles observed in MECC (i.e., broad peaks at high electrolyte concentration) and their higher retention in C18 columns using toluene-acetonitrile compared to toluene-methanol mobile phases (due to the formation of bigger aggregates), respectively.

RESUMEN

1. Nanotecnología

El famoso físico Richard Feynman introdujo en 1959 el concepto de "nanotecnología" como la capacidad de construir elementos con precisión atómica. Aunque Feynman nunca menciona explícitamente la palabra "nanotecnología" sugirió que con el tiempo sería posible manipular de manera precisa átomos y moléculas. Por lo tanto, mucho antes de que se inventaran los microscopios de efecto túnel y los microscopios de fuerza atómica, Feynman propuso ya estas ideas revolucionarias. Posteriormente en 1979, Eric Drexler a puso este concepto en circulación y acuñó el término "nanotecnología" que ha sido utilizado por numerosos investigadores. Actualmente, la investigación en nanotecnología se desarrolla de modo interdisciplinar y engloba la química, la física, la ciencia de los materiales, la biología y la medicina, y representa una nueva tendencia en el desarrollo científico, utilizando las propiedades de las moléculas de una manera única para producir y diseñar nuevos y fascinantes materiales y productos.

Hoy en día, la nanotecnología se ha convertido en una prioridad en la investigación en la mayoría de los países industrializados y se prevé que sus aplicaciones evolucionen generando nuevos productos nanotecnológicos en diferentes áreas que van desde una primera generación de nanoestructuras simples y pasivas y hasta llegar a una cuarta generación de sistemas moleculares altamente funcionalizados (Roco, 2004). En la Figura 1 se incluyen los productos correspondientes a las cuatro generaciones mencionadas que van desde los recubrimientos y materiales nanoestructurados (metales, polímeros, y cerámica) a la manipulación atómica para el diseño de moléculas y sistemas supramoleculares, máquinas moleculares y el diseño de grandes sistemas moleculares heterogéneos (Roco, 2004).

1.1. Nanopartículas

Las nanopartículas se consideran sustancias de un tamaño inferior a los 100 nm en más de una dimensión, aunque estos límites no son totalmente aceptados ya que existen varios nanomateriales que caen fuera de este intervalo. Las nanopartículas pueden ser esféricas, tubulares, o de forma irregular, pueden existir en formas fusionadas, agregados o aglomerados y pueden diferir de otros materiales a causa de su relativamente gran superficie específica. Los nanomateriales y nanopartículas presentan alta resistencia, alta estabilidad térmica, baja permeabilidad y su alta conductividad, entre otras propiedades únicas estimulan a la comunidad científica a centrar su investigación en el desarrollo de nuevas aplicaciones y productos

relacionados con la nanotecnología. Además, normalmente se realizan modificaciones físicas o químicas de los nanomateriales "nativos", como la funcionalización de superficies, para modificar o mejorar sus propiedades físico-químicas. Este tipo de nanopartículas reciben el prefijo 'ingeniería'.

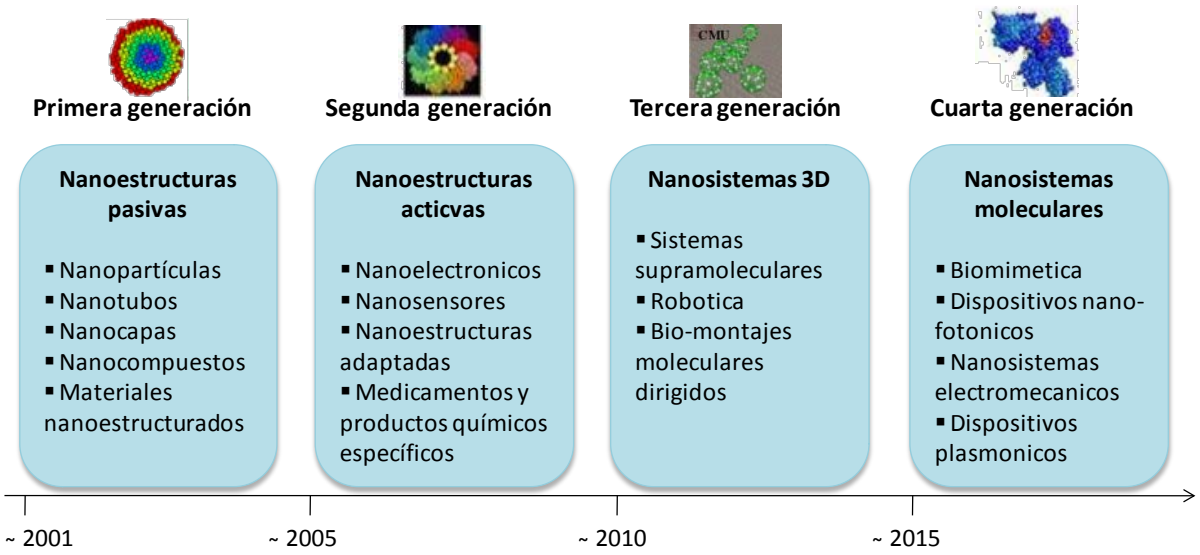

Figura 1. Evolución y aplicaciones de la nanotecnología, basado en Roco, 2004.

1.2. Nanopartículas

Las nanopartículas se consideran sustancias de un tamaño inferior a los 100 nm en más de una dimensión, aunque estos límites no son totalmente aceptados ya que existen varios nanomateriales que caen fuera de este intervalo. Las nanopartículas pueden ser esféricas, tubulares, o de forma irregular, pueden existir en formas fusionadas, agregados o aglomerados y pueden diferir de otros materiales a causa de su relativamente gran superficie específica. Los nanomateriales y nanopartículas presentan alta resistencia, alta estabilidad térmica, baja permeabilidad y su alta conductividad, entre otras propiedades únicas estimulan a la comunidad científica a centrar su investigación en el desarrollo de nuevas aplicaciones y productos relacionados con la nanotecnología. Además, normalmente se realizan modificaciones físicas o químicas de los nanomateriales "nativos", como la funcionalización de superficies, para modificar o mejorar sus propiedades físico-químicas. Este tipo de nanopartículas reciben el prefijo 'ingeniería'.

1.1.1. Clasificación y usos

Las nanopartículas se clasifican en dos grupos en función de su naturaleza, las de base de carbono (orgánicas) y las de base metálica (inorgánicas) y estos dos grupos principales se sub-clasifican en función de sus propiedades fisicoquímicas, como se muestra en la Figura 2. Las nanopartículas inorgánicas incluyen metales, óxidos metálicos y los *quantum dots* (plata, dióxido de titanio y seleniuro de cadmio). Los nanomateriales orgánicos ocupan un lugar destacado entre las nanopartículas artificiales (ENP) que engloban los nanotubos de carbono, los fullerenos, grafeno y muchos otros (Figura 3) y que se utilizan en productos tecnológicos, industriales y médicos. No obstante, la lista de nanomateriales es mucho más extensa y cada día se producen nuevas nanopartículas y en cantidades cada vez mayores para su aplicación en una amplia gama de sectores.

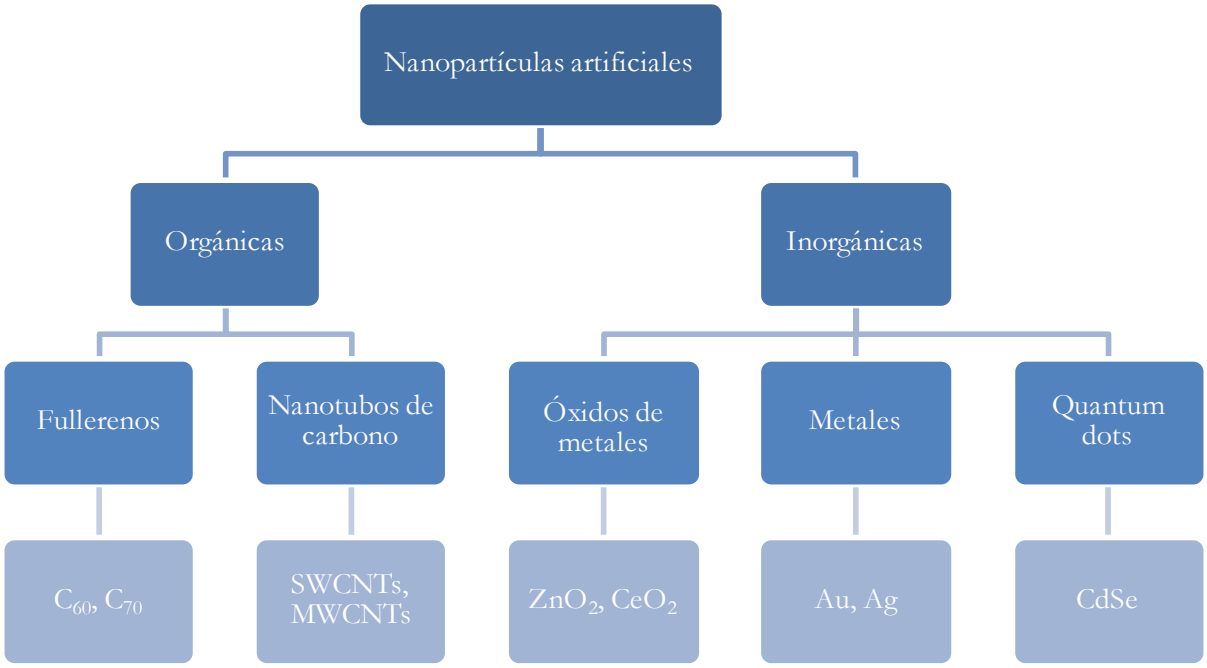

Figura 2. Clasificación de nanomateriales en relación a sus propiedades físico-químicas.

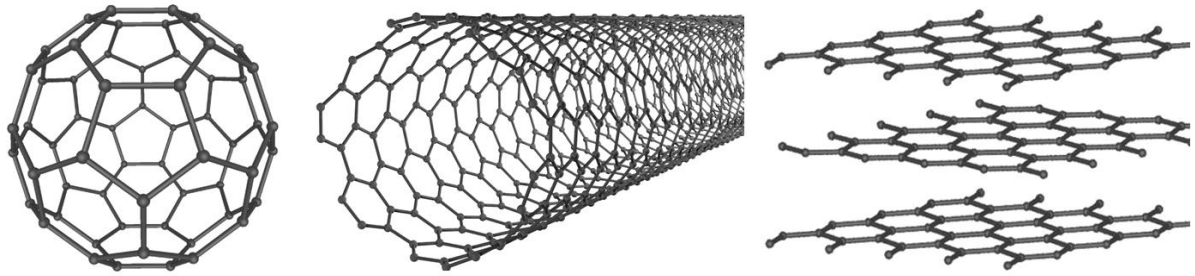

Figura 3. Ejemplos de nanopartículas de carbono (de izquierda a derecha: fullerenos, nanotubos de carbono y hojas de grafeno).

Las ENP, se utilizan, o están siendo evaluadas para ser utilizadas, en muchos campos, desde las aplicaciones biológicas y médicas a las ciencias ambientales y pueden abrir enormes perspectivas de progreso en ambas. Pueden contribuir a crear superficies y sistemas más resisitentes, más ligeros, más limpios y "más inteligentes" ya que a nanoescala las propiedades de las partículas pueden cambiar de forma impredecible.

Las estimaciones actuales sugieren que más de 1.600 productos de consumo, incluyendo baterías de teléfonos móviles, equipos deportivos, y cosméticos, contienen ENP (Miedos et al., 2011). Además de estos artículos de uso diario, se está trabajando en investigar el potencial de las ENP en las estrategias de remediación ambiental, para detectar y eliminar sustancias tóxicas, en la generación de energía y almacenamiento (Tratnyek and Johnson, 2006; Theron et al, 2008; Otto and Floyd, 2008; Karnt et al., 2009) y en procedimientos médicos avanzados (Freitas, 2005; Lacerda et al, 2006). Se espera que muchas de las aplicaciones ayuden a mejorar la salud humana y la calidad de vida. Por ejemplo, la aplicación médica de la nanotecnología es probablemente uno de los campos de más rápido crecimiento, con la evolución de los usos terapéuticos, de diagnóstico y de imagen (por ejemplo, en estudios de cáncer). La Figura 4 muestra el inventario de productos de consumo de la nanotecnología publicado en 2013 (Nanotechnology Inventory, 2013) de acuerdo a la categoría de productos de referencia (Figura 4a) y para los nanomateriales más utilizados (Figura 4b). Como se muestra en la Figura 4a la mayor parte (50%) se emplea en productos relacionados con la salud y forma física como son por ejemplo los cosméticos, los protectores solares y ropa. El material más común en los productos es la plata (51%), seguida del titanio (24%), de los compuestos de carbono (que incluyen fullerenos) (11%), la sílice (7%), el zinc (incluyendo óxido de zinc) (5%), y el oro (2%).

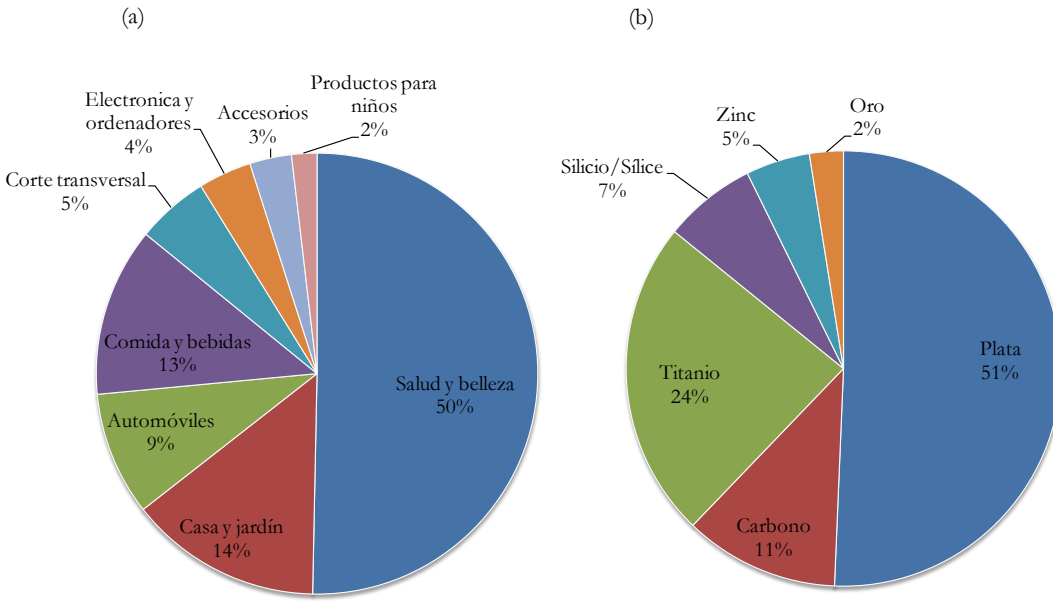

Figura 4. Inventario de productos de consumo basados en la nanotecnología de acuerdo con (a) categorías de productos principal pertinentes y (b) los nanomateriales más comunmente utilizados. Basado en: Nanotechnology Inventory, 2013.

1.1.2. La exposición y el peligro potencial

Las características únicas de la nanotecnología pueden producir numerosos beneficios sociales de largo alcance, pero también pueden plantear peligros y riesgos. Dado que hoy en dia se comercializan más productos nanotecnológicos, es probable que se produzca un aumento de la exposición a las NEP lo que conlleva un incremento de la preocupación sobre la seguridad de estos materiales en relación con la salud humana y el medio ambiente. En la Figura 5 se muestra un esquema de la producción, uso y presencia de los nanomateriales en el medio ambiente. Su liberación en el medio ambiente puede provenir de fuentes puntuales, tales como productos de consumo, eliminación, fábricas o rellenos sanitarios, y de fuentes no puntuales, como la deposición húmeda de la atmósfera y la escorrentía de aguas pluviales (Yah et al., 2012). Para su eliminación de aguas subterráneas y superficiales (utilizado para el agua potable) se utilizan métodos de tratamiento convencionales mientras que los filtros de aire y respiradores se pueden utilizar para eliminar los nanomateriales de aire. La exposición humana a los nanomateriales es más probable que ocurra durante la fabricación de nanomateriales, pero la inhalación de nanomateriales liberados a la atmósfera, la ingesta de agua potable o alimentos (por ejemplo, pescado) y la exposición cutánea a protectores solares y cosméticos también es probable (Hoet et

al, 2004; Yah et al, 2012). Dado que ciertas nanopartículas plantean riesgos para la salud ambiental y humana es importante llevar a cabo estudios de evaluación de riesgos. Hasta que no haya más información, los limitados datos disponibles hasta el momento sugieren que se debe tener cuidado ante posibles exposiciones a las nanopartículas.

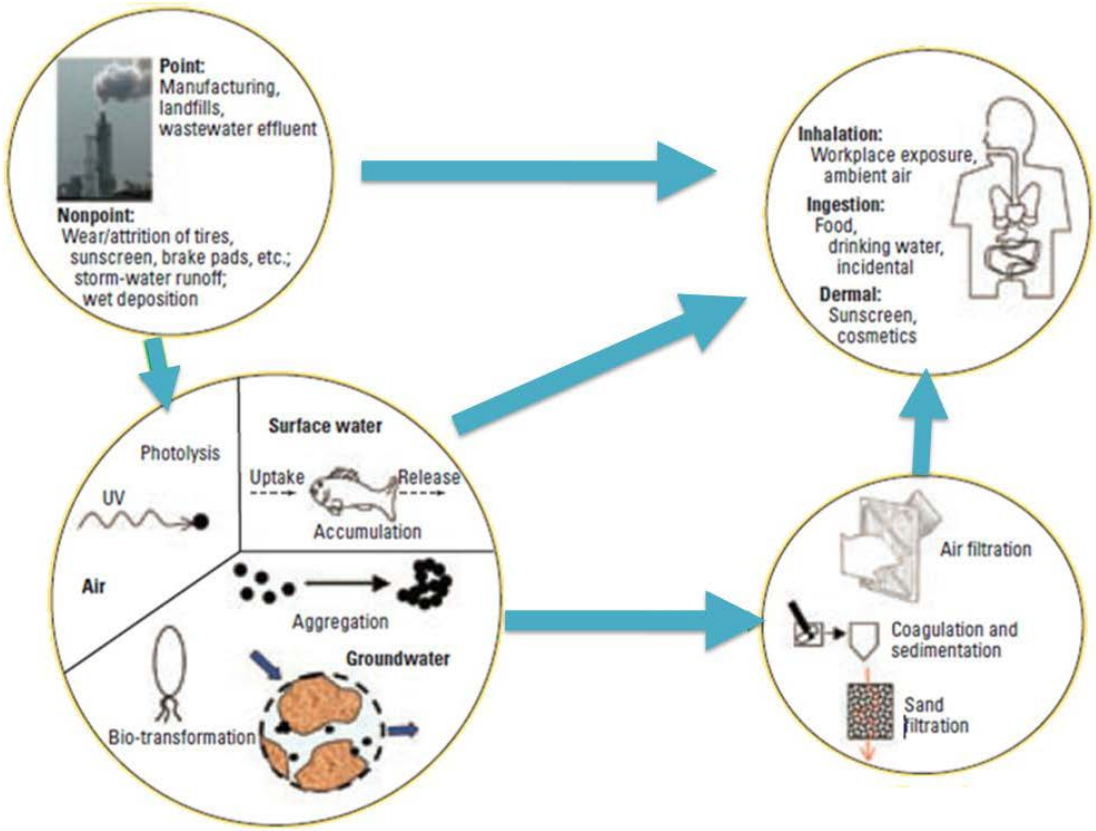

Figura 5. Esquema de la producción, uso y disposición de los nanomateriales en el aire, el agua, el suelo y los organismos. Reproducido con permiso del (Wiesner et al., 2006). Derecho de autor (2006) American Chemical Society.

Los problemas de seguridad derivados de las rutas de entrada de ENP y su potencial de bio-distribución dependen de la superficie, forma, aglomeración, agregación, solubilidad y interacciones de las partículas (Yah et al., 2012). Se requiere un examen detallado de estas propiedades para evaluar los riesgos que plantean. Por otra parte, la caracterización de los materiales de partida es esencial, ya que la pureza de las nanopartículas, basada únicamente en la información del fabricante, es a menudo poco fiable ya que pueden contener otras sustancias (incluyendo productos químicos conocidos por ser tóxicos), además de las propias nanopartículas (Liu et al., 2007; Jakubek et al, 2009; Hull et al, 2009). Las grandes diferencias en la toxicidad de las nanopartículas descritas en la literatura son probablemente una consecuencia

de estos hechos ya que los materiales contienen cantidades variables de contaminantes y además la agregación de las partículas varia en las propias disoluciones de ensayo.

Las nanopartículas no están reguladas en la actualidad, aunque la Comisión Europea (European Commision, 2002) y el Parlamento Europeo (European Parliament, 2008) han dado prioridad a la legislación sobre la manipulación y eliminación de nanomateriales. Además, la Agencia de Protección Ambiental de Estados Unidos está llevando a cabo un enfoque normativo completo bajo las *"Toxic Substances Control Act"* (EPA, 2015) para asegurarse que los materiales a nanoescala se fabrican y utilizan evitando riesgos para la salud humana y el medio ambiente. La evaluación de las concentraciones de exposición a los nanomateriales es muy dispersa y requiere una visión detallada de los procesos en los que intervienen estos materiales en los entornos correspondientes y, en la actualidad, el conocimiento disponible de estos procesos es insuficiente para permitir predicciones cuantitativas del destino ambiental de los nanomateriales Por otra parte, la regulación no es muy estricta debido a las incertidumbres en la definición, el comportamiento y la aplicación de nanomateriales en muchos sectores industriales y a la falta de normas y procedimientos de prueba adecuados y validados. Por lo tanto, los materiales y métodos para medir nanopartículas, así como métodos de referencia para su determinación después de su liberación al medio ambiente son cruciales. Además, también se necesitan ensayos in vivo que implican estudios de exposición a largo plazo para aumentar el conocimiento de los posibles riesgos para el ser humano y el medio ambiente.

1.3. Fulerenos

Los fulerenos o *Buckyballs* son un grupo de nanopartículas de carbono formados como nano-cajas de diferentes formas que van desde C_{20} a C_{720} (y superiores), que se componen de múltiples pentágonos y hexágonos (Figura 6). Su potencial impacto sobre el medio ambiente es tal vez una de las mayores preocupaciones contemporáneas.

Una propiedad importante de los fulerenos es la capacidad de atravesar las membranas celulares (Jensen et al., 1996) lo que permite su uso en medicina para la administración de fármacos y genes (por ejemplo, en estudio de la diabetes) y para la foto-escisión del ADN (da Ros et al., 1999; da Ros, 2008). Su estructura en forma de jaula les permite encapsular otras moléculas tales como átomos metálicos individuales que pueden servir como absorbentes en biomarcadores (Zhang et al., 2010) y en combinación con biomoléculas, para promover funciones específicas, tales como la catálisis (Willner and Willner, 2010). Su aplicación directa en medicina ha demostrado la capacidad de los fullerenos para regular a la baja el estrés oxidativo en

el tejido pulmonar de ratones portadores de tumores (Jiao et al., 2010). Además, los fullerenos se utilizan en la remediación ambiental, para la descontaminación de patógenos (Mauter and Elimelec, 2008) y en los sistemas de energía, tales como en células solares orgánicas (Shrotriya et al, 2006; Yuan et al., 2011) donde se añaden los derivados de fulereno como moléculas aceptoras a un polímero conductor para crear un material donador/aceptor (Anctil et al., 2011). Sin embargo, se han descrito algunos aspectos de salud adversos de los fulerenos en estudios realizados en ratas (por ejemplo, daño oxidativo en el hígado y los pulmones, y estrés oxidativo en el cerebro) desde principios de 1990 (Aschberger et al., 2010).

Los *buckyballs* son insolubles en agua pero forman suspensiones coloidales o agregados que son estables en ambientes acuosos (Andrievsky et al., 1995; Chen y Elimelec, 2006). Por ejemplo, cuando el C_{60} en un medio acuoso se organiza en un clúster icosaédrico de agua porque el tamaño de la molécula de fulereno y el diámetro interior de la agrupación de agua son similares (Figura 7). Estos grupos de fulereno-agua tienen propiedades ácidas debido a una reacción ácido-base por complejación mediante un sistema donador-aceptor de electrones entre el agua y carbonos sp^2 de los fulerenos resultando en una superficie cargada negativamente que aumenta la solubilidad de C_{60} en más de ocho órdenes de magnitud (Isaacson et al., 2009). Además, estos grupos esféricos de fulereno-agua se agregan en forma de estructuras irregulares más grandes, con tamaños de hasta 5 micras (Brant et al, 2005; Lyon et al, 2006).

La estabilidad coloidal de los fulerenos depende de sus propiedades fisicoquímicas en el medio acuoso dado y se refleja en última instancia en la agregación de partículas y el su comportamiento de deposición. La evaluación de los riesgos planteados por los fulerenos requiere una mejor comprensión de su movilidad, bio-disponibilidad y toxicidad. Adicionalmente, los compuestos de fulerenos pueden tener propiedades muy diferentes dependiendo de la funcionalización, así como del método para su síntesis que también tendrá implicaciones importantes para la evaluación de su comportamiento ambiental.

Con el fin de entender el comportamiento de los fulerenos tanto en productos de consumo como en matrices ambientales, así como su destino y toxicidad para los seres humanos, se requieren métodos fiables para su análisis cuantitativo y cualitativo. Para lograr esto, el acceso a metodologías analíticas robustas es esencial para la detección y caracterización de nanopartículas de fulereno en una amplia gama de matrices.

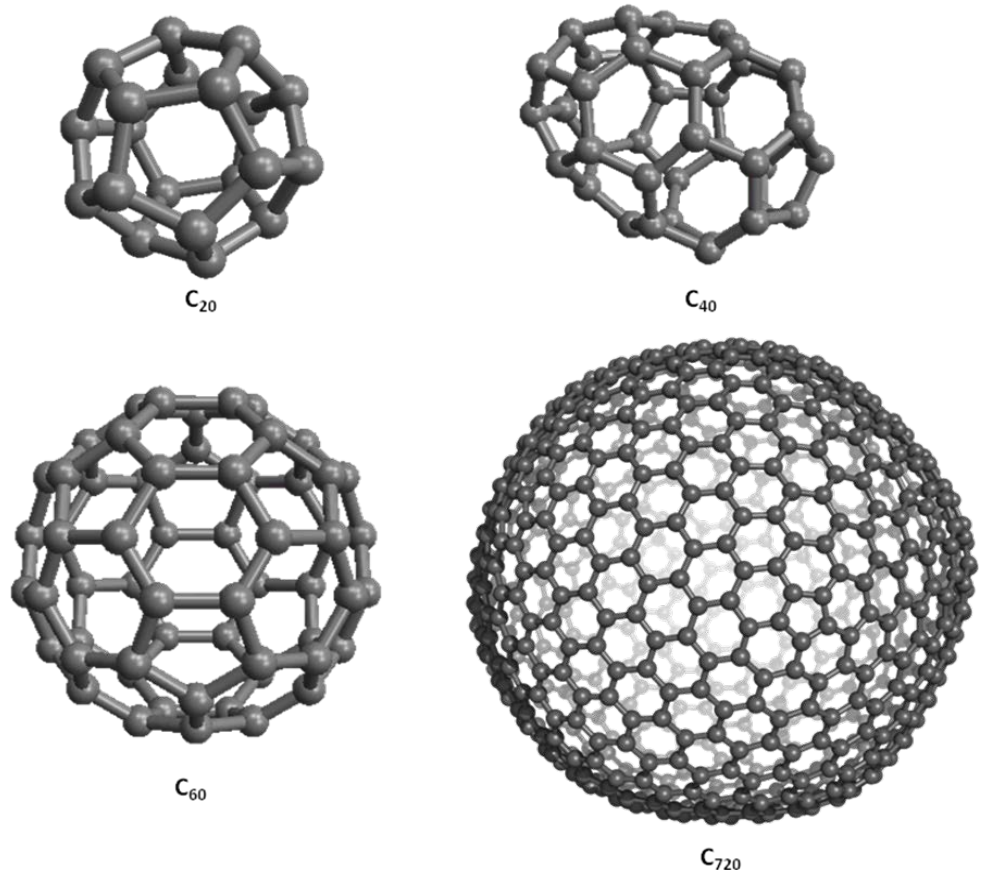

Figura 6. Estrucuras de fulerenos C_{20}, C_{40}, C_{60} y C_{720} (Tomanek, D. and Frederick, N., 2015) [38].

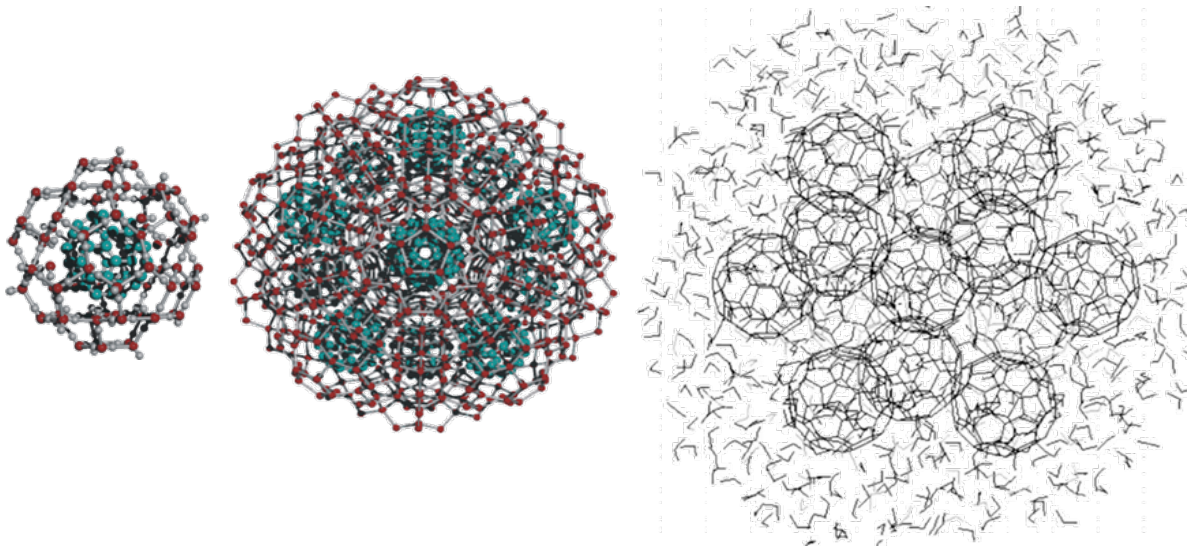

Figura 7. Un solo clúster de fulereno en agua, cluster de fulereno (modificado después de Chaplin M., 2015) y los agregados de fulerenos (de izquierda a derecha). Reproducido con permiso de (Andrievsky et al., 2002). Derechos de autor (2002) Elsevier.

2. Trabajo Experimental

2.1. Análisis de fulerenos en muestras ambientales y productos cosméticos

Dada la falta de estudios relacionados con la presencia y el comportamiento de los fulerenos en los productos de consumo y matrices ambientales, así como sus posibles riesgos tanto para el medio ambiente como para los humanos, es cada vez más importante caracterizar y cuantificar las nanopartículas de fulerenos y especialmente, de los derivados de éstos en matrices de diferente naturaleza. En cuanto los métodos de análisis de estos compuestos en muestras complejas, la cromatografía de líquidos (LC) acoplada a detección UV-Vis o a espectrometría de masas (MS) y la electroforesis capilar (CE) con detección UV-Vis son las técnicas más utilizadas. Hasta hoy en dia, los estudios descritos en la literatura se centran principalmente en el análisis de fullerenos convencionales y muy pocos estudios incluyen algunos derivados, y además se abordan un número limitado de matrices.

Con el fin de suplir esta falta de conocimiento, uno de los objetivos de esta tesis fue el desarrollo de metodologías analíticas para la determinación de fullerenos convencionales así como de algunos fulerenos funcionalizados. Para ello se han puesto a punto métodos basados en cromatografía de líquidos acoplada a espectrometría de masas (LC-MS) y en electroforesis capilar, tanto en medio no acuoso (NACE) como por cromatografía electrocinética micelar (MECC) con detección UV –Vis. Los métodos optimizado se han aplicado al análisis de diferentes matrices ambientales (muestras de agua y sedimentos) y productos cosméticos, respectivamente.

2.1.1 Análisis de fulerenos en muestras ambientales por LC-MS

Separación cromatográfica

Entre los desafíos actuales que enfrenta el análisis de los fulerenos existe la necesidad de separar y distinguir entre fullerenos convencionales de diferente tamaño, así como diferenciarlos de los que presentan diferentes grupos funcionales.

El orden de elución de los fulerenos hidrófobos en columnas de fase inversa se correlaciona con la presencia y el número de grupos funcionales (fulerenos funcionalizados eluyen antes que los fulerenos convencionales), y con el tamaño de la estructura ("jaula") del fulereno (mayor tamaño, mayor retención). Además, la retención de esta familia de compuestos en este tipo de columnas se controla mediante la adición de un disolvente polar (por ejemplo,

metanol o acetonitrilo) a un disolvente no-polar (tolueno) ya que la interacción de los fullerenos con disolventes aromáticos tales como el tolueno es más fuerte que con disolventes polares. En la Figura 1 se muestran las estructuras de los fulerenos estudiados.

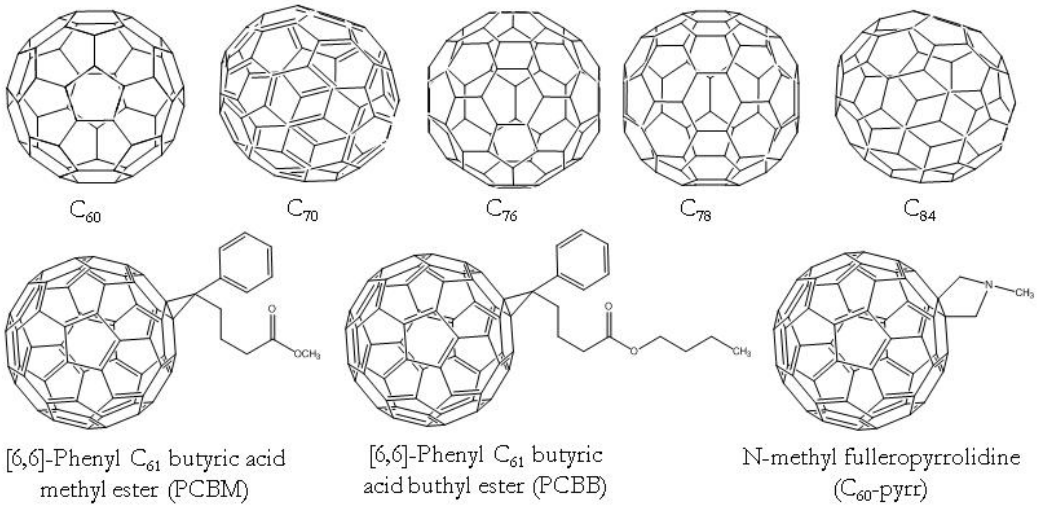

Figura 1. Estructura de los fulerenos estudiados.

Para llevar a cabo la separación cromatográfica de los fulerenos estudiados se evaluaron dos tipos de columnas C18, una con partículas totalmente porosas (Hypersil GOLD) y otra superficialmente porosa (*core-shell*) (Accucore C18) usando elución isocrática (toluno: metanol, 60:40, v/v). En ambas columnas, los derivados de los fulerenos (PCBM, PCBB y C_{60}-pyrr) eluyen antes que los fulerenos convencionales (C_{60}-C_{84}) debido a su mayor polaridad (Figura 2). Para estos últimos, los tiempos de retención aumentaron con el tamaño siendo mayor para los fulerenos con un mayor número de carbonos (C_{76}-C_{84}). El PCBM y el PCBB quedaron menos retenidos en la columna Accucore C18 (Figura 2b) que en la columna con partículas totalmente porosas (Hypersil GOLD) (Figura 2a) debido a la menor área superficial de la partícula frente a la de las partículas totalmente porosas (Staub et al, 2011; Gallart-Ayala et al, 2011; Yang et al, 2011; Destefano et al, 2012). Por el contrario, el C_{60}-pyrr y los fullerenos convencionales presentan una mayor retención en la columna superficialmente porosa (Accucore C18). Este comportamiento puede estar relacionado con el tamaño de los fulerenos y el tamaño de poro de la columna ya que los fulerenos con forma simétrica y tamaño relativamente grande (~ 10 Å para C_{60}) presentan mayor interacción con la columna de menor tamaño de poro (80 Å, Accucore C18) que con la columna totalmente porosa (175 Å, Hypersil GOLD). El diferente comportamiento mostrado por C_{60}-pyrr en comparación con los otros dos derivados del fulereno C_{60} podría estar relacionado con el tamaño de los grupos funcionales unidos a la estructura

buckyball, y en consecuencia a su geometría. De entre los tres compuestos evaluados, el C_{60}-pyrr tiene el grupo funcional más pequeño, y por lo tanto su simetría y el comportamiento de retención son más similares a las del C_{60} que a los de los otros derivados.

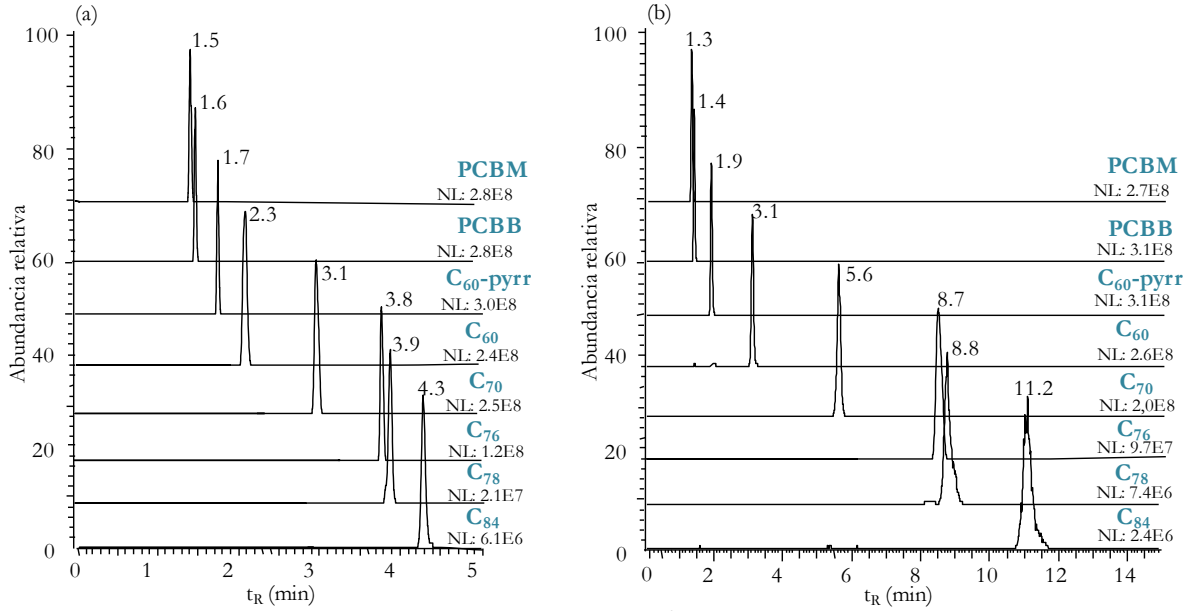

Figura 2. Separación de fulerenos por UHPLC–APPI-MS(/MS) utilizando columnas (a) Hypersil GOLD C18 (150 mm × 2.1 mm, 1.9 μm) y (b) Accucore C18 (150 x 2.1 mm, 2,6 μm) y tolueno:methanol (40:60, v/v) como fase móvil, flujo: 500 μL min^{-1}.

El comportamiento cromatográfico de los fulerenos en mezclas que contienen la misma proporción de tolueno- metanol y tolueno-acetonitrilo en modo isocrático ha sido uno de los aspectos más relevantes observado durante la optimización de la separación cromatográfica de los fulerenos estudiados. Sorprendentemente, se han obtenido tiempos de retención más elevados (hasta 1,65 veces mayor para C84) al usar de tolueno: acetonitrilo que con tolueno: metanol (véase la Figura 4 Sección 2.2, Capítulo 2.). En teoría, debería ocurrir lo contrario ya que la fuerza eluotrópica de la primera mezcla es mayor, y en consecuencia, se deberían obtener tiempos de retención inferiores. En cromatografía de fase invertida la retención de los fulerenos depende de su tamaño y cuanto mayor es el tamaño, mayor es su retención. Por lo tanto, el comportamiento de retención inesperado observado en estas mezclas de disolventes podría estar relacionado con su tamaño de partícula. Este hecho puede explicarse ya que, a pesar de la alta solubilidad de los fulerenos en disolventes no polares se ha descrito que tiene lugar una cierta agregación de estos compuestos en disolventes no polares puros (tolueno, benceno, etc.) (Nath et al, 1998; Rudalevige et al, 1998), y en mezclas binarias de tolueno con un disolvente

débil (metanol, acetonitrilo, etc.) (Sun et al, 1995; Rudalevige et al., 1998; Mrzel et al., 1999; Alargova et al, 2001). La presencia del disolvente débil fuerza que las moléculas de fullerenos se rodeen del disolvente fuerte lo que permite mantener estas entidades juntas formando gotitas de emulsión que cuando la concentración de fulereno alcanza el punto de saturación dan lugar a agregados de fulerenos (Ghosh et al., 1996; Mrzel et al, 1999; Alargova et al, 2001). Por otra parte, se ha descrito que los tamaños de los agregados formados disminuyen al aumentar la polaridad del disolvente débil (Mrzel et al., 1999; Alargova et al., 2001). Por lo tanto, los tiempos de retención más elevados observados en la fase móvile tolueno: acetonitrilo que en la de tolueno: metanol podría ser debido a la formación de agregados más grandes en la primera mezcla.

La separación cromatográfica de los ocho fulerenos estudiados se ha conseguido en menos de 4,5 min empleando una columna C18 de < 2 micras utilizando tolueno:metanol como fase móvil y elución por gradiente. La Figura 3 muestra el cromatograma obtenido en las condiciones óptimas de separación.

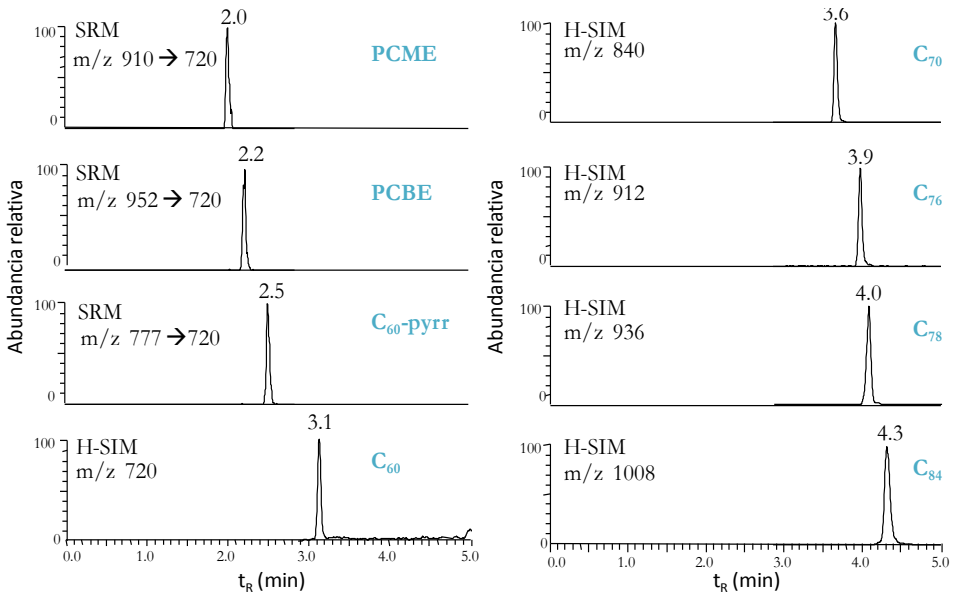

Figura 3. Separación de fulerenos por UHPLC–APPI-MS(/MS) utilizando una columna Hypersil GOLD C18 (150 mm × 2.1 mm, 1.9 μm) y tolueno:metanol como fase móvil (elución por gradiente) a un flujo de 500 μL min^{-1}.

Espectrometría de masas

Para el acoplamiento de la cromatografía de líquidos a la espectrometría de masas se han evaluado diferentes fuentes de ionización (ESI, H-ESI, APCI, APPI). Dependiendo de la fuente

de ionización utilizada, el modo de ionización (positivo y negativo) y las condiciones específicas de funcionamiento de la fuente de ionización (por ejemplo, temperatura de la fuente, voltaje aplicado, corriente de descarga, etc.) se han obtenido resultados diferentes en términos de selectividad y sensibilidad. Sin embargo, independientemente de la fuente, siempre se ha observado una eficiencia de ionización más alta en modo negativo. Los picos más abundantes en los espectros de MS corresponden al clúster isotópico del anión molecular $[M]^{-\bullet}$, que contiene los iones de m/z a M, M+1, M+2, y M+3 (ver Figura 4 para los fulerenos funcionalizados estudiados). Entre las fuentes de ionización evaluadas, el APCI ha proporcionado mejores resultados que el ESI y el H-ESI, lo que puede explicarse porque la captura de electrones se ve favorecida en el plasma del APCI. Sin embargo, la mayor respuesta se ha obtenido en APPI (véase la Figura 2, Sección 2.2., Capítulo 2), comportamiento que coincide con el de los los fullerenos convencionales (Núñez et al., 2012). Las elevadas respuestas en APPI están relacionadas, como se ha mencionado previamente, con el uso de tolueno en la fase móvil que mejora la eficiencia de ionización de estos compuestos.

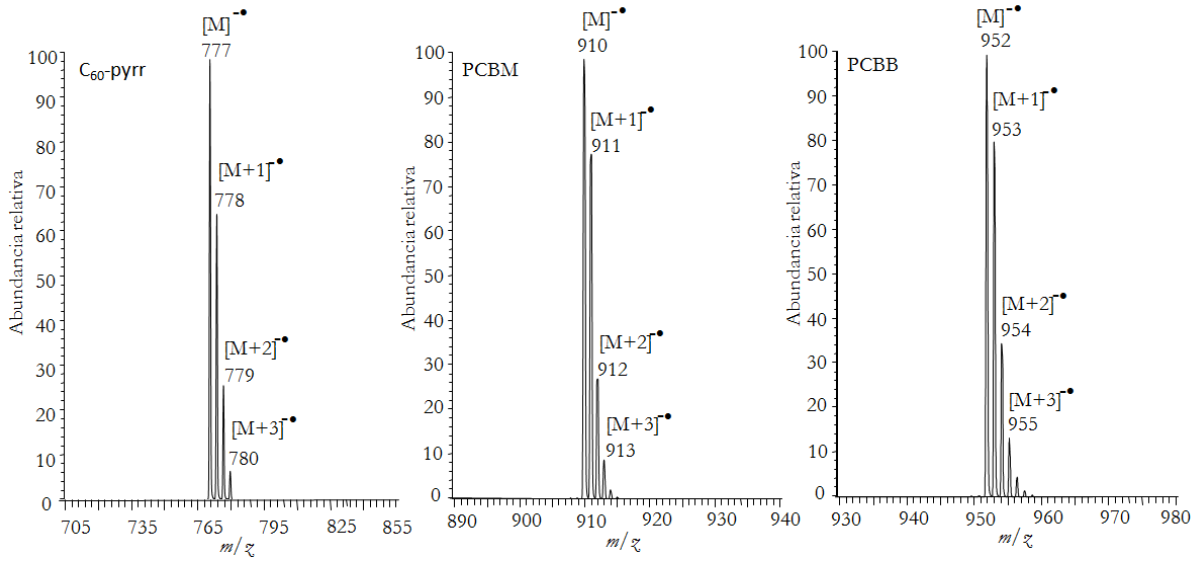

Figura 4. Espectros de los fullerenos funcionalizados obtenidos por UHPLC-(-)APPI-MS, toluene:metanol (45:55, v/v).

Al contrario que los fullerenos convencionales, que no pueden ser fragmentados debido a la alta estabilidad de su estructura, los derivados de C_{60} estudiados se fragmentan a altas energías de colisión (CE) (> 80 eV) perdiendo completamente el grupo funcional y proporcionando un ión producto principal a m/z 720 correspondiente a $[C_{60}]^{-\bullet}$. Para cumplir con

la legislación de la Unión Europea, se deben utilizar dos transiciones SRM para cada compuesto. En este caso, ya que el clúster isotópico de estos compuestos muestra una elevada abundancia de las contribuciones isotópicas del ^{13}C debido al elevado número de átomos de carbono en sus estructuras (véase la Figura 4), se han seleccionado las transiciones $[M]^{-\bullet} \rightarrow [C_{60}]^{-\bullet}$ para la cuantificación y $[M+1]^{-\bullet} \rightarrow [C_{60}+1]^{-\bullet}$ para la confirmación.

La utilización de APPI como fuente de ionización; el modo de adquisición H-SIM para fullerenos convencionales, trabajando a una resolución > 12 500 en el Q3 (0,06 *m/z* FWHM), y el modo de adquisición SRM (Q1 y Q3 en 0,7 *m/z* FWHM) para los fulerenos funcionalizados ha permitido obtener una adecuadas selectividad y sensibilidad, logrando MLODs entre 0,9 pg L^{-1} y 1,6 ng L^{-1} para las muestras de agua y entre 45 pg Kg^{-1} y 158 ng Kg^{-1} para los sedimentos.

Análisis de muestras ambientales

Para la extracción de los fulerenos de muestras de agua se ha utilizado la extracción líquido-líquido (LLE) con tolueno y la adición de sal para romper la estabilidad de los agregados de fullerenos y facilitar su partición en la fase de tolueno. Con este método de extracción, se han obtenido recuperaciones ligeramente más altas para los derivados de los fulerenos (93-96%) que para los fullerenos convencionales (83-89%), valores que son similares a los descritos previamente por LLE para algunos de estos compuestos. La ventaja del método de extracción utilizado en esta tesis es que permite extraer las partículas suspendidas y los agregados de fulerenos en una sola etapa, mientras que con la extracción en fase solida (SPE) es necesaria una etapa previa de filtración.

Para los sedimentos, se propone el uso de la extracción con líquidos presurizados (PLE) a una temperatura de extracción elevada (150 ° C) utilizando un ciclo de extracción de 10 min. Este método ha permitido obtener buenas recuperaciones para los fullerenos seleccionados (70-92%). Se han obtenido recuperaciones más elevadas para los derivados de los fullerenos (87-92%) que son además superiores a las descritas por UAE en la literatura para los mismos compuestos. Por otro lado, el método desarrollado en esta tesis es más rápido (10 minutos) e implica un menor consumo de disolvente que los métodos de UAE, los cuales requieren hasta 4 horas y cantidades de tolueno superiores. La metodología desarrollada nos ha permitido detectar por primera vez la presencia de C_{60}-pyrr, PCBM y PCBB en sedimentos (2,0-8,5 ng kg^{-1}) y en muestras de agua de estanques (0,1- 5,1 pg L^{-1}). Los fulerenos C_{60} y C_{70} fueron detectados en la mayoría de las muestras analizadas y cuantificados a niveles de hasta 25 ng L^{-1} y 330 ng L^{-1} (muestras de agua) y hasta 1 ng kg^{-1} y 7 ng kg^{-1} (sedimentos), respectivamente.

2.1.2 Análisis de fulerenos en productos cosméticos mediante técnicas electroforéticas

2.1.2.1 Electroforesis capilar en medio no-acuoso (NACE)

Separación

La utilización de NACE con un electrólito soporte (BGE) que contiene una sal de tetraalquilamonio de cadena larga (TDAB, 200 mM) capaz de interactuar con los analitos proporcionándoles carga y, en consecuencia, movilidad electroforética ha permitido la separación de dos fullerenos convencionales (C_{60} y C_{70}) y de dos derivados del C_{60} (C_{60}-pyrr y $C_{60}CHCOOH$). Ha sido necesario añadiral electrolito soporte una sal de tetraalquilamonio de cadena corta (TEAB, 40 mM) para reducir el flujo electroosmótico (EOF) y una mezcla de disolventes que contiene un 6% de metanol y un 10% de ácido acético en acetonitrilo:clorobenceno (1:1, v/v). En la Figura 5 se muestra el electroferograma obtenido en las condiciones óptimas.

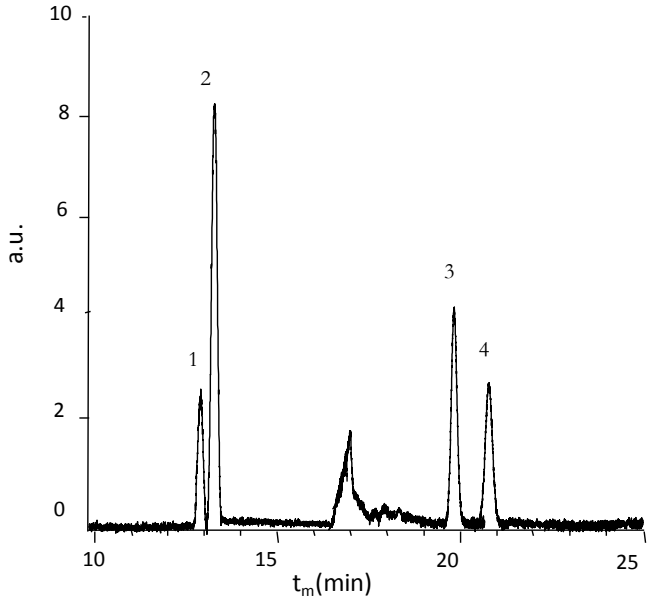

Figura 5. Separación de los fulerenos por NACE; 1: C_{70}; 2: C_{60}; 3: C_{60}-pyrr; 4: $C_{60}CHCOOH$; BGE: 200 mM TDAB, 40 mM TEAB, 6% metanol, 10% acido acético y acetonitrilo:clorobenzeno 1:1 (v/v); V= +30 kV; inyección hidrodinámica, 5 s (50 mbar), λ= 350 nm.

Análisis de productos cosméticos

Los límites de detección obtenidos, en base a una relación señal/ruido de 3:1, fueron de entre 1 y 3,7 mg L^{-1}. La metodología establecida por NACE se ha aplicado por primera vez a la cuantificación de C_{60} en un producto cosmético y el resultado obtenido (2,10 ± 0,20 mg L^{-1}) se

ha comparado con el obtenido mediante el análisis del mismo producto por LC-MS (1,93 ± 0,15 mg L^{-1}) y los resultados obtenidos muestran la buena veracidad del método NACE establecido. Por ello se propone el método NACE desarrollado como una alternativa a la LC convencional para la determinación de C_{60} en muestras de cosméticos donde este compuesto está presente a una concentración relativamente elevada, siendo un método menos caro y que implica un menor consumo de disolventes.

2.1.2.2 Cromatografía electrocinética micelar (MECC)

Se ha evaluado el uso de la MECC con micelas de SDS (100 mM) y 10 mM tetraborato de sodio-10 mM fosfato de sodio como BGE para el análisis de C_{60}, C_{70} y C_{60}-pyrr. Ahora bien, los electroferogramas obtenidos mediante el análisis por MECC de los complejos de fullereno-SDS indican que se produce una fuerte interacción entre los compuestos y las micelas de modo que quedan completamente unidos al núcleo hidrofóbico de las mismas, lo que conlleva que el tiempo de migración de los tres compuestos sea el mismo. Por lo tanto, esta técnica sólo se puede aplicar para el análisis individual de los fulerenos hidrófobos en control de calidad de productos donde sólo uno de estos compuestos este presente. La Figura 6 mustra como ejemplo el electroferograma de un patrón de C_{60} por MECC.

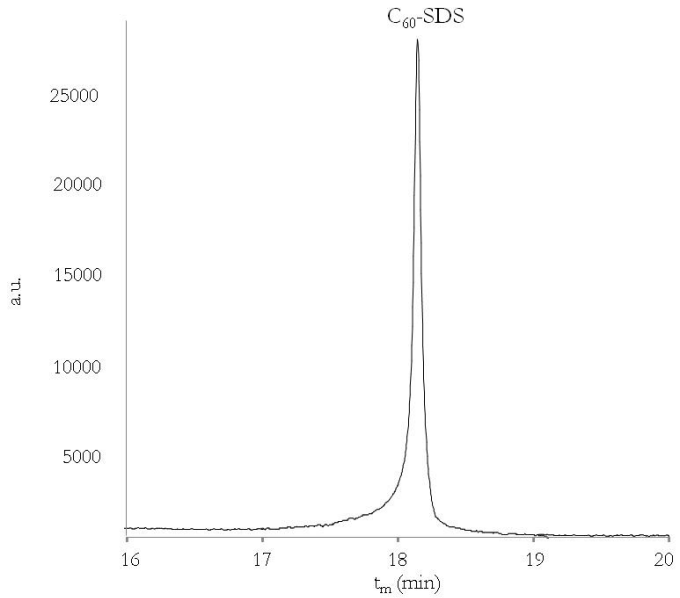

Figura 6. Análisis de C_{60} por MECC; BGE: 100 mM SDS, 10 mM tetraborato de sodio- 10 mM fosfato de sodio, V= +20 kV; inyección hidrodinámica, 5 s (50 mbar), λ= 254 nm.

Por lo tanto, se propone este método para el análisis individual de fullerenos en productos cosméticos mostrando una buena repetitividad y reproducibilidad, logrando LODs entre 0,6 y 2,2 mg L^{-1}, que son inferiores a los encontrados por NACE). La aplicabilidad del método se evaluó mediante la cuantificación de C_{60} en dos productos cosméticos donde se encontró a niveles de concentración de 1,86 ± 0,07 mg L^{-1} (suero anti-envejecimiento) y de 2,77 ± 0,16 mg kg^{-1} (mascarilla). La misma muestra de anti-envejecimiento también se analizó por el método NACE previamente propuesto y por LC-MS, obteniendo resultados similares. Por lo tanto, MECC podría ser utilizada como una alternativa a NACE y LC-MS para el análisis de C_{60} en productos cosméticos, ya que presenta la ventaja de ser menos contaminante que los otros dos métodos al no utilizar disolventes orgánicos.

2.2. Caracterización de los agregados de fulerenos funcionalizados en soluciones acuosas

La evaluación de la presencia y las cantidades detectadas de fulerenos en muestras ambientales no es suficiente para permitir una evaluación realista de los riesgos de estos compuestos. Los principales parámetros de interés con respecto a la seguridad de las nanopartículas son: el grado de agregación, la distribución por tamaños, la morfología de la superficie, la superficie específica y la estructura química. La movilidad y la toxicidad de los fulerenos en el medio ambiente dependen de la distribución por tamaño y de la forma de las partículas, así como de la estabilidad coloidal de los agregados formados. Los factores dominantes en la estabilidad coloidal en condiciones naturales son el pH, la fuerza iónica y la presencia de materia orgánica natural (Lead and Wilkinson, 2006).

En este contexto, otro objetivo de esta tesis ha sido la caracterización (tamaño de partículas, estructura de los agregados y distribución por tamaños) de fulerenos que presentan diferentes grupos funcionales en soluciones acuosas a diferentes valores de pH y fuerza iónica. Con el fin de obtener una imagen completa de los agregados formados y para aumentar la cantidad de información disponible sobre sus características en esta tesis se utilizaron y se combinaron varias técnicas (CE, AF4, MALS, TEM). Los compuestos seleccionados para estos estudios son fulerenos funcionalizados (Figura 7), los cuales presentan crecientes aplicaciones especialmente en el campo de la biomedicina y para los cuales hay muy poca o ninguna información disponible en la literatura.

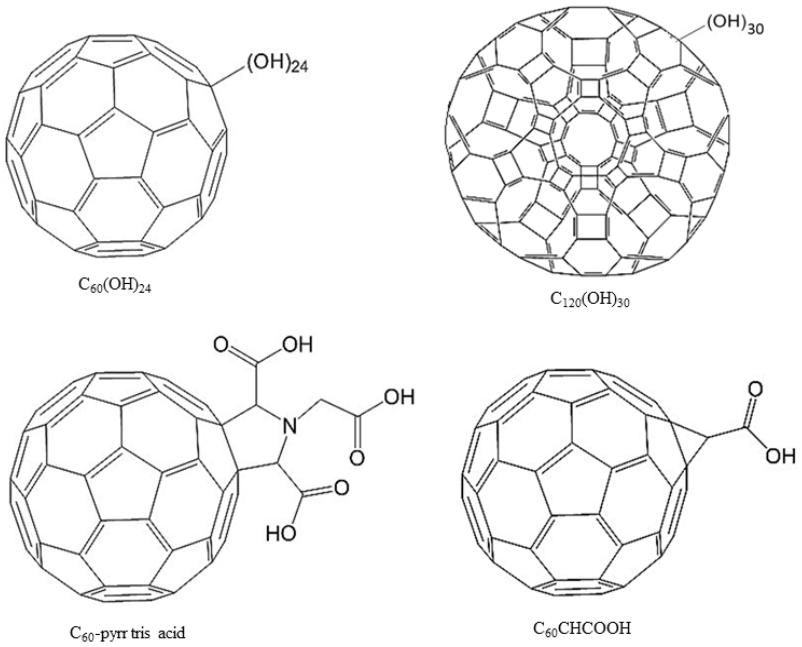

Figura 7. Estructura de los fulerenos funcionalizados estudiados

2.2.1 Tamaño y estructura de agregados de los fulerenos en soluciones acuosas (AF4 y TEM)

Mediante el uso de AF4 se ha conseguido separar las partículas de diferente grado de agregación presentes en las muestras y calcular su tamaño (radio hidrodinámico (r_H)) en soluciones acuosas de diferente fuerza iónica, pH y concentración de SDS. Además, mediante el acoplamiento del AF4 a la MALS, también se ha determinado la distribución por tamaños de las partículas en las condiciones estudiadas.

Una de las principales dificultades encontradas al optimizar el fraccionamiento de las partículas por AF4 ha sido establecer un valor de *cross-flow* óptimo para la separación de las fracciones. Debido a la alta polidispersidad de estas muestras, la elución isocrática no es eficiente y con ninguno de los valores de *cross-flow* utilizados se ha consiguido una separación eficiente en un tiempo razonable. Este problema se ha resuelto utilizando una programación del *cross-flow* (*time delayed exponential*, TDE). Los programas de TDE utilizados para el fraccionamiento de los analitos estudiados, aplicando un *cross-flow* y *focus-flow* inicial de 2 mL/min, y los valores de r_H calculados se muestran en la Figura 8. Al comienzo del programa, el *cross-flow* se ha mantenido constante durante un cierto tiempo y luego se ha disminuido exponencialmente con una constante de tiempo igual al tiempo de retardo (el tiempo que el *cross-flow* se mantiene constante). Para los polihidroxi-fulerenos, se requiere un tiempo de retardo/decadencia de 7 min y un

tiempo mínimo de enfoque (*focusing*) de 10 min para lograr una buena separación del pico del frente de elución y el fraccionamiento de las partículas en un tiempo razonable. Valores de *focus-flow* superiores a 10 min produce un aumento en el r_H de las partículas, debido a la agregación inducida ya que durante el enfoque las partículas están fuertemente concentradas cerca de la pared, y las interacciones partícula-partícula pueden ser más prominentes. Se ha observado un comportamiento similar al utilizar caudales de *cross-flow* y *focus-flow* mayores de 2 mL/min. Para los carboxi-fulerenos, el efecto de las condiciones de flujo (*cross-flow* y *focus-flow*) y el tiempo de enfoque es insignificante, y en contraste a los polihidroxi-fulerenos, los valores de r_H no estan afectados por estos parámetros experimentales. Para estos compuestos, las condiciones óptimas de fraccionamiento han sido un tiempo de enfoque de 3 min y un tiempo de retardo/decadencia de 3 min, utilizando un valor de *cross-flow* y *focus-flow* inicial de 2 mL/min. En cuanto al tipo de membrana, se ha empleado una membrana de celulosa regenerada (RC) de masa nominal 10 kDa y se han obtenido recuperaciones superiores a 79%. En las condiciones mencionadas anteriormente, se ha logrado la separación de varias fracciones lo que ha permitido la determinación de los r_H de las partículas presentes en estas muestras y también su distribución por tamaños mediante el acoplamiento del AF4 -UV al MALS. Los resultados obtenidos por AF4 muestran que $C_{60}(OH)_{24}$ y $C_{120}(OH)_{30}$ presentan tamaños significativamente inferiores (r_H: 4 nm, r_G: hasta 60 nm) a los de C_{60}CHCOOH y C_{60}-pyrr tris acid (r_H: 10-95 nm and r_G: 10-310 nm). Las Figuras 9 y 10 muestran los fractogramas obtenidos por AF4-UV y AF4-MALS, respetivamente. Como se observa en las figuras, los fractogramas de cada uno de los compuestos analizados revelan múltiples picos correspondientes a las partículas en diferentes grados de agregación. (Tabla 1).

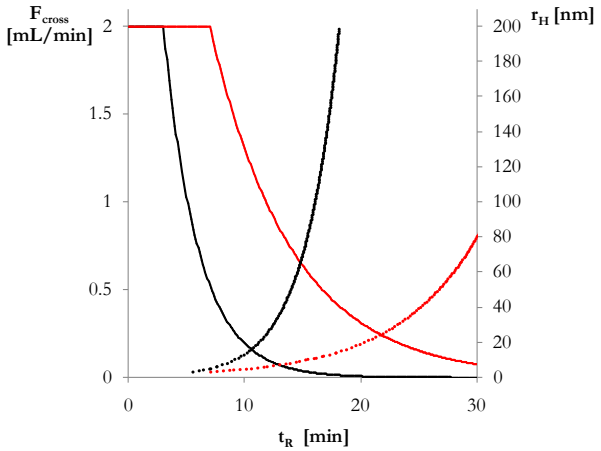

Figura 8. Programas TDE utilizados para el fraccionamiento de fulerenos, tiempo de retardo/decadencia de 3 min (negro) y 7 min (rojo), respectivamente, y los valores de radios hidrodinámicos calculados (r_H) (líneas discontinuas), negro: polihidroxi-fulerenos; rojo: carboxi - fulerenos.

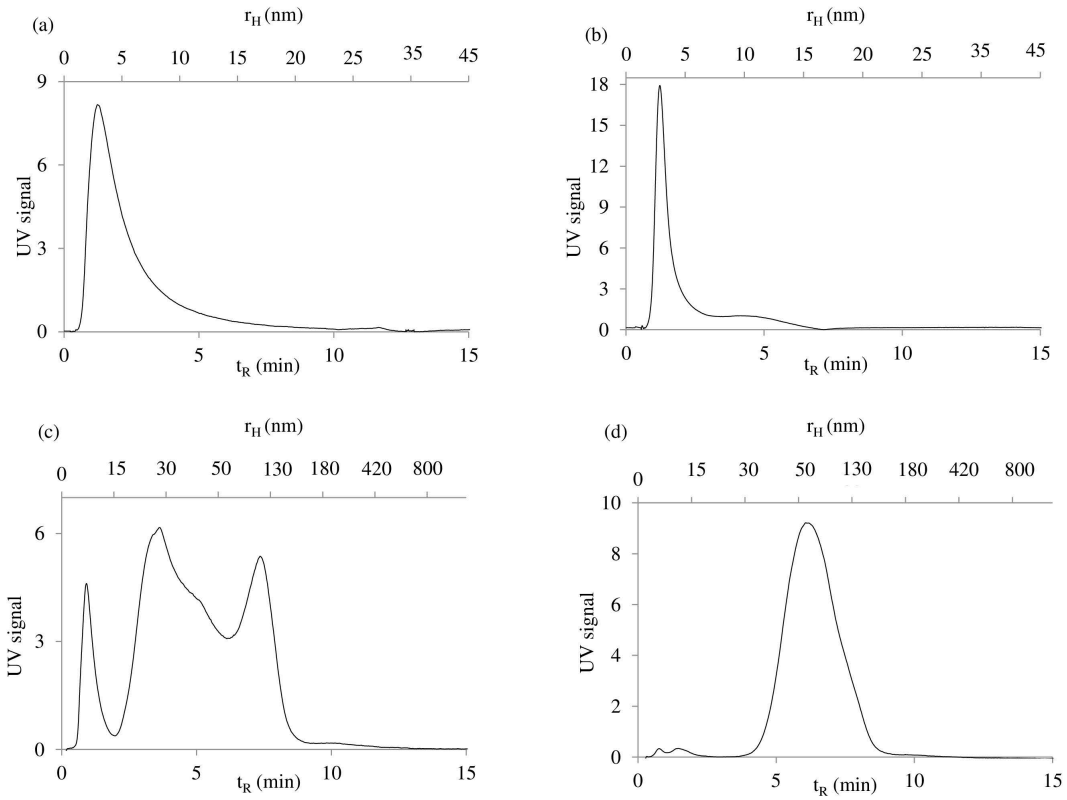

Figura 9. Fractogramas obtenidos por AF4 con detección UV en agua Milli-Q.

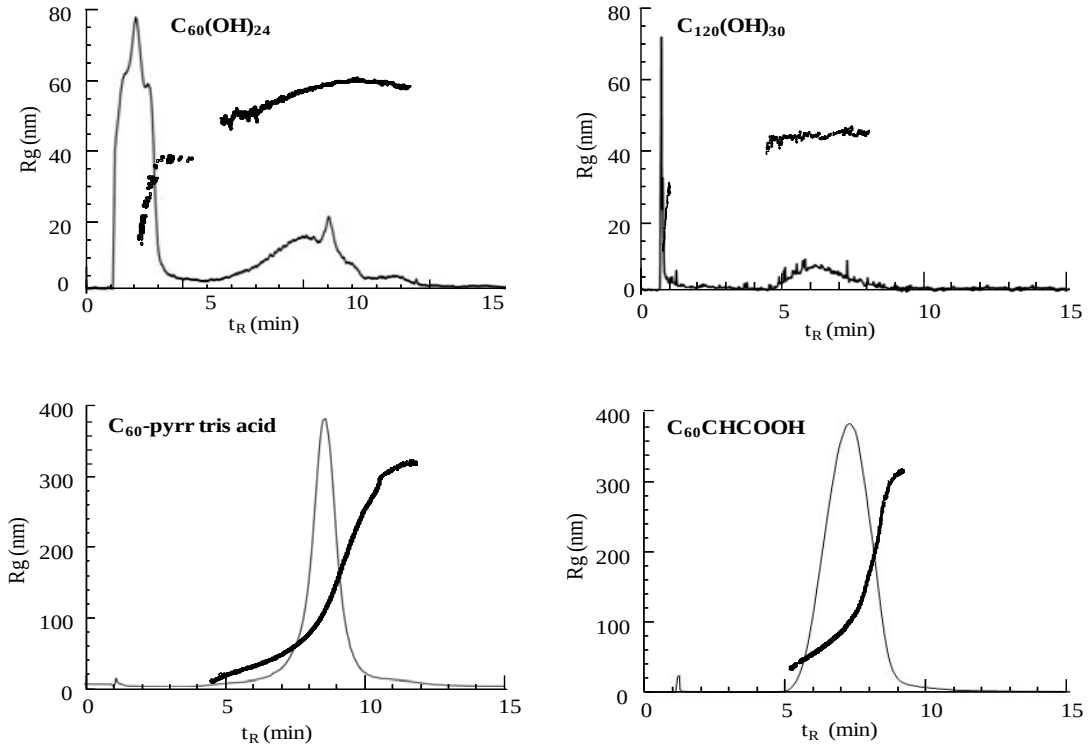

Figura 10. Fractogramas obtenidos por AF4 acoplado a MALS en agua Milli-Q.

Tabla 1. Tamaño de los agregados de fulerenos en soluciones acuosas de diferente fuerza iónica determinados por AF4-UV y AF4-MALS

	$C_{60}(OH)_{24}$		$C_{120}(OH)_{30}$		C_{60}-pyrr tris acid		$C_{60}CHCOOH$	
Fuerza iónica	r_H (nm)	r_G (nm)	r_H (nm)	r_G (nm)	r_H (nm)	r_G (nm)	r_H (nm)	r_G (nm)
0 (agua Milli-Q)	4	1er pico: 10-40 2º pico: 50-60	4 nm	1er pico: 10 -30 2º pico: ≈ 40	1er pico: 10 2º pico: 30 3er pico: 95	1er pico: < 10 2º pico: 15-310	1er pico: 10 2º pico: 55	1er pico: < 10 2º pico: 20-310
0.100	1er pico: 9 2º pico: 30	80-160	1er pico: 8 2º pico: 20	70-100	1er pico: 10 2º pico: 35 3er pico: 180	1er pico: < 10 2º pico: 15-325	1er pico: 10 2º pico: 65	1er pico: < 10 2º pico: 20-315
0.150	1er pico: 13 2º pico: 48	120-180	1er pico: 11 2º pico: 34	100-150	1er pico: 10 2º pico: 66 3er pico:-	1er pico: < 10 2º pico: 15-280	1er pico: 10 2º pico: 45	1er pico: < 10 2º pico: 20-290
0.200	1er pico: 14 2º pico: 50	140-180	1er pico: 12 2º pico: 40	120-160	1er pico: 10 2º pico: 65 3er pico: -	1er pico: < 10 2º pico: 15-280	1er pico: 10 2º pico: 45	1er pico: < 10 2º pico: 20-290

r_H: radio hidrodinámico (calculado a la altura máxima del pico)
r_G radio de giro (a la altura máxima del pico)

Las formas de los agregados formados se han estudiado calculando un factor de forma, utilizando los valores de los radios (r_G) obtenidos por MALS y los radios hidrodinámicos calculados a partir de los tiempos de retención en AF4 a la altura máxima de los picos. Los resultados indican una importante desviación de la forma esférica para los polihidroxi-fulerenos, y la presencia de partículas con forma esférica y forma irregular para los carboxi-fulerenos. Estos resultados están de acuerdo con los obtenidos por TEM que también muestran estructuras altamente ramificadas para los polihidroxi-fulerenos y la presencia de formas esféricas e irregulares para los carboxi-fulerenos (Figura 11).

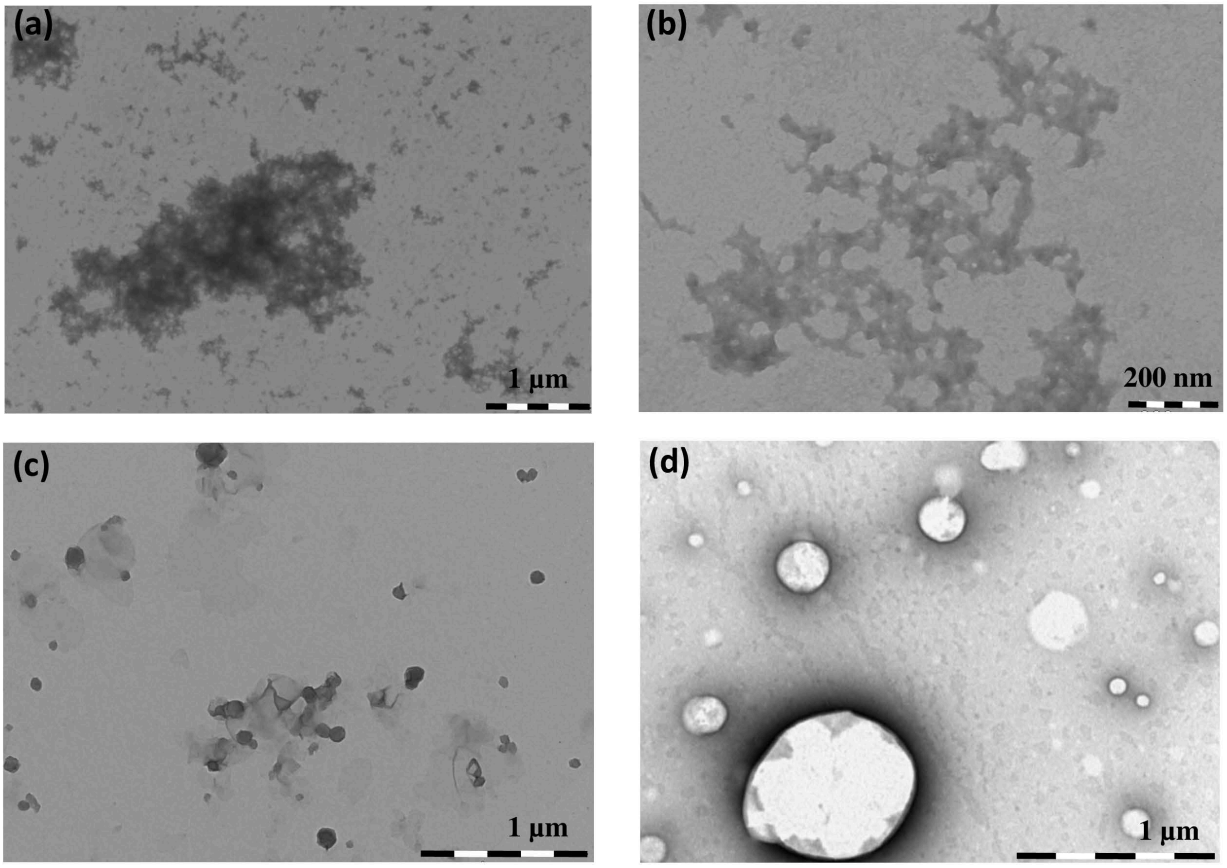

Figura 11. Imágenes de los agregados de fulerenos obtenidas por TEM (a): $C_{60}(OH)_{24}$; (b) $C_{120}(OH)_{30}$; (c) C_{60}-pyrr tris acid; (d) $C_{60}CHCOOH$.

El aumento de la fuerza iónica promueve la agregación de las partículas dando lugar a picos anchos y distorsionados en los fractogramas obtenidos por AF4. La Figura 12 muestra a modo de ejemplo las fractogramas obtenidos para el $C_{60}(OH)_{24}$ y el C_{60}-pyrr tris acid a diferentes valores de fuerza iónica. En los fractogramas de los polihidroxi-fulerenos y a valores de fuerza iónica ≥ 0.1 M, , aparece un pico adicional a un mayor tiempo de retención que corresponde a los agregados más grandes. Por otra parte, el área de este pico aumenta al aumentar la fuerza

iónica ya que la agregación se ve favorecida a altas concentraciones de sal. Por ejemplo, los valores de r_H del $C_{60}(OH)_{24}$, aumentan desde ≈ 4 nm (en agua Milli-Q) hasta 14 nm a un valor de fuerza iónica elevada (0.2 M) (Tabla 1). Los carboxi-fulerenos estudiados también han mostrado un cambio en el perfil de elución y una mayor agregación al aumentar la fuerza iónica. Por ejemplo, a una fuerza iónica de 0,1 M , su r_H es de 180 nm para C_{60}-pyrr tris acid (tercera pico) y de 65 nm para C_{60} - CHCOOH (segundo pico) (Tabla 1). Como se puede observar en la Figura 10, para valores de fuerza iónica superiores a 0.1 M el tercer pico observado para C_{60}-tris acid en agua Milli-Q (línea verde), que corresponde a grandes agregados, ya no es visible. Además, se obtuvieron recuperaciones inferiores al 10 % para ambos carboxi-fulerenos a 0.2 M NaCl ya que el aumento significativo de su tamaño produce su adsorción en la membrana utilizada para el análisis por AF4.

En resumen, se ha observado un aumento del r_G determinado por AF4-MALS para los polihidroxi-fulerenos y una ligera disminución para los carboxi-fulerenos debido a la adsorción de los agregados más grandes en la membrana después del fraccionamiento (Tabla 1). El aumento en la concentración de surfactante en la solución (SDS) permitió distinguir entre las partículas de diferente grado de agregación presentes en las muestras, revelando múltiples picos en los fractogramas obtenidos por AF4. No obstante, no se ha observado un aumento en el tamaño de las partículas con la concentración de SDS.

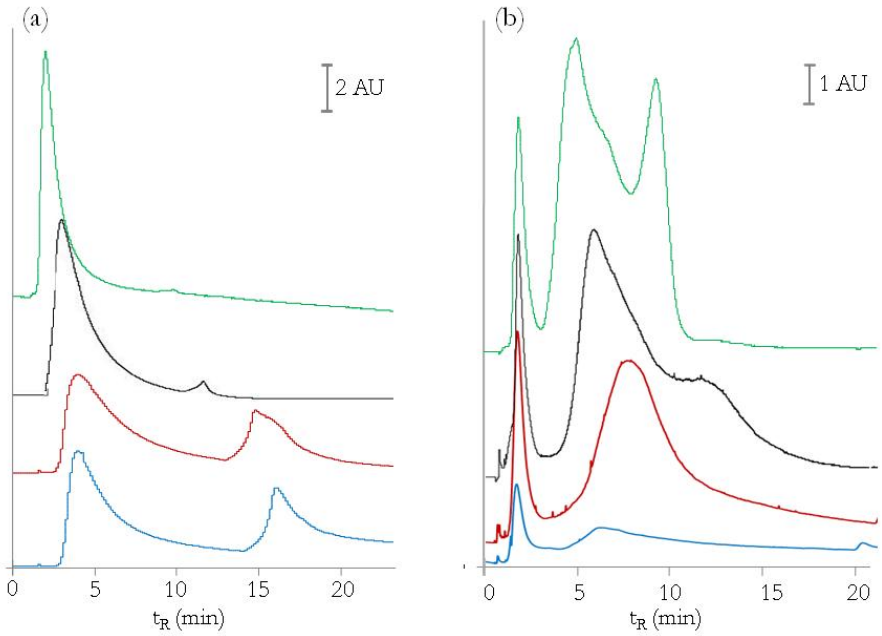

Figura 12. Fractogramas obtenidas por AF4-UV para (a) $C_{60}(OH)_{24}$ and (b) C_{60}-pyrr tris acid a diferentes valores de fuerza ionica: 0 (agua Milli-Q water) (verde), 0.100 (negro), 0.150 (rojo), 0.200 (azul).

2.2.2 Estudio de comportamiento de agregación de fulerenos por técnicas electroforéticas (MECC y CZE)

El mismo electrolito de separación (BGE) utilizado para en análisis de los fulerenos hidrofóbicos por MECC se ha utilizado como electrolito inicial para el análisis de los polihidroxi-fulerenos y los carboxi-fulerenos. En estas condiciones, se han obtenido picos anchos, y distorsionados, lo que ha dificultado la aplicación del método para el análisis de estos compuestos. Sin embargo se ha considerado de interés estudiar la razón por la que estos picos aparecían, y por otra parte, evaluar en qué medida su presencia se puede relacionar con la alta concentración de tampón y a la presencia de micelas en el BGE. Con este objetivo, se ha evaluado el efecto del tampón tetraborato de sodio- fosfato de sodio (entre 2,5 y 15 mM de cada componente) en el perfil electroforético de los derivados de los fulerenos seleccionados manteniendo constante la concentración de SDS (100 mM). El uso de concentraciónes elevadas de tampón tetraborato de sodio- fosfato de sodio (> 5 mM cada uno) ha producido notables diferencias en su perfil electroforético mostrando picos muy anchos, distorsionados y múltiples. A modo de ejemplo, los electroferogramas obtenidos para C_{60}-pyrr tris acid en MECC usando 100mM SDS, y los tampones anteriormente mencionados a concentraciones variables se muestran en la Figura 13. En esta figura se pueden observar dos picos anchos y con cola al usar 15 mM tetraborato de sodio- 15 mM fosfato de sodio (pico A, tm: 4,8 min; pico B, tm: 10.3 min) (Figura 13a). Teniendo en cuenta la elevada tendencia a la agregación de los fulerenos, es razonable pensar que estos picos podrían estar relacionados con la presencia de partículas de diferente grado de agregación que presentan diferentes constantes de distribución con la fase micelar. La disminución de la concentración del tampón conduce a una reducción en los tiempos de migración y en las colas de los picos mejorando las formas de los picos. Por ejemplo para el C_{60}-pyrr tris acid (Figura 13) el área del segundo pico (pico B) disminuye considerablemente, especialmente al utilizar 1 mM tetraborato de sodio (Figura 13d). Esto puede ser debido a una reducción de la fase micelar en disoluciones de electrolitos a concentraciones bajas y también a una disminución en el grado de agregación de los fullerenos que se ve afectada por la presencia de electrolitos.

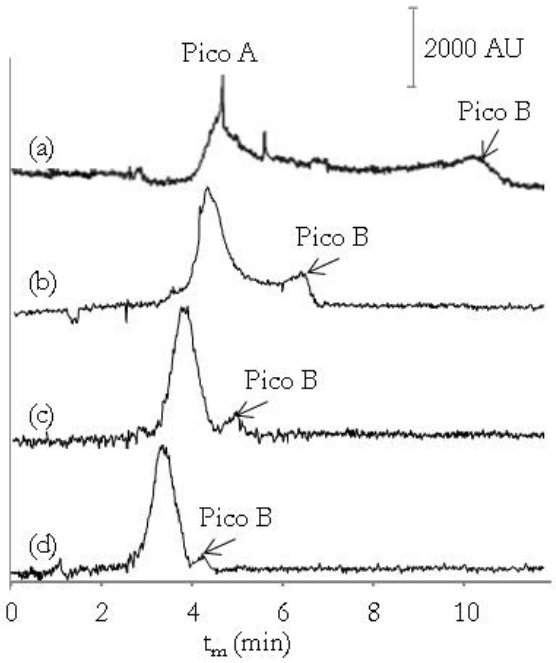

Figura 13. Electroferogramas obtenidas por MECC para C_{60}-pyrr tris acid utilizando como BGE: (a) 100 mM SDS y 15 mM tetraborate de sodio-15 mM fosfato de sodio (pH 9.4); (b) 100 mM SDS y 10 mM tetraborate de sodio-10 mM fosfato de sodio (pH 9.4), (c) BGE: 100 mM SDS y 2.5 mM sodium mM tetraborate de sodio-2.5 mM fosfato de sodio (pH 9.4) y (d) BGE: 100 mM SDS y 1 mM tetraborato de sodio (pH 9.2), V= +20 kV; inyección hidrodinamica (5psi); λ=254 nm.

Con respecto al efecto de la concentración de SDS en los picos electroforéticos, en general, se han obtenido picos más estrechos y tiempos de migración menores al reducir su concentración en el electrolito soporte y, en algunos casos, los perfiles de los picos también cambian. Por ejemplo, en la Figura 14 se puede observar que el segundo pico de C_{60}-pyrr tris acid ya no es visible a valores de concentración de SDS inferiores a 40 mM. Este hecho probablemente se puede relacionar con la fuerza iónica total de la BGE que en estas condiciones no es lo suficientemente elevada para favorecer la agregación de los fullerenos. Por otra parte, la agregación de las micelas a altas concentraciones de SDS, mejora la interacción con los fulerenos de modo que se pueden distinguir las partículas de diferente grado de agregación presentes en la muestra. Un comportamiento similar se ha descrito en la literatura para otro derivado del fulereno (el dendro-fullereno) que también mostró mayor número de picos a concentraciones elevadas de SDS en el BGE (Chan et al., 2007). Los autores atribuyen la aparición de varios picos a la heterogeneidad de la muestra (presencia de diferentes tamaños de partículas) como resultado del proceso de síntesis.

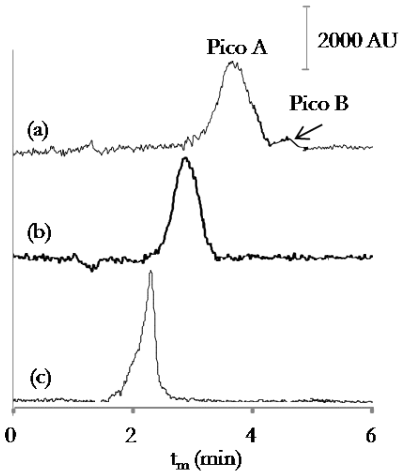

Figura 14. Electroferogramas obtenidos para C_{60}-pyrr tris acid a diferentes valores de concentraciones de SDS: (a) 100 mM SDS; (b) 40 mM SDS; (c) 2 mM SDS; otras condiciones de BGE: 1 mM tetraborato de sodio; inyección hidrodinamica (5psi); λ=254 nm.

La Figura 15 muestra los electroferogramas obtenidos para cada compuesto en MECC y CZE. Como se puede observar, se obtuvieron picos anchos y distorsionados trabajando en condiciones de MECC. Estos resultados indican un aumento en la agregación de los compuestos y la presencia de partículas de diferente grado de agregación.

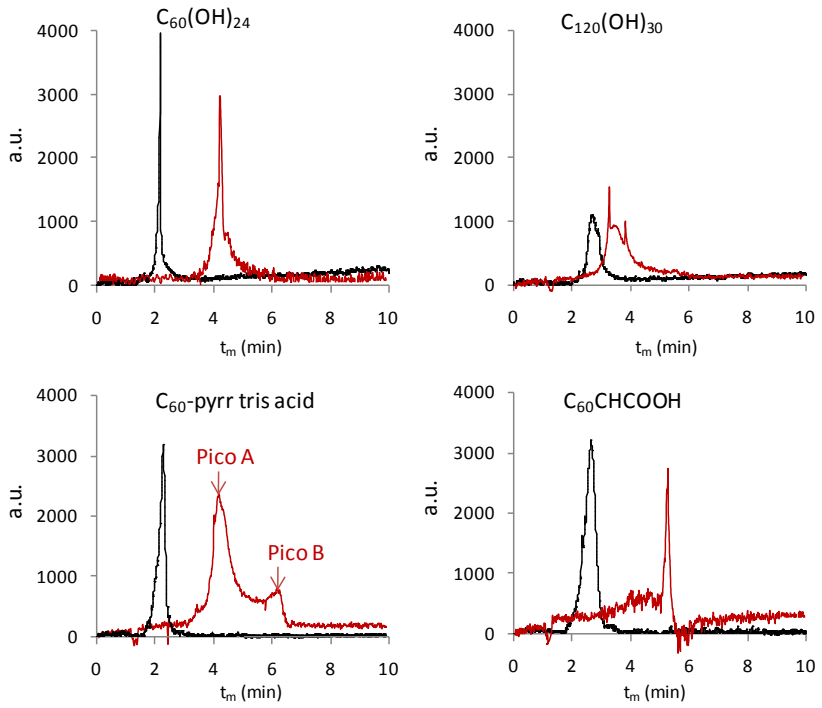

Figura 15. Electroferogramas de los compuestos estudiados obtenidos por MECC (rojo), BGE: 100 mM SDS, 10 mM tetraborate de sodio-10 mM fosfato de sodio (pH 9.4) y CZE (negro), BGE: 2 mM SDS, 1 mM tetraborato de sodio (pH 9.2); V= +20 kV, inyección hidrodinámica (5 psi); λ= 254 nm.

Morfología de los agregados de fulerenos (TEM)

Se ha utilizado TEM con el fin de examinar las estructuras de los agregados formados en el BGE utilizado en MECC. La Figura 12 muestra a modo de ejemplo las imágenes obtenidas para C_{60}-pyrr tris acid en agua Milli-Q (pH 6.5) (Figura 11a) y en 100 mM SDS y 10 mM tetraborato de sodio-10 mM fosfato de sodio (pH 9.4) (Figura 11b). Las imágenes muestran diferencias claras entre las estructuras de los agregados formados en agua y en el electrolito utilizado en MECC, y confirman el aumento de la agregación en este último. La formación de estructuras cristalinas más complejas y ramificadas tanto para los poilihidroxi-fulerenos como para los carboxi-fulerenos causadas por el aumento de la agregación (Figura 11b) explica los picos anchos y múltiples observados en MECC.

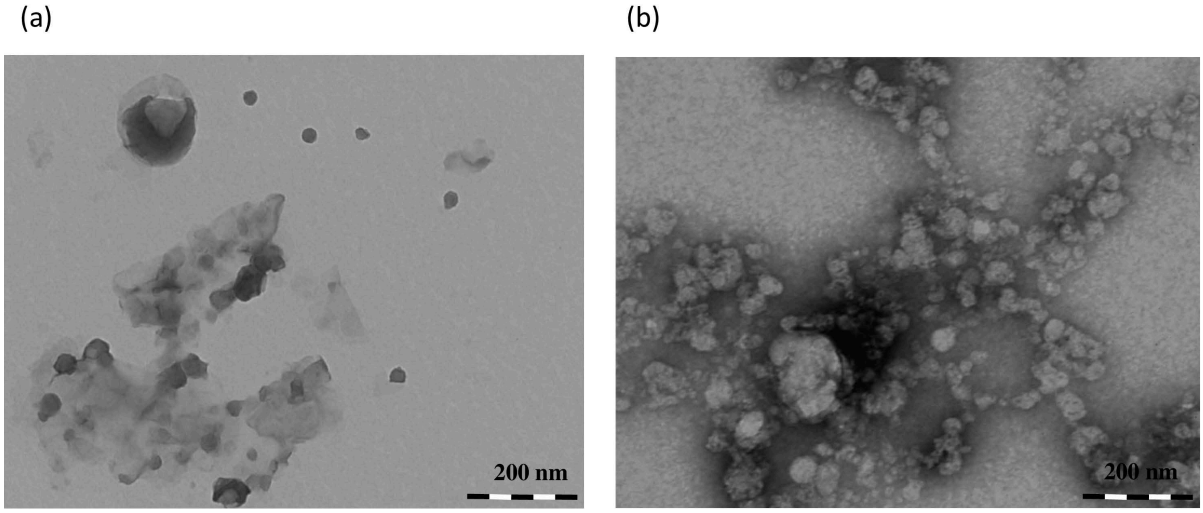

Figura 16. Imágenes obtenidas por TEM para C_{60}-pyrr tris acid en (a) aqua Milli-Q y (b) en 100 mM SDS y 10 mM tetraborato de sodio-10 mM fosfato de sodio.

References

Anctil, A., Babbitt, C.W., Raffaelle, R.P., Landi, B.J., Material and Energy Intensity of Fullerene Production, Environ. Sci. Technol. 45 (2011) 2353-2359.

Andrievsky, G.V., Kosevich, M.V., Vovk, O.M., Shelkovsky, V.S., Vashchenko, L.A., On the production of an aqueous colloidal solution of fullerenes, J. Chem. Soc., Chem. Commun. (1995) 1281-1282.

Andrievsky, G.V., Klochkov, V.K., Bordyuh, A.B., Bovbeshko, G.I., Comparative study of two aqueous colloidal solutions of C60 fullerene with help of FTIR reflactance and UV-VIS Spectroscopy, Chem. Phys. Lett. 364 (2002) 8-17.

Alargova, R.G., Deguchi, S., Tsujii, K., Stable colloidal dispersions of fullerenes in polar organic solvents, J. Am. Chem. Soc. 123(43) (2001) 10460-10467.

Aschberger, K., Johnston, H.J., Stone, V., Aitken, R.J., Tran, C.L., Hankin, S.M., Peters, S.A.K., Christensen, F.M., Review of fullerene toxicity and exposure - Appraisal of a human health risk assessment, based on open literature, Regul. Toxicol. Pharmacol. 58 (2010) 455-473.

Assemi, S., Tadjiki, S., Donose, B.C., Nguyen, A.V., Miller, J.D., Aggregation of Fullerol C60(OH)24 Nanoparticles as Revealed Using Flow Field-Flow Fractionation and Atomic Force Microscopy, Langmuir 26 (2010) 16063-16070.

Baalousha, M., Motelica-Heino, M., Le Coustumera, P., Conformation and size of humic substances: Effects of major cation concentration and type, pH, salinity, and residence time, Colloids and Surfaces A: Physicochemical and Engineering Aspects 272 (2006) 48-55.

Baalousha, M., B. Stolpe, B., J.R. Lead, Flow field-flow fractionation for the analysis and characterization of natural colloids and manufactured nanoparticles in environmental systems: a critical review, J. Chromatogr. A 1218 (2011) 4078-4103.

Benn, T.M., Westerhoff, P., Herckes, Detection of fullerenes (C60 and C70) in commercial cosmetics, Environ. Pollut. 159 (2011) 1334-1342.

Bermudez, O., Forciniti, D., Aggregation and denaturation of antibodies: a capillary electrophoresis, dynamic light scattering, and aqueous two-phase partitioning study, J. Chromatogr. B 807 (1) (2004) 17-24.

Bobylev, A.G., Kornev, A.B., Bobyleva, L.G., Shpagina, M.D., Fadeeva, I.S., Fadeev, R.S., Deryabin, D.G., Balzarini, J., Troshin, P.A., Podlubnaya, Z.A., Fulleronaltes:metalled polyhydroxylated fullerenes with potent anti-amyloid activity, Org. Biomol. Chem. 9 (2011) 5714-5719.

Bouchard, D., Ma, X., Extraction and high-performance liquid chromatographic analysis of C60, C70, and [6,6]-phenyl C61-butyric acid methyl ester in synthetic and natural waters, J. Chromatogr. A 1203 (2008) 153-159.

Botalina, O.V., Sidirov, L.V., Borschchevsky, A.Ya., Sukhanova, E.V., Skokan, E.V., Electron affinities of higher fullerenes, Rapid Commun. Mass Spectrom. 7 (1993) 7009-1011.

Brant, J., Lecoanet, H., Wiesner, M.R., Aggregation and deposition characteristics of fullerene nanoparticles in aqueous systems, J. Nanopart. Res. 7 (2005) 545-553.

Brant, J., Labille, J., Bottero, J.Y., Wiesener, M.R., Characterizing the impact of preparation method on fullerene clusters structure and chemistry, Langmuir 22 (2006) 3878-3885.

Brant, J.A., Labille, J., Robichaud, C.O., Wiesner, M., Fullerol cluster formation in aqueous solutions: Implications for environmental release, J. Colloid Interface Sci. 314 (2007) 281-288.

Cerar, J., Pompe, M., Gucek, M., Cerkovnik, J., Skerjanc, J., Analysis of sample of highly water-soluble Th-symmetric fullerenehexamalonic acid C66(COOH)12 by ion-chromatography and capillary electrophoresis, J. Chromatogr. A 1169 (2007) 86-94.

Carboni, A., Emke, E., Parsons, J.R., Kalbitz, K., de Voogt, P., An analytical method for determination of fullerenes and functionalized fullerenes in soils with high performance liquid chromatography and UV detection, Anal. Chim. Acta 807 (2014) 159-165.

Chan, K.C., Patri, A.K., Veenstra, T.D., McNeil, S.E., Issaq, H.J., Analysis of fullerene-based nanomaterial in serum matrix by CE, Electrophoresis 28 (2007) 1518-1524.Chaplin, M. 2015,

Fullerene hydration (Creative Commons Attribution). Available at: http://www1.lsbu.ac.uk/water/fullerene_hydration.html (accessed on 02/07/2015).

Charkin, O.P., Klimenko, N.M., Wang, Y.-S., Wang, C.-C., Chen, C.-H., Lin, S.H., Theoretical and Experimental Study of fullerenol molecules and ions C60(OH)24-n and C60(OH)24-

n(OL)nL+ succesively substituted by alkali metal atoms L (n=1-24), Russ. J. Inorg. Chem. 56 (2011) 580-590.

Chen, K.L., Elimelech, M., Aggregation and deposition kinetics of fullerene (C60) nanoparticles, Langmuir 22 (2006) 10994-11001.

Chen, H.C., Ding, W.H., Determination of aqueous fullerene aggregates in water by ultrasound-assisted dispersive liquid-liquid microextraction with liquid chromatography-atmospheric pressure photoionization-tandem mass spectrometry, J. Chromatogr. A 1223 (2012) 15-23.

Chen, Y., Cai, R.F., Chen, S., Huang, Z.-E., Synthesis and characterization of fullerenol derived from C60-n precursors, J. Phys. Chem. Solids 62 (2001) 999-1001.

da Ros, T., Prato, M., Medicinal chemistry with fullerenes and fullerene derivatives, Chem. Commun. (1999) 663-669.

da Ros, T., Twenty years of promises: fullerene in medicinal chemistry, Medicinal chemistry and pharmacological potential of fullerenes and carbon nanotubes, 2008, Eds. Cataldo, F., da Ros, T., Springer, The Netherlands, ISBN: 978-90-481-7736-3, pp. 1-21.

Deguchi, S., Alargova, R.G., Tsujii, K., Stable colloidal dispersions of fullerenes in polar organic solvents, J. Am. Chem. Soc. 123(43) (2001) 10460-10467.

Derjaguin, B., Landau, L., Theory of the stability of strongly charged lyophobic sols and of the adhesion of strongly charged particles in solutions of electrolytes, Acta Physicochim. URSS 14 (1941) 633-662.

Destefano, J.J., Schuster, S.A., Lawhorn, J.M., Kirkland, J.J., Performance characteristics of new superficially porous particles, J. Chromatogr. A 1258 (2012) 76-83.

Duffy, C.F., McEathron, A.A., Arriaga, E.A., Determination of individual microsphere properties by capillary electrophoresis with laser-induced fluorescence detection, Electrophoresis 23 (2002) 2040-2047.

Emke, E., Sanchis, J., Farre, M., Bäuerlein, P.S., de Voogt, P., Determination of several fullerenes in sewage water by LC HR-MS using atmospheric pressure photoionisation, Environmen Sci.: Nano (2015) DOI: 10.1039/C4EN00133H.

EPA Regulatory approach on nanomaterials under TSCA. Available at: http://www.epa.gov/oppt/nano/

European Commission (2002) Commission Decision of 12 August 2002 implementing Council Directive 96/23/EC concerning the performance of analytical methods and the interpretation of results. European Commission, Brussels.

European Parliament resolution on "Regulatory aspects of nanomaterials", 2008/2208(INI)

Farre, M., Perez, S., Gajda-Schrantz, K., Osorio, V., Kantiani, L., Ginebreda, A., Barcelo, D., First determination of C60 and C70 fullerenes and N-methylfulleropyrrolidine C60 on the suspended material of wastewater effluents by liquid chromatography hybrid quadrupole linear ion trap tandem mass spectrometry, J. Hydrol. 383 (2010) 44-51.

Fears, R., Kenneth, D., Krug, H., Aebi, K., Stamm, H., Monard, D., Kuhlbusch, T.A., Kreyling, W., Fadeel, B., Baun, A., Riediker, M., Anklam, E., Impact of Engineered Nanomaterials on Health: Considerations for Benefit-Risk Assessment, Joint Research Centre Corporate Activities, Publications Office of the European Union (2011) DOI 10.2788/29424.

Fortner, J.D., Lyon, D.Y., Sayes, C.M., Boyd, A.M., Falkner, J.C., Hotze, E.M., Alemany, L.B., Tao, Y.J., Guo, W., Ausman, K.D., Colvin, V.L., Hughes, J.B., C60 in Water: Nanocrystal Formation and Microbial Response, Environ. Sci. Technol. 39 (2005) 4307-4316.

Freitas, R.A.J., What is nanomedicine?, Nanomedicine 1 (2005) 2-9.

Gallart-Ayala, H., Moyano, E., Galceran, M.T., Fast liquid chromatography-tandem mass spectrometry for the analysis of bisphenol A-diglycidyl ether, bisphenol F-diglycidyl ether and their derivatives in canned food and beverages, J. Chromatogr. A 1218 (2011) 1603-1610.

Ghosh, H.N., Sapre, A.V., Mittal, J.P., Aggregation of C70 in solvent mixtures, J. Phys. Chem. 100 (1996) 9439-9443.

Giddings, J.C., Yang, F.J., Myers, M.N., Flow-field-flow fractionation: a versatile new separation method, Science 193 (1976) 1244-1245.

Gunasekera, N., Musier-Forsyth, K., Arriaga, E., Electrophoretic behavior of individual nuclear species as determined by capillary electrophoresis with laser-induced fluorescence detection, Electrophoresis 23 (2002) 2110-2116.

Hansen, S.H., Bjornsdottir, I., Tjornelund, J., Nonaqueous Capillary Electrophoresis, Electrophoresis (2000) 1293-1300.

Harrison A.G., Chemical ionization mass spectrometry, Boca Raton, FL: CRC Press, Inc. 1983. pp 12-22.

Herrero, P., Bäuerlein, P.S., Emke, E., Pocurull, E., de Voogt, P., Asymmetrical flow field-flow fractionation hyphenated to Orbitrap high resolution mass spectrometry for the determination of (functionalised) aqueous fullerene aggregates, J. Chromatogr. A 1356 (2014) 277-282.

Heymann, D., Korochantsev, A., Nazarov, M.A., Smit, Search for fullerenes C-60 and C-70 in Cretaceous-Tertiary boundary sediments from Turkmenistan, Kazakhstan, Georgia, Austria, and Denmark, Cretaceous Res. 17 (1996) 367-380.

Hoet, P.H., Brüske-Hohlfeld, I., Salata, O.V., Nanoparticles -known and unknown health risks, J. Nanobiotechnol. 2 (2004) 1-15.

Hull, M.S., Kennedy, A.J., Steevens, J.A., Bednar, A.J., Weiss, C.A.J., Vikesland, P.J., Release of Metal Impurities from Carbon Nanomaterials Influences Aquatic Toxicity, Environ. Sci. Technol. 43 (2009) 4169-4174.

Husebo, L.O., Sitharaman, B., Furukawa, K., Kato, T., Wilson, L.J., Fullerenols Revisited as Stable Radical Anions, J. Am. Chem. Soc. 126 (2004) 12055-12064.

Indeglia, P.A., Georgieva, A., Krishna, V.B., Bonzongo, J.J., Physicochemical characterization of fullerenol and fullerenol synthesis by-products prepared in alkaline media, J. Nanopart. Res. 16 (2014) 1-15.

Inventory of nanotechnology-based consumer products. Available at: http://www.nanotechproject.org/cpi/about/analysis/

Isaacson, C.W., Usenko, C.Y., Tanguay, R.L., Field, Quantification of Fullerenes by LC/ESI-MS and Its Application to in Vivo Toxicity Assays, Anal. Chem. 79 (2007) 9091-9097.

Isaacson, C.W., Bouchard, D., Asymmetric flow field flow fractionation of aqueous C60 nanoparticles with size determination by dynamic light scattering and quantification by liquid chromatography atmospheric pressure photo-ionization mass spectrometry, J. Chromatogr. A 1217 (2010) 1506-1512.

Isaacson, C.W., Kleber, M., Field, J.A., Quantitative analysis of fullerene nanomaterials in environmental systems: a critical review, Environ. Sci. Technol. 43 (2009) 6463-6474.

Jakubek, L.M., Marangoudakis, S., Raingo, J., Liu, X., Lipscombe, D., Hurt, R.H., The inhibition of neuronal calcium ion channels by trace levels of yttrium released from carbon nanotubes, Biomaterials 30 (2009) 6351-6357.

Jensen, A., Wilson, S., Schuster, D.I., Biological applications of fullerenes, Bioorg. Med. Chem. 44 (1996) 767-779.

Jiao, F., Qu, Y., Liu, Y., Li, W., Ge, C., Li, Y., Hi, W., Li, B., Gao, Y., Chen, C., Modulation of oxidative stress by functionalized fullerene materials in the lung tissues of female C57/BL mice with metastatic Lewis lung carcinoma, J. Nanosci. Nano-technol. 10 (2010) 8632-8637.

Karn, B., Kuiken, T., Otto, M., Nanotechnology and in situ remediation: a review of the benefits and potential risks. Eniviron. Health. Perspect. 117 (2009) 1813-1831.

Kato, H., Shinohara, N., Nakamura, A., Horie, M., Fujita, K., Takahashi, K., Iwahashi, H., Endoh, S., Kinugasa, S., Characterization of fullerene colloidal suspension in a cell culture medium for in vitro toxicity assessment, Mol. BioSyst. 6 (2010) 1238-1246.

Kawano, S.i., Murata, H., Mikami, H., Mukaibatake, K., Waki, H., Method optimization for analysis of fullerenes by liquid chromatography/atmospheric pressure photoionization mass spectrometry, Rapid Commun. Mass Spectrom. 20 (2006) 2783-2785.

Kolkman, A., Emke, E., Baeuerlein, P.S., Carboni, A., Tran, D.T., ter Laak, T.L., van Wezel, A.P., de Voogt, P., Analysis of (Functionalized) Fullerenes in Water Samples by Liquid Chromatography Coupled to High-Resolution Mass Spectrometry, Anal. Chem. 85 (2013) 5867-5874.

Lacerda, L., Bianco, A., Prato, M., Kostarelos, K., Carbon nanotubes as nanomedicines:from toxicology to pharmacology, Adv. Drug Delil. Rev. 1 (2006) 1460-1470.

Laitinena, T., Petaja, T., Backman, J., Hartonena, K., Junnienen, H., Ruiz-Jimenez, J., Worsnopb, D., Kumala, M., Riekkola, M.L., Carbon clusters in 50 nm urban air aerosol particles quantified by laser desorption–ionization aerosol mass spectrometer, Int. J. Mass Spectrom. 358 (2014) 17-24.

Lead, J.R., Wilkinson, K.J., Natural aquatic colloids: current knowledge and future trends, Environ. Chem. 3 (2006) 159-171.

Litzén, A., Separation Speed, Retention, and Dispersion in Asymmetrical Flow Field-Flow Fractionation as Functions of Channel, Dimensions and Flow rates, Anal. Chem. 65 (1993) 461-470.

Liu, X., Gurel, V., Morris, D., Murray, D.W., Zhitkovich, A., Kane, A.B., Hurt, R.H., , Bioavailability of nickel in single-wall carbon nanotubes, Adv. Mater. 19 (2007) 2790-2796.

Lyon, D.Y., Adams, L.K., Falkner, J.C., Alvarez, P.J.J., Antibacterial activity of fullerene water suspensions: Effects of preparation method and particle size, Environ. Sci. Technol. 40 (2006) 4360-4366.

Ma, X., Bouchard, D., Formation of Aqueous Suspensions of Fullerenes, Environ. Sci. Technol. 43 (2009) 330-336.

Mauter, M.S., Elimelech, M., Environmental Applications of Carbon-Based Nanomaterials, Environ. Sci. Technol. 42 (2008) 5843-5859.

Messaud, F.A., Runyon, J.R., Otte, T., Pasch, H., Ratanathanawongs Williams, S.K., An overview on field-flow fractionation techniques and their applications in the separation and characterization of polymers, Prog. Polym. Sci. (2009) doi:10.1016/j.progpolymsci.2008.11.001.

Mitra, S., Sample Preparation Techniques in Analytical Chemistry, John Wiley & Sons, Inc., New York, 2004.

Moussa, F., Pressac, M., Genin, E., Roux, S., Trivin, F., Rassat, A., Ceolin, R., Szwarc, H., Quantitative analysis of C60 fullerene in blood and tissues by high-performance liquid chromatography with photodiode-array and mass spectrometric detection, J. Chromatogr. B: Biomed. Sci. Appl. 696 (1997) 153-159.

Mrzel, A., Mertelj, A., Omerzu, A., Copic, M., Mihailovic, D., Investigation of Encapsulation and Solvatochromism of Fullerenes in Binary Solvent Mixtures, J. Phys. Chem. B 103 (1999) 11256-11260.

Nath, S., Pal, H., Palit, D.K., Sapre, A.V., Mittal, J.P., Aggregation of fullerene, C60, in benzonitrile, J. Phys. Chem. B 102 (1998) 10158-10164.

Nowack, B, Pollution Prevention and Treatment Using Nanotechnology, Nanotechnology, Volume 2: Environmental Aspects, Ed. Krug, H., 2008, 1-15 Wiley-VCH Verlag, Weinheim.

Núñez, O., Gallart-Ayala, H., Martins, C.P.B., Moyano, E., Galceran, M.T., Atmospheric Pressure Photoionization Mass Spectrometry of Fullerenes, Anal. Chem. 84 (2012) 5316-5326.

Otto, M., Floyd, S., Bajpai, S., Nanotechnology for site remediation, Remed. J 19 (2008) 99-108.

Perez, R.A., Albero, B., Miguel, E., Tadeo, J.L., Sanchez-Brunete, C., A rapid procedure for the determination of C60 and C70 fullerenes in soil and sediments by ultrasound-assisted extraction and HPLC-UV, Anal. Sci. 29 (2013) 533-538.

Pryor, E., Kotarek, J.A., Moss, M., Hestekin, C.N., Monitoring Insulin Aggregation via Capillary Electrophoresis, Int. J. Mol. Sci. 12 (2011) 9369-9388.

Raffaelli, A., Saba, A., Atmospheric pressure photoionization mass spectrometry, Mass Spectrom. Rev. 22 (2003) 318-331.

Rezenom, Y.H., Wellman, A.D., Tilstra, L., Medley, C.D., Gilman, S.D., Separation and detection of individual submicron particles by capillary electrophoresis with laser-light-scattering detection, Anayst 132 (2007) 1215-1222.

Roco, M.C., Nanoscale Science and Engineering: Unifying and Transforming Tools, AIChE J. 50 (2004) 890-897.

Rudalevige, T., Francis, A.H., Zand, R., Spectroscopic Studies of Fullerene Aggregates, J. Phys. Chem. A 102 (1998) 9797-9802.

Sabella, S., Quaglia, M., Lanni, C., Racchi, M., Govoni, S., Caccacialanza, G., Calligaro, A., Belloti, V., De Lorenzi, E., Capillary electrophoresis studies on the aggregation process of -amyloid 1-42 and 1-40 peptides, Electrophoresis 25 (2004) 3186-3194.

Saleh, N.M., Sanagi, M.M., Comparison of pressurized liquid extraction with soxhlet extraction in the determination of polycyclic aromatic hydrocarbons in soil, M. J. Anal. Sci. 13 (2009) 141-145.

Sanchis, J., Bozovic, D., Al-Harbi, N.A., Silva, L.F., Farre, M., Barcelo, D., Quantitative trace analysis of fullerenes in river sediment from Spain and soils from Saudi Arabia, Anal. Bioanal. Chem. 405 (2013) 5915-5923.

Sanchis, J., Berrojalbiz, N., Caballero, G., Dachs, J., Farre, M., Barcelo, D., Occurrence of Aerosol-Bound Fullerenes in the Mediterranean Sea Atmosphere, Environ. Sci. Technol. 46 (2012) 1335-1343.

Sanchis, J., Bosch-Orea, C., Farre, M., Barcelo, D., Nanoparticle tracking analysis characterisation and parts-per-quadrillion determination of fullerenes in river samples from Barcelona catchment area, Anal. Bioanal. Chem. 407 (2015a) 4261-4275.

Sanchis, J., Oliviera, L.F., Leão, F.B., Farre, M., Barcelo, D., Liquid chromatography-atmospheric pressure photoionization-Orbitrap analysis of fullerene aggregates on surface soils and river sediments from Santa Catarina (Brazil), Sci. Total Eniron. 505 (2015b) 172-179.

Schimpf, M.E., Caldwell, C.K., Giddings, J.C., Field Flow Fractionation Handbook, John Wiley & Sons, New York, 2000.

Semenov, K.N., Letenko, D.G., Charykov, N.A., Nikitin, V.A., Matuzenko, M.Y., Keskinov, V.A., Postnov, V.N., Kopyrin, A.A., Synthesis and identification of fullerenol prepared by the direct oxidation route, Russ. J. Inorg. Chem. 83 (2010) 2076-20803.

Shrotriya, V., Yao, Y., Li, G., Yang, Y., Effect of self-organization in polymer/fullerene bulk heterojunctions on solar cell performance, Appl. Phys. Lett. 89 (2006) 063505-1-063505-3.

Silion, M., Dascalu, A., Pinteala, M., Simionescu, B.C., Ungurenasu, C., A study on electrospray mass spectrometry of fullerenol C60(OH)24, Beilstein J. Org. Chem. 9 (2013) 1285-1295.

Staub, A., Zurlino, D., Rudaz, S., Veuthey, J.L., Guillarme, D., Analysis of peptides and proteins using sub-2μm fully porous and sub 3-μm shell particles., J. Chromatogr. A 1218 (2011) 8903-8914.

Su, H.L., Kao, W.C., Lee, C.y., Chuang, S.C., Hsieh, Y.Z., Separation of open-cage fullerenes using nonaqueous capillary electrophoresis, J. Chromatogr. A 1217 (2010) 4471-4475.

Sun, Y.P., Ma, B., Bunker, C.E., Liu, B., , All-Carbon Polymers (Polyfullerenes) from Photochemical Reactions of Fullerene Clusters in Room-Temperature Solvent Mixtures , J. Am. Chem. Soc. 117 (1995) 12705-12711.

Tamisier-Karolak, S.L., Pagliarusco, S., Herrenknecht, C., Brettreich, M., Hirsch, A., Ceolin, R., Bensasson, R.V., Szwarc, H., Moussa, F., Electrophoretic behavior of a highly water-soluble dendro[60]fullerene, Electrophoresis 22 (2001) 4341-4346.

Theron, J., Walker, J.A., Cloete, T.E., Nanotechnology and water treatment: applications and emerging opportunities, Crit. Rev. Microbiol. 34 (2008) 43-69.

Tomanek, D. and Frederick, N, Guide through the Nanocarbon Jungle: Buckyballs, Nanotubes, Graphene. Available at:
http://www.nanotube.msu.edu/fullerene/ (accessed on 27/05/2015)

Tratnyek, P.G., Johnson, R.L., Nanotechnologies for environmental cleanup, Nano Today 1 (2006) 44-48.

Treubig, J.M., Brown, P.R., Novel approach to the analysis and use of fullerenes in capillary electrophoresis, J. Chromatogr. A 873 (2000) 257-267.

Utsunomiya, S., Jensen, K.A., Ewing, G.J., Uranitite and fullerene in atmospheric particulates, Environ. Sci. Technol. 36 (2002) 4943-4947.

van Wezel, A.P., Moriniere, V., Emke, E., ter Laak, T., Hogenboom, A.C., Quantifying summed fullerene nC60 and related transformation products in water using LC LTQ Orbitrap MS and application to environmental samples, Environ. Int. 37 (2011) 1063-1067.

Wahlund, K.G., Improved terminology for experimental field-flow fractionation, Anal. Bioanal. Chem. 406 (2014) 1579-1583.

Wahlund, K.G., Giddings, Properties of an asymmetrical flow field-flow fractionation channel having one permeable wall, Anal. Chem. 59 (1987) 1332-1339.

Wan, T.S.M., Leung, G.N.W., Tso, T.S.C., Komatsu, K., Murata, Y., Non-aqueous capillary electrophoresis as a new method for the separation of fullerenes, Proc. - Electrochem. Soc. 95 (1995) 1474-1487.

Wang, C., Shang, C., Westerhoff, P., Quantification of fullerene aggregate nC60 in wastewater by high-performance liquid chromatography with UV-vis spectroscopic and mass spectrometric detection, Chemosphere 80 (2010) 334-339.

Wang, X.B., Ding, C.F., Wang, L.S., High resolution photoelectron spectroscopy of C60-, J. Chem. Phys. 110 (1999) 8217-8220.

Warheit, D.B., How meaningful are the results of nanotoxicity studies in the absence of adequate material characterization? Toxicol. Sci. 101 (2008) 183-185.

Wiesner, M., Lowry, G.V., Alvarez, P., Biswas, P.R., Assessing the risks of manufactured nanomaterials, Environ. Sci. Technol. 40 (2006) 4336-4345.

Willner, I., Willner, B., Biomolecule-based nanomaterials and nanostructures, Nano Lett. 10 (2010) 3805-3815.

Wyatt, P.J., Light scattering and the absolute characterization of macromolecules, Analytica Chimica Acta 272 (1993) 1-40.

Xia, X.R., Monteiro-Riviere, N.A., Riviere, J.E., Trace analysis of fullerenes in biological samples by simplified liquid-liquid extraction and high-performance liquid chromatography, J. Chromatogr. A 1129 (2006) 216-222.

Yah, S.C., Simate, G.S., Iyuke, S.E., Nanoparticles toxicity and their routes of exposures, J. Pharm. Sci. 25 (2012) 477-491.

Yang, P., McCabe, T., Pursch, M., Practical comparison of LC columns packed with different superficially porous particles for the separation of small molecules and medium size natural products, J. Sep. Sci. 34 (2011) 2975-2982.

Yuan, Y., Reece, T.J., Sharma, P., Poddar, S., Stephen, D., Gruverman, A., Yang, Y., Huang, J., Efficiency enhancement in organic solar cells with ferroelectric polymers, Nature Mat. 10 (2011) 296-302.

Zhang, M., Xing, G., Yuan, H., Transmembrane delivery of aggregated [Gd@C82(OH)22]n nanoparticles, J. Nanosci. Nano-technol. 10 (2010) 8556-8566.

First of all I would like to thank my parents, my grandparents and my brother for their understanding, support, enthusiasm and encouragement. Especially to my mother, who was always close and gave me all the support and strength that I needed to handle the stress, pressure, and sacrifices that came along with this PhD. All that I am and hope to be I owe it to you, my warrior, my role model and my best friend. Without your dedication, patience and guidance I would not have gotten where I am now. Mulțumesc din suflet pentru toate sacrificiile iubita mea.

My deepest gratitude goes to my main supervisor Dr. Maria Teresa Galceran for providing me the opportunity to work in her research group when I was looking for a PhD position back in 2010. I am fortunate to be your PhD student and I am grateful for your continuous support and valuable ideas which helped me to complete this PhD. Thank you for your patience, wisdom and encouragement and for pushing me further than I thought I could go. Moltes gràcies.

I would like to express my gratefulness to my other supervisor, Dr. Oscar Núñez for his guidance, support and for sharing his knowledge and expertise in CE and LC-MS. Thank you for always being present in the lab and for helping me whenever I looked-for.

I also acknowledge Dr. Encarnación Moyano who made great efforts resolving specific LC-MS problems. Thank you for sharing your knowledge and for your contributions to this research project. I must not forget to thank Dr. Francisco Javier Santos for his contribution with valuable ideas for specific topics of my research and for guiding and helping me with the preparation of the paperwork required for the submission of this thesis.

My warm thanks to all my colleagues from CECEM group, especially to Élida and Héctor for their help with the MS instruments and their good advice. Moltes gràcies. Alba, Gabino, Helena, Eloy, Raquel, Anna, Paolo, Marsela, Rocio, and Juanfra, thank you for the great moments we shared. Special thanks to my Venezuelan colleagues and friends, Luz and Luis, who stood by me through this journey. Thank you both for your support and advice. Gracias amigos.

At the University of Amsterdam I had the opportunity to be part of the esteemed research group of one of the most influential people in the analytical sciences, Prof. Peter Schoenmakers. My wholehearted gratitude for your enthusiastic motivation, continuous support and guidance, your kind help and recommendations, and for opening many doors for my future career. Dank U wel.

I also thank Dr. Wim Kok for his exceptional supervision during my stay in the Analytical Chemistry group at UvA. Thank you for showing me the doors to FFF and sharing your professional expertise in this field and for helping me to achieve one of the goals of my research.

I appreciate your support in sorting out the challenges faced during my stay in Amsterdam. Dank U wel.

I would like to thank Peter V. and Tom for their kind help fixing the FFF and MALS instruments whenever I needed. I shall not forget to thank my friendly and joyful colleagues in the international office at UvA. Many thanks to Maria for being very helpful with FFF instrument, for the nice talks and great company. I would also like to thank Jana for her help in the lab, and for the great time we had together. My sincerest gratitude goes to my sweet friend, Anna. Thank you for our Thursdays, your delightful company and your jokes, the moral support and for helping me to overcome the difficult times in the last two years. Спасибо большое. Many thanks to my kind friend Nick. Thank you for your continuous help and support and your good advice. I would like to thank my office mates Daniela and Rudy for the great moments we shared and your support. Special thanks to Bob, thank you for your friendship, your support, enthusiasm and for the great time we had in Dordrecht. Best of luck with your PhD. Gabriel, Casi, Katja, Martin, Henrik, Andjoe, Michelle and Andrea it was nice meeting you. Petra Aarnoutse, thank you for your help and for the good talks.

I would like to acknowledge Prof. Pim de Voogt for his help and support during the last part of my PhD. Thank you for encouraging me to write the Marie Curie proposal, for your valuable contribution and for wanting me to become part of your team. Also, many thanks for giving me the opportunity to collaborate with your students and with your team at KWR. Dank U wel.

My gratitude to Dr. Patrick Bäuerlein for his hospitality and help with the FFF instrument at KWR. Thank you for sharing your knowledge, for all the effort, support and help with the experiments and the data. Vielen Dank.

I also have to thank Andrea Carboni from UvA for providing some of the fullerene aqueous solutions for the experiments carried in Amsterdam. Grazie mille.

My sincerest gratitude to my supervisors at the University Al. I. Cuza and University Babes Bolyai in Romania where I carried my Bachelor's and Master degree in Chemistry, Mirela Goanta and Codruta Cobzac. Thank you for all the guidance and the chemistry you have thought me. Mulţumesc frumos.

I would also like to acknowledge the Spanish Ministry of Economy and Competitiveness for a Ph.D. grant (FPI-MICINN) which enabled me to carry out this research.

Last but not the least many thanks to my friends, Gina, Roxana, Idoya, Maria, Llúis, Carles and Alvaro, who always encouraged and supported me. Special thanks to Edfran who stood by me from the beginning of this PhD. It is hard to summarise in few lines how grateful I am. Thank you for your patience, understanding and moral support. Gracias por todo.

Finally, I would like to thank you Bert, for your immense patience, professional and moral support and motivation. Bedankt voor alles! Ik ben dankbaar dat ik zo een prachtig persoon in mijn leven heb.